HEREDITARY HEARING IMPAIRMENT IN THE NETHERLANDS

Diagnostics, genotype-phenotype correlations and identification of novel deafness genes

Mieke Wesdorp

Hereditary hearing impairment
in the Netherlands

Diagnostics, genotype-phenotype correlations
and identification of novel deafness genes

Mieke Wesdorp

Hereditary hearing impairment in the Netherlands

Diagnostics, genotype-phenotype correlations and identification of novel deafness genes

Proefschrift

ter verkrijging van de graad van doctor
aan de Radboud Universiteit Nijmegen
op gezag van de rector magnificus prof. dr. J.H.J.M. van Krieken,
volgens besluit van het college van decanen
in het openbaar te verdedigen op
woensdag 6 december 2017
om 14.30 uur precies

door

Francina Maria Wesdorp
geboren op 29 april 1989
te Goes

Contents

1

General introduction

Anatomy and physiology of the inner ear

The inner ear consists of the vestibular system and the cochlea (Figure 1a). The cochlea is coiled in a spiral shape, like a snail shell, and contains three parallel compartments: the scala media, scala vestibuli and scala tympani (Figure 1b). The scala media is filled with potassium-rich endolymph, whereas the other two compartments are filled with sodium-rich perilymph. The difference in ion concentration between the compartments results in a positive voltage in the scala media, known as the encodochlear potential. Endolymph is produced by the stria vascularis, localized in the lateral wall of the scala media, which is responsible for maintainance of high potassium concentration of the endolymph.[1] The scala media is separated from the scala vestibuli by Reissner's membrane, and from the scala tympani by the basilar membrane. The organ of Corti is positioned on the thin basilar membrane and contains a single row of inner hair cells and three rows of outer hair cells. Inner hair cells transduce the vibration of sound into electrochemical signals, whereas outer hair cells enhance the sound sensitivity and selectivity.[2] The hair cells are surrounded by various supporting cells, which play a pivotal role in development of sensory epithelia, preservation of structural integrity and homeostasis.[3] Junctions between the hair cells and supporting cells ensure a selective barrier between endolymph and perilymph and enable exchange of electric and chemical signals.[4] On the apical surface of hair cells, stereocilia are located, the mechano-sensory structures of the cochlea.[5] Atop the stereocilia lays a gelatinous structure, the tectorial membrane (Figure 1c).

When sound reaches the ear, it travels through the external auditory canal to the tympanic membrane, which starts vibrating. These vibrations are transmitted to the cochlea by the three middle ear ossicles (Figure 1a). Sound transmission to the cochlea generates vibration of the basilar membrane, causing vertical movement of the organ of Corti. This results in deflection of stereocilia against the tectorial membrane. Deflections of the stereocilia bundle leads to influx of calcium and potassium from the endolymph into the hair cell, inducing depolarization of the cell and release of neurotransmitters at the basal end of the hair cell.[1] The neurotransmitters stimulate the cochlear nerve, which transmits the signal to the auditory cortex.

Due to variation in stiffness and width of the basilar membrane, variation in length of the stereocilia and outer hair cell bodies, and variation in width of the tectorial membrane, the basal part of the cochlea perceives high-frequency sounds, while low-frequency sounds are perceived in the apex.[6] Loudness of a tone is determined by the amplitude of basilar membrane motion.[7]

The vestibular system consists of three semicircular canals, which detect rotational accelerations, and of the utricule and saccule, which detect linear accelerations (Figure 1a). Although the anatomy of the vestibular organ is different from the cochlea, the physiology is very similar. The vestibular structures contain perilymph and endolymph, the latter being produced by dark cells in the vestibular system and by the stria vascularis in the cochlea. The vestibular system harbors supporting cells, and hair cells with stereocilia and one kinocilium per hair cell. In the ampulla of the semicircular canals, the stereocilia and kinocilia are embedded in a gelatinous mass, called the cupula (Figure 1d). In the utricule and saccule, the gelatinous mass is known as the otolithic membrane, which is covered by otoconia (Figure 1e).[8,9]

Rotation of the head causes movement of endolymph that bends the cupula and causes movement of the otoliths. This leads to deflection of stereocilia and kinocilia in the semicircular canals, and saccule and utricule. As a result, the hair cells depolarize and release neurotransmitters, causing signals to be transduced to the brainstem. Here, the peripheral vestibular signals are integrated with visual signals from the ocular system, and orientation signals from proprioceptors, to maintain balance.[8,9]
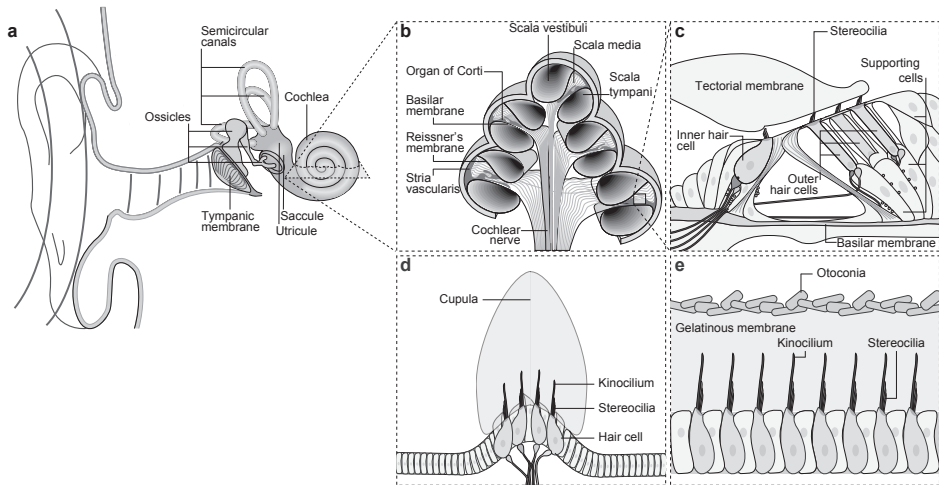
Figure 1 The auditory system (cochlea) and vestibular system (semicircular canals, utricule and saccule) are part of the inner ear **(a)**. The snail shell shaped cochlea, consists of the scala media, scala vestibuli and scala tympani **(b)**. Within the scala media, the organ of Corti is located, which transduces sound waves into electrochemical signals. It contains the basilar membrane, hair cells, supporting cells and the tectorial membrane **(c)**. The stereocilia and kinocilia of the semicircular canals, located on the apical surface of the hair cells, are embedded in a membranous mass, called the cupula **(d)**. The utricule and saccule contain hair cells with stereocilia and kinocilia that are overlaid by a gelatinous membrane, which is covered by otoliths **(e)**. The figure was adapted from Frolenkov *et al.* (2004)[10], with approval from the Nature Publishing Group.

Molecular aspects of hereditary hearing impairment

Given the complexity of the auditory system, defects in many biological processes can lead to hearing impairment (HI). Functions of known genes active in the auditory system differ from hair bundle morphogenesis, to ion homeostasis, to gene regulation and synaptic signal transmission.[11,12] Some of the encoded proteins co-function in specific biological pathways. Currently, deleterious mutations in more than 100 genes have been associated with nonsyndromic HI (NSHI) (Hereditary Hearing Loss Homepage, http://hereditaryhearingloss.org/) and even more in syndromic HI (OMIM, https://www.omim.org/), illustrating the extreme genetic heterogeneity of HI. Mutations in *GJB2* are the leading cause of NSHI, accounting for up to 50% of the NSHI population.[13] Although a number of other genes are relatively frequently involved in HI (*e.g. MYO6, MYO7A, MYO15A, SLC26A4, STRC* and *USH2A*)[14-21], many genes have been reported in only one or a few families, demonstrating that most types of hereditary HI are (extremely) rare.

In this manuscript, we focus on monogenic (Mendelian) forms of HI, meaning that HI is caused by defect(s) in a single gene. Monogenic inheritance can be classified as autosomal recessive (70-80% of early onset NSHI cases), autosomal dominant (20-30% of NSHI), mitochondrial (1-2% of NSHI), X-linked (1-2% of NSHI) and Y-linked (rare in NSHI).[22,23] Nonsyndromic deafness loci and genes involved in monogenic forms of HI are named according to the DFN (DeaFNess) nomenclature: DFNA, autosomal dominant; DFNB, autosomal recessive; DFN, X-linked; DFNY, Y-linked inheritance; DFNM, modifier.

Clinical aspects of hereditary hearing impairment

Worldwide, 360 million people suffer from disabling HI, of whom 32 million are children, making HI the most prevalent sensorineural disorder.[24] One to two in every 1000 newborns has permanent HI; about half of the cases is assumed to be inherited.[25]

Very diverse genetic HI phenotypes are known. In most forms of monogenic HI, there is a congenital or childhood onset of HI, although onset can vary up to the 6th decade in patients with DFNA9.[26] Hereditary HI can be syndromic or nonsyndromic, accounting for 30% and 70% of cases, respectively.[27] Syndromic HI is characterized by HI associated with one or more particular symptoms. The most common types of syndromic HI are Pendred, Usher, Waardenburg and Branchio- oto-renal syndrome. NSHI can be defined as isolated HI without additional symptoms.

Auditory phenotypes investigated in this thesis are described according to the recommendations of the GENDEAF study group.[28] Vestibular characteristics in this thesis

are described in accordance with current standards[29] and the international standard ANSI S3.45 2009. Tables 1 and 2 provide an overview of the audiological and vestibular terms and definitions. Although the auditory and vestibular phenotype can be objectively investigated and described, it is often impossible to predict the genotype based on the HI phenotype. Many monogenic types of NSHI have a similar phenotype, characterized by early onset HI with a downsloping audiogram configuration, making it impossible

Table 1 Audiological terms and definitions, as described by the GENDEAF study group[28]

Auditory characteristic	Term	Definition
Type of HI	Conductive	Related to disease or deformity of outer/middle ear. Normal bone-conduction thresholds (<20 dB HL) and an air-bone gap >15 dB HL averaged over 0.5, 1 and 2 kHz.
	Sensorineural	Related to disease/deformity of the inner ear/cochlear nerve. Air/bone gap <15 dB HL averaged over 0.5, 1 and 2 kHz.
	Mixed	Related to combined involvement of the outer/middle ear and the inner ear/cochlear nerve. >20 dB HL in the bone conduction threshold together with >15 dB HL air-bone gap averaged over 0.5, 1 and 2 kHz.
Severity of HI (applied to the better hearing ear, averaged over 0.5, 1, 2 and 4 kHz)	Mild	20-40 dB HL
	Moderate	41-70 dB HL
	Severe	71-95 dB HL
	Profound	in excess of 95 dB HL
Audiometric configuration	Low frequency ascending	>15 dB HL difference from the poorer low frequency thresholds to the higher frequencies
	Mid frequency U-shaped	>15 dB HL difference between the poorest thresholds in the mid-frequencies, and those at higher and lower frequencies
	High frequency gently sloping	15-29 dB HL difference between the mean of 0.5 and 1 kHz and the mean of 4 and 8 kHz
	High frequency steeply sloping	>30 dB HL difference between the mean of 0.5 and 1 kHz and the mean of 4 and 8 kHz
	Flat	<15 dB HL difference between the mean of 0.25, 0.5 kHz thresholds, the mean of 1 and 2 kHz and the mean of 4 and 8 kHz
Frequency ranges	Low frequencies	≤ 0.5 kHz
	Mid frequencies	>0.5 kHz ≤ 2 kHz
	High frequencies	>2 kHz ≤ 8 kHz
	Extended high frequencies	> 8 kHz
Unilateral/bilateral		>10 dB HL difference between the ears in at least two frequencies. The average over 0.5, 1 and 2 kHz of the better ear should be worse than 20 dB HL.
Progression		Deterioration of >15 dB HL in the average over the frequencies of 0.5, 1, and 2 kHz within a 10 year period.

to clinically differentiate them. There are, however, a few types of HI with a very distinct phenotype, such as HI in Pendred syndrome, Usher syndrome, and DFNA9. These types of HI are therefore easily recognized, enabling targeted diagnostic analysis.

Mutations in a specific deafness gene can lead to different phenotypes, which has implications for counseling. Some deafness genes are involved in both syndromic and nonsyndromic HI, such as *CDH23*, which is known for DFNB12 and Usher syndrome type 1D.[30] Other deafness genes have been associated with both dominantly and recessively inherited forms of HI. Mutations in *TECTA* can, for example, lead to DFNA8/12 and DFNB21.[31] It is important to realize that even differences in phenotypes between patients with exactly the same genetic defect do exist. Therefore, counseling for these types of HI, particularly on prognosis, may be difficult. In general, phenotypic differences can be due to the type or location of the mutation (such as in DNFA9[26,32]), environmental factors (*e.g.* noise exposure[33]) or genetic modifiers[34] (*e.g.* DFNM1[35]). The penetrance of the mutation within a family can be complete or incomplete, but is usually complete.

Table 2 Vestibular terms and definitions in accordance with current standards[29] and the international standard ANSI S3.45 2009

Vestibular test	Term	Definition
Caloric irrigation test[a]	Hyporeflexia	Slow phase velocities of the nystagmus <10°/sec cold water irrigation or <7°/sec warm water irrigation
	Hyperreflexia	Slow phase velocities of the nystagmus >52°/sec cold water irrigation or >31°/sec warm water irrigation
Rotary chair test	Hyporeactivity	Gain <33% and maximum velocity at deceleration <30°/sec and decay time <11 sec
	Hyperreactivity	Gain >72% and maximum velocity at deceleration >65°/sec and decay time >26 sec
vHIT	Hyporeactivity	Gain <82%
cVEMP	Hyporeactivity	Thresholds >100 dB
	Hyperreactivity	Thresholds <82 dB

sec, second; vHIT, video head impulse test; cVEMP, cervical vestibular evoked myogenic potentials. [a]Caloric irrigation tests were performed with water irrigation during 30 seconds.

The impact of hereditary hearing impairment on life

HI can have a significant impact on social life and professional performance. Patients with HI may have to deal with feelings of shame and insecurity, lack of energy, depression, loneliness, isolation, dependence, and frustration.[36-39] Parents sometimes experience feelings of guilt.[40] It can be very difficult for parents to cope with a (syndromic) diagnosis, especially (presymptomatic) Usher syndrome. Presymptomatic diagnosis of syndromic HI has become more frequent with the introduction of next generation sequencing (NGS),

targeting a panel of syndromic and nonsyndromic HI-related genes or the whole exome. A presymptomatic diagnosis can induce feelings of insecurity and lead to coping problems with unanswered questions, such as for parents when and how to tell their child, and what the future of their child will hold. A genetic diagnosis can also entail difficult decisions on family planning and career.

It is essential to assist patients and their relatives, by counseling them on their diagnosis, recurrence risk, prognosis and rehabilitation options, and by providing aftercare.[41] It has been shown that a genetic diagnosis positively impacts the psychological status of individuals and families affected by HI.[42] In addition, a genetic diagnosis can prevent further diagnostic testing and may identify possible medical comorbidities[43] (*e.g.* hypothyroidism in Pendred syndrome). Knowledge on phenotype characteristics and genotype-phenotype correlations is crucial for proper counseling, however, evidence based information lacks for many types of HI.

Diagnostic work-up of patients with hereditary hearing impairment

In the Netherlands, patients suspected of hereditary HI can be referred to an (oto)genetic outpatient clinic in one of the eight university medical centers, where they are clinically and genetically examined. In the Radboud university medical center outpatient clinic, expertise center Hearing & Genes, a standardized protocol is used (see flowchart, Figure 2). Clinical evaluation has been described in detail before.[44] In brief, patients and their relatives are seen by an otologist, clinical geneticist, and/or audiologists, who takes medical history and family history, and performs physical examination including otoscopy. Special attention is paid to possible acquired causes of HI[12], such as cytomegalovirus infection[45] and perinatal hypoxia/ asphyxia.[46] Hearing is evaluated to determine the auditory phenotype. When indicated, additional examinations can be performed, such as high-resolution computed tomography, magnetic resonance imaging, cytomegalovirus test, full blood count, and additional audiometric or vestibular tests.

If a patient is clinically suspected of Usher syndrome type 2, Pendred syndrome or DFNA9, a single gene test is requested (*USH2A, SLC26A4* or *COCH,* respectively). In patients with early-onset HI, gene tests for DFNB1 are performed (*GJB2/GJB6)*. In all other cases, whole exome sequencing (WES) is performed and subsequently a panel of known (non) syndromic HI-related genes is targeted and analyzed. This gene panel is constantly updated according to newest insights on genes involved in HI. Patients or their legal representatives are counseled by the clinician on potential findings related to syndromic HI, prior to testing. If gene panel analysis is negative, analysis of all WES data (open exome analysis)

1
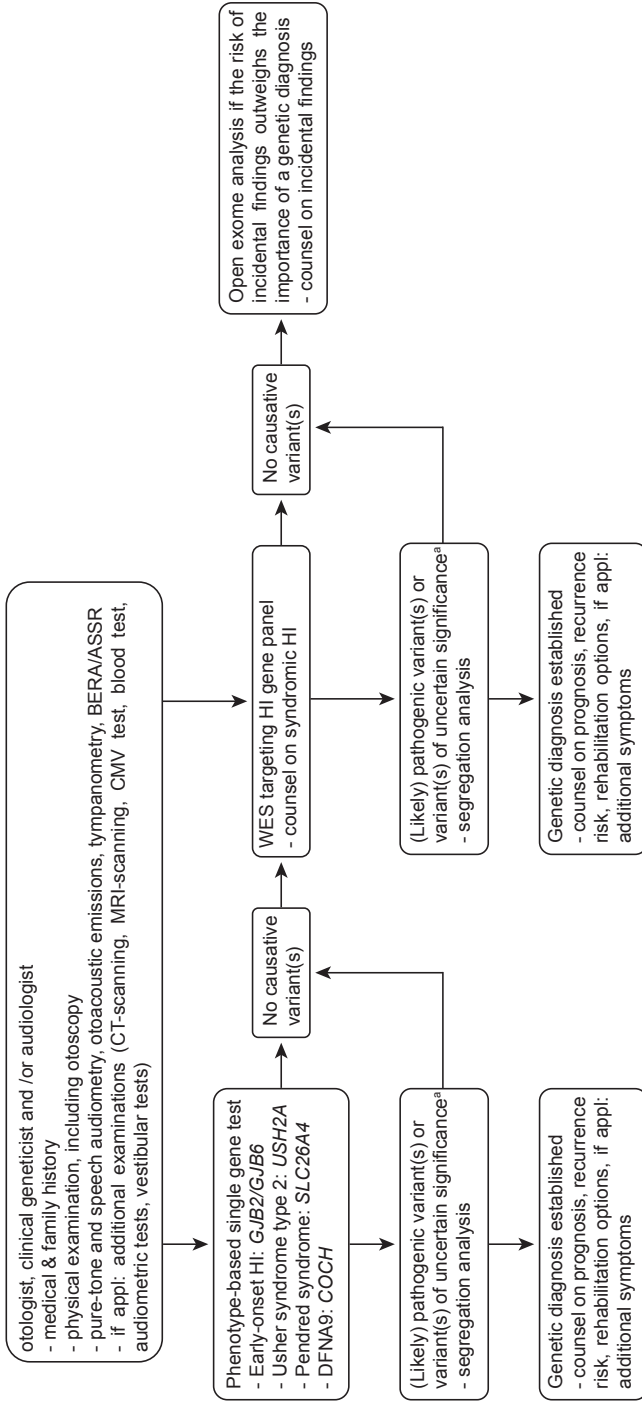
Figure 2 Flowchart of the diagnostic work-up of patients with hereditary HI, used in the Radboud university medical center Hearing & Genes outpatient clinic. BERA, brainstem evoked response audiometry; ASSR, auditory steady-state response; CT, computed tomography; MRI magnetic resonance signaling; CMV, cytomegalovirus. [a]According to the guidelines of the American College of Medical Genetics and Genomics.[49]

can be performed. Open exome analysis is used for identification of (likely) pathogenic variants in candidate genes for HI. The risk of incidental findings[47] (0.7%, unpublished data), the extremely low diagnostic yield of open exome analysis, and the importance to establish a genetic diagnosis, are carefully considered and counseled. If an incidental finding occurs, the results are discussed in a panel of independent specialists who decide whether the incidental finding is important for the patient to know, in accordance with the recommendations by the European Society of Human Genetics[48], and the guidelines for diagnostic next generation sequencing as published by Eurogentest (http://www.eurogentest.org/). The turnaround time for single gene tests is approximately 6 weeks, for gene panel analysis 4 months, and for open exome analysis 2 additional months. In the Netherlands, genetic tests are all reimbursed by the health insurance company of the patient. Genetic testing for nonsyndromic HI and the most common syndromic forms is centered in the Radboud university medical center, Nijmegen, and the Erasmus University Medical Center, Rotterdam; the Netherlands.

All patients seen in the outpatient clinic Hearing & Genes in the Radboud university medical center Nijmegen, are discussed in a multidisciplinary meeting with otologists, clinical geneticists, molecular geneticists, audiologists and social workers. Here, we discuss the interpretation of variants and whether the identified genetic defect is in accordance with the phenotype known to be associated with defects in a specific gene. If a genetic diagnosis can be established, we discuss who (otologist and/or clinical geneticist) should perform the counseling and whether patients or their parents may possibly need aftercare (*e.g.* in case of a presymptomatic Usher diagnosis). Patients are counseled on prognosis, recurrence risk, rehabilitation options and, if applicable, additional symptoms.

Scientific research into hereditary hearing impairment

Molecular diagnostic results often raise questions regarding the causality of identified variants, because novel variants of uncertain significance have been identified in a known deafness gene, or because the identified genetic defect does not match with the phenotype of the patient. These questions can be answered by performing research into the effect of the mutation on protein level. There can also be uncertainty about the associated phenotype due to insufficient phenotype data, which hampers proper counseling. Therefore, studies into phenotype characteristics and genotype-phenotype correlations are essential. Negative results from diagnostic genetic tests can be a reason to investigate presence of variants in candidate genes for HI in a scientific research setting. Identification of novel (candidate) deafness genes and functional analysis of the encoded proteins

contribute to knowledge of the complex physiology of the hearing apparatus.[11] When a novel deafness gene is identified in research, it can also be included in the diagnostic gene panel. Finally, there is high demand for development of genetic therapies and for data that enable personalized medicine in hearing rehabilitation. Worldwide, many research projects currently focus on these issues. In this thesis, we focused on the identification of novel deafness genes and characterization of genotype-phenotype correlations for known and novel deafness genes.

Several techniques can be used to identify novel genes associated with the disease of interest, such as homozygosity mapping, linkage analysis, WES and whole genome sequencing (WGS).

Homozygosity mapping is used to identify the genetic region, in which the causative variant of a disorder is located. It is only applicable in families with autosomal recessive disorders, and can determine disease haplotypes inherited from a common ancestor (founder effect)[50] or within consanguineous families[51]. This technique detects homozygous genotypes shared by affected individuals, but not by unaffected individuals within a family. Genome-wide Single Nucleotide Polymorphism (SNP) arrays are used to determine individual genotypes. Subsequently, these genotypes are compared amongst affected and/or unaffected individuals within the same family to identify large regions (usually >1 Mb) of homozygosity.

Linkage analysis can be used for localization of the genetic defect located in a specific chromosomal region, in families with autosomal dominant[52], recessive[53], and X-linked[54] HI. It can also provide statistical evidence that a chromosomal region is excluded to harbor the genetic defect.

Whereas since 1977 Sanger sequencing has been used to sequence DNA[55], the need for large-scale, rapid and inexpensive sequencing has increased exponentially over the years. With the advent of NGS, which is based on massively parallel sequencing, complete exomes (WES) or the whole genome (WGS) can be analyzed in one experiment. It is also possible to perform targeted sequencing of a gene panel using NGS methods, such as in OtoSCOPE.[56] Many recently identified deafness genes have been discovered using WES, often in combination with homozygosity mapping or linkage analysis.[57] However, the large number of variants identified with WES and WGS poses challenges for interpretation of variants, storage of data and managing of incidental findings. To reduce the risk of incidental findings, pathogenic variants in 59 genes associated with severe diseases, can be excluded from analysis. For this purpose, the list of genes compiled and updated by the American College of Medical Genetics and Genomics, for reporting of secondary findings in clinical exome and genome sequencing, can be used.[58]

For characterization of genotype-phenotype correlations in this thesis, the pathogenicity of the identified variant(s) was first classified according to the guidelines of the American College of Medical Genetics and Genomics.[49] In this context, DNA of affected and unaffected family members was collected for segregation analysis. Subsequently, audiovestibular phenotypes were investigated and described according to the recommendations of the GENDEAF study group.[28] Need for investigation of additional symptoms was based on the phenotype of animal models, expression and function of the gene and complaints reported by the investigated individuals.

1

Scope of this thesis

The research presented in this thesis has the aim to contribute to optimal diagnostics and counseling for patients with hereditary HI in the Netherlands and beyond, by identification of novel deafness genes and (further) characterizing phenotypes and correlations between types of HI and the underlying genetic causes. Ultimately, we aim to identify causative mutations and provide personal, evidence-based counseling in >90% of individuals with hereditary HI.

In **chapter 2**, the diagnostic yield of WES targeting a deafness gene panel has been investigated in 200 Dutch patients with HI. This chapter serves as the starting point of this thesis. It provides insight into the most frequent causes of HI in the Netherlands, the yield and (dis)advantages of WES targeting a deafness gene panel, the issues that are faced in the interpretation of genetic variants, and genotype-phenotype correlations in the Dutch population. In **chapter 3**, the phenotypes of two recessive types of HI, DFNB28 and DFNB77, are further characterized and genotype-phenotype correlations are extended. These chapters contribute to our knowledge on the phenotypic spectrum of DFNB28 and DFNB77 and to our understanding of the relationship between specific mutations and the associated phenotype. The findings are particularly useful for counseling of patients. Both chapters emphasize the huge genetic and phenotypic heterogeneity of HI. In **chapter 4**, two novel deafness genes (*MPZL2* and *LMX1A*) are described for autosomal recessive and autosomal dominant HI, respectively. A combination of thorough genetic research, phenotype characterization, and for *MPZL2,* localization studies and investigation of a mouse model, reveals that both genes are associated with NSHI and thus that both encoded proteins are essential for normal hearing. For patients with HI caused by defects of *MPZL2* or *LMX1A*, the identification of these two novel genes enables establishment of a genetic diagnosis and subsequently genotype-based counseling.

As part of this thesis, a clinical and scientific collaboration with four university medical centers in the Netherlands was started, called "DOOFNL: Diagnostiek en Onderzoek Oto-genotype Fenotype Nederland", freely translated as: "DEAFNL: Diagnostics and Research Oto-genotype Phenotype the Netherlands". The goal of this collaboration is fully in line with the aim of this thesis: contribute to the best diagnostics and information for patients with HI in the Netherlands. Participating centers are: Radboud university medical center, Erasmus University Medical Center, Leiden University Medical Center, Maastricht University Medical Center+, and University Medical Center Groningen. Genetic and phenotypic data obtained by this collaboration is shared in a national database.

References

1.   Hudspeth AJ. Integrating the active process of hair cells with cochlear function. Nature reviews. Neuroscience. Sep 2014;15(9):600-614.

2.   Jahan I, Pan N, Kersigo J, Fritzsch B. Beyond generalized hair cells: molecular cues for hair cell types. Hearing research. Mar 2013;297:30-41.

3.   Wan G, Corfas G, Stone JS. Inner ear supporting cells: rethinking the silent majority. Seminars in cell & developmental biology. May 2013;24(5):448-459.

4.   Wang B, Hu B, Yang S. Cell junction proteins within the cochlea: A review of recent research. Journal of Otology. 2015;10:131-135.

5.   Zhao B, Muller U. The elusive mechanotransduction machinery of hair cells. Current opinion in neurobiology. Oct 2015;34:172-179.

6.   Mann ZF, Kelley MW. Development of tonotopy in the auditory periphery. Hearing research. Jun 2011;276(1-2):2-15.

7.   Oghalai JS. The cochlear amplifier: augmentation of the traveling wave within the inner ear. Current opinion in otolaryngology & head and neck surgery. Oct 2004;12(5):431-438.

8.   Khan S, Chang R. Anatomy of the vestibular system: a review. NeuroRehabilitation. 2013;32(3):437-443.

9.   Kingma H, van de Berg R. Anatomy, physiology, and physics of the peripheral vestibular system. Handbook of clinical neurology. 2016;137:1-16.

10.   Frolenkov GI, Belyantseva IA, Friedman TB, Griffith AJ. Genetic insights into the morphogenesis of inner ear hair cells. Nature reviews. Genetics. Jul 2004;5(7):489-498.

11.   Dror AA, Avraham KB. Hearing loss: mechanisms revealed by genetics and cell biology. Annual review of genetics. 2009;43:411-437.

12.   Korver AM, Smith RJ, Van Camp G, et al. Congenital hearing loss. Nature reviews. Disease primers. Jan 12 2017;3:16094.

13.   Kenneson A, Van Naarden Braun K, Boyle C. GJB2 (connexin 26) variants and nonsyndromic sensorineural hearing loss: a HuGE review. Genetics in medicine : official journal of the American College of Medical Genetics. Jul-Aug 2002;4(4):258-274.

14.   Zazo Seco C, Wesdorp M, Feenstra I, et al. The diagnostic yield of whole-exome sequencing targeting a gene panel for hearing impairment in The Netherlands. European journal of human genetics : EJHG. Feb 2017;25(3):308-314.

15.   Sommen M, Schrauwen I, Vandeweyer G, et al. DNA Diagnostics of Hereditary Hearing Loss: A Targeted Resequencing Approach Combined with a Mutation Classification System. Human mutation. Aug 2016;37(8):812-819.

16.   Yan D, Tekin D, Bademci G, et al. Spectrum of DNA variants for non-syndromic deafness in a large cohort from multiple continents. Human genetics. Aug 2016;135(8):953-961.

17.   Shearer AE, Black-Ziegelbein EA, Hildebrand MS, et al. Advancing genetic testing for deafness with genomic technology. J Med Genet. Sep 2013;50(9):627-634.

18.   Sloan-Heggen CM, Babanejad M, Beheshtian M, et al. Characterising the spectrum of autosomal recessive hereditary hearing loss in Iran. J Med Genet. 2015;52:823-829.

19.   Sloan-Heggen CM, Bierer AO, Shearer AE, et al. Comprehensive genetic testing in the clinical evaluation of 1119 patients with hearing loss. Human genetics. Apr 2016;135(4):441-450.

20.   Atik T, Onay H, Aykut A, et al. Comprehensive Analysis of Deafness Genes in Families with Autosomal Recessive Nonsyndromic Hearing Loss. PLoS One. 2015;10(11):e0142154.

21.   Bademci G, Diaz-Horta O, Guo S, et al. Identification of copy number variants through whole-exome sequencing in autosomal recessive nonsyndromic hearing loss. Genetic testing and molecular biomarkers. Sep 2014;18(9):658-661.

22.   Morton NE. Genetic epidemiology of hearing impairment. Annals of the New York Academy of Sciences. 1991;630:16-31.

23.   Mahboubi H, Dwabe S, Fradkin M, Kimonis V, Djalilian HR. Genetics of hearing loss: where are we standing now? European archives of oto-rhino-laryngology : official journal of the European Federation of Oto-Rhino-Laryngological Societies. Jul 2012;269(7):1733-1745.

24.   WHO. Factsheet deafness and hearing loss. 2017; http://www.who.int/. Accessed May, 2017.

25.   Morton CC, Nance WE. Newborn hearing screening--a silent revolution. The New England journal of medicine. May 18 2006;354(20):2151-2164.

26.   Bae SH, Robertson NG, Cho HJ, et al. Identification of pathogenic mechanisms of COCH mutations, abolished cochlin secretion, and intracellular aggregate formation: genotype-phenotype correlations in DFNA9 deafness and vestibular disorder. Human mutation. Dec 2014;35(12):1506-1513.

27.   Van Laer L, Cryns K, Smith RJ, Van Camp G. Nonsyndromic hearing loss. Ear and hearing. Aug 2003;24(4):275-288.

28.   Mazzoli M, Van Camp G, Newton V, Giarbini N, Declau F, Parving A. Recommendations for the description of genetic and audiological data for families with nonsyndromic hereditary hearing impairment. Audiological Medicine. 2003;1:148-150.

29.   Jacobson GP, Shepard NT. Balance Function Assessment and Management. Plural Phublishing Inc; 2014.

30.   Bork JM, Peters LM, Riazuddin S, et al. Usher syndrome 1D and nonsyndromic autosomal recessive deafness DFNB12 are caused by allelic mutations of the novel cadherin-like gene CDH23. American journal of human genetics. Jan 2001;68(1):26-37.

31.   Balciuniene J, Dahl N, Jalonen P, et al. Alpha-tectorin involvement in hearing disabilities: one gene--two phenotypes. Human genetics. Sep 1999;105(3):211-216.

32.   Kim BJ, Kim AR, Han KH, et al. Distinct vestibular phenotypes in DFNA9 families with COCH variants. European archives of oto-rhino-laryngology : official journal of the European Federation of Oto-Rhino-Laryngological Societies. Oct 2016;273(10):2993-3002.

33.   Liberman MC. Noise-Induced Hearing Loss: Permanent Versus Temporary Threshold Shifts and the Effects of Hair Cell Versus Neuronal Degeneration. Advances in experimental medicine and biology. 2016;875:1-7.

34.   Yan D, Liu XZ. Modifiers of hearing impairment in humans and mice. Current genomics. Jun 2010;11(4):269-278.

35.   Riazuddin S, Castelein CM, Ahmed ZM, et al. Dominant modifier DFNM1 suppresses recessive deafness DFNB26. Nature genetics. Dec 2000;26(4):431-434.

36.   Ciorba A, Bianchini C, Pelucchi S, Pastore A. The impact of hearing loss on the quality of life of elderly adults. Clinical interventions in aging. 2012;7:159-163.

37.   Kvam MH, Loeb M, Tambs K. Mental health in deaf adults: symptoms of anxiety and depression among hearing and deaf individuals. Journal of deaf studies and deaf education. Winter 2007;12(1):1-7.

38.   Carlsson PI, Hjaldahl J, Magnuson A, et al. Severe to profound hearing impairment: quality of life, psychosocial consequences and audiological rehabilitation. Disability and rehabilitation. 2015;37(20):1849-1856.

39.   Oonk AMM, Ariens S, Kunst HPM, Admiraal RJC, Kremer H, Pennings RJE. Psychological impact of a genetic diagnosis on hearing impairment - an exploratory study. Clinical otolaryngology : official journal of ENT-UK ; official journal of Netherlands Society for Oto-Rhino-Laryngology & Cervico-Facial Surgery. May 29 2017.

40.   Withrow KA, Burton S, Arnos KS, Kalfoglou A, Pandya A. Consumer motivations for pursuing genetic testing and their preferences for the provision of genetic services for hearing loss. Journal of genetic counseling. Jun 2008;17(3):252-260.

41. Alford RL, Arnos KS, Fox M, et al. American College of Medical Genetics and Genomics guideline for the clinical evaluation and etiologic diagnosis of hearing loss. Genetics in medicine : official journal of the American College of Medical Genetics. Apr 2014;16(4):347-355.

42. Withrow KA, Tracy KA, Burton SK, et al. Impact of genetic advances and testing for hearing loss: results from a national consumer survey. American journal of medical genetics. Part A. Jun 2009;149A(6):1159-1168.

43. Shearer AE, Smith RJ. Genetics: advances in genetic testing for deafness. Current opinion in pediatrics. Dec 2012;24(6):679-686.

44. Hoefsloot LH, Feenstra I, Kunst HP, Kremer H. Genotype phenotype correlations for hearing impairment: approaches to management. Clinical genetics. Jun 2014;85(6):514-523.

45. Dumanch KA, Holte L, O'Hollearn T, Walker E, Clark J, Oleson J. High Risk Factors Associated With Early Childhood Hearing Loss: A 3-Year Review. American journal of audiology. May 06 2017:1-14.

46. Borg E. Perinatal asphyxia, hypoxia, ischemia and hearing loss. An overview. Scandinavian audiology. 1997;26(2):77-91.

47. Johnston JJ, Rubinstein WS, Facio FM, et al. Secondary variants in individuals undergoing exome sequencing: screening of 572 individuals identifies high-penetrance mutations in cancer-susceptibility genes. American journal of human genetics. Jul 13 2012;91(1):97-108.

48. van El CG, Cornel MC, Borry P, et al. Whole-genome sequencing in health care: recommendations of the European Society of Human Genetics. European journal of human genetics : EJHG. Jun 2013;21(6):580-584.

49. Wallis Y, Payne S, McAnulty C, et al. Practice Guidelines for the Evaluation of Pathogenicity and the Reporting of Sequence Variants in Clinical Molecular Genetics. ACGS /VGKL. 2013.

50. Schraders M, Oostrik J, Huygen PL, et al. Mutations in PTPRQ are a cause of autosomal-recessive nonsyndromic hearing impairment DFNB84 and associated with vestibular dysfunction. American journal of human genetics. Apr 09 2010;86(4):604-610.

51. Seco CZ, Oonk AM, Dominguez-Ruiz M, et al. Progressive hearing loss and vestibular dysfunction caused by a homozygous nonsense mutation in CLIC5. European journal of human genetics : EJHG. Feb 2015;23(2):189-194.

52. Zazo Seco C, Serrao de Castro L, van Nierop JW, et al. Allelic Mutations of KITLG, Encoding KIT Ligand, Cause Asymmetric and Unilateral Hearing Loss and Waardenburg Syndrome Type 2. American journal of human genetics. Nov 05 2015;97(5):647-660.

53. Zazo Seco C, Castells-Nobau A, Joo SH, et al. A homozygous FITM2 mutation causes a deafness-dystonia syndrome with motor regression and signs of ichthyosis and sensory neuropathy. Disease models & mechanisms. Feb 01 2017;10(2):105-118.

54. Schraders M, Haas SA, Weegerink NJ, et al. Next-generation sequencing identifies mutations of SMPX, which encodes the small muscle protein, X-linked, as a cause of progressive hearing impairment. American journal of human genetics. May 13 2011;88(5):628-634.

55. Sanger F, Nicklen S, Coulson AR. DNA sequencing with chain-terminating inhibitors. Proceedings of the National Academy of Sciences of the United States of America. Dec 1977;74(12):5463-5467.

56. Shearer AE, DeLuca AP, Hildebrand MS, et al. Comprehensive genetic testing for hereditary hearing loss using massively parallel sequencing. Proceedings of the National Academy of Sciences of the United States of America. Dec 07 2010;107(49):21104-21109.

57. Vona B, Nanda I, Hofrichter MA, Shehata-Dieler W, Haaf T. Non-syndromic hearing loss gene identification: A brief history and glimpse into the future. Molecular and cellular probes. Oct 2015;29(5):260-270.

58. Kalia SS, Adelman K, Bale SJ, et al. Recommendations for reporting of secondary findings in clinical exome and genome sequencing, 2016 update (ACMG SF v2.0): a policy statement of the American College of Medical Genetics and Genomics. Genetics in medicine : official journal of the American College of Medical Genetics. Feb 2017;19(2):249-255.

2
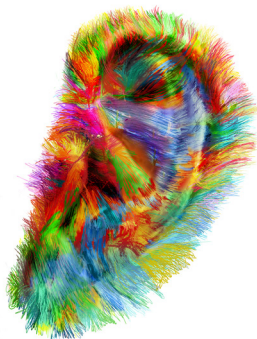
The diagnostic yield of whole-exome sequencing targeting a gene panel for hearing impairment in the Netherlands

Celia Zazo Seco*, Mieke Wesdorp*, Ilse Feenstra*, Rolph Pfundt, Jayne Y. Hehir Kwa, Stefan H. Lelieveld, Steven Castelein, Christian Gilissen, Ilse J. de Wijs, Ronald J.C. Admiraal, Ronald J.E. Pennings, Henricus P. M. Kunst, Jiddeke M. van de Kamp, Saskia Tamminga, Arjan C. Houweling, Astrid S. Plomp, Saskia M. Maas, Pia A.M. de Koning Gans, Sarina G. Kant, Christa M. de Geus, Suzanna G.M. Frints, Els K. Vanhoutte, Marieke F. van Dooren, Marie-José H. van den Boogaard, Hans Scheffer, Marcel Nelen, Hannie Kremer, Lies Hoefsloot, Margit Schraders[#] and Helger G. Yntema[#]

*,[#] These authors contributed equally to this work

Abstract

Hearing impairment (HI) is genetically heterogeneous, which hampers genetic counseling and molecular diagnosis. Testing of several single HI-related genes is laborious and expensive. In this study, we evaluate the diagnostic utility of whole-exome sequencing (WES) targeting a panel of HI-related genes. Two hundred index patients, mostly of Dutch origin, with presumed hereditary HI underwent WES followed by targeted analysis of an HI gene panel of 120 genes. We found causative variants underlying the HI in 67 of 200 patients (33.5%). Eight of these patients have a large homozygous deletion involving *STRC, OTOA* or *USH2A*, which could only be identified by copy number variation detection. Variants of uncertain significance were found in 10 patients (5.0%). In the remaining 123 cases no potentially causative variants were detected (61.5%). In our patient cohort, causative variants in *GJB2*, *USH2A, MYO15A* and *STRC*, and in *MYO6* were the leading causes for autosomal recessive and dominant HI, respectively. Segregation analysis and functional analyses of variants of uncertain significance will probably further increase the diagnostic yield of WES.

Introduction

DNA diagnostics of any genetically heterogeneous disease based on single gene testing is highly inefficient, laborious and expensive. High throughput sequencing technologies such as whole exome sequencing (WES) have coped with these disadvantages allowing the analysis of all protein-coding exons in a single cost-effective attempt.[1]

Hearing impairment (HI) is the most common sensory disorder with an incidence of one in 750 newborns (> 40 dB hearing loss) in developed countries.[2] About half of the cases are attributed to genetic factors with more than a hundred syndromic and non-syndromic genes known to date (http://hereditaryhearingloss.org/). HI is most frequently manifested as non-syndromic (NSHI) accounting for about 70% of the hereditary cases. About 77% of hereditary NSHI cases exhibit autosomal recessive inheritance (arNSHI) with 62 genes and 92 loci known to date, whereas it is dominant (adNSHI) in about 22% of the cases with 36 genes and 58 loci known. The remaining 1% shows an X-linked, a Y-linked or a mitochondrial type of inheritance pattern with seven loci and six genes known to date (http://hereditaryhearingloss.org/). Thus, NSHI is a perfect example of a genetically heterogeneous disorder. Many genes have been described to be involved in only one or a few families with HI.[3-5] Some exceptions are known, for example, mutations in *GJB2* followed by mutations in *STRC* and *MYO15A* are the most common causes for arNSHI worldwide.[6-9]

Since many genes contribute to hereditary HI, targeting all or a selection of protein-coding exons in a single experiment, as in WES, might currently be the best option for a comprehensive genetic analysis of HI individuals. The implementation of WES in a diagnostic setting has been much slower than in scientific research due to the relatively low sensitivity of this method in detection of genetic variation in some exonic regions, for example, extremely GC-rich regions, as compared to Sanger sequencing.[10] Despite this fact, the diagnostic yield in hereditary HI obtained by WES is expected to be higher compared with the approach of phenotype-based pretesting of one or two genes by Sanger sequencing.[11] Therefore, the aim of this study is to evaluate the diagnostic utility of WES targeting a panel of HI-related genes in a group of 200 Dutch index patients with presumed hereditary HI.

Patients and Methods

Patients
A retrospective cohort study was performed in 200 patients with HI, mainly of Dutch origin, who underwent WES in diagnostics in the period of 2011-2014. Only index cases were

included. Non-genetic causes of the HI were considered to be unlikely on basis of medical history and ENT examination. Type of inheritance, age of onset, and phenotype were based on family history, medical history and available audiogram(s) (Supplemental Tables S2-S4). The inheritance pattern indicated by the referring clinician was autosomal dominant in 66 cases, autosomal recessive in 31 cases, X-linked in one case and the remaining 102 cases were isolated. In the majority of subjects, the age of onset of HI was congenital (n=79) or in the first decade of life (n=60). Patients with both nonsyndromic and syndromic HI were included. The audiometric phenotype was assessed according to the recommendations by the GENDEAF study group.[12] Thirty-six patients have been previously reported in a study on the utility of WES,[11] and one patient has been reported before in a publication on novel and recurrent *CIB2* variants.[13] Prior to WES, causative variants in one or more genes involved in HI had been excluded by Sanger sequencing in 137 patients. Prescreening was performed in these patients because WES was not available at that time or because the clinician had a high clinical suspicion for mutations in a specific gene. Diagnostic WES was approved by the medical ethics committee of the Radboud university medical center, Nijmegen, the Netherlands (registration number 2011-188). For all patients, written informed consent for WES was obtained after counseling by a clinical geneticist.

WES and bioinformatics

Prior to sequencing, genomic DNA fragments of all patients were enriched for exome sequences using the Agilent SureSelectXT Human All Exon 50 Mb kit (n=30) or the version 4 (V4) kit (n=170). For 44 patients (30 cases Agilent 50 Mb, 14 cases Agilent V4), WES was performed with a 5500xl SOLiD system (Life Technologies) at the department of Human Genetics, Radboudumc Nijmegen, and data were analyzed using LifeScopeTM software as previously reported.[11] For the remaining patients (n=156, Agilent V4) WES was performed at BGI-Europe (Copenhagen, Denmark), employing an Illumina HiSeq2000TM machine. For these samples, 'read alignment' using BWA and 'variant calling' with GATK were performed at BGI.[14]

For all patients, variants were annotated with an in-house developed annotation and prioritization pipeline.[11] Variants in genes associated with HI were selected and analyzed. In the first 44 patients, a panel of 98 HI genes was analyzed (gene list DGD07092012).[11] In 2014, the gene panel was updated to 120 genes: four genes were deleted from the gene list, because proof for the involvement of the gene in HI is questionable, and 26 published novel HI-related genes were added (gene list DGD20062014). The remaining 156 patients were analyzed with the updated list of 120 HI genes. In retrospect, the WES data of the first 44 patients were analyzed for variants in the 26 genes added to gene list DGD20062014. Detailed information on both gene lists can be found in Supplemental Table S1.

The coverage was determined for the HI-related genes. The targeted genes enriched with the Agilent 50 Mb and Agilent V4 were compared with the longest RefSeq transcript to identify untargeted exons (Supplemental Table S1). These exons were omitted from coverage calculations. The coverage was calculated per sample on a base pair resolution, using the *coverage* function of BEDtools (v2.19.1; PMID 20110278). Subsequently, the mean percentage of base pairs with at least 20 reads (≥20x coverage) was determined per sample, for each gene and technological WES condition. Finally, the median ≥20x coverage was calculated per gene and technological WES condition. For all patients 'copy number variant calling' was carried out using CoNIFER 0.2.0,[15] and variant annotation was performed using an in-house developed strategy.[16]

Interpretation and classification of variants

To systematically predict their pathogenicity, variants were classified according to the existing guidelines from the American College of Medical Genetics and Genomics: benign (class 1), likely benign (class 2), uncertain significance (class 3), likely pathogenic (class 4) and pathogenic (class 5).[17] Patients were grouped based on the variant classification, segregation analysis and associated phenotype known from literature. Three groups were distinguished: (1) patients with causative variants, that is, (likely) pathogenic variant(s) matching the phenotype and segregating with the HI in the family; (2) patients with variants of uncertain significance, that is, variants that could not be further classified by segregation analysis or not matching the phenotype; and (3) patients without detected causative variants. All detected variants were submitted to the Leiden Open Variant Database (LOVD, http://databases.lovd.nl/shared/genes, patient IDs 79876, 79998, 80001-80064, 80136, and 80138-80147).

Validation of selected variants

All reported sequence variants have been validated by Sanger sequencing (primer sequences and PCR conditions are available upon request). Copy number variants (CNVs) were validated by MLPA (*STRC*, homemade MLPA kit s139; *USH2A*, MRC-Holland kits P361A1 and P362A2) or deletion-specific PCR (*OTOA*, kindly provided by Guney Bademci, MD).

Results

The exomes of 200 individuals with presumed hereditary HI, mostly of Dutch origin, were sequenced in this study. Subsequently, targeted analysis of WES data was performed for a panel of 120 genes (DGD20062014) associated with HI. A median coverage of at least 20x

was reached for 72.0% and 97.8% of the targeted genes with the SOLiD system (n=44), for the Agilent 50 Mb and V4 enrichment kits, respectively (Supplemental Figure S1a and b, Supplemental Table S1). The median coverage was 97.5% with the HiSeq system (n=156; Supplemental Figure S1c). The percentage of identified causative variants did not increase with improvement of the technological WES conditions. In 31.8% (n=14) of the samples performed with the SOLiD system causative variants were identified, compared to 34.0% (n=53) of the samples performed with the Illumina HiSeq2000TM (Supplemental Table S3).

Diagnostic yield with WES in HI patients

We identified causative variants in 33.5% (67 cases) out of 200 cases with presumed hereditary HI (Table 1, Supplemental Tables S2 and S3). In 44 of these patients, homozygous or compound heterozygous variants in genes associated with autosomal recessive HI (arHI) were detected, being large homozygous deletions of several exons or complete genes in eight of these cases. No causative heterozygous CNVs were identified. *GJB2* was found to be the most frequently mutated gene (13.4% of positive cases), followed by *USH2A, MYO15A* and *STRC*, together accounting for 34.3% of the positive cases (Figure 1a).

In the remaining 23 cases heterozygous causative variants in 11 different genes associated with autosomal dominant HI (adHI) were found (Supplemental Table S2, Figure 1b). In four cases, the heterozygous variants were *de novo*. Causative variants in *MYO6* were the leading cause in this cohort of presumed adHI cases (Figure 1b).

The diagnostic yield was related to the type of inheritance and the age of onset of HI in the patients. For patients with suspected arHI, the diagnostic yield was 58.1%, of which 16.7% (n=3) caused by variants in *GJB2* (Table 1, Supplemental Table S3). In 30.4% of the cases without a (known) family history of HI (isolated cases), the molecular etiology could be identified, the majority harboring causative variants in genes associated with arHI. In 19.4% (n=6) of these cases causative variants in *GJB2* were found (Table 1, Supplemental Table S3). For adHI, causative variants were found in 27.3% of the cases (Table 1, Supplemental Table S3). Causative variant(s) could be identified in 49.4% and 36.7% of the subjects with congenital and 1st decade onset HI, respectively (Supplemental Table S3, Supplemental Figure S2). This percentage strongly declines with the increase in age of onset.

We identified variants of uncertain significance in 10 cases (5.0%) (Supplemental Tables S3 and S4). In eight of these, segregation analysis of the variant(s) could not be performed, because DNA of family members was unavailable. Segregation analysis is essential in order to classify these variants as causative or non-causative. In the remaining two cases segregation analysis was performed, but the variants could neither be classified as the cause of the HI, nor could they be discarded as not disease causing. In one case (AD19), the reported phenotype (unilateral HI) is different from the type of HI known to
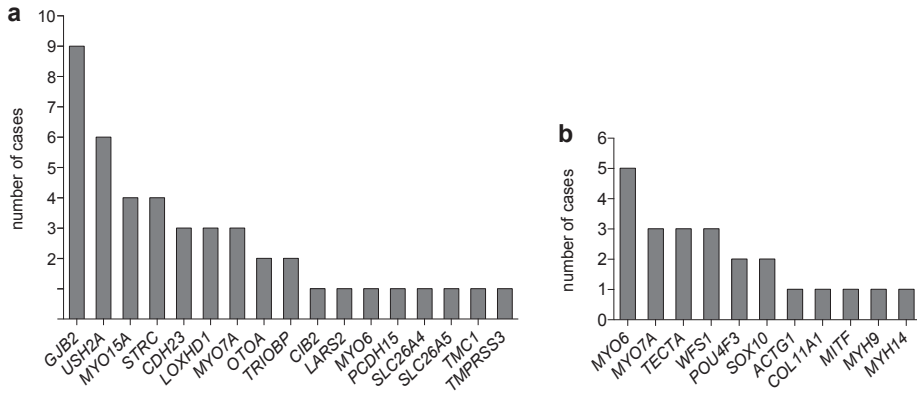
Figure 1 Overview of HI genes and number of cases in which causative variant(s) were identified in these genes. **(a)** Cases with autosomal recessive HI. **(b)** Cases with autosomal dominant HI.

Table 1 List of patients with causative variants in HI-related genes

Patient	Gene, RefSeq transcript ID	Variant 1 nucleotide change (protein change)	Variant 2 nucleotide change (protein change)	Zygosity[a]	Segre-gating with HI[b]
AD1[c]	*MYO6* NM_004999.3	c.1546+1G>T (p.?)	-	het	yes
AD2	*WFS1* NM_006005.3	c.2051C>T (p.Ala684Val)[c]	-	het	ND
AD3	*TECTA* ENST00000392793.1	c.6002G>T (p.Cys2001Phe)	-	het	*de novo*
AD4	*MYO7A* NM_000260.3	c.1373A>T (p.Asn458Ile)[c]	-	het	yes
AD5[c]	*MYO6* NM_004999.3	c.1211del (p.Gly404Glufs*4)	-	het	yes
AD6[c]	*MYH9* NM_002473.5	c.2507C>T (p.Pro836Leu)	-	het	yes
AD7	*POU4F3* NM_002700.2	c.828_829insT (p.Lys277*)	-	het	ND
AD8	*MYO7A* NM_000260.3	c.652G>A (p.Asp218Asn)	-	het	yes
AD9	*POU4F3* NM_002700.2	c.668T>C (p.Leu223Pro)[c]	-	het	ND
AD10	*MYO6* NM_004999.3	c.3395del (p.Lys1132Serfs*12)	-	het	yes
AD11	*SOX10* NM_006941.3	c.1195C>T (p.Gln399*)	-	het	ND
AD12	*MITF* NM_000248.3	c.649del (p.Arg217Aspfs*4)[c]	-	het	yes
AD13	*MYO7A* NM_000260.3	c.2617C>T (p.Arg873Trp)[c]	-	het	yes
AD14	*TECTA* ENST00000392793.1	c.5794A>C (p.Thr1932Pro)	-	het	yes
AD15	*MYH14* NM_001145809.1	c.5176C>T (p.Arg1726Trp)	-	het	yes
AD16	*WFS1* NM_006005.3	c.2032T>C (p.Trp678Arg)	-	het	yes

Table 1 (continued)

Patient	Gene, RefSeq transcript ID	Variant 1 nucleotide change (protein change)	Variant 2 nucleotide change (protein change)	Zygosity[a]	Segregating with HI[b]
AD17	*MYO6* NM_004999.3	c.584C>A (p.Ala195Glu)	-	het	yes
AD18	*TECTA* ENST00000392793.1	c.5597C>T (p.Thr1866Met)[c]	-	het	yes
AR1[c]	*USH2A* NM_206933.2	c.(9371+1_9372-1)_(9570+1_9571-1)del (p.?)	c.(9371+1_9372-1)_(9570+1_9571-1)del (p.?)	hom	ND
AR2	*OTOA* ENST00000388958	c.(?_-1)_(*1_?)del[c]	c.(?_-1)_(*1_?)del[c]	hom	ND
AR3[c]	*CIB2* NM_006383.3	c.97C>T (p.Arg33*)	c.196C>T (p.Arg66Trp)	compound het	yes
AR4	*STRC* NM_153700.2	c.(?_-1)_(*1_?)del[c]	c.(?_-1)_(*1_?)del[c]	hom	yes
AR5	*USH2A* NM_206933.2	c.(8845+1_8846-1)_(9371+1_9372-1)del (p.?)	c.(8845+1_8846-1)_(9371+1_9372-1)del (p.?)	hom	yes
AR6	*TMC1* NM_138691.2	c.646del (p.Leu216Serfs*54)	c.790C>T (p.Arg264*)	ND	ND
AR7	*CDH23* NM_022124.5	c.6442G>A (p.Asp2148Asn)[c]	c.1545_1547del (p.Ile515del)[c]	compound het	ND
AR8	*USH2A* NM_206933.2	c.1606T>C (p.Cys536Arg)[c]	c.9815C>T (p.Pro3272Leu)[c]	compound het	yes
AR9	*GJB2* NM_004004.5	c.35del (p.Gly12Valfs*2)[c]	c.71G>A (p.Trp24*)[c]	ND	ND
AR10	*GJB2* NM_004004.5	c.35del (p.Gly12Valfs*2)[c]	c.35del (p.Gly12Valfs*2)[c]	hom	ND
AR11	*CDH23* NM_022124.5	c.2096A>G (p.Asp699Gly)	c.4562A>G (p.Asn1521Ser)	compound het	yes
AR12	*GJB2* NM_004004.5	c.-23+1G>A (p.?)[c]	c.35del (p.Gly12Valfs*2)[c] c.5227C>T (p.Arg1743Trp)[c]	compound het	ND
AR13	*MYO7A* NM_000260.3	c.3289C>T (p.Gln1097*)	c.3862G>C (p.Ala1288Pro)[c]	compound het	ND
AR14	*STRC* NM_153700.2	c.(?_-1)_(*1_?)del[c]	c.(?_-1)_(*1_?)del[c]	hom	ND
AR15	*PCDH15* NM_033056.3	c.3374-2A>G (p.?)	c.4127C>A (p.Ala1376Asp)	compound het	yes
AR16	*STRC* NM_153700.2	c.(?_-1)_(*1_?)del[c]	c.(?_-1)_(*1_?)del[c]	hom	ND
AR17	*LOXHD1* NM_144612.6	c.1618dup (p.Thr540Asnfs*24)	c.1730T>G (p.Leu577Arg)	compound het	yes
AR18	*USH2A* NM_206933.2	c.5018T>C (p.Leu1673Pro) c.7871C>T (p.Pro2624Leu)	c.2299del (p.Glu767Serfs*21)	compound het	ND
ISO1[c]	*MYO15A* NM_016239.3	c.625G>T (p.Glu209*)	c.1137del (p.Tyr380Metfs*64)[c]	ND	ND
ISO2[c]	*USH2A* NM_206933.2	c.5385T>A (p.Tyr1795*)	c.6846_6849dup (p.His2284Asnfs*48)	ND	ND

Table 1 (continued)

Patient	Gene, RefSeq transcript ID	Variant 1 nucleotide change (protein change)	Variant 2 nucleotide change (protein change)	Zygosity[a]	Segregating with HI[b]
ISO3	*CDH23* NM_022124.5	c.8480_8481del (p.Leu2827Hisfs*23)	c.8480_8481del (p.Leu2827Hisfs*23)	hom	ND
ISO4[c]	*MYO15A* NM_016239.3	c.6764+2T>A (p.?)	c.3844C>T (p.Arg1282Trp) c.5287C>T (p.Arg1763Trp)	ND	ND
ISO5	*GJB2* NM_004004.5	c.101T>C (p.Met34Thr)[17]	c.109G>A (p.Val37Ile)[17]	compound het	ND
ISO6	*WFS1* NM_006005.3	c.2051C>T (p.Ala684Val)[2]	-	het	ND
ISO7	*MYO15A* NM_016239.3	c.6787G>A (p.Gly2263Ser)	c.7893+1G>A (p.?)	compound het	ND
ISO8	*TRIOBP* NM_001039141.2	c.2653del (p.Arg885Alafs*120)	c.5014G>T (p.Gly1672*)	compound het	ND
ISO9	*USH2A* NM_206933.2	c.2299del (p.Glu767Serfs*21)	c.920_923dup (p.His308Glnfs*16)	compound het	ND
ISO10	*MYO7A* NM_000260.3	c.3476G>T (p.Gly1159Val)[c]	c.5560G>A (p.Val1854Met)[c]	compound het	ND
ISO11	*GJB2* NM_004004.5	c.250G>C(p.Val84Leu)	c.269T>C (p.Leu90Pro)[c]	ND	ND
ISO12	*GJB2* NM_004004.5	c.109G>A (p.Val37Ile)[c]	c.109G>A (p.Val37Ile)[c]	hom	ND
ISO13	*TMPRSS3* NM_024022.2	c.916G>A (p.Ala306Thr)[c]	c.1276G>A (p.Ala426Thr)[c]	ND	ND
ISO14	*STRC* NM_153700.2	c.(?_-1)_(*1_?)del[c]	c.(?_-1)_(*1_?)del[c]	hom	ND
ISO15	*GJB2* NM_004004.5	c.35del (p.Gly12Valfs*2)[c]	c.101T>C (p.Met34Thr)[c]	compound het	ND
ISO16	*ACTG1* NM_001199954.1	c.773C>T (p.Pro258Leu)	-	het	*de novo*
ISO17	*GJB2* NM_004004.5	c.35del (p.Gly12Valfs*2)[c]	c.508_511dup (p.Ala171Glufs*40)[c]	compound het	ND
ISO18	*MYO15A* NM_016239.3	c.3311dup (p.Glu1105*)	c.3311dup (p.Glu1105*)	hom	ND
ISO19	*TRIOBP* NM_001039141.2	c.3460_3461del (p.Leu1154Alafs*29)	c.3232dup (p.Arg1078Profs*6)[c]	compound het	ND
ISO20	*MYO7A* NM_000260.3	c.5618G>A (p.Arg1873Gln)[c]	c.6028G>A (p.Asp2010Asn)[c]	compound het	ND
ISO21	*MYO6* NM_004999.3	c.3610C>T (p.Arg1204Trp)[c]	-	het	*de novo*
ISO22	*SLC26A5* NM_198999.2	c.355C>T (p.Pro119Ser)	c.355C>T (p.Pro119Ser)	hom	ND
ISO23	*GJB2* NM_004004.5	c.101T>C (p.Met34Thr)c	c.109G>A (p.Val37Ile)c	compound het	ND
ISO24	*SOX10* NM_006941.3	c.482G>A (p.Arg161His)c	-	het	de novo
ISO25	*MYO6* NM_004999.3	c.3335A>G (p.Tyr1112Cys)	c.1897del (p.Gln633Lysfs*19)	compound het	ND
ISO26	*LARS2* NM_015340.3	c.683G>A (p.Arg228His)	c.880G>A (p.Glu294Lys)	compound het	ND

Table 1 (continued)

Patient	Gene, RefSeq transcript ID	Variant 1 nucleotide change (protein change)	Variant 2 nucleotide change (protein change)	Zygosity[a]	Segregating with HI[b]
ISO27	*OTOA* ENST00000388958	c.(?_-1)_(*1_?)del[c]	c.(?_-1)_(*1_?)del[c]	hom	ND
ISO28[c]	*COL11A1* NM_001854.3	c.1630-2del (p.?)	-	het	ND
ISO29	*LOXHD1* NM_144612.6	c.3061+1G>A (p.?)	c.6353G>A (p.Gly2118Glu)	ND	ND
ISO30	*LOXHD1* NM_144612.6	c.3061C>T (p.Arg1021*)	c.5885C>T (p.Thr1962Met)	compound het	ND
ISO31	*SLC26A4* NM_000441.1	c.505del (p.Thr169Leufs*3)	c.1334T>G (p.Leu445Trp)[c]	compound het	ND

AD, autosomal dominant; AR, autosomal recessive; HI, hearing impairment; het, heterozygous; hom, homozygous; ISO, isolated; ND, not determined or not conclusive. [a]Zygosity, determined on basis of segregation analysis in the parents. [b]Segregating with HI, determined on basis of segregation analysis in affected and/or unaffected family members. [c]Mutations that have been described in literature before, the corresponding references are provided in Supplemental Table S2.

be associated with mutations in the gene (*MYO7A*). In another patient (AR19), two class 3 variants in *USH2A* were found. The patient was 14 years old and had no signs of retinitis pigmentosa. The significance of the (previously unreported) *USH2A* missense variants in this patient is unclear and they cannot be definitely classified as causative for the HI in this patient, although they are located in *trans* and co-segregate with the HI.

In our study, 61.5% of the 200 exomes (123 cases) did not reveal causative or putative causative variants. In the majority of them (95 cases), no putative causative variants remained after the data-filtering procedure. In 24 cases, the variants were not segregating with the HI in the family. In three cases, only a single variant was identified in a gene known to underlie arHI. In two of these patients (ISO41 and ISO45), the genes were analyzed with Sanger sequencing and/or MLPA, which did not reveal a second variant. In the third patient (AD65) a heterozygous variant c.1322C>T (p.Ser441Leu) was found in *SLC26A5*. As the patient had autosomal dominant, profound, asymmetric HI with an onset in the sixth decade, the phenotype was not compatible with DFNB61. Therefore, the *SLC26A5* gene was not further analyzed. Finally, in one case (ISO87), a class 3 variant was identified in *NLRP3*, a gene known to underlie autosomal dominant cryporin-associated periodic syndromes, for example, Muckle-Wells syndrome.[18] Further clinical evaluation in the patient revealed, however, no evidence for this syndrome and the variant was therefore considered not to be the cause of the HI.

Prescreening of single genes
In 137 patients (68.5%), one or more HI-related genes had been prescreened with Sanger

sequencing prior to WES (Tables 2a and b). On average, 1.5 genes were pretested per individual. The numbers of individuals with pretests and the number of pretested genes were comparable between the groups of inheritance and between the groups of patients with causative variants, variants of uncertain significance and without detected causative variants. *GJB2* was most frequently tested (80 times), followed by *TECTA* (36 times). Although prescreening in these 137 patients was negative and therefore WES was performed, it is known that patients with a specific phenotype associated with mutations in one or a few genes (eg, Pendred syndrome) are quite often solved by targeted testing.[19]

To evaluate the utility of prescreening in individuals with HI, we made an overview of all in-house gene analysis requests for HI in 2013-2014 and the diagnostic yield (Supplemental Table S5). The vast majority of these tests were performed in patients of Dutch origin. The three genes with the highest diagnostic yield were *COCH* (36.8%), *KCNQ4* (15.4%) and *GJB2* (7.2%). For these three genes, founder or hotspot mutations occur in the Dutch population explaining the high incidence of mutations found in DNA diagnostics.[20-22] The diagnostic yield for *COL11A1, DFNA5, EYA1, MYO7A, NDP, OTOF, SLC26A4* and *USH2A* was higher than 10%, but the number of requests was less than 10 times. Therefore, the diagnostic yield for these genes is not reliable.

Table 2a Single gene tests prior to WES per category

Categories	Subcategories	No. of individuals with single gene test(s) (%)	No. of single gene tests (per individual)	No. of individuals with GJB2/GJB6 test (%)
WES result	Causative variant(s)	45 (67.2%)	101 (1.5)	32 (47.8%)
	Variant(s) of uncertain significance	8 (80.0%)	17 (1.7)	4 (36.4%)
	No detected causative variant(s)	84 (68.3%)	188 (1.5)	44 (35.8%)
Inheritance	adHI	45 (68.2%)	106 (1.6)	11 (16.7%)
	arHI	24 (77.4%)	43 (1.4)	17 (54.8%)
	Isolated HI	67 (55.8%)	154 (1.5)	51 (50.0%)
	X-linked HI	1 (100.0%)	3 (3.0)	1 (100.0%)

Discussion

In this study, we aimed to evaluate the diagnostic yield of WES-based targeted analysis of genes involved in HI. WES technology allowed the efficient identification of single-nucleotide variants, small insertions or deletions (indels) and large deletions that affect the protein coding regions of HI genes in a single experiment.[11] Our study underlines the great

Table 2b Single gene tests prior to WES per gene

Gene	No. of requests	Gene (continued)!	No. of requests (continued)
Total	306	COLL11A2	2
GJB2/GJB6	80	POUF4F3	2
TECTA	36	PTPRQ	2
KCNQ4	18	TMC1	2
COCH	16	CDH23	1
COL11A2	15	DFNB59	1
SLC26A4	15	EYA	1
TMPRSS3	14	EYA1	1
MYO6	10	FMR1	1
POU4F3	10	KCNE1	1
ACTG1	9	KCNQ	1
WFS1	8	KCNQ1	1
Asper array	6	POLR1C	1
EYA4	6	POLR1D	1
USH2A	6	POU3F4	1
MITF	5	RP-R	1
MYO7A	5	SIX1	1
DFNA5	4	SIX5	1
MYO15A	4	SMPX	1
PAX3	4	SNAI2	1
DIAPH1	3	SOS1	1
OTOF	3	TCOF1	1
Array	2	TIMM8A	1

adHI, autosomal dominant hearing impairment; arHI, autosomal recessive hearing impairment.

genetic heterogeneity of HI, as causative variants were found in 26 different genes (Table 1, Figure 1).

In 61.5% of the cases, no causative variants were identified in the targeted HI-related genes. A part of these cases might be explained by variants that are not identified due to insufficient enrichment or coverage.[23] Although coverage has greatly improved over time (Supplemental Figure S1, Supplemental Table S1), the identification rate of causative variants has remained stable (Supplemental Table S3). This implies that part of the causative variants in known HI genes cannot be identified by WES, for example deep intronic variants affecting splicing, variants in non-coding exons, repeat regions and regulatory regions.

Another part of the cases without detected causative variants may be explained by mutations in yet undiscovered genes. There are tens of HI-related loci known, of which the causative gene is still not identified (http://www.hereditaryhearingloss.org/). As *de novo* variants in known adNSHI genes were identified in four of the cases in our study, we hypothesize that novel genes for adNSHI can be identified by a *de novo* strategy (ie, sequencing affected individuals and their unaffected parents).[24] For the isolated cases, comprising about half of the subjects in this study, involvement of non-genetic causes cannot be fully excluded. Also, in subjects with late-onset HI non-genetic causes or a combination of (multiple) genetic and non-genetic factors cannot be discarded, despite the thorough patient evaluation. This could well explain why no variants were identified in the 16 subjects with an age of onset in the fifth or sixth decade (Supplemental Table S3, Supplemental Figure S2).

Variants of uncertain significance were mainly reported for patients without a family history of HI (isolated cases) or presumed adHI (Supplemental Tables S3 and S4). As in most of these cases no family members were available for segregation analysis, the causality of these variants remained unclear. This highlights the importance of taking an accurate family history and collecting clinical data and DNA samples of family members. In addition, it is essential to provide a thorough description of the phenotype of the patient in order to evaluate whether the gene with the identified variant has previously been associated with this specific phenotype.

A subset of patients (36 cases) in the present study was previously reported by Neveling *et al*.[11] In 16 out of these 36 cases likely causative variants were identified, leading to a diagnostic yield of 44.4% for WES in HI.[11] However, in nine of these families segregation analysis was still needed to confirm the genetic diagnosis. This analysis was performed in the current study and in seven families the variants did not segregate with the HI. This lowers the diagnostic yield of the cases included in the study by Neveling *et al.* to 22%, which is comparable to the yield in our study and again underlines the importance of segregation analysis.

The wide use of WES in routine diagnostics and research is producing large amounts of data on sequence variants in HI. Variants that have initially been reported as causative, based on the knowledge at that time, might be reclassified as benign due to increasing availability of allele frequency data.[25] This highlights the importance of population-based allele frequency data to evaluate the causality of variants. However, rare variants can still be difficult to classify. We identified novel missense variants in *USH2A* (AR19) and classified these as variants of uncertain significance, despite the fact that (1) they are predicted to be damaging, (2) they were not reported in any public database so far and (3) they segregated with the hearing impairment in the corresponding family. The patient did

not show symptoms of retinitis pigmentosa at the age of 14 years, but visual symptoms in Usher syndrome type 2 normally start in the second decade of life.[26] Without support from functional studies, the pathogenicity of these missense variants will remain uncertain, since Petrovski *et al.*[27] calculated a residual variation score of 4.18 for *USH2A* (75th percentile of scored genes, frequency data based on NHLBI Exome Sequencing Project) suggestive of a great tolerance of this gene to genetic variation. This is casting some doubt on the extensive variation in *USH2A* reported as likely pathogenic in public databases such as the LOVD. Importantly, these uncertainties are extremely difficult for genetic counseling, as parents have to be informed about the possible development of Usher syndrome in their children.

CNV detection in our cohort could identify large homozygous deletions in 4% of the cases, which is comparable to the 1.5-7.3% presented in the literature.[28-34] A relatively high frequency of *STRC* deletions was found in our Dutch population (2%), as has also been reported in other populations.[8,9] In one case (ISO31), we found causative variants in a gene that is associated with an identifiable phenotype and segregating with a recessive inheritance pattern. This patient had an incomplete partition of the cochlea and mutations in *SLC26A4.*[35] We did not find other cases with an identifiable phenotype such as progressive HI with a downsloping audiogram caused by *TMPRSS3* mutations,[7,36] and the stable HI with a cookie-bite audiogram configuration caused by mutations in *TECTA.*[7] This is most likely due to the fact that these genes are generally pretested in patients with these identifiable phenotypes.

In our cohort, the diagnostic yield of WES targeting a panel of HI-related genes is 33.5%. Other studies using massively parallel sequencing have reported similar overall diagnostic rates, despite of using different technologies and testing different populations.[32-34,37,38] We found that causative variants in *GJB2*, *USH2A*, *MYO6, STRC* and *MYO15A* underlie HI in 14.0% of the cases in our cohort. This is in agreement with previously published studies on the involvement of HI genes in other populations.[6-9,32-34,36,38-40] The diagnostic yield of WES targeting a panel of HI-related genes is generally higher than that of single gene testing. Therefore, we recommend to reduce prescreening of single genes to a minimum. As the utility and yield of prescreening of single genes prior to WES is population specific, our recommendations apply in particular for the Dutch population. We suggest that for nonsyndromic congenital or 1st decade onset HI it would be cost-effective to prescreen *GJB2*, because of its relatively frequent association with HI. For recognizable phenotypes (such as Pendred syndrome, Waardenburg syndrome and Usher syndrome) or for genes with a relatively common founder mutation in a specific population (such as mutations in *COCH* in the Dutch and Belgian population)[20] prescreening of specific genes might still be useful. This is supported by the relatively high diagnostic yield of targeted sequencing of

GJB2 (7.2%) and *COCH* (36.8%). In all other cases, we recommend to perform WES targeting a panel of HI-related genes as a first diagnostic test.

2

Acknowledgements

References

1. Shearer AE, DeLuca AP, Hildebrand MS, et al. Comprehensive genetic testing for hereditary hearing loss using massively parallel sequencing. *Proceedings of the National Academy of Sciences of the United States of America.* Dec 7 2010;107(49):21104-21109.

2. Morton CC, Nance WE. Newborn hearing screening--a silent revolution. *The New England journal of medicine.* May 18 2006;354(20):2151-2164.

3. Seco CZ, Oonk AM, Dominguez-Ruiz M, et al. Progressive hearing loss and vestibular dysfunction caused by a homozygous nonsense mutation in CLIC5. *European journal of human genetics : EJHG.* Feb 2015;23(2):189-194.

4. Schraders M, Ruiz-Palmero L, Kalay E, et al. Mutations of the gene encoding otogelin are a cause of autosomal-recessive nonsyndromic moderate hearing impairment. *American journal of human genetics.* Nov 2 2012;91(5):883-889.

5. Yariz KO, Duman D, Seco CZ, et al. Mutations in OTOGL, encoding the inner ear protein otogelin-like, cause moderate sensorineural hearing loss. *American journal of human genetics.* Nov 2 2012;91(5):872-882.

6. Miyagawa M, Nishio SY, Hattori M, et al. Mutations in the MYO15A Gene Are a Significant Cause of Nonsyndromic Hearing Loss: Massively Parallel DNA Sequencing-Based Analysis. *The Annals of otology, rhinology, and laryngology.* Mar 19 2015.

7. Hoefsloot LH, Feenstra I, Kunst HP, Kremer H. Genotype phenotype correlations for hearing impairment: approaches to management. *Clinical genetics.* Jun 2014;85(6):514-523.

8. Francey LJ, Conlin LK, Kadesch HE, et al. Genome-wide SNP genotyping identifies the Stereocilin (STRC) gene as a major contributor to pediatric bilateral sensorineural hearing impairment. *American journal of medical genetics. Part A.* Feb 2012;158A(2):298-308.

9. Vona B, Hofrichter MA, Neuner C, et al. DFNB16 is a frequent cause of congenital hearing impairment: implementation of STRC mutation analysis in routine diagnostics. *Clinical genetics.* Jan 2015;87(1):49-55.

10. Gilissen C, Hoischen A, Brunner HG, Veltman JA. Disease gene identification strategies for exome sequencing. *European journal of human genetics : EJHG.* May 2012;20(5):490-497.

11. Neveling K, Feenstra I, Gilissen C, et al. A post-hoc comparison of the utility of sanger sequencing and exome sequencing for the diagnosis of heterogeneous diseases. *Human mutation.* Dec 2013;34(12):1721-1726.

12. Mazzoli M, Van Camp G, Newton V, Giarbini N, Declau F, Parving A. Recommendations for the description of genetic and audiological data for families with nonsyndromic hereditary hearing impairment. *Audiological Medicine.* 2003;1:148-150.

13. Seco CZ, Giese AP, Shafique S, et al. Novel and recurrent CIB2 variants, associated with nonsyndromic deafness, do not affect calcium buffering and localization in hair cells. *European journal of human genetics : EJHG.* Jul 15 2015.

14. Van der Auwera GA, Carneiro MO, Hartl C, et al. From FastQ data to high confidence variant calls: the Genome Analysis Toolkit best practices pipeline. *Current protocols in bioinformatics / editoral board, Andreas D. Baxevanis ... [et al.].* Oct 15 2013;11(1110):11 10 11-11 10 33.

15. Krumm N, Sudmant PH, Ko A, et al. Copy number variation detection and genotyping from exome sequence data. *Genome research.* Aug 2012;22(8):1525-1532.

16. Pfundt R, del Rosario M, Vissers LELM, et al. Detection of clinically relevant copy number variants by exome sequencing in a large cohort of genetic disorders. *Genetics in Medicine.* 2016.

17. Richards S, Aziz N, Bale S, et al. Standards and guidelines for the interpretation of sequence variants: a joint consensus recommendation of the American College of Medical Genetics and Genomics and the Association for Molecular Pathology. *Genetics in medicine : official journal of the*

American College of Medical Genetics. May 2015;17(5):405-424.

18. Sarrabay G, Grandemange S, Touitou I. Diagnosis of cryopyrin-associated periodic syndrome: challenges, recommendations and emerging concepts. *Expert review of clinical immunology.* 2015;11(7):827-835.

19. Dai P, Stewart AK, Chebib F, et al. Distinct and novel SLC26A4/Pendrin mutations in Chinese and U.S. patients with nonsyndromic hearing loss. *Physiological genomics.* Aug 7 2009;38(3):281-290.

20. Fransen E, Verstreken M, Bom SJ, et al. A common ancestor for COCH related cochleovestibular (DFNA9) patients in Belgium and The Netherlands bearing the P51S mutation. *Journal of medical genetics.* Jan 2001;38(1):61-65.

21. Gasparini P, Rabionet R, Barbujani G, et al. High carrier frequency of the 35delG deafness mutation in European populations. Genetic Analysis Consortium of GJB2 35delG. *European journal of human genetics : EJHG.* Jan 2000;8(1):19-23.

22. Topsakal V, Pennings RJ, te Brinke H, et al. Phenotype determination guides swift genotyping of a DFNA2/KCNQ4 family with a hot spot mutation (W276S). *Otology & neurotology : official publication of the American Otological Society, American Neurotology Society [and] European Academy of Otology and Neurotology.* Jan 2005;26(1):52-58.

23. Lelieveld SH, Spielmann M, Mundlos S, Veltman JA, Gilissen C. Comparison of Exome and Genome Sequencing Technologies for the Complete Capture of Protein-Coding Regions. *Human mutation.* Aug 2015;36(8):815-822.

24. Vissers LE, de Ligt J, Gilissen C, et al. A de novo paradigm for mental retardation. *Nature genetics.* Dec 2010;42(12):1109-1112.

25. Shearer AE, Eppsteiner RW, Booth KT, et al. Utilizing ethnic-specific differences in minor allele frequency to recategorize reported pathogenic deafness variants. *American journal of human genetics.* Oct 2 2014;95(4):445-453.

26. Smith RJ, Berlin CI, Hejtmancik JF, et al. Clinical diagnosis of the Usher syndromes. Usher Syndrome Consortium. *American journal of medical genetics.* Mar 1 1994;50(1):32-38.

27. Petrovski S, Wang Q, Heinzen EL, Allen AS, Goldstein DB. Genic intolerance to functional variation and the interpretation of personal genomes. *PLoS genetics.* 2013;9(8):e1003709.

28. Tsai EA, Berman MA, Conlin LK, et al. PECONPI: a novel software for uncovering pathogenic copy number variations in non-syndromic sensorineural hearing loss and other genetically heterogeneous disorders. *American journal of medical genetics. Part A.* Sep 2013;161A(9):2134-2147.

29. Bademci G, Diaz-Horta O, Guo S, et al. Identification of copy number variants through whole-exome sequencing in autosomal recessive nonsyndromic hearing loss. *Genetic testing and molecular biomarkers.* Sep 2014;18(9):658-661.

30. Shearer AE, Kolbe DL, Azaiez H, et al. Copy number variants are a common cause of non-syndromic hearing loss. *Genome medicine.* 2014;6(5):37.

31. Ji H, Lu J, Wang J, Li H, Lin X. Combined examination of sequence and copy number variations in human deafness genes improves diagnosis for cases of genetic deafness. *BMC ear, nose, and throat disorders.* 2014;14:9.

32. Sommen M, Schrauwen I, Vandeweyer G, et al. DNA Diagnostics of Hereditary Hearing Loss: A Targeted Resequencing Approach Combined with a Mutation Classification System. *Human mutation.* Aug 2016;37(8):812-819.

33. Yan D, Tekin D, Bademci G, et al. Spectrum of DNA variants for non-syndromic deafness in a large cohort from multiple continents. *Human genetics.* Aug 2016;135(8):953-961.

34. Sloan-Heggen CM, Bierer AO, Shearer AE, et al. Comprehensive genetic testing in the clinical evaluation of 1119 patients with hearing loss. *Human genetics.* Apr 2016;135(4):441-450.

35. Phelps PD, Coffey RA, Trembath RC, et al. Radiological malformations of the ear in Pendred syndrome. *Clinical radiology.* Apr 1998;53(4):268-273.

36.   Bademci G, Foster J, 2nd, Mahdieh N, et al. Comprehensive analysis via exome sequencing uncovers genetic etiology in autosomal recessive nonsyndromic deafness in a large multiethnic cohort. *Genetics in medicine : official journal of the American College of Medical Genetics.* Jul 30 2015.

37.   Shearer AE, Smith RJ. Massively Parallel Sequencing for Genetic Diagnosis of Hearing Loss: The New Standard of Care. *Otolaryngology--head and neck surgery : official journal of American Academy of Otolaryngology-Head and Neck Surgery.* Aug 2015;153(2):175-182.

38.   Shearer AE, Black-Ziegelbein EA, Hildebrand MS, et al. Advancing genetic testing for deafness with genomic technology. *Journal of medical genetics.* Sep 2013;50(9):627-634.

39.   Atik T, Onay H, Aykut A, et al. Comprehensive Analysis of Deafness Genes in Families with Autosomal Recessive Nonsyndromic Hearing Loss. *PloS one.* 2015;10(11):e0142154.

40.   Sloan-Heggen CM, Babanejad M, Beheshtian M, et al. Characterising the spectrum of autosomal recessive hereditary hearing loss in Iran. *Journal of medical genetics.* 2015;52:823-829.

Supplemental Data

2
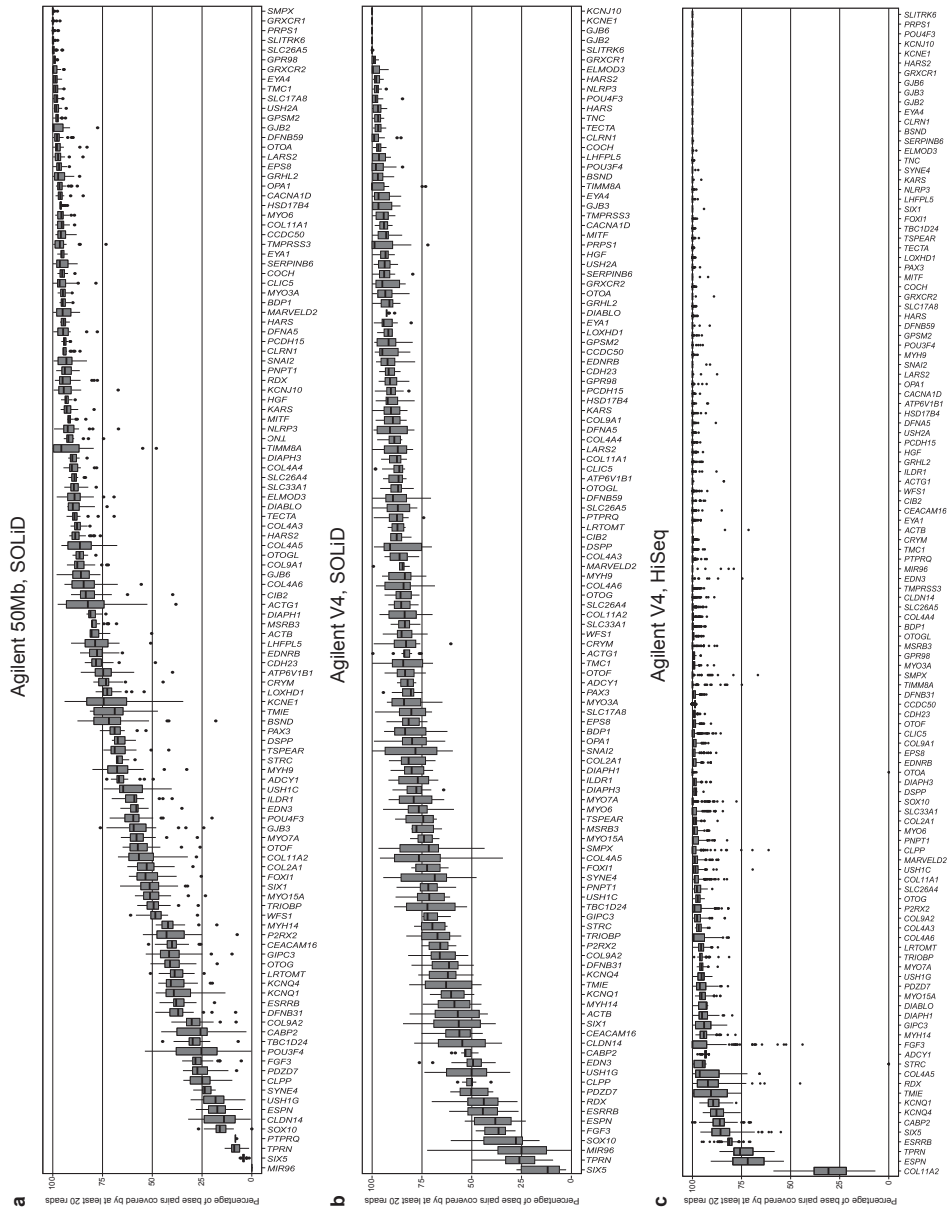
Figure S1 Percentage of ≥20x coverage per gene for each technological WES condition.
The boxplots show the percentage of base pairs covered by at least 20 reads per gene (DGD20062014, 120 genes) and technological WES condition. Outliers are depicted as dots, representing individual samples. **(a)** Coverage of samples (n=30) enriched with the Agilent 50Mb kit and sequenced on the 5000xl SOLiD system. **(b)** Coverage of samples (n=14) enriched with the Agilent V4 kit and sequenced on the 5000xl SOLiD system. **(c)** Coverage of samples (n=156) enriched with the Agilent V4 kit and sequenced on the HiSeq2000TM system.
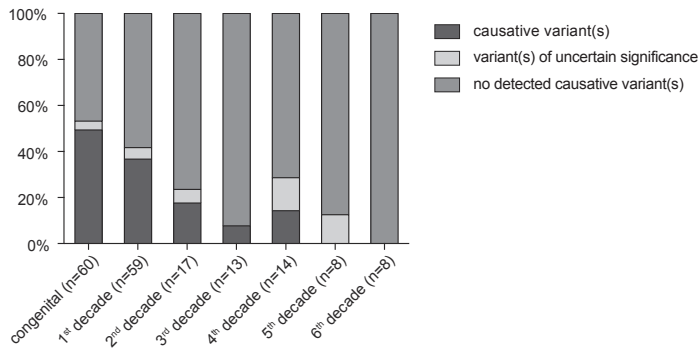
Figure S2 Diagnostic yield of WES targeting a panel of HI-related genes, based on age of onset of HI. One individual with late-onset HI was ommited from this analysis, because the exact age of onset was unknown.

2

Table S1 Details on gene lists DGD07092012 and DGD20062014, and coverage

Gene name	RefSeq transcript ID	HI panel DGD 07092012	HI panel DGD 20062014	Median % covered ≥20x Agilent 50Mb (n=30): 72.0	SOLiD Agilent V4 (n=14): 79.8	Median % covered ≥20x HiSeq Agilent V4 (n=156): 97.5	Untargeted exons, coding exons shown in bold
Total		98 genes	120 genes				
ACTB	NM_001101.3	x	x	80,5	57,0	100	Agilent 50Mb: 121 exons Agilent V4: 121 exons
ACTG1	NM_0011999954.1	x	x	82,4	83,8	100	Agilent 50Mb: 1 Agilent V4: 1
ADCY1	NM_021116.2		x	66,7	82,2	93,4	Agilent 50Mb: 1 Agilent V4: 1
ATP6V1B1	NM_001692.3	x	x	74,7	86,7	100	
BDP1	NM_018429.2		x	95,0	83,4	100	
BSND	NM_057176.2	x	x	71,8	97,1	100	
CABP2	NM_016366.2	x	x	25,8	53,1	86,1	
CACNA1D	NM_000720.3	x	x	96,2	94,0	100	
CC2D2A	NM_001080522.2	x		89,4	84,7		Agilent 50Mb: 1, 2, **30**
CCDC50	NM_178335.2	x	x	95,9	94,8	98,7	Agilent V4: **12**
CDH23	NM_022124.5	x	x	78,3	91,7	99,0	Agilent 50Mb: 1 Agilent V4: **63**
CEACAM16	NM_001039213.3		x	40,1	56,2	100	Agilent 50Mb: **7** Agilent V4: **7**
CIB2	NM_006383.3		x	83,4	87,6	100	Agilent 50Mb: 1, 2
CLDN14	NM_144492.2	x	x	14,0	54,7	100	Agilent V4: 1, 2
CLIC5	NM_0011114086.1		x	96,6	86,3	100	
CLPP	NM_006012 .2		x	24,9	49,9	100	
CLRN1	NM_0011195794.1	x	x	94,6	99,0	100	Agilent 50Mb: **3**
COCH	NM_0011135058.1	x	x	95,3	96,8	100	Agilent V4: **2**
COL11A1	NM_001854.3	x	x	95,5	87,5	98,9	Agilent V4: **28**
COL11A2	NM_080680.2	x	x	56,7	83,7	30,7	Agilent V4: **10, 22, 47, 50**
COL2A1	NM_001844.4		x	52,8	81,7	98,6	
COL4A3	NM_000091.4	x	x	87,8	86,2	96,8	
COL4A4	NM_000092.4	x	x	90,4	88,8	100	Agilent 50Mb: 1

Table S1 (continued)

Gene name	RefSeq transcript ID	HI panel DGD 07092012	HI panel DGD 20062014	Median % covered ≥20x SOLiD	Median % covered ≥20x HiSeq	Untargeted exons, coding exons shown in bold
COL4A5	NM_033380.2	×		86,4	76,5	96,3	Agilent V4: 1
COL4A6	NM_001287758.1		×	84,5	84,2	99,4	Agilent V4: **5, 44** Agilent 50Mb: **1, 10, 24** Agilent V4: **1, 10, 24**
COL9A1	NM_001851.4	×	×	87,7	89,6	99,6	Agilent v4: **28**
COL9A2	NM_001852.3		×	30,2	66,0	97,7	
CRYM	NM_001888.4	×	×	73,3	83,0	100	Agilent 50Mb: 1, 2 Agilent V4: 1, 2
DFNA5	NM_004403.2	×	×	94,8	91,0	100	Agilent 50Mb: 1 Agilent V4: 1
DFNB31	NM_015404.3	×	×	37,0	61,4	99,6	
DFNB59	NM_001042702.3	×	×	97,9	89,5	100	Agilent 50Mb: 1 Agilent V4: 1
DIABLO	NM_019887.5	×	×	89,9	92,7	92,8	Agilent 50Mb: 1 Agilent V4: 1
DIAPH1	NM_005219.4	×	×	81,1	80,1	95,1	Agilent 50Mb: **18** Agilent V4: **18**
DIAPH3	NM_001042517.1	×	×	90,2	77,8	99,2	
DSPP	NM_014208.3	×	×	67,3	91,0	98,5	Agilent 50Mb: 1 Agilent V4: 1
EDN3	NM_207034.2	×	×	58,0	49,3	100	
EDNRB	NM_001201397.1	×	×	77,8	92,2	99,7	
ELMOD3	NM_032213.4		×	89,1	99,6	100	Agilent 50Mb: 1 Agilent V4: 1
EPS8	NM_004447.5		×	96,8	81,6	99,8	Agilent 50Mb: 1 Agilent V4: 1
ESPN	NM_031475.2	×	×	17,3	38,2	71,8	
ESRRB	NM_004452.3	×	×	38,0	44,4	81,3	Agilent 50Mb: 1-3 Agilent V4: 1-3
EYA1	NM_000503.5	×	×	95,5	94,2	100	Agilent 50Mb: 1

2

Table S1 (continued)

Gene name	RefSeq transcript ID	HI panel DGD 07092012	HI panel DGD 20062014	Median % covered ≥20x SOLiD	Median % covered ≥20x HiSeq	Untargeted exons, coding exons shown in bold
EYA4	NM_001301013.1	×	×	98,7	100	Agilent V4: 1 Agilent 50Mb: 1 Agilent V4: 1
FAM189A2	NM_004816.3	×		84,4		Agilent 50Mb: 1
FGF3	NM_005247.2	×	×	28,3	100	
FOXI1	NM_012188.4	×	×	53,4	100	
GIPC3	NM_133261.2	×	×	41,6	94,1	
GJB2	NM_004004.5	×	×	99,6	100	Agilent 50Mb: 1 Agilent V4: 1
GJB3	NM_024009.2	×	×	59,4	100	Agilent 50Mb: 1 Agilent V4: 1
GJB6	NM_001110219.2	×	×	85,9	100	Agilent 50Mb: 1-4 Agilent V4: 1-4
GPR98	NM_032119.3	×	×	99,1	99,4	Agilent V4: 1
GPSM2	NM_013296.4	×	×	97,7	100	Agilent 50Mb: 1 Agilent V4: 1
GRHL2	NM_024915.3	×	×	97,3	100	
GRXCR1	NM_001080476.2	×	×	100,0	100	
GRXCR2	NM_001080516.1		×	99,7	100	
HARS	NM_002109.5		×	94,6	100	
HARS2	NM_012208.2		×	88,7	100	
HGF	NM_000601.4	×	×	93,4	100	
HSD17B4	NM_001199291.1		×	96,2	100	Agilent 50Mb: **6** Agilent V4: **6**
ILDR1	NM_001199799.1	×	×	59,0	100	Agilent V4: **8**
KARS	NM_001130089.1	×	×	93,0	100	
KCNE1	NM_000219.4	×	×	74,4	100	Agilent 50Mb: 1-3 Agilent V4: 1-3
KCNJ10	NM_002241.4	×	×	94,5	100	Agilent 50Mb: 1 Agilent V4: 1

Table S1 (continued)

Gene name	RefSeq transcript ID	HI panel DGD 07092012	HI panel DGD 20062014	Median % covered ≥20x SOLiD	Median % covered ≥20x	HiSeq	Untargeted exons, coding exons shown in bold
KCNQ1	NM_000218.2	×	×	39,2	60,3	89,5	
KCNQ4	NM_004700.3	×	×	40,7	62,0	87,8	
LARS2	NM_015340.3		×	97,3	87,1	100	Agilent 50Mb: 1, 2 Agilent V4: 1, 2
LHFPL5	NM_182548.3	×	×	78,7	96,5	100	Agilent 50Mb: 4 Agilent V4: 4
LOXHD1	NM_144612.6	×	×	72,6	91,8	100	
LRTOMT	NM_001145309.3	×	×	38,8	87,3	95,6	Agilent 50Mb: 1, 2 Agilent V4: 1, **5**
MARVELD2	NM_001038603.2	×	×	95,1	84,6	98,8	Agilent 50Mb: 1 Agilent V4: 1
MIR96	NR_029512.1	×	×	0,0	25,0	100	
MITF	NM_198159.2	×	×	91,9	92,9	100	
MSRB3	NM_198080.3	×	×	80,3	77,7	100	
MYH14	NM_001145809.1	×	×	42,1	58,7	94,2	Agilent 50Mb: 1 Agilent V4: 1
MYH9	NM_002473.5	×	×	67,7	83,6	100	Agilent 50Mb: 1 Agilent V4: 1
MYO15A	NM_016239.3	×	×	51,1	73,9	95,4	Agilent 50Mb: 1 Agilent V4: 1, 9, **25**
MYO1A	NM_001256041.1	×		96,7	94,8		Agilent 50Mb: 1, 2
MYO3A	NM_017433.4	×	×	94,9	84,0	99,5	Agilent 50Mb: 1, 2 Agilent V4: 1, 2
MYO6	NM_004999.3	×	×	95,7	76,6	99,2	Agilent 50Mb: 1 Agilent V4: 1
MYO7A	NM_000260.3	×	×	57,9	79,1	95,5	Agilent 50Mb: 1 Agilent V4: 1
NLRP3	NM_001079821.2	×	×	92,5	97,6	100	Agilent 50Mb: 1, **2** Agilent V4: 1, **2**
OPA1	NM_130837.2	×	×	96,7	79,9	100	Agilent 50Mb: 31

Table S1 (continued)

Gene name	RefSeq transcript ID	HI panel DGD 07092012	HI panel DGD 20062014	Median % covered ≥20x SOLiD	Median % covered ≥20x HiSeq	Untargeted exons, coding exons shown in bold
OTOA	NM_144672.3	x	x	97,9	100	Agilent V4: **1, 31**
OTOF	NM_194248.2	x	x	57,3	99,4	Agilent V4: **20, 22-28**
OTOG	NM_001277269.1		x	41,1	97,3	
OTOGL	NM_173591.3	x	x	86,6	99,8	Agilent 50Mb: **1, 2**
P2RX2	NM_170683.3		x	42,9	99,0	
PAX3	NM_181459.3	x	x	68,9	100	
PCDH15	NM_033056.3	x	x	94,2	100	Agilent 50Mb: 1; Agilent V4: 1
PDZD7	NM_001195263.1	x	x	27,3	96,2	Agilent 50Mb: 1; Agilent V4: 1
PNPT1	NM_033109.4		x	93,9	99,8	
POU3F4	NM_000307.4	x	x	25,3	100	
POU4F3	NM_002700.2	x	x	59,6	100	
PRPS1	NM_002764.3	x	x	100,0	100	Agilent V4: 1
PTPRQ	NM_001145026.1	x	x	8,3	100	Agilent 50Mb: **1-36, 41, 42**
RDX	NM_002906.3	x	x	95,1	92,1	Agilent 50Mb: 1; Agilent V4: 1
SERPINB6	NM_001271823.1	x	x	96,4	100	Agilent 50Mb: **1**; Agilent V4: **1**
SIX1	NM_005982.3	x	x	51,3	100	
SIX5	NM_175875.4	x	x	4,2	85,7	
SLC17A8	NM_139319.2	x	x	98,2	100	
SLC26A4	NM_000441.1	x	x	89,1	97,7	
SLC26A5	NM_198999.2	x	x	100,0	100	Agilent 50Mb: 1, 2; Agilent V4: 1, 2
SLC33A1	NM_004733.	x		89,4	100	
SLITRK6	NM_032229.2	x	x	100,0	100	Agilent 50Mb: 1; Agilent V4: 1

2

Table S1 (continued)

Gene name	RefSeq transcript ID	HI panel DGD 07092012	HI panel DGD 20062014	Median % covered ≥20x SOLiD	Median % covered ≥20x HiSeq	Untargeted exons, coding exons shown in bold
SMPX	NM_014332.2	x	x	100,0	71,5	100	Agilent 50Mb: 1, 5 / Agilent V4: 1, 5
SNAI2	NM_003068.4	x	x	93,2	78,2	100	
SOX10	NM_006941.3	x	x	16,1	27,8	100	Agilent 50Mb: 1 / Agilent V4: 1
STRC	NM_153700.2	x	x	67,5	69,7	94,8	Agilent V4: **1-18, 20, 27-29**
SYNE4	NM_001039876.2		x	23,6	68,5	100	
TBC1D24	NM_001199107.1		x	29,7	72,2	100	Agilent 50Mb: 1 / Agilent V4: 1
TECTA	NM_005422.2	x	x	89,1	96,9	100	
TIMM8A	NM_004085.3	x	x	95,7	100,0	100	
TJP2	NM_004817.3	x		75,6	77,6		
TMC1	NM_138691.2	x	x	98,7	84,4	100	Agilent 50Mb: 1-4 / Agilent V4: 1-4
TMIE	NM_147196.2	x	x	68,9	62,9	90,6	
TMPRSS3	NM_024022.2	x	x	96,4	94,2	100	
TNC	NM_002160.3		x	92,2	96,9	100	Agilent 50Mb: 1 / Agilent V4: 1
TPRN	NM_001128228.2	x	x	8,8	26,1	75,8	
TRIOBP	NM_001039141.2	x	x	49,3	67,2	96,0	Agilent 50Mb: 1, 2, **24** / Agilent V4: 1, 2, **24**
TSPEAR	NM_144991.2		x	68,9	74,3	100	
USH1C	NM_153676.3	x	x	64,6	71,3	98,5	Agilent V4: **6**
USH1G	NM_173477.4	x	x	18,2	50,0	95,4	
USH2A	NM_206933.2	x	x	98,3	93,7	100	Agilent 50Mb: 1 / Agilent V4: 1
WFS1	NM_006005.3	x	x	48,5	85,2	100	Agilent 50Mb: 1 / Agilent V4: 1

HI, hearing impairment; DFNA, nonsyndromic autosomal dominant deafness; DFNB, nonsyndromic autosomal recessive deafness; DFNX, nonsyndromic X-linked deafness, AD, autosomal dominant; AR, autosomal recessive; ≥20x, ≥20 reads per base pair.

Table S2 Additional phenotype and single gene test information regarding patients with causative variants indicated in Table 1

Patient	Age of onset	Phenotype	Previous single gene tests	Gene RefSeq transcript ID	Variant 1 nucleotide change (protein change)	Variant 2 nucleotide change (protein change)	Zygosity[a]	Segregating with HI[b]
AD1[1]	1st decade	SNHI, bilateral, sym, stable, moderate, MF	TECTA, COL11A2, POU4F3	MYO6 NM_004999.3	c.1546+1G>T (p.?)	-	het	yes
AD2	congenital	HI, bilateral, sym, optic atrophy	WFS1	WFS1 NM_006005.3	c.2051C>T (p.Ala684Val)[2]	-	het	ND
AD3	congenital	SNHI, bilateral, sym, severe, flat, juvenile arthritis, cataract, childhood onset glaucoma	-	TECTA ENST00000392793.1	c.6002G>T (p.Cys2001Phe)	-	het	de novo
AD4	congenital	SNHI, bilateral, profound, HF	GJB2/GJB6	MYO7A NM_000260.3	c.1373A>T (p.Asn458Ile)[3]	-	het	yes
AD5[1]	1st decade	SNHI, bilateral, sym, stable, moderate, HF, myocardial infarction	TECTA, POU4F3, DFNA5	MYO6 NM_004999.3	c.1211del (p.Gly404Glufs*4)	-	het	yes
AD6[1]	1st decade	SNHI, bilateral, sym, prog, moderate, right HF, left flat, vestibular symptoms	KCNQ4	MYH9 NM_002473.5	c.2507C>T (p.Pro836Leu)	-	het	yes
AD7	1st decade	SNHI, bilateral, sym, stable, moderate, flat	TECTA, COL11A2	POU4F3 NM_002700.2	c.828_829insT (p.Lys277*)	-	het	ND
AD8	4th decade	SNHI, bilateral, prog, moderate, LF/MF	COCH, MYO6	MYO7A NM_000260.3	c.652G>A (p.Asp218Asn)	-	het	yes
AD9	2nd decade	SNHI, bilateral, asym, stable, moderate, HF	DFNA5, KCNQ4, ACTG1	POU4F3 NM_002700.2	c.668T>C (p.Leu223Pro)[4]	-	het	ND
AD10	1st decade	SNHI, bilateral, sym, prog, moderate, LF	TECTA, COL11A2	MYO6 NM_004999.3	c.3395del (p.Lys1132Serfs*12)	-	het	yes
AD11	congenital	SNHI, bilateral, sym, profound, flat, bilateral hypoplasia cochlea and dysplasia labyrinth	-	SOX10 NM_006941.3	c.1195C>T (p.Gln399*)	-	het	ND

2

Table S2 (continued)

Patient	Age of onset	Phenotype	Previous single gene tests	Gene RefSeq transcript ID	Variant 1 nucleotide change (protein change)	Variant 2 nucleotide change (protein change)	Zygosity[a]	Segregating with HI[b]
AD12	congenital	SNHI, bilateral, sym, stable, profound, flat	GJB2/GJB6	MITF NM_000248.3	c.649del (p.Arg217Aspfs*4)[15]	-	het	yes
AD13	4th decade	SNHI, bilateral, sym, prog, moderate, flat	MYO6	MYO7A NM_000260.3	c.2617C>T (p.Arg873Trp)[25]	-	het	yes
AD14	congenital	SNHI, bilateral, moderate, HF	GJB2/GJB6, KCNQ4	TECTA ENST00000392793.1	c.5794A>C (p.Thr1932Pro)	-	het	yes
AD15	congenital	SNHI, bilateral, mild, flat	KCNQ4, GJB2/GJB6	MYH14 NM_011145809.1	c.5176C>T (p.Arg1726Trp)	-	het	yes
AD16	1st decade	SNHI, bilateral, asym, prog, MF	-	WFS1 NM_006005.3	c.2032T>C (p.Trp678Arg)	-	het	yes
AD17	1st decade	SNHI, asym, moderate, MF	-	MYO6 NM_004999.3	c.584C>A (p.Ala195Glu)	-	het	yes
AD18	congenital	SNHI, bilateral, sym, moderate, HF	-	TECTA ENST00000392793.1	c.5597C>T (p.Thr1866Met)[30]	-	het	yes
AR1[1]	1st decade	SNHI, bilateral, sym, stable, moderate, HF, retinitis pigmentosa	USH2A, RP-R	USH2A NM_206933.2	c.(9371+1_9372-1)_(9570+1_9571-1)del (p.?)	c.(9371+1_9372-1)_(9570+1_9571-1)del (p.?)	hom	ND
AR2	congenital	SNHI, moderate, HF	GJB2/GJB6, SLC26A4	OTOA ENST0000388958	complete Δ[5]	complete Δ[5]	hom	ND
AR3[6]	congenital	SNHI, bilateral, sym, profound, flat	GJB2/GJB6, Asper array	CIB2 NM_006383.3	c.97C>T (p.Arg33*)	c.196C>T (p.Arg66Trp)	compound het	yes
AR4	1st decade	SNHI, bilateral, sym, stable, mild, flat	COCH, KCNQ4, WFS1, TECTA	STRC NM_153700.2	complete Δ[7]	complete Δ[7]	hom	yes
AR5	congenital	mixed HI, asym, severe, HF	GJB2/GJB6, SLC26A4, OTOF, MYO15A	USH2A NM_206933.2	c.(8845+1_8846-1)_(9371+1_9372-1)del (p.?)	c.(8845+1_8846-1)_(9371+1_9571-1)del (p.?)	hom	yes
AR6	1st decade	SNHI, bilateral, sym,	GJB2/GJB6,	TMC1	c.646del	c.790C>T	ND	ND

Table S2 (continued)

Patient	Age of onset	Phenotype	Previous single gene tests	Gene RefSeq transcript ID	Variant 1 nucleotide change (protein change)	Variant 2 nucleotide change (protein change)	Zygosity[a]	Segregating with HI[b]
		profound, HF	TMPRSS3	NM_138691.2	(p.Leu216Serfs*54)	(p.Arg264*)	compound het	ND
AR7	congenital	SNHI, bilateral, profound, flat	GJB2/GJB6	CDH23 NM_022124.5	c.6442G>A (p.Asp2148Asn)[8]	c.1545_1547del (p.Ile515del)[8]	compound het	yes
AR8	2nd decade	SNHI, bilateral, HF, night blindness	-	USH2A NM_206933.2	c.1606T>C (p.Cys536Arg)[9]	c.9815C>T (p.Pro3272Leu)[9]	compound het	ND
AR9	1st decade	SNHI, bilateral, asym, mild, HF	-	GJB2 NM_004004.5	c.35del (p.Gly12Valfs*2)[10]	c.71G>A (p.Trp24*)[11]	ND	ND
AR10	congenital	SNHI, bilateral, sym, mild	-	GJB2 NM_004004.5	c.35del (p.Gly12Valfs*2)[10]	c.35del (p.Gly12Valfs*2)[10]	hom	ND
AR11	congenital	SNHI, profound, flat	GJB2/GJB6	CDH23 NM_022124.5	c.2096A>G (p.Asp699Gly)	c.4562A>G (p.Asn1521Ser)	compound het	yes
AR12	congenital	SNHI, bilateral, sym, moderate, HF	-	GJB2 NM_004004.5	c.-23+1G>A (p.?)[12]	c.35del (p.Gly12Valfs*2)[10]	compound het	ND
AR13	congenital	SNHI, moderate, HF	-	MYO7A NM_000260.3	c.3289C>T (p.Gln1097*)	c.3862G>C (p.Ala1288Pro)[13]; c.5227C>T (p.Arg1743Trp)[14]	compound het	ND
AR14	1st decade	SNHI, bilateral, moderate, HF	GJB2/GJB6	STRC NM_153700.2	complete Δ[7]	complete Δ[7]	hom	ND
AR15	congenital	SNHI, bilateral, sym, profound, HF	GJB2/GJB6	PCDH15 NM_033056.3	c.3374-2A>G (p.?)	c.4127C>A (p.Ala1376Asp)	compound het	yes
AR16	congenital	SNHI, bilateral, sym, mild, MF	GJB2/GJB6, SLC26A4	STRC NM_153700.2	complete Δ[7]	complete Δ[7]	hom	ND
AR17	congenital	SNHI, bilateral, sym, severe, HF	GJB2/GJB6, USH2A	LOXHD1 NM_144612.6	c.1618dup (p.Thr540Asnfs*24)	c.1730T>G (p.Leu577Arg)	compound het	yes
AR18	congenital	SNHI, moderate	-	USH2A NM_206933.2	c.5018T>C (p.Leu1673Pro); c.7871C>T (p.Pro2624Leu)	c.2299del (p.Glu767Serfs*21)	compound het	ND

Table S2 (continued)

Patient	Age of onset	Phenotype	Previous single gene tests	Gene RefSeq transcript ID	Variant 1 nucleotide change (protein change)	Variant 2 nucleotide change (protein change)	Zygosity[a]	Segregating with HI[b]
ISO1[1]	1st decade	SNHI, bilateral, asym, prog, right profound flat, left severe HF	GJB2/GJB6, TMPRSS3	MYO15A NM_016239.3	c.625G>T (p.Glu209*)	c.1137del (p.Tyr380Metfs*64)[1] [6]	ND	ND
ISO2[1]	congenital	SNHI, bilateral, sym, stable, moderate, MF/HF	GJB2/GJB6, TMPRSS3	USH2A NM_206933.2	c.5385T>A (p.Tyr1795*)	c.6846_6849dup (p.His2284Asnfs*48)	ND	ND
ISO3	congenital	HI, retinitis pigmentosa, vestibular symptoms	GJB2/GJB6, CDH23, MYO7A, Asper array	CDH23 NM_022124.5	c.8480_8481del (p.Leu2827Hisfs*23)	c.8480_8481del (p.Leu2827Hisfs*23)	hom	ND
ISO4[1]	congenital	SNHI, bilateral, asym, stable, profound, flat	GJB2/GJB6	MYO15A NM_016239.3	c.6764+2T>A (p.?)	c.3844C>T (p.Arg1282Trp) c.5287C>T (p.Arg1763Trp)	ND	ND
ISO5	congenital	SNHI, bilateral, sym, stable, mild, MF/HF U-shaped	-	GJB2 NM_004004.5	c.101T>C (p.Met34Thr)[17]	c.109G>A (p.Val37Ile)[17]	compound het	ND
ISO6	congenital	SNHI, bilateral, asym, stable, profound, HF, optical atrophy	GJB2/GJB6, MITF	WFS1 NM_006005.3	c.2051C>T (p.Ala684Val)[2]	-	het	ND
ISO7	congenital	SNHI, bilateral, sym, severe	GJB2/GJB6, MYO7A, KCNE1, KCNQ1,PTPRQ	MYO15A NM_016239.3	c.6787G>A (p.Gly2263Ser)	c.7893+1G>A (p.?)	compound het	ND
ISO8	1st decade	SNHI, bilateral, sym, stable, moderate, HF	COL11A2, EYA, TECTA	TRIOBP NM_001039141.2	c.2653del (p.Arg885Alafs*120)	c.5014G>T (p.Gly1672*)	compound het	ND
ISO9	congenital	SNHI, moderate, flat	GJB2/GJB6	USH2A NM_206933.2	c.2299del (p.Glu767Serfs*21)	c.920_923dup (p.His308Glnfs*16)	compound het	ND
ISO10[1]	1st decade	SNHI, bilateral, sym, stable, moderate, HF	GJB2/GJB6, TMPRSS3, TMC1	MYO7A NM_000260.3	c.3476G>T (p.Gly1159Val)[18]	c.5560G>A (p.Val1854Met)[19]	compound het	ND
ISO11	congenital	SNHI, bilateral, sym, mild	-	GJB2 NM_004004.5	c.250G>C (p.Val84Leu)	c.269T>C (p.Leu90Pro)[20]	ND	ND

Table S2 (continued)

Patient	Age of onset	Phenotype	Previous single gene tests	Gene RefSeq transcript ID	Variant 1 nucleotide change (protein change)	Variant 2 nucleotide change (protein change)	Zygosity[a]	Segregating with HI[b]
ISO12	1st decade	SNHI, bilateral, sym, mild, HF	-	GJB2 NM_004004.5	c.109G>A (p.Val37Ile)[17]	c.109G>A (p.Val37Ile)[17]	hom	ND
ISO13	2nd decade	SNHI, bilateral, sym, prog, HF	-	TMPRSS3 NM_024022.2	c.916G>A (p.Ala306Thr)[21]	c.1276G>A (p.Ala426Thr)[22]	ND	ND
ISO14	congenital	SNHI, bilateral, moderate, MF/HF	GJB2/GJB6	STRC NM_153700.2	complete Δ[7]	complete Δ[7]	hom	ND
ISO15	congenital	SNHI, bilateral, moderate, MF	-	GJB2 NM_004004.5	c.35del (p.Gly12Valfs*2)[10]	c.101T>C (p.Met34Thr)[17]	compound het	ND
ISO16	congenital	SNHI, bilateral, sym, prog, severe, MF, night blindness, ID, clubfoot, hip luxation	-	ACTG1 NM_001199954.1	c.773C>T (p.Pro258Leu)	-	het	de novo
ISO17	congenital	SNHI, bilateral, sym, profound, ID	-	GJB2 NM_004004.5	c.35del (p.Gly12Valfs*2)[10]	c.508_511dup (p.Ala171Glufs*40)[23]	compound het	ND
ISO18	congenital	mixed HI, bilateral, sym, prog, profound, HF	GJB2/GJB6	MYO15A NM_016239.3	c.3311dup (p.Glu1105*)	c.3311dup (p.Glu1105*)	hom	ND
ISO19	congenital	SNHI, bilateral, sym, mild, flat	-	TRIOBP NM_001039141.2	c.3460_3461del (p.Leu1154Alafs*29)	c.3232dup (p.Arg1078Profs*6)[2,4]	compound het	ND
ISO20	1st decade	SNHI, bilateral, asym, prog, moderate, HF, heterochromia iridis, cataract	GJB2/GJB6, TMPRSS3, MITF, PAX3	MYO7A NM_000260.3	c.5618G>A (p.Arg1873Gln)[25]	c.6028G>A (p.Asp2010Asn)[26]	compound het	ND
ISO21	1st decade	SNHI, bilateral, prog, moderate, MF	GJB2/GJB6, TECTA, OTOF, MYO15A, TMC1	MYO6 NM_004999.3	c.3610C>T (p.Arg1204Trp)[27]	-	het	de novo
ISO22	congenital	SNHI, bilateral, mild, HF	GJB2/GJB6, SLC26A4	SLC26A5 NM_198999.2	c.355C>T (p.Pro119Ser)	c.355C>T (p.Pro119Ser)	hom	ND
ISO23	1st decade	SNHI, bilateral, sym, prog,	-	GJB2	c.101T>C	c.109G>A	compound	ND

2

Table S2 (continued)

Patient	Age of onset	Phenotype	Previous single gene tests	Gene RefSeq transcript ID	Variant 1 nucleotide change (protein change)[17]	Variant 2 nucleotide change (protein change)	Zygosity[a]	Segregating with HI[b]
		mild, HF		NM_004004.5	(p.Met34Thr)[17]	(p.Val37Ile)[17]	het	
ISO24	congenital	HI, bilateral, severe, flat	-	SOX10 NM_006941.3	c.482G>A (p.Arg161His)[28]	-	het	de novo
ISO25	congenital	SNHI, moderate, HF	GJB2/GJB6, SLC26A4, Asper array	MYO6 NM_004999.3	c.3335A>G (p.Tyr1112Cys)	c.1897del (p.Gln633Lysfs*19)	compound het	ND
ISO26	1st decade	SNHI, bilateral, sym, profound, flat, vestibular areflexia, ovarian failure	GJB2/GJB6, USH2A, MYO7A, PTPRQ	LARS2 NM_015340.3	c.683G>A (p.Arg228His)	c.880G>A (p.Glu294Lys)	compound het	ND
ISO27	1st decade	SNHI, bilateral, sym, moderate, MF	GJB2/GJB6, SLC26A4, TECTA	OTOA ENST00000388958	complete Δ[5]	complete Δ[5]	hom	ND
ISO28[1]	3rd decade	SNHI, bilateral, sym, stable, moderate, LF/MF	TECTA, ACTG1, POU4F3, COL11A2	COL11A1 NM_001854.3	c.1630-2del (p.?)	-	het	ND
ISO29	congenital	SNHI, bilateral, symm, moderate, MF/HF	GJB2/GJB6	LOXHD1 NM_144612.6	c.3061+1G>A (p.?)	c.6353G>A (p.Gly2118Glu)	ND	ND
ISO30	1st decade	SNHI, bilateral, sym, prog, severe, MF/HF	GJB2/GJB6, TMPRSS3	LOXHD1 NM_144612.6	c.3061C>T (p.Arg1021*)	c.5885C>T (p.Thr1962Met)	compound het	ND
ISO31	congenital	SNHI, bilateral, profound, bilateral incomplete partition cochlea	-	SLC26A4 NM_000441.1	SLC26A4:c.505del (p.Thr169Leufs*3)	SLC26A4:c.1334T>G (p.Leu445Trp)[29]	compound het	ND

AD, autosomal dominant; AR, autosomal recessive; ISO, isolated; SNHI, sensorineural hearing impairment; HI, hearing impairment; sym, symmetric; asym, asymmetric; LF, low frequency; MF, mid frequency; HF, high frequency; flat, flat audiogram configuration; prog, progressive; ID, intellectual disability; RP-R, recessive retinis pigmentosa gene package; het, heterozygous; hom, homozygous; ND, not determined or not conclusive; Δ, deletion. [a]Zygosity, determined on basis of segregation analysis in the parents. [b]Segregating with HI, determined on basis of segregation analysis in affected and/or unaffected family members.

2

Table S3 Diagnostic rates of WES targeting a panel of HI-related genes, based on type of inheritance, age of onset, and technological WES conditions

Categories	Subcategories	total (n)	Causative variant(s)		Variant(s) of uncertain significance		No causative variant(s) detected	
			n	%	n	%	n	%
Total		200	67	33.	10	5.0	123	61.5
Type of inheritance	adHI	66	18	27.3	4	6.1	44	66.7
	arHI	31	18	58.1	1	3.2	12	38.7
	GJB2		*3*	*16.7*				
	Isolated HI	102	31	30.4	4	3.9	67	65.7
	GJB2		*6*	*19.4*				
	X-linked HI	1	0	0.0	1	100	0	0.0
Age of onset	congenital	79	39	49.4	3	3.8	37	46.8
	1st decade	60	22	36.7	3	5.0	35	58.3
	2nd decade	17	3	17.6	1	5.9	13	76.5
	3rd decade	13	1	7.7	0	0.0	12	92.3
	4th decade	14	2	14.3	2	14.3	10	71.4
	5th decade	8	0	0.0	1	12.5	7	87.5
	6th decade	8	0	0.0	0	0.0	8	100
	unknown[a]	1	0	0.0	0	0.0	1	100
Technological WES conditions	Agilent 50Mb, SOLiD	30	9	30.0	3	10.0	18	60.0
	Agilent V4, SOLiD	14	5	35.7	0	0.0	9	64.3
	Agilent V4, HiSeq	156	53	34.0	7	4.5	96	61.5

adHI, autosomal dominant hearing impairment; arHI, autosomal recessive hearing impairment; HI, hearing impairment. [a] In one patient with late-onset HI the exact age of onset was unknown.

Table S4 Information on inheritance pattern, phenotype, and pretested genes of HI patients with variants of uncertain significance identified by WES targeting a panel of HI-related genes

Patient	Age of onset	Phenotype	Previous single gene tests	Gene RefSeq transcript ID	Variant 1 nucleotide change (protein change)	Variant 2 nucleotide change (protein change)	Zygosity[a]	Segregating with HI[b]
AD19	4th decade	SNHI, unilateral, asym, stable, moderate, HF	POU4F3, MYO6	MYO7A NM_000260.4	c.6122T>A (p.Ile2041Asn)	-	het	yes
AD20	congenital	SNHI, unilateral, asym, profound, flat	PAX3, MITF	MYO6 NM_004999.3	c.271G>A (p.Ala91Thr)	-	het	ND
AD21	4th decade	SNHI, bilateral, sym, prog, moderate, MF/HF	EYA4, COL11A2, POU4F3	COL11A1 NM_001854.3 TECTA ENST00000392793.1	COL11A1:c.2799del (p.Gly934Alafs*48)	TECTA:c.2128G>A (p.Glu710Lys)	het	ND
AD22	1st decade	SNHI, bilateral, sym, prog, severe, LF, hypermobility	EYA4, TECTA, COL11A2	WFS1 NM_006005.3	c.941G>T (p.Trp314Leu)	-	het	ND
AR19	1st decade	SNHI, severe, flat	GJB2/GJB6	USH2A NM_206933.2	c.1772A>G (p.Asp591Gly)	c.5018T>C (p.Leu1673Pro)	compound het	yes
ISO32	2nd decade	SNHI, bilateral, sym, moderate, MF	-	TECTA ENST00000392793.1	c.5818G>A (p.Ala1940Thr)	-	het	ND
ISO33	congenital	SNHI, bilateral, asym, stable, right severe MF, left profound flat, mild vestibular hyporeflexia	GJB2/GJB6	OTOGL NM_173591.3	c.2533T>C (p.Phe845Leu)	c.4833G>A (p.?)	ND	ND
ISO34	5th decade	SNHI, bilateral, sym, prog, moderate, HF	GJB2/GJB6, MYO6	CEACAM16 NM_001039213.3	c.859del (p.Gln287Argfs*34)	-	het	ND
ISO35	congenital	SNHI, bilateral, asym, right profound, left moderate, bilateral EVA	-	SLC26A4 NM_000441.1	c.1246A>C (p.Thr416Pro)	-	het	ND
XL1[1]	1st decade	SNHI, bilateral, sym, prog, severe, HF, unilateral mild ptosis	GJB2/GJB6, KCNQ4, TMPRSS3	SMPX NM_014332.2	c.132G>A (p.?)	-	hem	ND

AD, autosomal dominant; AR, autosomal recessive; ISO, isolated; SNHI, sensorineural hearing impairment; sym, symmetric; asym, asymmetric; LF, low frequency; MF, mid frequency; HF, high frequency; flat, flat audiogram configuration; prog, progressive; het, heterozygous; hom, homozygous; hem, hemizygous; ND, not determined or not conclusive. [a]Zygosity, determined on basis of segregation analysis in the parents. [b]Segregating with HI, determined on basis of segregation analysis in affected and/or unaffected family members.

Table S5 Diagnostic yield for targeted sequencing of single genes

Gene symbol	No. of requests	No. of positive[a] requests	% of positive[a] requests per gene
ACTG1	17	0	0
BSND	1	0	0
CLRN1	1	0	0
COCH	19	7	36.8
COL11A1	1	1	100
COL11A2	35	0	0
COL2A1	1	0	0
DFNA5	5	1	20
DFNB59	2	0	0
DIAPH1	8	0	0
EYA1	9	1	11.1
EYA4	22	0	0
GJB2	69	5	7.2
GRXCR1	1	0	0
HOXA2	1	0	0
KCNQ4	26	4	15.4
MITF	18	1	5.6
MYO15A	3	0	0
MYO6	16	0	0
MYO7A	3	1	33.3
NDP	1	1	100
OTOF	4	2	50
OTOG	3	0	0
OTOGL	3	0	0
PAX3	14	1	7.1
POU3F4	1	0	0
POU4F3	11	0	0
PTPRQ	1	0	0
SIX1	5	0	0
SIX5	5	0	0
SLC26A4	8	2	25
SNAI2	10	0	0
SOX10	2	0	0
TECTA	47	2	4.3
TMC1	2	0	0

2

Table S5 (continued)

Gene symbol	No. of requests	No. of positive[a] requests	% of positive[a] requests per gene
TMPRSS3	36	2	5.6
TSHZ1	3	0	0
USH2A	5	1	20
WFS1	17	1	5.9

[a]Positive indicates that causative variants were identified.

References

1. Neveling K, Feenstra I, Gilissen C, et al. A post-hoc comparison of the utility of sanger sequencing and exome sequencing for the diagnosis of heterogeneous diseases. Human mutation. Dec 2013;34(12):1721-1726.

2. Rendtorff ND, Lodahl M, Boulahbel H, et al. Identification of p.A684V missense mutation in the WFS1 gene as a frequent cause of autosomal dominant optic atrophy and hearing impairment. American journal of medical genetics. Part A. Jun 2011;155A(6):1298-1313.

3. Luijendijk MW, Van Wijk E, Bischoff AM, et al. Identification and molecular modelling of a mutation in the motor head domain of myosin VIIA in a family with autosomal dominant hearing impairment (DFNA11). Human genetics. Jul 2004;115(2):149-156.

4. Collin RW, Chellappa R, Pauw RJ, et al. Missense mutations in POU4F3 cause autosomal dominant hearing impairment DFNA15 and affect subcellular localization and DNA binding. Human mutation. Apr 2008;29(4):545-554.

5. Bademci G, Diaz-Horta O, Guo S, et al. Identification of copy number variants through whole-exome sequencing in autosomal recessive nonsyndromic hearing loss. Genetic testing and molecular biomarkers. Sep 2014;18(9):658-661.

6. Seco CZ, Giese AP, Shafique S, et al. Novel and recurrent CIB2 variants, associated with nonsyndromic deafness, do not affect calcium buffering and localization in hair cells. European journal of human genetics : EJHG. Jul 15 2015.

7. Verpy E, Masmoudi S, Zwaenepoel I, et al. Mutations in a new gene encoding a protein of the hair bundle cause non-syndromic deafness at the DFNB16 locus. Nature genetics. Nov 2001;29(3):345-349.

8. Astuto LM, Bork JM, Weston MD, et al. CDH23 mutation and phenotype heterogeneity: a profile of 107 diverse families with Usher syndrome and nonsyndromic deafness. American journal of human genetics. Aug 2002;71(2):262-275.

9. Dreyer B, Tranebjaerg L, Rosenberg T, Weston MD, Kimberling WJ, Nilssen O. Identification of novel USH2A mutations: implications for the structure of USH2A protein. European journal of human genetics : EJHG. Jul 2000;8(7):500-506.

10. Zelante L, Gasparini P, Estivill X, et al. Connexin26 mutations associated with the most common form of non-syndromic neurosensory autosomal recessive deafness (DFNB1) in Mediterraneans. Human molecular genetics. Sep 1997;6(9):1605-1609.

11. Rehman AU, Santos-Cortez RL, Drummond MC, et al. Challenges and solutions for gene identification in the presence of familial locus heterogeneity. European journal of human genetics : EJHG. Dec 10 2014.

12. Denoyelle F, Marlin S, Weil D, et al. Clinical features of the prevalent form of childhood deafness, DFNB1, due to a connexin-26 gene defect: implications for genetic counselling. Lancet. Apr 17 1999;353(9161):1298-1303.

13. Bharadwaj AK, Kasztejna JP, Huq S, Berson EL, Dryja TP. Evaluation of the myosin VIIA gene and visual function in patients with Usher syndrome type I. Experimental eye research. Aug 2000;71(2):173-181.

14. Pennings RJ, Huygen PL, Orten DJ, et al. Evaluation of visual impairment in Usher syndrome 1b and Usher syndrome 2a. Acta ophthalmologica Scandinavica. Apr 2004;82(2):131-139.

15. Tassabehji M, Newton VE, Liu XZ, et al. The mutational spectrum in Waardenburg syndrome. Human molecular genetics. Nov 1995;4(11):2131-2137.

16. Vona B, Muller T, Nanda I, et al. Targeted next-generation sequencing of deafness genes in hearing-impaired individuals uncovers informative mutations. Genetics in medicine : official journal of the American College of Medical Genetics. Dec 2014;16(12):945-953.

17. Hoefsloot LH, Feenstra I, Kunst HP, Kremer H. Genotype phenotype correlations for hearing impairment: approaches to management. Clinical genetics. Jun 2014;85(6):514-523.

18. Roux AF, Faugere V, Vache C, et al. Four-year follow-up of diagnostic service in USH1 patients. Investigative ophthalmology & visual science. Jun 2011;52(7):4063-4071.

19.   Neveling K, Collin RW, Gilissen C, et al. Next-generation genetic testing for retinitis pigmentosa. Human mutation. Jun 2012;33(6):963-972.

20.   Batissoco AC, Abreu-Silva RS, Braga MC, et al. Prevalence of GJB2 (connexin-26) and GJB6 (connexin-30) mutations in a cohort of 300 Brazilian hearing-impaired individuals: implications for diagnosis and genetic counseling. Ear and hearing. Feb 2009;30(1):1-7.

21.   Elbracht M, Senderek J, Eggermann T, et al. Autosomal recessive postlingual hearing loss (DFNB8): compound heterozygosity for two novel TMPRSS3 mutations in German siblings. Journal of medical genetics. Jun 2007;44(6):e81.

22.   Weegerink NJ, Schraders M, Oostrik J, et al. Genotype-phenotype correlation in DFNB8/10 families with TMPRSS3 mutations. Journal of the Association for Research in Otolaryngology : JARO. Dec 2011;12(6):753-766.

23.   Wu BL, Lindeman N, Lip V, et al. Effectiveness of sequencing connexin 26 (GJB2) in cases of familial or sporadic childhood deafness referred for molecular diagnostic testing. Genetics in medicine : official journal of the American College of Medical Genetics. Jul-Aug 2002;4(4):279-288.

24.   Riazuddin S, Khan SN, Ahmed ZM, et al. Mutations in TRIOBP, which encodes a putative cytoskeletal-organizing protein, are associated with nonsyndromic recessive deafness. American journal of human genetics. Jan 2006;78(1):137-143.

25.   Roux AF, Faugere V, Le Guedard S, et al. Survey of the frequency of USH1 gene mutations in a cohort of Usher patients shows the importance of cadherin 23 and protocadherin 15 genes and establishes a detection rate of above 90%. Journal of medical genetics. Sep 2006;43(9):763-768.

26.   Jacobson SG, Aleman TS, Sumaroka A, et al. Disease boundaries in the retina of patients with Usher syndrome caused by MYO7A gene mutations. Investigative ophthalmology & visual science. Apr 2009;50(4):1886-1894.

27.   Oonk AM, Leijendeckers JM, Lammers EM, et al. Progressive hereditary hearing impairment caused by a MYO6 mutation resembles presbyacusis. Hearing research. May 2013;299:88-98.

28.   Chaoui A, Watanabe Y, Touraine R, et al. Identification and functional analysis of SOX10 missense mutations in different subtypes of Waardenburg syndrome. Human mutation. Dec 2011;32(12):1436-1449.

29.   Van Hauwe P, Everett LA, Coucke P, et al. Two frequent missense mutations in Pendred syndrome. Human molecular genetics. Jul 1998;7(7):1099-1104.

30.   Brownstein Z, Friedman LM, Shahin H, et al. Targeted genomic capture and massively parallel sequencing to identify genes for hereditary hearing loss in Middle Eastern families. Genome biology. 2011;12(9):R89.

3

Genotype-phenotype characterization of known deafness genes
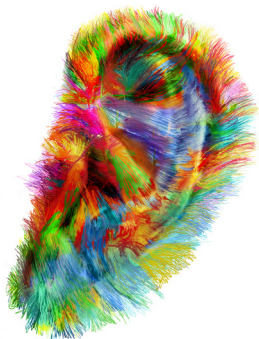
3.1

Broadening the phenotype of DFNB28: mutations in *TRIOBP* are associated with moderate, stable hereditary hearing impairment

Mieke Wesdorp, Jiddeke M. van de Kamp, Erik F. Hensen, Margit Schraders, Jaap Oostrik, Helger G. Yntema, Ilse Feenstra, Ronald J.C. Admiraal, Henricus P.M. Kunst, Mustafa Tekin, Moien Kanaan, Hannie Kremer* and Ronald J.E. Pennings*

* These authors contributed equally to this work
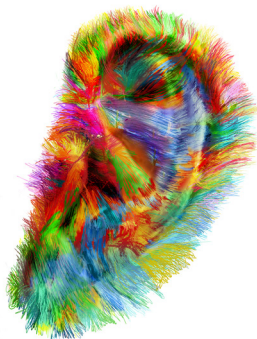
Abstract

DFNB28 is characterized by prelingual, severe to profound sensorineural hearing impairment (HI). It is associated with mutations in exon 6 and 7 of *TRIOBP* and has not been reported in the European population. Here, we describe two isolated cases of Dutch origin with congenital, moderate HI and compound heterozygous mutations in *TRIOBP*. Three of the mutations are novel, one nonsense mutation (c.5014G>T (p.Gly1672*) and two frameshift mutations (c.2653del (p.Arg885Alafs*120) and c.3460_3461del (p.Leu1154Alafs*29). The fourth mutation is the known c.3232dup (p.Arg1078Profs*6) mutation. Longitudinal audiometric analyses in one of the subjects revealed that HI was stable over a period of 15 years. Vestibular function was normal. Predicted effects of the mutations do not explain the relatively mild phenotype in the presented subjects, whereas location of the mutation might well contribute to the milder HI in one of the subjects. It is known that isoform classes TRIOBP-4 and TRIOBP-5 are important for stereocilia stability and rigidity. To our knowledge, p.Gly1672* is the first pathogenic variant identified in DFNB28 that does not affect isoform class TRIOBP-4. This suggests that a single *TRIOBP* copy to encode wild-type TRIOBP-4 is insufficient for normal hearing, and that at least one *TRIOBP* copy to encode TRIOBP-5 is indispensable for normal inner ear function. Furthermore, this study demonstrates that DFNB28 can be milder than reported so far and that mutations in *TRIOBP* are thus associated with a heterogeneous phenotype.

Introduction

DFNB28 (MIM #609823) is a rare type of autosomal recessive hereditary hearing impairment (HI), caused by mutations in *TRIOBP* (MIM #609761). It was first described by Riazuddin *et al.* and Shahin *et al.* in 2006, who mapped DFNB28 to chromosome 22q13.1 and found that mutations in *TRIOBP* were segregating with HI in 15 families.[1,2] To date, 22 families with (likely) pathogenic mutations in *TRIOBP* have been reported in literature, originating from the USA, China, India, Iran, Pakistan, Palestine, South Africa and Turkey. The majority of these families are consanguineous. All patients show prelingual, severe to profound HI.[1-7] To our knowledge, DFNB28 has not been described in the European population.

TRIOBP encodes TRIO - and filamentous-actin-Binding Protein, which plays an important role in the stability and rigidity of hair cell stereocilia in the inner ear.[8] Stereocilia are mechano-sensory structures, which are located on the apical surface of hair cells. Sound-induced deflections of the stereocilia bundle change the open probability of the mechanotransduction channel and thereby induce electrochemical signals that are transmitted via the cochlear nerve to the auditory cortex.[9] Hair cell stereocilia need to endure an infinite number of sound-induced deflections. Especially the pivot point of stereocilia, which is located at its insertion point in the cuticular plate of the cochlear hair cell,[10] needs to sustain the repeated mechanical stress. Rigidity and stability of stereocilia is secured by rootlets, flexible structures that anchor the base of the stereocilia into the cuticular plate.[11,12] Rootlets are formed by densely packed, tapered actin filaments at the base of each stereocilium.[13] It has been shown that the *Triobp* mouse mutant (*Triobp*^Δex8/Δex8) fails to form normal rootlets, although the remaining part of the stereocilia develop normally. Upon stimulation of stereocilia of the *Triobp*^Δex8/Δex8 mouse, hyperflexibility of the stereocilia and decreased pivot stiffness was observed, followed by progressive degeneration of the stereocilia. As a result, *Triobp*^Δex8/Δex8 mice are profoundly deaf from an early age.[8] This mimics DFNB28 in human and explains the severity and prelingual onset of HI.

It has been shown that specific classes of TRIOBP isoforms are involved in the formation of stereocilia rootlets.[8] According to Kitajiri *et al*. (2010), TRIOBP isoforms can be grouped into three classes: TRIOBP-5, TRIOBP-4 and TRIOBP-1.[8] TRIOBP-5 (NM_001039141) is encoded by the longest transcripts (exons 1-24) with a translation start site in exon 3. TRIOBP-4 (DQ228004) is encoded by exons 2-7 (previously known as exons 1-6) and translation occurs from an alternative translation start site in exon 6. TRIOBP-1 (NM_007032) is encoded by exons 11a-24 and translated from a translation start site in exon 11a (Figure 2). TRIOBP-4 and TRIOBP-5 are preferentially expressed in the inner ear and the eye; TRIOBP-1 is ubiquitously expressed. As already indicated, *Triobp*^Δex8/Δex8 mice, which lack exon 8, are

deaf. Mouse exon 8 is orthologous to human exon 7, previously known as human exon 6, and present in TRIOBP-4 and TRIOBP-5. Mice deficient for TRIOBP-1 are not viable. This indicates that TRIOBP-4 and/or TRIOBP-5 are essential for hearing, whereas TRIOBP-1 is indicated to be involved in processes essential for mouse development.[8] This is in line with the fact that all known pathogenic mutations associated with DFNB28 are located in exon 7, and only affect TRIOBP-4 and TRIOBP-5.[1-4,8] Localization experiments by Kitajiri *et al.* (2010) revealed that TRIOBP-4 localizes along the length of the stereocilia actin filaments, whereas TRIOBP-5 is only detected in the rootlets. Further in vitro studies showed that TRIOBP-4 alone is sufficient to organize filamentous-actin into dense bundles, which resemble stereocilia rootlets in vivo.[8] The interfilament spacing of the bundles is unusually small, which might suggest that TRIOBP wraps around the actin filaments externally instead of cross-linking.[8,14] The precise formation and maintenance of stereocilia rootlets and the role of TRIOBP-4 and/or TRIOBP-5 in this process is still elusive.

The present study describes mutations in *TRIOBP* in two Dutch isolated cases with moderate, stable HI. This demonstrates that HI in DFNB28 can be milder than reported so far and also occurs in the European population. We provide an overview of the genotype-phenotype characteristics of DFNB28 and seek to find a correlation between the severity of HI and the genotype.

Subjects and Methods

Subject evaluation
Medical history was obtained from the participants of the Dutch families 14-00692 and W15-2079, using a questionnaire focusing on hearing and balance. Ear, nose and throat examination was performed in all subjects to exclude acquired causes of HI. Pure-tone audiometry was performed in a sound-treated room according to current standards. Air conduction thresholds were determined at 0.25, 0.5, 1, 2, 4, and 8 kHz in dB HL. Bone conduction thresholds were determined at 0.5, 1, 2, 4, and 8 kHz in dB HL, to exclude conductive HI. In the proband (II:1) of family 14-00692, hearing was assessed at the age of one month, by use of Brainstem Evoked Response Audiometry (BERA) according to current standards. At the age of two years, visual reinforcement audiometry with a bone conductor and with headphones was performed by an experienced paediatric audiologist and hearing thresholds were determined at 0.5, 1, 2 and 4 kHz in dB of HL. For all participants, the 95th percentile threshold values of presbyacusis (p95) were calculated for each frequency and matched to the individual's sex and age, according to the ISO 7029 standard. HI was described according to the recommendations by the GENDEAF study group.[15] In

the index case (III:1) of family W15-2079, speech-recognition and vestibular function were assessed. Speech audiometry was performed in quiet, using standard monosyllabic Dutch word lists.[16] Vestibular function was assessed by electronystagmography, including a video head impulse test, rotary, and caloric tests.[17] This study was approved by the medical ethics committee of the Radboud university medical center. Informed consent was obtained from all participants or their legal representatives.

Mutation analysis

Genomic DNA was isolated from peripheral blood using standard techniques. In the index cases (family 14-00692, II:1 and family W15-2079, III:1) whole exome sequencing (WES) was performed. First, the exome was enriched using the Agilent SureSelect version 4 kit. Subsequently, WES was performed on an Illumina HiSeq system by BGI-Europe (Denmark). A panel of 120 HI-related genes (Supplemental Table S1) was analyzed and variants were selected based on variant classification guidelines,[18] for short description also see Neveling *et al.* (2012).[19] A potential effect of the *TRIOBP* variants was predicted with Alamut Visual (Interactive Biosoftware). Allele frequencies of the identified variants were obtained from the Exome Aggregation Consortium (ExAC) database and our in-house database that contains whole exome sequencing data of 13314 individuals, the vast majority of Dutch origin, affected by a large number of different diseases (including 810 patients with hearing impairment) and also non-affected individuals. Exons of *TRIOBP* that were not completely covered in WES were Sanger sequenced. The identified variants in *TRIOBP* (NM_001039141) were confirmed by Sanger sequencing. Segregation analysis in family members was performed to determine compound zygosity and co-segregation of the mutation with the HI in the family. Primer sequences and PCR conditions are available upon request.

Results

Moderate HI in family 14-00692

The index case (II:1) of family 14-00692 (Figure 1a) presented with congenital, bilateral HI, detected during neonatal hearing screening and confirmed by BERA at the age of one month. This BERA revealed hearing thresholds of 70 dB HL in the lower frequencies and 80 dB HL in the higher frequencies with slight total wave delay, indicating a conductive or mixed HI. Repeated visual reinforcement audiometry with a bone conductor, performed at the ages of 1 and 2 years, showed moderate HI on the left side. Visual reinforcement audiometry with headphones, performed at the age of 2 years, showed a conductive component of the hearing impairment (Figure 1b). Repeated tympanometry displayed

a flat curve, indicating otitis media with effusion. Hearing thresholds on the right ear were not determined during these examinations. There were no associated symptoms, such as dysmorphology, vestibular problems, delayed motor development or intellectual disability. Acquired causes of HI could most certainly be excluded by history taking, physical examination and a negative cytomegalovirus test. The parents (I:1 and I:2) had normal hearing. There were no other family members with HI and there was no history of consanguinity in the family.

With HI gene-panel analysis, a heterozygous mutation was detected in *TRIOBP*, c.3232dup (p.Arg1078Profs*6) in exon 7 (Figure 2). This mutation has been reported homozygously in two Indian families with profound HI (Table 1).[1] Sanger sequencing of the exons that were not completely covered in the WES data resulted in detection of a second variant, c.3460_3461del (p.Leu1154Alafs*29) in exon 7 (Figure 2). This variant was novel and considered to be pathogenic as it is predicted to introduce a premature stop codon, and because it is very rare (Table 1). Segregation analysis in the unaffected parents demonstrated that the father carried the c.3232dup mutation (Figure 1a). The second mutation could not be traced in the parents. A common SNP (rs5756795, C/T) is located in proximity to the c.3460_3461del mutation. Segregation analysis of this SNP and the c.3460_3461del mutation revealed that this mutation occurred *de novo* on the maternal allele or that germline mosaicism existed in the mother (Supplemental Figure S1). No potentially pathogenic variants were identified in other HI-related genes that were targeted in our analysis.

Moderate, stable HI in family W15-2079

The proband (III:1) of family W15-2079 suffered from congenital, symmetric, moderate, high frequency sensorineural HI (Figure 1). Longitudinal analyses of audiograms over a period of 15 years revealed no progression of HI up to the age of 28 years. Speech audiometry showed a maximum phoneme score of 100% without hearing aids. Acquired causes of HI could be excluded by medical history and ear, nose and throat examination. There were no complaints of balance problems and electronystagmography showed normal vestibular function. Audiological evaluation of family members I:2, II:1, III:2 and III:3 demonstrated normal hearing. The father (II:2) of the proband was physically not able to participate in the study. Family history was negative for HI and consanguinity.

HI gene-panel analysis revealed two novel variants in *TRIOBP*: c.2653del (p.Arg885Alafs*120 in exon 7 and c.5014G>T (p.Gly1672*) in exon 9 (Figure 2). The variants were considered to be causative, because 1) they are damaging (a premature stop codon is predicted to be introduced), 2) they have a very low global and population-specific minor allele frequency (Table 1), 3) they are located in trans, and 4) they co-segregate with the HI

in the family (Figure 1a). No possibly pathogenic variants were identified in other HI-related genes that were targeted in our analysis.

a

14-00692   W15-2079

M1: c.3232dup (p.Arg1078Profs*6)
M2: c.3460_3461del (p.Leu1154Alafs*29)
M3: c.2653del (p.Arg885fs*120)
M4: c.5014G>T (p.Gly1672*)
+ : wildtype

b
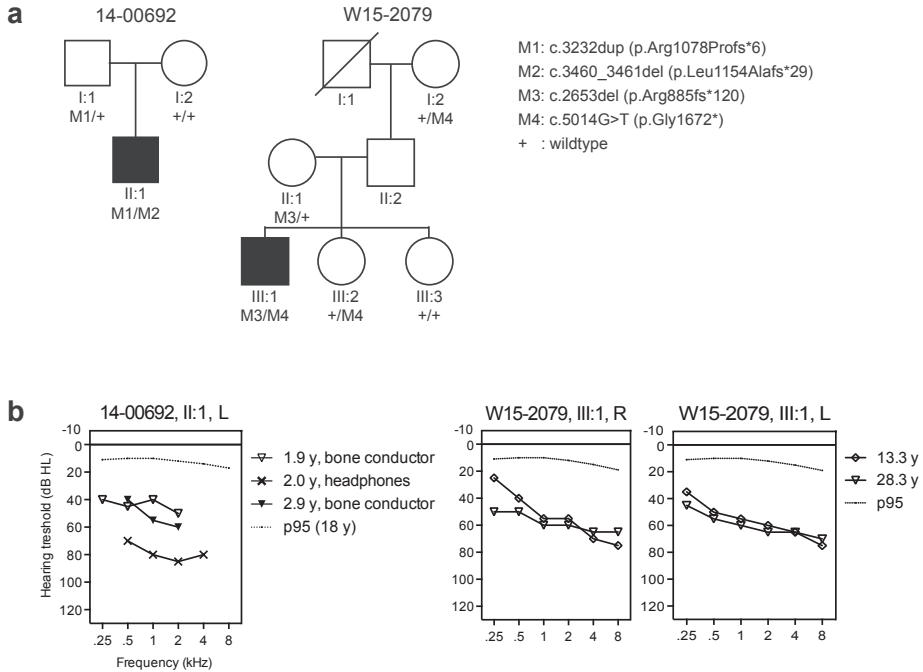
Figure 1 Family 14-00692 and W15-2079
(a) Pedigrees and segregation analyses of the identified mutations in *TRIOBP*. **(b)** Pure-tone audiograms of the affected individuals, showing moderate HI (14-00692, II:1 measured with visual reinforcement audiometry, besides the sensorineural HI there is a conductive component due to otitis media with effusion). HI in W15-2079, III:1 was stable over a period of 15 years.
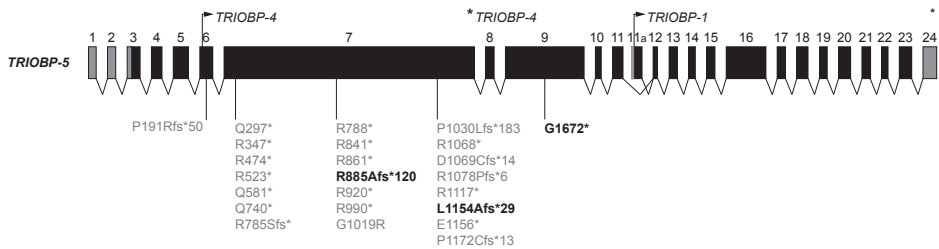
Figure 2 Pathogenic mutations in *TRIOBP*
Schematic representations of the genomic structure and alternative transcript classes of *TRIOBP*: *TRIOBP-5* (NM_001039141, RefSeq), *TRIOBP-4* (DQ228004, GenBank) and *TRIOBP-1* (NM_007032, RefSeq). Previously published (likely) pathogenic mutations (depicted in grey) and novel mutations identified in this study (depicted in black) are shown.

⌐ , alternative translation start site; * (alternative) stop codon.

Table 1 Genotypic and phenotypic characteristics of DFNB28

Genotype						Phenotype				
Allele 1 nucleotide change (predicted protein change)	Allele 2 nucleotide change (predicted protein change)	Exon	Segregation analysis[a]	ExAC MAF	Pathogenicity of variant(s)[b]	Ethnicity	Age of onset	Severity	Audiogram configuration	Ref.
c.154G>A (p.Asp52Asn)	unknown[c]	4	unknown	GL 0.020 EA 0.165	uncertain significance	Japanese	unknown	unknown	unknown	20
c.572del (p.Pro191Argfs*50)	c.3510_3513dup (p.Pro1172Cysfs*13)	1) 6 2) 7	unknown	1) NR 2) NR	likely pathogenic	South African	prelingual	unknown	unknown	6
c.889C>T (p.Gln297*)	c.889C>T (p.Gln297*)	7	yes	NR	pathogenic	Indian	prelingual	profound	all freq. affected	1
c.1039C>T (p.Arg347*)	c.1039C>T (p.Arg347*)	7	yes	0.004	pathogenic	Palestinian	prelingual	severe	flat	2
c.1039C>T (p.Arg347*)	c.1741C>T (p.Gln581*)	7	yes	1) 0.004 2) NR	pathogenic	Palestinian	prelingual	severe	MF	2
c.1039C>T (p.Arg347*)	c.3055G>A (p.Gly1019Arg)	7	yes	1) 0.004 2) NR	pathogenic	Palestinian	prelingual	profound	all freq. affected	2
c.1420C>T (p.Arg474*)	c.1420C>T (p.Arg474*)[d]	7	unknown	NR	pathogenic	unknown	unknown	unknown	unknown	8
c.1567C>T (p.Arg523*)	c.1567C>T (p.Arg523*)[d]	7	unknown	0.001	pathogenic	unknown	unknown	unknown	unknown	8
c.1741C>T (p.Gln581*)	c.1741C>T (p.Gln581*)	7	yes	NR	pathogenic	Palestinian	prelingual	severe-profound	all freq. affected	2;e
c.2218C>T (p.Gln740*)	c.2218C>T (p.Gln740*)[d]	7	unknown	NR	pathogenic	unknown	unknown	unknown	unknown	8
c.2355_2356del (p.Arg785Serfs*50)	c.2355_2356del (p.Arg785Serfs*50)	7	yes	NR	pathogenic	Turkish	unknown	unknown	unknown	3
c.2362C>T (p.Arg788*)	c.2362C>T (p.Arg788*)	7	yes	GL 0.003 SA NR	pathogenic	Pakistani	prelingual	profound	all freq. affected	1
c.2521C>T (p.Arg841*)	c.2521C>T (p.Arg841*)	7	unknown	NR	pathogenic	Turkey	prelingual	severe - profound	MF, HF, flat	6;f
c.2581C>T (p.Arg861*)	c.2758C>T (p.Arg920*)	7	no	1) GL 0.001 EA NR 2) NR	pathogenic[g]	Chinese	unknown	severe – profound (asymmetric)	HF, flat	21

Table 1 (continued)

Genotype						Phenotype				
Allele 1 nucleotide change (predicted protein change)	Allele 2 nucleotide change (predicted protein change)	Exon	Segregation analysis[a]	ExAC MAF	Pathogenicity of variant(s)[b]	Ethnicity	Age of onset	Severity	Audiogram configuration	Ref.
c.2581C>T (p.Arg861*)	c.3089del (p.Pro1030Leufs*183)	1) 7 2) 7	unknown	1) 0.001 2) NR	pathogenic	American	prelingual	unknown	unknown	6
c.2653del (p.Arg885Alafs*120)	c.5014G>T (p.Gly1672*)	1) 7 2) 9	yes	1) GL NR IHD NR 2) GL 0.057 NFE 0.095 IHD 0.049	pathogenic	Dutch	prelingual	moderate	HF	This study
c.2968C>T (p.Arg990*)	c.2968C>T (p.Arg990*)	7	yes	NR	pathogenic	Pakistani	unknown	severe	unknown	7
c.2992G>A (p.Ala998Thr)	c.5767G>A (p.Ala1923Thr)	1) 7 2) 16	no	1) 0.070 2) 0.151	uncertain significance	unknown	prelingual	mild – moderate	unknown	22
c.3202C>T (p.Arg1068*)	c.3202C>T (p.Arg1068*)	7	yes	GL 0.001 SA NR	pathogenic	Pakistani	prelingual	profound	all freq. affected	1
c.3202_3203del (p.Asp1069Cysfs*14)	c.3202_3203del (p.Asp1069Cysfs*14)	7	yes	NR	pathogenic	Indian	prelingual	profound	all freq. affected	1
c.3232dup (p.Arg1078Profs*6)	c.3232dup (p.Arg1078Profs*6)	7	yes	GL 0.015 SA 0.007	pathogenic	Indian	prelingual	profound	all freq. affected	1
c.3232dup (p.Arg1078Profs*6)	c.3460_3461del (p.Leu1154Alafs*29)	7	yes	1) GL 0.015 NFE 0.016 IHD NR 2) GL 0.004 NFE 0.006 IHD NR	pathogenic	Dutch	prelingual	mild	NA[h]	This study
c.3349C>T (p.Arg1117*)	c.3349C>T (p.Arg1117*)	7	yes	NR	pathogenic	Indian	prelingual	profound	all freq affected	1
c.3349C>T (p.Arg1117*)	c.4691G>C (p.Gly1564Ala)	1) 7 2) 9	no	1) NR 2) NR	uncertain significance	unknown	unknown	unknown	unknown	22

3.1

Table 1 (continued)

Genotype						Phenotype				
Allele 1 nucleotide change (predicted protein change)	Allele 2 nucleotide change (predicted protein change)	Exon	Segregation analysis[a]	ExAC MAF	Pathogenicity of variant(s)[b]	Ethnicity	Age of onset	Severity	Audiogram configuration	Ref.
c.3451A>G (p.Met1151Val)	c.4187C>G (p.Pro1396Arg)	1) 7 2) 9	unknown	1) GL 0.012 EA 0.012 2) GL 0.001 EA 0.019	uncertain significance	Chinese	unknown	moderate – severe (asymmetric)	HF	21
c.3466G>T (p.Glu1156*)	c.3466G>T (p.Glu1156*)[d]	7	unknown	NR	pathogenic	unknown	unknown	unknown	unknown	8
c.3662G>A (p.Arg1221Gln) c.3942G>C (p.Glu1314Asp)	c.6736G>A (p.Glu2246Lys)	1) 7 2) 7 3) 21	no	1) 0.033 2) 0.040 3) 0.612	uncertain significance	unknown	prelingual	severe – profound	unknown	22
c.4840G>T (p.Gly1614Cys)	unknown[c]	9	unknown	GL 0.015 EA 0.210	uncertain significance	Japanese	unknown	unknown	unknown	20
c.5519G>A (p.Arg1840His)	unknown[c]	14	unknown	GL 0.003 EA 0.012	uncertain significance	Japanese	unknown	unknown	unknown	20
c.6362C>T (p.Ser2121Leu)	c.6362C>T (p.Ser2121Leu)	18	yes	GL 0.291 SA 0.578	uncertain significance	Iranian	prelingual	unknown	unknown	5
c.6860G>A (p.Arg2287His)	unknown[c]	22	unknown	NR	uncertain significance	Japanese	unknown	unknown	unknown	20

ExAC MAF, minor allele frequency from the Exome Aggregation Consortium (global MAF, unless stated otherwise); Ref, Reference; GL, global MAF; EA, East Asian MAF; NFE, Non-Finnish European MAF; SA, South Asian MAF; IHD, minor allele frequency from our in-house database; NR, not reported; freq, frequency; MF, mid frequency; HF, high frequency. [a]segregation analysis performed to confirm zygosity or co-segregation of the mutations with the HI in the family. [b]pathogenicity of variant(s) classified as uncertain significance if the mutation on the second allele and/or segregation analysis is unknown or not performed. [c]reported as variants of uncertain significance, unclear whether mutations were found in compound heterozygous or homozygous state. [d]reported as pathogenic mutations, unclear whether mutations were found in homozygous state, here assumed to be homozygous; [e]unpublished data provided by M. Kanaan. [f]unpublished data provided by M. Tekin. [g]segregation analysis was not performed, but analysis of WES read-pairs demonstrated that the variants are located in trans, [h]too young to determine.

Discussion

In this study, we present two isolated cases of Dutch origin with hereditary moderate HI caused by compound heterozygous mutations in *TRIOBP*. The three novel and one known truncating mutations were identified by WES targeting a panel of HI-related genes and Sanger sequencing, and segregated with HI in the family. Table 1 represents an overview of the *TRIOBP* variants that have been reported in this and previous studies. DFNB28 displays allelic heterogeneity, as many other types of genetic HI. To date, 21 (likely) pathogenic mutations have been reported in homozygous or compound heterozygous state, *viz.* 14 nonsense, 6 frameshift and 1 missense mutations, all located in exons 6 and 7, which were previously described as exons 5 and 6 (Table 1, Figure 2).[1-4,8] We assumed the 4 mutations described by Kitajiri *et al.* (2010) to be present in homozygous state although this is not clearly indicated by the authors. In addition, 13 missense variants of uncertain significance have been published.[4,20] The pathogenicity of these variants is unclear, because no mutations of the second allele were identified, prediction programs were inconclusive about the pathogenicity of the variant, and/or segregation analysis has not been performed. In addition, some of these missense variants are relatively frequent found in control populations, which casts doubt on their pathogenicity (Table 1, minor allele frequency ExAC database).

Published phenotypic data of DFNB28 families showed that affected individuals suffered from prelingual, severe to profound HI (Table 1).[1,2,4-7,22] One case reported by Gu *et al.* (2015) had asymmetric, moderate (right ear) to severe (left ear) HI.[4] Another case reported by Sloan-Heggen *et al.* (2016) suffered from mild to moderate HI. However, in both cases the identified missense variants are of uncertain significance. In this study, sensorineural HI in both cases is moderate. The reliability of the thresholds determined in visual reinforcement audiometry could be questioned as the index case of family 14-00692 is only 2 years old. However, the thresholds measured with headphones are comparable to those measured with BERA. In addition, repeated measurements with a bone conductor show comparable sensorineural thresholds. Until now, repeated audiometry shows no hearing deterioration of the subject, although future progression of HI cannot be excluded. Importantly, HI in the affected subject of family W15-2079 was stable over a period of 15 years and remains moderate at the age of 28 years. This indicates that the moderate HI is not related to an early stage of disease. Our results therefore provide evidence that mutations in *TRIOBP* can be associated with moderate, stable HI.

All but two previously reported (likely) pathogenic mutations are predicted to result in premature protein truncation as are the mutations presented in this study (Table 1). Therefore, we conclude that the relatively mild phenotype observed in the subjects

presented here is unlikely to be explained by the type of mutations.

The *TRIOBP* mutations in family W15-2079 are located in exon 7 (c.2653del) and exon 9 (c.5014G>T). The latter exon is only present in the mRNA for isoform class TRIOBP-5. Since the isoform classes TRIOBP-4 and TRIOBP-5 have a different distribution along the stereocilia and their rootlets,[8] it may well be that the location of the mutations and thus the affected isoform(s) explain the milder HI in this family. However, the mutations identified in family 14-00692 are both located in exon 7, and affect both isoform classes TRIOBP-4 and TRIOBP-5, as is the case in all previously published mutations associated with DFNB28 and severe to profound HI. In this family, therefore the location of the mutations is unlikely to explain the milder DFNB28 phenotypes. This implies that different genetic factors may underlie or contribute to the milder phenotype in the two families. Candidate factors are variants in other proteins that function in the stereociliary rootlet or variation in their level of expression and differences in efficacy of nonsense mediated decay of the mutated *TRIOBP* mRNA.

To our knowledge, c.5014G>T is the first pathogenic *TRIOBP* variant identified in a patient with DFNB28 that does not affect TRIOBP-4. This implies that a single gene copy to encode wild-type TRIOBP-4 is insufficient for the formation of normal stereocilia rootlets, and/or that at least one gene copy to encode wild-type TRIOBP-5 is required for normal hearing. This is in line with the differential localization of the protein isoforms, showing that TRIOBP-4 was detected along the entire length of the stereocilia, whereas TRIOBP-5 was only found to be located at the rootlets of stereocilia.[8]

We assessed the vestibular function to extend the insight in the DFNB28 phenotype. The lack of complaints of imbalance and normal motor development in the presented subjects in combination with normal electronystagmography in family W15-2079 suggested vestibular function to be normal. This is in line with previous research by Riazuddin *et al.* (2006), who described that subjects with DFNB28 have no vestibular symptoms and normal vestibular function.[1] Whether the vestibular organ is dysfunctioning in *Triobp* mouse mutants has not been reported.

Our findings highlight the importance of providing an extensive description of the phenotype when mutations underlying HI are reported in literature, including audiometric data, vestibular symptoms and/or function and presence of syndromic features. Such descriptions were not available for a number of the published *TRIOBP* mutations. Phenotypic characterizations are essential for expanding our knowledge on genotype – phenotype correlations for HI. This enables clinicians to provide adequate counseling on prognosis and rehabilitation options.

Conclusions

DFNB28, caused by mutations in *TRIOBP*, was known to be associated with prelingual, severe to profound HI. We identified three novel mutations and one known mutation in *TRIOBP* in two Dutch isolated cases with moderate HI. Longitudinal audiometric analysis in one of these subjects demonstrated that the HI is stable over a period of 15 years. These data indicate that DFNB28 can be less severe than reported so far and that the phenotype associated with mutations in *TRIOBP* is heterogeneous. Predicted effect of the mutations does not explain the less severe phenotype in the presented subjects, whereas location of the mutations could probably explain the milder HI in only one of the subjects. Vestibular function was found to be normal.

Acknowledgements

Webresources

The URLs for data presented herein are as follows:
Alamut Visual, http://www.interactive-biosoftware.com/alamut- visual/
ExAC Browser, http://exac.broadinstitute.org/
ExonPrimer, http://ihg.gsf.de/ihg/ExonPrimer.html
GenBank, http://www.ncbi.nlm.nih.gov/genbank/
OMIM, http://www.omim.org/
OMIM Phenotypic Series, http://www.omim.org/phenotypicSeriesTitle/all
RefSeq, http://www.ncbi.nlm.nih.gov/refseq/

References

1. Riazuddin S, Khan SN, Ahmed ZM, et al. Mutations in TRIOBP, which encodes a putative cytoskeletal-organizing protein, are associated with nonsyndromic recessive deafness. *American journal of human genetics.* Jan 2006;78(1):137-143.

2. Shahin H, Walsh T, Sobe T, et al. Mutations in a novel isoform of TRIOBP that encodes a filamentous-actin binding protein are responsible for DFNB28 recessive nonsyndromic hearing loss. *American journal of human genetics.* Jan 2006;78(1):144-152.

3. Diaz-Horta O, Duman D, Foster J, 2nd, et al. Whole-exome sequencing efficiently detects rare mutations in autosomal recessive nonsyndromic hearing loss. *PloS one.* 2012;7(11):e50628.

4. Seco CZ, Oonk AM, Dominguez-Ruiz M, et al. Progressive hearing loss and vestibular dysfunction caused by a homozygous nonsense mutation in CLIC5. *European journal of human genetics : EJHG.* Feb 2015;23(2):189-194.

5. Fardaei M, Sarrafzadeh S, Ghafouri-Fard S, Miryounesi M. Autosomal Recessive Nonsyndromic Hearing Loss: A Case Report with a Mutation in TRIOBP Gene. *International journal of molecular and cellular medicine.* Fall 2015;4(4):245-247.

6. Yan D, Tekin D, Bademci G, et al. Spectrum of DNA variants for non-syndromic deafness in a large cohort from multiple continents. *Human genetics.* Aug 2016;135(8):953-961.

7. Naz S, Imtiaz A, Mujtaba G, et al. Genetic causes of moderate to severe hearing loss point to modifiers. *Clinical genetics.* Oct 6 2016.

8. Kitajiri S, Sakamoto T, Belyantseva IA, et al. Actin-bundling protein TRIOBP forms resilient rootlets of hair cell stereocilia essential for hearing. *Cell.* May 28 2010;141(5):786-798.

9. Zhao B, Muller U. The elusive mechanotransduction machinery of hair cells. *Current opinion in neurobiology.* Oct 2015;34:172-179.

10. Howard J, Ashmore JF. Stiffness of sensory hair bundles in the sacculus of the frog. *Hearing research.* 1986;23(1):93-104.

11. Flock A, Cheung HC. Actin filaments in sensory hairs of inner ear receptor cells. *The Journal of cell biology.* Nov 1977;75(2 Pt 1):339-343.

12. Furness DN, Mahendrasingam S, Ohashi M, Fettiplace R, Hackney CM. The dimensions and composition of stereociliary rootlets in mammalian cochlear hair cells: comparison between high- and low-frequency cells and evidence for a connection to the lateral membrane. *The Journal of neuroscience : the official journal of the Society for Neuroscience.* Jun 18 2008;28(25):6342-6353.

13. Tilney LG, Derosier DJ, Mulroy MJ. The organization of actin filaments in the stereocilia of cochlear hair cells. *The Journal of cell biology.* Jul 1980;86(1):244-259.

14. Boutet de Monvel J, Petit C. Wrapping up stereocilia rootlets. *Cell.* May 28 2010;141(5):748-750.

15. Mazzoli M, Van Camp G, Newton V, Giarbini N, Declau F, Parving A. Recommendations for the description of genetic and audiological data for families with nonsyndromic hereditary hearing impairment. *Audiological Medicine.* 2003;1:148-150.

16. Bosman AJ. *Speech Perception by the Hearing Impaired*, University of Utrecht; 1989.

17. Theunissen EJ, Huygen PL, Folgering HT. Vestibular hyperreactivity and hyperventilation. *Clinical otolaryngology and allied sciences.* Jun 1986;11(3):161-169.

18. Wallis Y, Payne S, McAnulty C, et al. Practice Guidelines for the Evaluation of Pathogenicity and the Reporting of Sequence Variants in Clinical Molecular Genetics. *ACGS /VGKL.* 2013.

19. Neveling K, Collin RW, Gilissen C, et al. Next-generation genetic testing for retinitis pigmentosa. *Human mutation.* Jun 2012;33(6):963-972.

20. Miyagawa M, Naito T, Nishio SY, Kamatani N, Usami S. Targeted exon sequencing successfully discovers rare causative genes and clarifies the molecular epidemiology of Japanese deafness patients. *PloS one.* 2013;8(8):e71381.

21.   Gu X, Guo L, Ji H, et al. Genetic testing for sporadic hearing loss using targeted massively parallel sequencing identifies 10 novel mutations. *Clinical genetics.* Jun 2015;87(6):588-593.
22.   Sloan-Heggen CM, Bierer AO, Shearer AE, et al. Comprehensive genetic testing in the clinical evaluation of 1119 patients with hearing loss. *Human genetics.* Apr 2016;135(4):441-450.

3.1

Supplemental data

Figure S1 Segregation analysis family 14-00692.
(**a**) Sequence analysis showed that both the index patient and the father carry the c.3232dup mutation in *TRIOBP*. (**b**) Sequence analysis demonstrated that the index case and the father carry a heterozygous SNP (rs5756795, C/T), which lies in proximity to the c.3460_3461 del mutation. (**c**) Analysis of the WES paired-reads demonstrated that the second variant c.3460_3461del was located in reads that do not harbor the SNP (indicated by the red boxes), revealing that this mutation occurred *de novo* on the maternal allele or that germline mosaicism existed in the mother.

Table S1 Analyzed panel of 120 HI-related genes

Gene name	RefSeq transcript ID	Gene name (continued)	RefSeq transcript ID (continued)	Gene name (continued)	RefSeq transcript ID (continued)
ACTB	NM_001101.3	GPR98	NM_032119.3	SLC17A8	NM_139319.2
ACTG1	NM_001199954.1	GPSM2	NM_013296.4	SLC26A4	NM_000441.1
ADCY1	NM_021116.2	GRHL2	NM_024915.3	SLC26A5	NM_198999.2
ATP6V1B1	NM_001692.3	GRXCR1	NM_001080476.2	SLC33A1	NM_004733.
BDP1	NM_018429.2	GRXCR2	NM_001080516.1	SLITRK6	NM_032229.2
BSND	NM_057176.2	HARS	NM_002109.5	SMPX	NM_014332.2
CABP2	NM_016366.2	HARS2	NM_012208.2	SNAI2	NM_003068.4
CACNA1D	NM_000720.3	HGF	NM_000601.4	SOX10	NM_006941.3
CCDC50	NM_178335.2	HSD17B4	NM_001199291.1	STRC	NM_153700.2
CDH23	NM_022124.5	ILDR1	NM_001199799.1	SYNE4	NM_001039876.2
CEACAM16	NM_001039213.3	KARS	NM_001130089.1	TBC1D24	NM_001199107.1
CIB2	NM_006383.3	KCNE1	NM_000219.4	TECTA	NM_005422.2
CLDN14	NM_144492.2	KCNJ10	NM_002241.4	TIMM8A	NM_004085.3
CLIC5	NM_001114086.1	KCNQ1	NM_000218.2	TMC1	NM_138691.2
CLPP	NM_006012 .2	KCNQ4	NM_004700.3	TMIE	NM_147196.2
CLRN1	NM_001195794.1	LARS2	NM_015340.3	TMPRSS3	NM_024022.2
COCH	NM_001135058.1	LHFPL5	NM_182548.3	TNC	NM_002160.3
COL11A1	NM_001854.3	LOXHD1	NM_144612.6	TPRN	NM_001128228.2
COL11A2	NM_080680.2	LRTOMT	NM_001145309.3	TRIOBP	NM_001039141.2
COL2A1	NM_001844.4	MARVELD2	NM_001038603.2	TSPEAR	NM_144991.2
COL4A3	NM_000091.4	MIR96	NR_029512.1	USH1C	NM_153676.3
COL4A4	NM_000092.4	MITF	NM_198159.2	USH1G	NM_173477.4
COL4A5	NM_033380.2	MSRB3	NM_198080.3	USH2A	NM_206933.2
COL4A6	NM_001287758.1	MYH14	NM_001145809.1	WFS1	NM_006005.3
COL9A1	NM_001851.4	MYH9	NM_002473.5		
COL9A2	NM_001852.3	MYO15A	NM_016239.3		
CRYM	NM_001888.4	MYO3A	NM_017433.4		
DFNA5	NM_004403.2	MYO6	NM_004999.3		
DFNB31	NM_015404.3	MYO7A	NM_000260.3		
DFNB59	NM_001042702.3	NLRP3	NM_001079821.2		
DIABLO	NM_019887.5	OPA1	NM_130837.2		
DIAPH1	NM_005219.4	OTOA	NM_144672.3		
DIAPH3	NM_001042517.1	OTOF	NM_194248.2		
DSPP	NM_014208.3	OTOG	NM_001277269.1		
EDN3	NM_207034.2	OTOGL	NM_173591.3		
EDNRB	NM_001201397.1	P2RX2	NM_170683.3		
ELMOD3	NM_032213.4	PAX3	NM_181459.3		
EPS8	NM_004447.5	PCDH15	NM_033056.3		
ESPN	NM_031475.2	PDZD7	NM_001195263.1		
ESRRB	NM_004452.3	PNPT1	NM_033109.4		
EYA1	NM_000503.5	POU3F4	NM_000307.4		
EYA4	NM_001301013.1	POU4F3	NM_002700.2		
FGF3	NM_005247.2	PRPS1	NM_002764.3		
FOXI1	NM_012188.4	PTPRQ	NM_001145026.1		
GIPC3	NM_133261.2	RDX	NM_002906.3		
GJB2	NM_004004.5	SERPINB6	NM_001271823.1		
GJB3	NM_024009.2	SIX1	NM_005982.3		
GJB6	NM_001110219.2	SIX5	NM_175875.4		

3.1
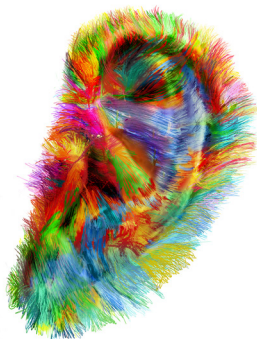
3.2

Further audiovestibular characterization of DFNB77, caused by deleterious variants in *LOXHD1*, and investigation into the involvement of fuchs corneal dystrophy in carriers

Mieke Wesdorp, Vivian Schreur, Andy J. Beynon, Jaap Oostrik, Jiddeke M. van de Kamp, Mariet W. Elting, Marie-José H. van den Boogaard, Ilse Feenstra, Ronald J.C. Admiraal, Henricus P.M. Kunst, Carel B. Hoyng, Hannie Kremer, Helger G. Yntema*, Ronald J.E. Pennings* and Margit Schraders*

* These authors contributed equally to this work

Abstract

This study focuses on further characterization of the audiovestibular phenotype and on genotype-phenotype correlations of DFNB77, an autosomal recessive type of hereditary hearing impairment (HI). DFNB77 is associated with disease-causing variants in *LOXHD1*, and is both genetically and phenotypically highly heterogeneous. So far, a clear correlation between variant- and phenotypic characteristics has not been established. Heterozygous deleterious missense variants in *LOXHD1* have been associated with late-onset Fuchs corneal dystrophy (FCD). However, up to now screening for FCD of heterozygous carriers in DFNB77 families has not been reported. Enhanced knowledge on phenotype characteristics, potential genotype-phenotype correlations and the involvement of FCD will lead to improved care and personal counseling of patients and their relatives. This study describes the genotype, and audiometric and vestibular phenotypes of nine families with HI, caused by pathogenic variants in *LOXHD1*. In addition, carriers within the families were screened for FCD. Fifteen pathogenic missense and truncating variants were identified, of which twelve were novel. The hearing phenotype showed high inter- and intrafamilial variation in severity and progression, which could not be related to the type or location of the variant. There was no evidence for involvement of the vestibular system. None of the carriers showed (preclinical) symptoms of FCD. Our findings expand the genotypic and phenotypic spectrum of DFNB77, but a clear correlation between the type or location of the variant and the severity or progression of HI could not be established. We hypothesize that environmental factors or genetic modifiers are responsible for phenotypic differences. No association was found between heterozygous pathogenic variants in *LOXHD1* and the occurrence of FCD in carriers.

Introduction

Nonsyndromic hereditary hearing impairment (HI) is clinically and genetically very heterogeneous. Currently, more than 100 genes (http://hereditaryhearingloss.org/) have been associated with this disorder and for many of the genes only a single or a few families have been described. As a result, knowledge on genotype-phenotype correlations for many forms of hereditary HI is limited. This hampers evidence-based counseling on prognosis and rehabilitation options.[1] The introduction of massive parallel sequencing approaches, such as whole exome sequencing (WES), has enabled efficient molecular diagnosis for hereditary HI.[2,3] The number of families or patients with a genetic diagnosis will thus increase, allowing the determination of novel and more detailed genotype-phenotype correlations.

DFNB77 (MIM #613079) is an example of an autosomal recessive type of nonsyndromic HI, of which knowledge on its genotype-phenotype correlation is limited due to its rareness. It is known to be caused by deleterious truncating and missense variants in *LOXHD1* (MIM #613072).[4] *LOXHD1* encodes lipoxygenase homology domain 1, which consists of 15 PLAT (polycystin-1, lipoxygenase, alpha-toxin) domains. PLAT domains are thought to target proteins to the plasma membrane and mediate protein interactions.[5-7] Based on studies in mice, it is known that *Loxhd1* is mainly expressed in stereocilia of cochlear hair cells and plays an important role in maintaining normal hair cell function. Mice with homozygous *Loxhd1* missense variants are profoundly deaf from an early age.[4] To date, 41 cases with DFNB77 from 22 families have been reported worldwide, harboring 27 different disease-causing variants.[4,8-18] In 17 of these families the auditory characteristics have been described, showing different audiometric phenotypes, varying from mild to profound and stable to progressive sensorineural HI.[4,8,9,11,12,14-17] So far, a clear correlation between variant- and phenotypic characteristics has not been established.

Variants in *LOXHD1* have not only been linked to HI; Riazuddin *et al.* (2012) associated heterozygous pathogenic missense variants in *LOXHD1* with dominantly inherited late-onset Fuchs corneal dystrophy (FCD).[19] FCD is a genetic disorder of the corneal endothelium and is characterized by an increasing number of central corneal guttae, which are excrescences of Descemet's membrane. In more advanced stages of the disease it can be accompanied by corneal edema.[20] The onset of FCD is generally in the fourth or fifth decade of life. Over time, corneal edema and endothelial loss lead to deterioration of visual acuity and can eventually lead to painful epithelial bullae.[20] Riazuddin *et al.* (2012) demonstrated that a heterozygous pathogenic variant in *LOXHD1* segregated in a multiplex family with autosomal dominant late-onset FCD. Subsequent screening of sporadic cases with late

onset FCD and unaffected, unrelated control samples revealed that in both groups rare missense variants occur, which were predicted to be damaging. However, the variant load in affected individuals was significantly higher (7.5% versus 2.7%, p = 0.003).[19] Expression of *LOXHD1* was demonstrated in human corneal endothelium and in mouse corneal epithelial and endothelial cells. Results of corneal immunohistochemistry led to the hypothesis that allelic deleterious variants of *LOXHD1* lead to protein aggregation in the endothelium and Descemet membrane, which might have long-term cytotoxic effects.[19]

It is essential to determine whether family members who carry a heterozygous pathogenic variant in *LOXHD1* are at risk of FCD. Besides, further characterization of the audiovestibular phenotype and investigation of potential genotype-phenotype correlations of DFNB77 is needed in order to enable personal and evidence-based counseling of patients and their relatives with deleterious variants in *LOXHD1*. The present study evaluated the audiovestibular phenotype of nine families with DFNB77, mainly of Dutch origin, with novel and known compound heterozygous pathogenic variants in *LOXHD1*. Characterization of the phenotype was established by otoscopic evaluation, audiometric analyses and vestibular testing. Heterozygous carriers of pathogenic variants in *LOXHD1* were evaluated for presence of FCD.

Subjects and methods

Subject evaluation
Medical history was obtained from all participants, using a questionnaire focusing on hearing and balance, and otoscopic examination and external ear inspection was performed in all subjects. Special attention was paid to possible causes of acquired deafness.

Pure-tone audiometry was performed in a sound-treated room according to the ISO 8253-1:2010 standard. Air conduction thresholds were determined at 0.25, 0.5, 1, 2, 4, and 8 kHz in dB HL. Bone conduction thresholds were determined at 0.5, 1, 2, 4, and 8 kHz in dB HL, to determine if the HI had a conductive component. The better hearing ear was defined using the mean air conduction thresholds averaged over the frequencies of 0.5, 1, 2 and 4 kHz. HI characteristics were described according to the recommendations of the GENDEAF study group.[21] In the index cases of families 5 and 7, hearing was evaluated by click-evoked Brainstem Evoked Response Audiometry (BERA) because of young age, according to current standards[22], and severity of HI was based on the BERA thresholds, displaying hearing thresholds at about 3 kHz. Individual progression of HI was calculated with longitudinal linear regression analyses, using all available audiograms for the better hearing ear. Audiograms were used only if they were obtained after the age of 5 years. The

onset level of HI (threshold intercept, in dB HL at age 0 years) and progression of HI (slope in dB/year) were determined for each frequency (0.25, 0.5, 1, 2, 4 and 8 kHz). Progression of HI was considered to be significant, if the regression coefficient differed significantly (p ≤ 0.05) from 0 for at least two of the six evaluated frequencies, and if the slopes were positive.

Vestibular function was assessed with cervical vestibular evoked myogenic potentials (cVEMP; Interacoustics EP25, Denmark), video head impulse test (Ulmer vHIT, Synapsys, France) and electronystagmography (ENG; BalanceLab, Ekida, Germany) in one affected individual per family and in both affected siblings of family 8. ENG consisted of rotary chair testing (trapezium stimulated velocity step test: acceleration of $2°/s^2$, deceleration of $-200°/s^2$, with an adaptation time of 60 seconds and a velocity of 90°/s) and caloric tests with water irrigation (cold 30°C and warm 44°C, 30 seconds irrigation).[23] Prior to vestibular testing, oculomotor testing was performed to exclude central lesions. Vestibular function was defined as abnormal when slow phase velocities of the nystagmus elicited by caloric irrigation was less than 10°/s or 7°/s (hyporeflexia) or more than 52°/s or 31°/s (hyperreflexia) for warm and cold water irrigation, respectively. Rotary chair testing was considered to be significantly deviant when the gain was less than 33% (hyporeactivity) or more than 72% (hyperreactivity), maximum velocity at deceleration less than 30°/s or more than 65°/s, and decay time less than 11 seconds or more than 26 seconds. cVEMP responses were elicited using 500 Hz tone burst stimuli with 6 ms duration (1 cycle rise/fall, 1 cycle plateau) at a presentation rate of 5.1 Hz. EMG responses were band pass filtered between 10 Hz and 750 Hz, and typical P13/N23 peaks were obtained in steps of 2 dBnHL down to threshold level. Peak-to-peak (P-P) amplitudes of the P13/N23 component were used to determine cVEMP thresholds. To compare cVEMPs from both sides, P-P amplitudes were corrected and normalized for interaural differences in background EMG activity. cVEMP responses were defined as abnormal when thresholds were lower than 82 dBnHL or higher than 100 dBnHL.[24] Responses to the video head impulse tests were defined as abnormal when the gain of the vestibulo-ocular reflex (*i.e.* head/ eye movement) was less than 0.72 for each of the three semicircular canals.

Parents of affected individuals, who carry a heterozygous deleterious variant in *LOXHD1*, were assessed for presence of FCD. They were asked to fill out a questionnaire focusing on vision problems. Slit lamp biomicroscopy was performed to evaluate the presence of FCD. To support the diagnosis, specular microscopy was performed in order to visualize corneal endothelial cells and assess the endothelial cell density. All hearing impaired individuals were younger than the described age of onset of FCD and were therefore not examined.

This study was approved by the medical ethics committee of the Radboud university medical center and is in accordance with the principles of the World Medical Association

Declaration of Helsinki. Written informed consent was obtained from all participants or their legal representatives.

Whole Exome Sequencing
Genomic DNA was isolated from peripheral blood using standard techniques. In the index cases of families 1, 2, 4–7 and 9, whole exome sequencing (WES) was performed. First, the exome was enriched using the Agilent SureSelect version 4 kit. Subsequently, WES was performed on an Illumina HiSeq system by BGI-Europe (Denmark). A panel of 120 (DGD_200614), 123 (DGD_250214) or 127 (DGD_141114) HI-related genes was analyzed and variants were selected based on variant classification guidelines.[25] A list of analyzed genes can be found at https://www.radboudumc.nl/Informatievoorverwijzers/Genoom-diagnostiek/en/Pages/Hearingimpairment.aspx. The index cases of families 1, 6 and 7 have been reported previously.[3] The identified variants in *LOXHD1* (NM_144612.6 and NM_001145472.2) were confirmed using PCR and sequence analysis, as described below.

STR-marker analysis for LOXHD1
Short Tandem Repeat (STR) markers flanking *LOXHD1,* D18S1145, D18S1143, D18S970, and D18S470, were genotyped under standard PCR conditions and analyzed on an ABI Prism 3730 Genetic Analyzer. The alleles were assigned with GeneMapper software (Applied Biosystems, Foster City, CA, USA) according to the manufacturer's protocol.

PCR and sequence analysis
Amplification of all exons and exon-intron boundaries of *LOXHD1* was performed using standard PCR conditions. PCR fragments were purified with Exonuclease I and FastAP™ (Thermo Fisher Scientific, Waltham, MA, USA) according to the manufacturer's protocol. Sequence analysis was performed with the ABI PRISM BigDye Terminator Cycle Sequencing V2.0 Ready Reaction kit and analyzed with the ABI PRISM 3730 DNA analyzer (Applied Biosystems Foster City, CA, USA). For all families in which the index patient carried putative pathogenic variants in *LOXHD1*, segregation analysis in available family members was performed to determine zygosity and co-segregation of the variant with the HI in the family using PCR and sequence analysis as described above. Primer sequences and PCR conditions are available upon request.

Minigene Construction and Splicing Assay
To determine the effect of the synonymous c.5934C>T variant on splicing, a minigene was constructed and a splicing assay was performed, as described previously.[37] A PCR amplified fragment of wild-type *LOXHD1* exons 38 and

39, along with flanking intronic sequences, was generated with the following primers: 5'-   GGGGACAAGTTTGTACAAAAAAGCAGGCTTCatctccattttgcatctcacc-3' and 5'-   GGGGACCACTTTGTACAAGAAAGCTGGGTCcagatggaccattggattacc-3'. This fragment was inserted in a pCI-NEO vector between exons 3 and 5 of RHO. The c.5934C>T variant was introduced with site-directed mutagenesis using primers 5'-ggctcatcctggagggtaggaagaaccgatcc-3' and 5'- ggatcggttcttcctaccctccaggatgagcc-3', and using Q5® High-Fidelity DNA Polymerase (New England Biolabs, Ontario, Canada). Recombinant vectors were employed for transfection of HEK293T cells, which were incubated at 37 oC for 24 hours. RNA was isolated from transfected cells and reverse transcribed into cDNA. Primers 5'-cggaggtcaacaacgagtct-3' and 5'-aggtgtaggggatgggagac-3' were used to amplify and sequence the amplified cDNA fragments of exon 38-39 of *LOXHD1*, along with flanking RHO sequences as present in the vector. The RT-PCR fragments were excised from gel and purified using a Qiaquick gel extraction kit (Qiagen, Hilden, Germany) according to the manufacturer's protocol prior to sequencing.

3.2

Results

LOXHD1 variants

Nine families with DFNB77, comprising of 14 affected individuals, were included in this study (Figure 1). *LOXHD1* variants that were predicted to be damaging were identified in seven families by WES targeting a HI gene panel. In a parallel approach a panel of seven families with progressive HI was tested for possible linkage to the DFNB77 locus. In five families linkage to *LOXHD1* could not be excluded and *LOXHD1* variant analysis of the index case was performed. This resulted in the identification of variants in two additional families (Figure 1 and Table 1). All variants were detected in a compound heterozygous state and all segregated with HI in the families. In total, fifteen missense and truncating variants were identified, of which twelve were novel. All patients carried a missense variant in one *LOXHD1* allele. The type of variant on the second allele varied; nonsense (3 families), canonical splice site (2 families), missense (2 families), frameshift (1 family) and synonymous (1 family) variants were identified. The synonymous variant was predicted to introduce a novel splice donor site (Supplemental Figure 1a). Usage of this splice site would lead to a frameshift and a premature stop codon. To determine the effect of this synonymous variant a minigene approach was used. This showed correct splicing of the wild-type exon 38, while the c.5934C>T variant indeed abolished normal splicing (Supplemental figure 1b) by usage of the predicted novel splice donor site.
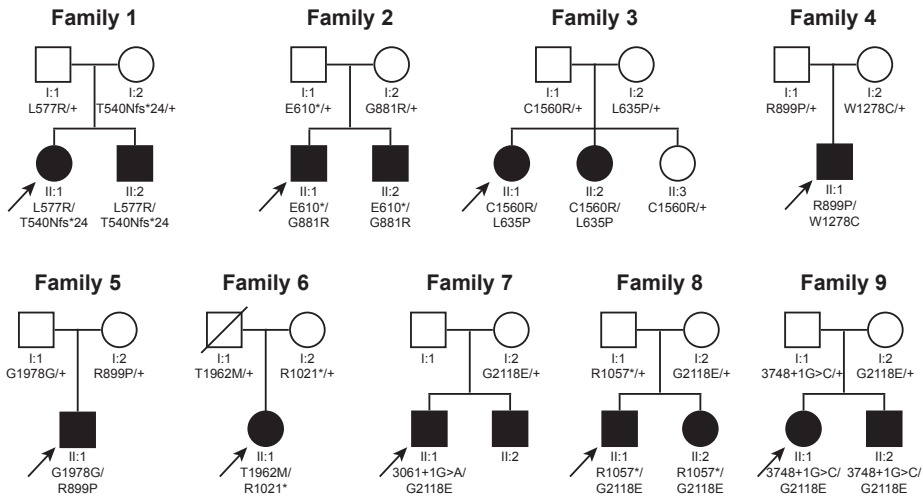
Figure 1 Families and identified pathogenic variants in *LOXHD1*

Pedigrees of nine families with DFNB77 and segregation analyses of the identified variants in *LOXHD1*. Only those family members are depicted who were relevant for the study. I:1 and II:2 of family 7 did not participate in genetic analysis. Index cases are indicated by arrows. + means wild-type.
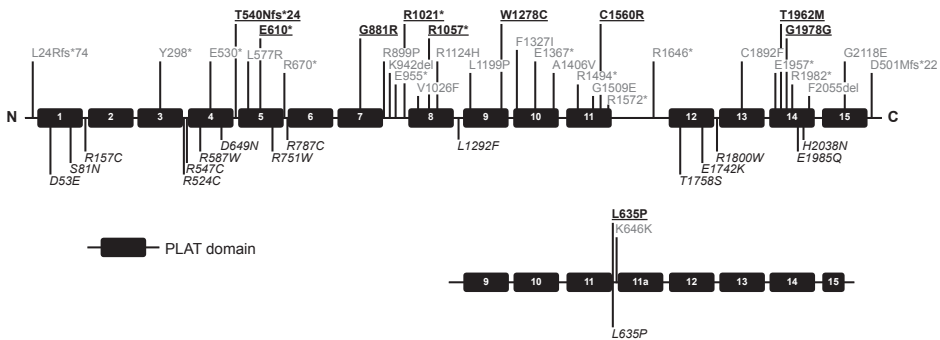
Figure 2 Deleterious variants in *LOXHD1* associated with DFNB77 and FCD

Schematic representations of two of the five LOXHD1 protein isoforms (NP_653213.6, known as isoform 1; and NP_001138944.1, known as isoform 2) and identified pathogenic variants in *LOXHD1*. Two variants (L635P and splice site variant K646K), only affect the shorter isoform 2; the L635P variant has also been reported in a subject with FCD.[19] PLAT protein domains are predicted with Pfam 29.0 (http://pfam.xfam.org/) and are numbered. Previously published variants associated with DFNB77 are depicted in grey, published variants associated with FCD are depicted in italic, and novel variants identified in this study are underlined.

Table 1 Identified compound heterozygous variants in *LOXHD1*

Family	Nucleotide change (protein change)	Type of variant	ExAC MAF all pop. (%)	ExAC MAF ENF pop. (%)	PhyloP[a]	Grantham[b]	Polyphen-2[c]	SIFT[d]	CADD[e]	In PLAT domain	Variant analysis[f]
1[g]	c.1618dup (p.Thr540Asnfs*24)	frameshift	0	0	NA	NA	NA	NA	35.0	NA	WES, DGD_200614
	c.1730T>G (p.Leu577Arg)[h]	missense	0.005	0.011	4.81	102	0.999	deleterious (0)	23.8	yes	WES, DGD_200614
2	c.1828G>T (p.Glu610*)	nonsense	0	0	NA	NA	NA	NA	42.0	NA	WES, DGD_200614
	c.2641G>A (p.Gly881Arg)	missense	0.006	0.016	1.58	125	0.778	tolerated (0.06)	20.0	yes	WES, DGD_200614
3	c.1904T>C (p.Leu635Pro)[i] NM_001145472.2	missense	0.037	0.035	4.64	98	0.978	deleterious (0)	25.2	no	panel screening
	c.4678T>C (p.Cys1560Arg)	missense	0	0	4.64	180	0.999	deleterious (0)	26.8	yes	
4	c.2696G>C (p.Arg899Pro)[h]	missense	0	0	1.58	103	0.980	deleterious (0.02)	20.5	no	WES, DGD_250214
	c.3834G>C (p.Trp1278Cys)	missense	0	0	5.69	215	1.000	deleterious (0)	32.0	yes	
5	c.2696G>C (p.Arg899Pro)[h]	missense	0	0	1.58	103	0.980	deleterious (0.02)	20.5	no	WES, DGD_141114
	c.5934C>T[k] (p.Gly1978Gly)	synonymous splice site	0	0	NA	NA	NA	NA	11.9	yes	
6[g]	c.3061C>T (p.Arg1021*)	nonsense	0	0	NA	NA	NA	NA	20.5	NA	WES, DGD_200614
	c.5885C>T (p.Thr1962Met)	missense	0.004	0	5.37	81	1.000	deleterious (0)	34.0	yes	WES, DGD_200614

Table 1 (continued)

Family	Nucleotide change (protein change)	Type of variant	ExAC MAF all pop. (%)	ExAC MAF ENF pop. (%)	PhyloP[a]	Grantham[b]	Polyphen-2[c]	SIFT[d]	CADD[e]	In PLAT domain	Variant analysis[f]
7[g]	c.3061+1G>A p.(?)	canonical splice site	0	0	NA	NA	NA	NA	21.4	NA	WES, DGD_200614
	c.6353G>A (p.Gly2118Glu)[h]	missense	0.005	0.011	5.77	98	1.000	deleterious (0)	32.0	yes	
8	c.3169C>T (p.Arg1057*)	nonsense	0	0	NA	NA	NA	NA	19.9	NA	panel screening
	c.6353G>A (p.Gly2118Glu)	missense	0.005	0.011	5.77	98	1.000	deleterious (0)	32.0	yes	
9	c.3748+1G>C p.(?)	canonical splice site	0	0	NA	NA	NA	NA	24.2	NA	WES, DGD_141114
	c.6353G>A (p.Gly2118Glu)	missense	0.005	0.011	5.77	98	1.000	deleterious (0)	32.0	yes	

ExAC MAF, minor allele frequency from the Exome Aggregation Consortium; pop., population; ENF, European non-Finnish; NA, not applicable; WES, whole exome sequencing. [a-e]Higher scores are considered more deleterious. [a]PhyloP score represents the evolutionary conservation of the mutated residue; a higher score means that nucleotide is better conserved.[26] [b]Grantham score is a prediction of the effect of substitutions between amino acids; a higher score reflects a greater evolutionary distance between the wild-type and the mutant amino acid.[27] [c]Polyphen-2 is a pathogenicity score based on sequence conservation and structural properties of the mutated amino acid.[28] [d]SIFT is a pathogenicity score that is exclusively based on sequence conservation.[30] [f]DGD means genelist used for WES analysis (genelists can be found at https://www.radboudumc.nl/Informatievoor-verwijzers/Genoomdiagnostiek/en/Pages/Hearingimpairment.aspx). [g]Families 1, 6 and 7 have been reported previously (Seco *et al.* 2016). [h]Reported previously by Sloan-Heggen *et al.* 2016. [i]This variant does not affect the longest LOXHD1 isoform (NM_144612.6); [k]this variant introduces a splice donor site in exon 38.

Clinical history

HI was diagnosed in the affected subjects between 0 and 5 years. The affected sibling (II:2) of family 7 did not participate in clinical evaluation, but had congenital HI, according to information provided by the parents. In the individuals with a congenital onset (n=8), HI was discovered after failed neonatal hearing screening. The subjects who were diagnosed in the first years after birth did not have neonatal hearing screening (family 2 and 3), or the results of the screening were inconclusive (index cases of family 1 and 4). There were no known causes of acquired hearing loss identified by history or physical examination of the affected subjects. Otoscopic examination and external ear inspection were normal in all subjects. The index cases of families 5, 7 and 8 had a negative cytomegalovirus test; the other affected individuals could not be tested because of age or because the parents did not give consent. There were no associated symptoms, such as dysmorphology, delayed motor development or intellectual disability. All parents had normal hearing sensitivity. In family 1, there is a positive family history of Usher syndrome type 2, but variants in *USH2A* were ruled out previously in the affected subjects of family 1. In all other families, there were no additional relatives with childhood onset HI and there was no history of consanguinity.

Audiometric analysis

In all subjects, HI was sensorineural and symmetric. In most cases, the audiogram configuration was downsloping (Figure 3). Families 2–5 and 7 showed mild to moderate HI; in family 6 HI was severe. In families 1, 8 and 9, severity of HI varied between affected individuals. Hearing in the index cases of families 5 and 7 was assessed by click-evoked BERA (data not shown). The index case of family 5 demonstrated binaural sensorineural HI, with hearing thresholds of 30 dB HL at the age of 6 months. BERA in the index case of family 7 was performed at the age of 6 weeks, 5 months, 1 year and 3 years; all showed bilateral sensorineural HI, with thresholds of about 60 dB HL.

To determine whether HI was progressive, longitudinal linear regression analyses of hearing thresholds were performed in the affected individuals of families 1-4, 6, 8 and 9. On average, 6 audiograms per individual were available. In four of the families (2, 4, 6 and 8) HI was stable, which means that less than two out of six frequencies showed significant progression. In the index cases of families 1, 3 and 9, significant progression of HI was observed. The siblings (II:2) of families 1, 3 and 9 all demonstrated stable HI. However, the follow-up time in the cases with stable hearing loss was on average 8 years (3-17 years); hence deterioration of hearing over a longer period of time cannot be excluded in all cases (Figure 3).
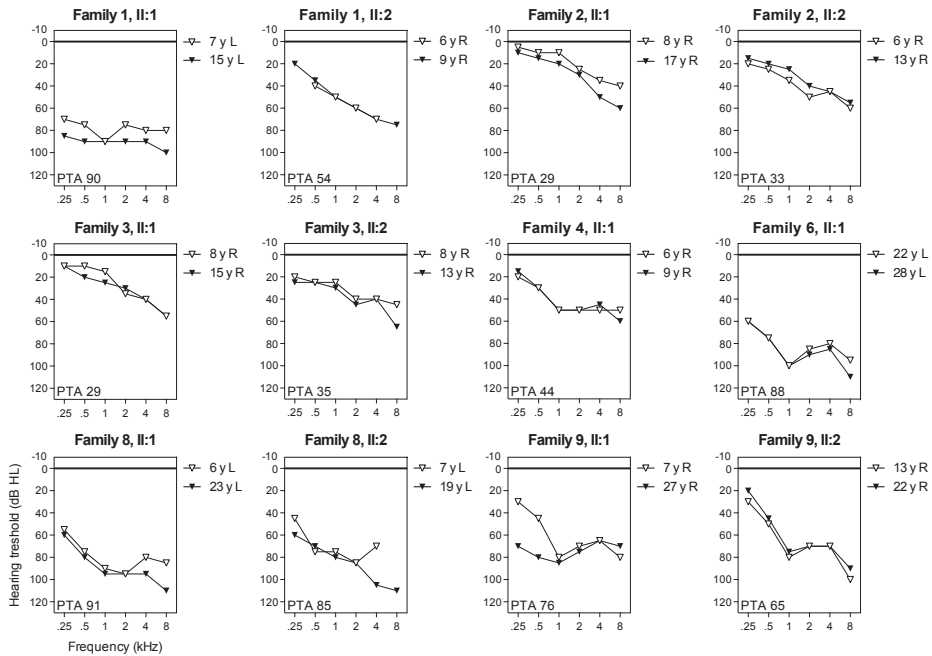
Figure 3 Hearing thresholds of affected individuals

Air conduction thresholds of the better hearing ear of all hearing impaired participants, except for the index cases of families 5 and 7, because hearing in these individuals was investigated with click-evoked BERA. The better hearing ear was determined by calculating the mean air conduction thresholds averaged over the frequencies of 0.5, 1, 2 and 4 kHz of the last audiogram. First-visit and last-visit audiograms are shown. Pure tone average (PTA) was calculated over frequencies 0.5, 1, 2 and 4 kHz of the last-visit audiogram. R, right ear; L, left ear; PTA, pure tone average.

Assessment of vestibular function

None of the affected subjects reported vestibular symptoms, including vertigo, dizziness, instability or motoric developmental delay, except for the index case of family 1 who reported motion sickness. Vestibular function of the index cases of families 1-4 and 6, and both affected siblings of family 8 was examined with ENG and cVEMP. These showed normal or slightly higher vestibular reactivity, the latter one based on higher gains measured with ENG and lower cVEMP thresholds (Table 3). There was slight asymmetry of the cVEMPS in the index cases of families 2 and 8, also after correction for muscle tone. All responses to the video head impulse test showed normal gains, demonstrating that all subjects have a normal vestibulo-ocular reflex (data not shown).

Table 2 Genotype – phenotype correlation of DFNB77

Allele 1 nucleotide change (protein change)	Allele 2 nucleotide change (protein change)	SA[a]	ExAC MAF	Ethnicity	Age of HI diagnosis	Severity of HI	Audiogram config.	Progression of HI	# of reported fam. (cases)	Ref.
c.71delT (p.Leu24Argfs*74)	c.71delT (p.Leu24Argfs*74)	yes	0.005	Turkish	NA (cong. or prel.)	NA (severe or profound)	NA	NA	1 (1)	13
c.442A>T (p.K148*)	c.4217C>T (p.Ala1406Val)*	yes	1) 0 2) 0.792	NA	NA	NA	NA	NA	1 (1)	18
c.894T>G (p.Tyr298*)	c.6353G>A (p.Gly2118Glu)	no	1) 0 2) 0.005	NA	cong.	mild - moderate	NA	NA	1 (1)	15
c.1588G>T (p.Glu530*)	c.1588G>T (p.Glu530*)	yes	0	Qatary	early onset	severe - profound	MF – HF, flattening over time	progressive	1 (3)	11
c.1618dup (p.Thr540Asnfs*24)	**c.1730T>G (p.Leu577Arg)**	**yes**	**1) 0 2) 0.005**	**Dutch**	**cong. - 1 year old**	**moderate - severe**	**HF - flat**	**stable – progressive**	**1 (2)**	**this study**
c.1730T>G (p.Leu577Arg)	c.5944C>T (p.Arg1982*)	no	1) 0.005 2) 0	NA	cong.	severe - profound	NA	NA	1 (1)	15
c.1828G>T (p.Glu610*)	**c.2641G>A (p.Gly881Arg)**	**yes**	**1) 0.000 2) 0.006**	**Dutch**	**2 - 4 years old**	**mild**	**HF**	**stable**	**1 (2)**	**this study**
c.1904T>C (p.Leu635Pro) NM_001145472.2	**c.4678T>C (p.Cys1560Arg)**	**yes**	**1) 0.037 2) 0**	**Dutch**	**2 - 3 years old**	**mild**	**HF**	**stable – progressive**	**1 (2)**	**this study**
c.1938G>A (p.Lys646Lys)[c] NM_001145472.2	c.4936C>T (p.Arg1646*)	no	1) 0 2) 0	NA	childhood	mild - moderate	NA	NA	1 (1)	15
c.2008C>T (p.Arg670*)	c.2008C>T (p.Arg670*)	yes	0	Iranian	7 - 8 years old	mild - profound	MF - HF	progressive	1 (5)	4
c.2696G>C (p.Arg899Pro)	c.3596T>C (p.Leu1199Pro)	no	1) 0 2) 0	NA	NA	NA	NA	NA	1 (1)	15
c.2696G>C (p.Arg899Pro)	**c.3834G>C (p.Trp1278Cys)**	**yes**	**1) 0 2) 0**	**Dutch**	**5 years old**	**moderate**	**MF - HF**	**stable**	**1 (1)**	**this study**
c.2696G>C (p.Arg899Pro)	**c.5934C>T (p.Gly1978Gly)**	**yes**	**1) 0 2) 0**	**Dutch**	**cong.**	**mild[±]**	**HF**	**too young to determine**	**1 (1)**	**this study**

3.2

Table 2 (continued)

Allele 1 nucleotide change (protein change)	Allele 2 nucleotide change (protein change)	SAᵃ	ExAC MAF	Etnicity	Age of HI diagnosis	Severity of HI	Audiogram config.	Progession of HI	# of reported fam. (cases)	Ref.
c.2825_2827delAGA (p.Lys942del)#	c.4217C>T (p.Ala1406Val)ᵇ	no	1) 2.700 2) 0.792	NA	childhood	mild - moderate	NA	NA	1 (1)	15
c.2863G>T (p.Glu955*)	c.2863G>T (p.Glu955*)	yes	0	Turkish	NA	NA	NA	NA	1 (2)	10
c.3061C>T (p.Arg1021*)	**c.5885C>T p.Thr1962Met**	yes	1) 0 2) 0.004	Indian	cong.	severe	MF/HF	stable	1 (1)	this study
c.3061+1G>A (p.?)	**c.6353G>A (p.Gly2118Glu)**	yes	1) 0 2) 0.005	Dutch	cong.	moderateᵈ	too young to determine	too young to determine	1 (1)	this study
c.3076G>T (p.Val1026Phe)	c.4375+1G>T (p.?)	yes	1) 0 2) 0	Japanese	3 years old	profound	downsloping	stable	1 (1)	16
c.3169C>T (p.Arg1057*)	**c.6353G>A (p.Gly2118Glu)**	yes	1) 0 2) 0.005	Dutch	cong.	severe	MF - HF	stable	1 (2)	this study
c.3371G>A (p.Arg1124His)	c.3979T>A (p.Phe1327Ile)	yes	1) 0.005 2) 0.010	Cameroonian	prel.	profound	NA	NA	1 (2)	17
c.3748+1G>C (p.?)	**c.6353G>A (p.Gly2118Glu)**	yes	1) 0 2) 0.005	Dutch	cong.	moderate - severe	MF - HF, flattening over time	stable - progressive	1 (2)	this study
c.4099G>T (p.Glu1367*)	c.6162_6164delCCT (p.Phe2055del)	no	1) 0.004 2) 0	NA	cong.	severe - profound	NA	NA	1 (1)	15
c.4212+1G>A (p.?)	c.4212+1G>A (p.?)	yes	0	Japanese	cong.	profound	all frequencies	stable	1 (2)	12
c.4212+1G>A (p.?)	c.5674G>T (p.Val1892Phe)	yes	1) 0 2) 0.005	Japanese	cong. - 7 years old	mild - profound	MF - HF	progressive	1 (2)	14
c.4480C>T (p.Arg1494*)	c.4480C>T (p.Arg1494*)	yes	0.058	Turkish	NA	NA	NA	NA	1 (2)	10
c.4480C>T (p.Arg1494*)	c.4480C>T (p.Arg1494*)	yes	0.058	NA	cong.	mild - moderate	NA	NA	1 (1)	15

3.2

Table 2 (continued)

Allele 1 nucleotide change (protein change)	Allele 2 nucleotide change (protein change)	SA[a]	ExAC MAF	Ethnicity	Age of HI diagnosis	Severity of HI	Audiogram config.	Progression of HI	# of reported fam. (cases)	Ref.
c.4480C>T (p.Arg1494*)	c.4526G>A (p.Gly1509Glu)[b]	no	1) 0.058 2) 0.609	Caucasian	40 years old	severe - profound	NA	progressive	1 (1)	9
c.4480C>T (p.Arg1494*)	c.5869G>T (p.Glu1957*)	yes	1) 0.058 2) 0	Japanese	1 - 6 years old	moderate - severe	MF - HF	stable	1 (2)	12
c.4480C>T (p.Arg1494*)	c.6598delG (p.Asp2200Metfs*2 2)	no	1) 0.058 2) 0	NA	childhood	severe - profound	NA	NA	1 (1)	15
c.4714C>T (p.Arg1572*)	c.4714C>T (p.Arg1572*)	yes	0.028	Ashkenazi Jewish	cong. - prel.	severe - profound	all frequencies	NA	2 (9)	8

Severity of HI and audiogram configuration were determined according to the recommendation of the GENDEAF study group (Mazolli *et al.* 2003).[21] SA, segregation analysis; ExAC MAF, minor allele frequency from the Exome Aggregation Consortium; audiogram config., audiogram configuration; HI, hearing impairment; fam, families; ref, references; NA, not applicable; cong, congenital; prel, prelingual; MF, mid frequency; HF, high frequency. [a]Segregation analysis performed to determine zygosity or co-segregation of the variants with the HI in the family. [b]Variant is likely benign due to high frequency in the ExAC database. [c]This variant does not affect the longest LOXHD1 isoform (NM_144612.6). [d]Severity of HI in the index cases of families 5 and 7 was based on click-evoked BERA thresholds, displaying hearing thresholds at about 3 kHz.

Table 3 Vestibular assessment

Family	Subjects	Age (yrs)	cVEMP (dBnHL)		Ny-velocity caloric irrigation (°/s)				Gain (%)		SCV (°/s)		Tau (s)	
			right	left	warm right	warm left	cold right	cold left	CW	CCW	CW	CCW	CW	CCW
			(82-100)	(82-100)	(10-52)	(10-52)	(7-31)	(7-31)	(33-72)	(33-72)	(30-65)	(30-65)	(11-26)	(11-26)
1	II:1	15	77	80	30	46	21	21	72	57	65	52	17	14
2	II:1	17	95	82	15	25	14	19	22	42	20	38	27	13
3	II:1	15	80	77	33	24	17	20	46	80	42	73	18	16
4	II:1	9	82	82	NA	NA	24	32	117	106	106	96	11	13
8	II:1	23	97	87	20	13	17	17	90	78	81	70	14	13
8	II:2	19	87	87	33	39	34	28	68	76	61	68	17	15

Thresholds of cVEMPs, nystagmus velocity of caloric irrigational testing at culmination point, Gain, Slow Component Velocity of nystagmus at time of deceleration (SCV) and time constant (tau) after rotary chair velocity step testing. Yrs, years; CW, clockwise; CCW, counter-clockwise; normative values are shown in parentheses; NA, not available.

Ophthalmological evaluation

The parents of families 1–4, 8 and the mother (I:2) of family 6 (n=11) were examined for symptoms of FCD (Table 4). The age of the parents ranged from 39 to 56 years, with a median age of 48 years. None of the parents had symptoms of blurred vision, glare, distorted vision or pain in the eye. Ophthalmological examination with slit lamp biomicroscopy in all parents was normal, and did not show any signs of FCD. Specular microscopy of endothelial cells showed normal appearance and density. History taking revealed that also none of the grandparents suffered from FCD or symptoms resembling FCD.

Table 4 Evaluation of pathogenic *LOXHD1* variant carriers for FCD

Family	Subject	nucleotide change (protein change)	Type of variant	Age at time of assessment for FCD (years)	Endothelial cell count (cells/mm^2)
1	I:1	c.1730T>G (p.Leu577Arg)	missense	44	OD 3091 OS 3055
	I:2	c.1618dup (p.Thr540Asnfs*24)	frameshift	44	OD 2744 OS 2593
2	I:1	c.1828G>T (p.Glu610*)	nonsense	50	OD 3138 OS 2870
	I:2	c.2641G>A (p.Gly881Arg)	missense	50	OD 3099 OS 2556
3	I:1	c.4678T>C (p.Cys1560Arg)	missense	48	OD 2541 OS 2716
	I:2	c.1904T>C (p.Leu635Pro)[a]	missense	48	OD 2400 OS 2827
4	I:1	c.2696G>C (p.Arg899Pro)	missense	39	OD 3234 OS 3375
	I:2	c.3834G>C (p.Trp1278Cys)	missense	40	OD 3081 OS 3451
6	I:2	c.3061C>T (p.Arg1021*)	nonsense	56	OD 3328 OS 3882
8	I:1	c.3169C>T (p.Arg1057*)	nonsense	52	OD 2458 OS 2300
	I:2	c.6353G>A (p.Gly2118Glu)	missense	49	OD 3231 OS 2808

Endothelial cell density (cells/mm^2) determined with specular microscopy. The healthy endothelium has a hexagonal cell pattern and normal endothelial cell density in adults ranges from 2000 to 4000 cells/mm^2.[31,32] In FCD, variation in endothelial cell size and shape can be seen, as well as a decreased endothelial cell density.[33,34]
[a]The c.1904T>C (NM_001145472.2) variant only affects two of the five LOXHD1 isoforms (transcript variants 2 and 5, UCSC Genome Browser).

Discussion

In this study, we present nine families with hereditary HI caused by compound heterozygous deleterious variants in *LOXHD1*. Different types of pathogenic variants were identified, namely truncating, splice site and missense variants, which is in line with previously published *LOXHD1* genotypes.[9,14-17] Twelve of the identified variants were novel. The c.1904T>C (NM_001145472.2) variant identified in family 3 only affects two of the five LOXHD1 isoforms (transcript variants 2 and 5, UCSC Genome Browser). The pathogenicity of this variant is therefore uncertain, however the allele frequency in control populations is very low (EXAC, http://exac.broadinstitute.org/) and the variant co-segregates with another missense variant in this family.

Table 2 presents an overview of the (likely) causative *LOXHD1* variants that have been reported in this study and previous studies. The causality of several published variants could be questioned, as in some studies segregation analysis was not performed and consequently the bi-allelic origin of the variants and segregation with the HI in the family is not proven. In addition, three of these variants (c.2825_2827delAGA, c.4217C>T and c.4526G>A) are found relatively frequently in control populations (EXAC database, all populations 2.70%, 0.79% and 0.61%, respectively), which makes it unlikely that these variants are pathogenic (Table 2).

The affected individuals were diagnosed with HI at birth or in the first years of life. It is not unlikely that the individuals with non-congenital HI in fact have congenital HI, but that delayed diagnosis occurred due to lack of neonatal hearing screening or inconclusive test results. In literature, the reported onset of HI is mainly congenital, but varies from congenital to 8 years old (Table 2).[4,8,12-17] One individual, described by Eppsteiner *et al.* (2012), had progressive HI that started at the age of 40 years.[9] However, the pathogenicity of one of the reported variants in this individual can be questioned, because the minor allele frequency of the c.4526G>A variant is rather high (ExAC database, all populations 0.61%, 3 times homozygous). Moreover, the two reported variants might reside on the same allele, as both variants have been reported before in homozygous state in another individual (Table 2).[15] Audiometry performed in our study demonstrated that mainly the high frequencies are affected, although in some cases the mid frequencies and/or low frequencies are equally affected. Audiometric analyses revealed interfamilial and intrafamilial variation in severity and progression of HI. Severity varied from mild to profound and progression varied from stable to progressive HI in some frequencies. This phenotypic variability and audiogram configuration is in line with previous research on DFNB77 (Table 2).[4,8-14,16,17]

To explain the variation in phenotype, we sought to identify genotype characteristics that correlate with the severity of HI. First of all, the type of variant (truncating *versus*

missense variant) does not seem to explain the severity of HI. Comparing families 2, 3 and 4 shows that the combination of a truncating and a missense variant can be associated with the same audiometric phenotype as two missense variants (Table 2, Figure 3). Besides, the combination of a truncating and a missense variant can lead to different audiometric phenotypes. This is illustrated by the affected individuals from family 2 and 8, who all have a nonsense and a missense variant, but show mild *versus* severe HI, respectively (Table 2, Figure 3). Second, the location of the missense variants (*i.e.* in or outside a PLAT domain) does not correlate with the severity of the phenotype. This is illustrated by families 2, 8 and 9, who all have a truncating variant and a missense variant in a PLAT domain, but demonstrate a completely different phenotype with mild stable *versus* severe *versus* moderate progressive to severe HI, respectively (Figure 2, Figure 3).

Even between affected individuals from the same family large variation is seen in the HI phenotype (*e.g.* family 1). The same deleterious variants can thus lead to different phenotypes, indicating that other factors are probably underlying the phenotypic differences. These could be genetic factors (*e.g.* genetic modifiers) or environmental factors. Almost all of the missense variants are located within the PLAT domains of the LOXHD1 protein. These domains are known to be mostly involved in lipid binding, but also protein binding and protein localization have been described.[5,7,35,36] Possibly, variants in other genes encoding proteins that interact with the PLAT domains influence the phenotype of DFNB77. Identification of these "modifiers" would require studies in large cohorts of patients with deleterious *LOXHD1* variants.

Previous studies on the DFNB77 phenotype reported no vestibular symptoms[4,11,12], however, objective evaluation of vestibular function was not reported. In the present study, ENG and cVEMP were performed in seven affected individuals and revealed normal or even increased vestibular reactivity (Table 3). These findings, in combination with the lack of complaints, suggests that the vestibular organ is not affected by disease-causing variants in *LOXHD1*.

We could not find an association between heterozygous pathogenic variants in *LOXDH1* and FCD. In none of the parents, who are carriers of a deleterious heterozygous missense or truncating variant in *LOXHD1,* was FCD present. This is in contrast to previous research by Riazuddin *et al.* (2012), who showed that pathogenic heterozygous missense variants are associated with dominantly inherited late-onset FCD.[19] At the time of our ophthalmological examination, the median age of the parents was 48 years (Table 4). Since the first signs of late-onset FCD generally appear in the fourth or fifth decade of life, it could be expected that (preclinical) symptoms of FCD would be detectable at the age of the examined individuals, if FCD was present. In addition, none of the grandparents suffered from FCD or

had symptoms resembling FCD.

Since eye abnormalities nor FCD have been reported in previous research on DFNB77 and could also not be confirmed in this study, monogenic involvement of deleterious *LOXHD1* variants in FCD is unlikely. As described by Riazuddin *et al.* (2012)*, LOXHD1* variants were found in both individuals with FCD and unaffected subjects, with a significantly higher variant load in affected subjects (7.5% versus 2.7%, respectively).[19] This could suggest that heterozygous pathogenic variants in *LOXHD1* are a risk factor for FCD. However, we cannot exclude that the association between rare allelic variants in *LOXDH1* and FCD are related to specific variants in *LOXHD1*. There is no overlap between the missense variants identified by Riazuddin *et al.* and the variants identified in this study, except for the c.1904T>C (p.Leu635Pro) variant, which only affects two smaller isoforms of *LOXHD1* (transcript variant 2 and 5). This pathogenic variant was found in family 3, and was inherited from the mother (I:2) who carried the variant heterozygously. Although the mother was already 48 years during the time of examination no symptoms of FCD were found. This strengthens the hypothesis that rare *LOXHD1* alleles are a risk factor for FCD, rather than a monogenic cause.

Based on type and location of variants, we could not find clear differences between variants associated with FCD and with DNB77 (Figure 2). However, since homozygous truncating variants of *LOXHD1* have been associated with DFNB77, it could be argued that all *LOXHD1* variants associated with HI, including missense variants, are null variants. Riazuddin *et al.* (2012) described that subjects with FCD and mono-allelic missense variants of *LOXHD1* have multiple corneal aggregates, most likely due to the increased LOXHD1 protein levels in FCD subjects.[19] This could indicate a gain-of-function effect of these variants. Therefore, one could hypothesize that bi-allelic loss-of-function variants cause HI, whereas mono-allelic gain-of-function variants are a risk factor for FCD. Further research into the effect of the variants on protein function is needed to confirm or reject this hypothesis.

In conclusion, our study confirms that the HI phenotype associated with deleterious variants in *LOXHD1* can differ in onset, type and severity. No clear genotype-phenotype correlation could be established based on type or location of the variant and severity or progression of HI. Extensive vestibular examination confirmed that vestibular function is not affected in DFNB77. In addition, no association was found in this study between pathogenic *LOXHD1* variants and FCD.

Acknowledgements

Web resources

3.2

The URLs for data presented herein are as follows:
ExAC Browser, http://exac.broadinstitute.org/
Pfam, http://pfam.xfam.org/
OMIM, http://www.omim.org/
OMIM Phenotypic Series, http://www.omim.org/phenotypicSeriesTitle/all
UCSC Genome Browser, http://genome.ucsc.edu

References

1. Toriello HV, Smith SD. *Hereditary Hearing Loss and Its Syndromes.* Third edition ed. New York: Oxford University Press; 2013.

2. Shearer AE, DeLuca AP, Hildebrand MS, et al. Comprehensive genetic testing for hereditary hearing loss using massively parallel sequencing. *Proceedings of the National Academy of Sciences of the United States of America.* Dec 07 2010;107(49):21104-21109.

3. Zazo Seco C, Wesdorp M, Feenstra I, et al. The diagnostic yield of whole-exome sequencing targeting a gene panel for hearing impairment in The Netherlands. *European journal of human genetics : EJHG.* Dec 21 2016.

4. Grillet N, Schwander M, Hildebrand MS, et al. Mutations in LOXHD1, an evolutionarily conserved stereociliary protein, disrupt hair cell function in mice and cause progressive hearing loss in humans. *American journal of human genetics.* Sep 2009;85(3):328-337.

5. Bateman A, Sandford R. The PLAT domain: a new piece in the PKD1 puzzle. *Current biology : CB.* Aug 26 1999;9(16):R588-590.

6. Hu J, Barr MM. ATP-2 interacts with the PLAT domain of LOV-1 and is involved in Caenorhabditis elegans polycystin signaling. *Molecular biology of the cell.* Feb 2005;16(2):458-469.

7. Aleem AM, Jankun J, Dignam JD, et al. Human platelet 12-lipoxygenase, new findings about its activity, membrane binding and low-resolution structure. *Journal of molecular biology.* Feb 8 2008;376(1):193-209.

8. Edvardson S, Jalas C, Shaag A, et al. A deleterious mutation in the LOXHD1 gene causes autosomal recessive hearing loss in Ashkenazi Jews. *American journal of medical genetics. Part A.* May 2011;155A(5):1170-1172.

9. Eppsteiner RW, Shearer AE, Hildebrand MS, et al. Prediction of cochlear implant performance by genetic mutation: the spiral ganglion hypothesis. *Hearing research.* Oct 2012;292(1-2):51-58.

10. Diaz-Horta O, Duman D, Foster J, 2nd, et al. Whole-exome sequencing efficiently detects rare mutations in autosomal recessive nonsyndromic hearing loss. *PloS one.* 2012;7(11):e50628.

11. Vozzi D, Morgan A, Vuckovic D, et al. Hereditary hearing loss: a 96 gene targeted sequencing protocol reveals novel alleles in a series of Italian and Qatari patients. *Gene.* Jun 1 2014;542(2):209-216.

12. Mori K, Moteki H, Kobayashi Y, et al. Mutations in LOXHD1 gene cause various types and severities of hearing loss. *The Annals of otology, rhinology, and laryngology.* May 2015;124 Suppl 1:135S-141S.

13. Atik T, Onay H, Aykut A, et al. Comprehensive Analysis of Deafness Genes in Families with Autosomal Recessive Nonsyndromic Hearing Loss. *PloS one.* 2015;10(11):e0142154.

14. Minami SB, Mutai H, Namba K, Sakamoto H, Matsunaga T. Clinical characteristics of a Japanese family with hearing loss accompanied by compound heterozygous mutations in LOXHD1. *Auris, nasus, larynx.* Mar 10 2016.

15. Sloan-Heggen CM, Bierer AO, Shearer AE, et al. Comprehensive genetic testing in the clinical evaluation of 1119 patients with hearing loss. *Human genetics.* Apr 2016;135(4):441-450.

16. Sakuma N, Moteki H, Takahashi M, et al. An effective screening strategy for deafness in combination with a next-generation sequencing platform: a consecutive analysis. *Journal of human genetics.* Mar 2016;61(3):253-261.

17. Lebeko K, Sloan-Heggen CM, Noubiap JJ, et al. Targeted genomic enrichment and massively parallel sequencing identifies novel nonsyndromic hearing impairment pathogenic variants in Cameroonian families. *Clinical genetics.* Sep 2016;90(3):288-290.

18. Posey JE, Harel T, Liu P, et al. Resolution of Disease Phenotypes Resulting from Multilocus Genomic Variation. *The New England journal of medicine.* Jan 05 2017;376(1):21-31.

19. Riazuddin SA, Parker DS, McGlumphy EJ, et al. Mutations in LOXHD1, a recessive-deafness locus, cause dominant late-onset Fuchs corneal dystrophy. *American journal of human genetics.* Mar 9 2012;90(3):533-539.

20. Krachmer JH, Purcell JJ, Jr., Young CW, Bucher KD. Corneal endothelial dystrophy. A study of 64 families. *Archives of ophthalmology.* Nov 1978;96(11):2036-2039.

21. Mazzoli M, Van Camp G, Newton V, Giarbini N, Declau F, Parving A. Recommendations for the description of genetic and audiological data for families with nonsyndromic hereditary hearing impairment. *Audiological Medicine.* 2003;1:148-150.

22. Hall JW. *New Handbook of Auditory Evoked Responses.* Boston, USA: Pearson Allyn & Bacon Publishers; 2006.

23. Theunissen EJ, Huygen PL, Folgering HT. Vestibular hyperreactivity and hyperventilation. *Clinical otolaryngology and allied sciences.* Jun 1986;11(3):161-169.

24. Jacobson GP, Shepard NT. *Balance Function Assessment and Management.* Plural Phublishing Inc; 2014.

25. Wallis Y, Payne S, McAnulty C, et al. Practice Guidelines for the Evaluation of Pathogenicity and the Reporting of Sequence Variants in Clinical Molecular Genetics. *ACGS /VGKL.* 2013.

26. Pollard KS, Hubisz MJ, Rosenbloom KR, Siepel A. Detection of nonneutral substitution rates on mammalian phylogenies. *Genome research.* Jan 2010;20(1):110-121.

27. Grantham R. Amino acid difference formula to help explain protein evolution. *Science.* Sep 06 1974;185(4154):862-864.

28. Adzhubei IA, Schmidt S, Peshkin L, et al. A method and server for predicting damaging missense mutations. *Nature methods.* Apr 2010;7(4):248-249.

29. Ng PC, Henikoff S. SIFT: Predicting amino acid changes that affect protein function. *Nucleic acids research.* Jul 01 2003;31(13):3812-3814.

30. Kircher M, Witten DM, Jain P, O'Roak BJ, Cooper GM, Shendure J. A general framework for estimating the relative pathogenicity of human genetic variants. *Nature genetics.* Mar 2014;46(3):310-315.

31. Wilson RS, Roper-Hall MJ. Effect of age on the endothelial cell count in the normal eye. *The British journal of ophthalmology.* Aug 1982;66(8):513-515.

32. Edelhauser HF. The balance between corneal transparency and edema: the Proctor Lecture. *Investigative ophthalmology & visual science.* May 2006;47(5):1754-1767.

33. Zhang J, Patel DV. The pathophysiology of Fuchs' endothelial dystrophy--a review of molecular and cellular insights. *Experimental eye research.* Jan 2015;130:97-105.

34. Mustonen RK, McDonald MB, Srivannaboon S, Tan AL, Doubrava MW, Kim CK. In vivo confocal microscopy of Fuchs' endothelial dystrophy. *Cornea.* Sep 1998;17(5):493-503.

35. van Tilbeurgh H, Sarda L, Verger R, Cambillau C. Structure of the pancreatic lipase-procolipase complex. *Nature.* Sep 10 1992;359(6391):159-162.

36. Recacha R, Boulet A, Jollivet F, et al. Structural basis for recruitment of Rab6-interacting protein 1 to Golgi via a RUN domain. *Structure.* Jan 14 2009;17(1):21-30.

37. Shafique S, Siddiqi S, Schraders M, et al. Genetic spectrum of autosomal recessive non-syndromic hearing loss in Pakistani families. PloS one. 2014;9(6):e100146.

3.2

Supplemental data

a

b
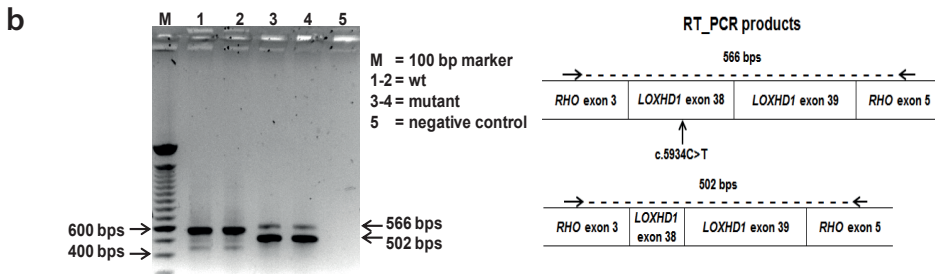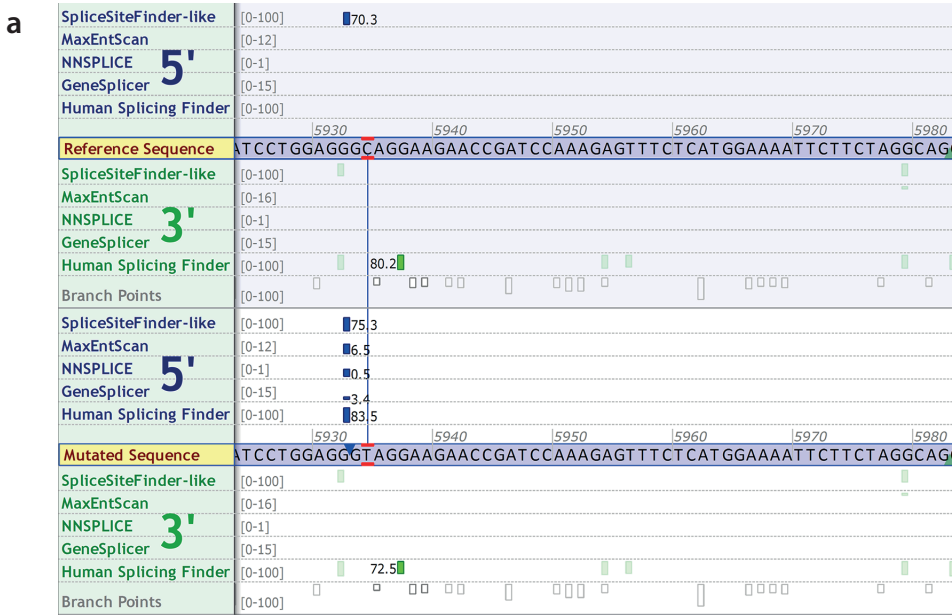
Figure S1 (**a**) The synonymous variant c.5934C>T (p.(Gly1978Gly)) introduces a novel splice donor site. Splice site prediction scores and figure were obtained from Alamut (Interactive Biosoftware, Rouen, France). (**b**) An agarose gel containing RT-PCR products detected from HEK293T cells transfected with the wild-type and mutant minigene construct, and a schematic representation of the identified splicing products (the two bands with the highest intensity). All of the RT-PCR products were verified by sequence analysis. The c.5934C>T variant leads to a shortened exon 38 due to usage of the predicted splice donor site. Two RT-PCR products are visible in the wild-type (wt) samples. The larger product is the expected RT-PCR product containing both wild-type exon 38 and 39 of *LOXHD1* (566 bps). The smaller RT-PCR product only contains exon 39 of *LOXHD1*; exon 38 is not present in this product. Also in the mutant samples two RT-PCR products seem to be present. However, sequence analysis of both bands showed products of the same length and sequence with a shortened exon 38, due to use of the novel predicted splice donor size, and a wild-type exon 39 (502 bps). It seems that the two bands represent the same product with a different migration pattern.

4

Identification of novel deafness genes

4.1

MPZL2, encoding the epithelial junctional protein Myelin Protein Zero-like 2, is essential for hearing in man and mouse

Mieke Wesdorp*, Silvia Murillo-Cuesta*, Theo Peters, Adelaida M. Celaya, Anne Oonk, Margit Schraders, Jaap Oostrik, Elena Gomez-Rosas, Andy J. Beynon, Bas P. Hartel, Kees Okkersen, Hans J.P.M. Koenen, Jack Weeda, Stefan Lelieveld, Nicol C. Voermans, Irma Joosten, Carel B. Hoyng, Peter Lichtner, Henricus P.M. Kunst, Ilse Feenstra, DOOFNL consortium, Ronald J.C. Admiraal, Helger G. Yntema, Erwin van Wijk, Ignacio del Castillo, Pau Serra, Isabel Varela-Nieto[#], Ronald J.E. Pennings[#] and Hannie Kremer[#]

*,[#] These authors contributed equally to this work

Abstract

In a Dutch consanguineous family with recessively inherited nonsyndromic hearing impairment (HI), homozygosity mapping combined with whole exome sequencing revealed a homozygous truncating variant of *MPZL2*, c.72del (p.Ile24Metfs*22). By screening a cohort of phenotype-matched subjects and a cohort of HI subjects in whom WES was performed previously, we identified two additional families with biallelic truncating variants of *MPZL2*. Affected individuals demonstrated symmetric, progressive, mild to moderate, sensorineural HI. Onset of HI was in the first decade and high-frequency hearing was more severely affected. There was no vestibular involvement. *MPZL2* encodes Myelin protein zero-like 2, an adhesion molecule that mediates epithelial cell-cell interactions in several (developing) tissues. Involvement of MPZL2 in hearing was confirmed by audiometric evaluation of *Mpzl2^{ko/ko}* mice. These displayed early-onset progressive sensorineural HI that was more pronounced in the high frequencies. Histological analysis of adult *Mpzl2^{ko/ko}* mice demonstrated an altered organization of outer hair cells and supporting cells and degeneration of the organ of Corti. In addition, mild degeneration of spiral ganglion neurons was observed, most pronounced at the cochlear base. Although MPZL2 is known to function in cell adhesion in several tissues, HI is so far the only phenotype associated with MPZL2 defects. This indicates MPZL2 to have a unique function in the inner ear. The present study suggests that deleterious variants of *Mplz2/MPZL2* affect adhesion of the inner ear epithelium resulting in loss of structural integrity of the organ of Corti and progressive degeneration of hair cells, supporting cells, and spiral ganglion neurons.

Introduction

The identification of novel genes for hereditary nonsyndromic hearing impairment (NSHI) has accelerated in the last decade with the introduction of next generation sequencing. But despite the fact that currently more than 100 deafness genes are known (Hereditary Hearing loss Homepage), over 60 percent of subjects with hereditary NSHI can still not be genetically diagnosed.[1-6] These individuals and their relatives receive suboptimal care, because of insufficient counseling on prognosis and recurrence risk. In addition, syndromic features can be overlooked, or in the opposite case, unnecessary and costly tests are performed to screen for additional symptoms that are not present.

Given the number of deafness loci for which the causative gene is not known yet (Hereditary Hearing loss Homepage), it is estimated that still many monogenic forms of NSHI await identification. Discovery of these NSHI-associated genes will contribute to the full understanding of the complex physiology of hearing. However, the search for novel deafness genes has become more challenging, as most frequently involved genes are already known and those that remain are most likely involved in less than 1 percent of the cases, or even in only one or a few families with NSHI. Also, identification of deleterious variant(s) in a novel deafness gene in one family with NSHI alone is insufficient proof for causality. Functional studies and animal models are important tools to provide evidence for involvement of the identified gene in hearing.[7,8]

In this study, we report on the identification of a novel gene for recessive NSHI, *MPZL2,* by combining homozygosity mapping and whole exome sequencing (WES) in a family of Dutch origin. Subsequent screening of a phenotype-matched cohort and analysis of WES data of genetically undiagnosed individuals with NSHI led to the identification of two additional families of Turkish origin with truncating variants in *MPZL2*. We characterized the phenotype of affected individuals and of mice with an intragenic deletion of *Mpzl2*.[9] In addition, we observed histological abnormalities in the cochleae of the mutant mice.

Subjects And Methods

Subject evaluation
This study was approved by the medical ethics committee of the Radboud University Medical Center and is in accordance with the principles of the World Medical Association Declaration of Helsinki. Written informed consent was obtained from all participants or their legal representatives.

4.1

Medical history was obtained from all participants, using a questionnaire focusing on hearing and balance, and possible acquired causes of HI. Otoscopy was performed in all subjects to assess the tympanic membrane and aeration of the middle ear. Pure-tone audiometry was performed in a sound-treated room according to current standards. Air conduction thresholds were determined at 0.25, 0.5, 1, 2, 4, and 8 kHz in dB HL. Bone conduction thresholds were determined at 0.5, 1, 2, 4, and 8 kHz in dB HL, to exclude conductive HI. HI was described according to the recommendations of the GENDEAF study group.[10] Progression of HI was evaluated by cross-sectional linear regression analysis of last-visit audiograms of the better hearing ear and used to construct Age Related Typical Audiograms (ARTA), as described previously.[11] Individual progression of HI was calculated for each frequency with longitudinal linear regression analyses, using GraphPad Prism 6.0 (GraphPad, San Diego, CA, USA). Tympanometry was performed, and click-evoked ABR and otoacoustic emissions (OAEs) were obtained, according to current standards. Contralateral and ipsilateral acoustic reflexes were measured at 0.5, 1, 2 and 4 kHz up to loudness discomfort level. Speech perception thresholds and maximum speech recognition scores were determined using speech audiometry, which was performed in a sound-treated room with standard monosyllabic consonant-vowel-consonant Dutch word lists.[12]

Vestibular function was assessed using electronystagmography (ENG) rotary chair stimulation and caloric irrigation testing, according to current standards. Additionally, cervical vestibular evoked myogenic potentials (cVEMP) and video head impulse tests (vHIT) were performed to assess sacculus and vestibulo-ocular reflex (VOR) functionality, respectively. To assess the presence of polyneuropathy, standardized neurological screening was performed in accordance with a predefined protocol (Supplemental Methods). Immunological screening was performed to evaluate presence of immunodeficiencies by asking participants about symptoms of allergies, autoimmune diseases, and frequent, prolonged or severe infections or inflammations. In addition, the numbers of CD4- and CD8-expressing human T cells were analyzed, using flow cytometry, as indicated in the legend of Figure S12. Screening for corneal abnormalities and vision problems was performed by history, slit lamp biomicroscopy and evaluation of visual acuity using a Snellen chart.

Description of subject cohorts
Two cohorts were screened for the presence of *MPZL2* variants, a phenotype-based cohort and a WES cohort. The phenotype-based cohort consisted of 138 individuals with a phenotype comparable to that of individuals of family W05-682, demonstrating sensorineural NSHI and a flat, cookie-bite or downsloping audiogram configuration. Of these, 70 subjects were Dutch and displayed stable, mild to severe NSHI; 68 subjects were Spanish and displayed mild to profound NSHI. Only isolated cases and subjects with

suspected autosomal recessive inheritance were included. All subjects were previously tested for a phenotype-based selection of single genes.

The WES cohort consisted of 270 subjects with presumed recessive HI for whom WES was performed previously. In these subjects, pathogenic variants in known deafness genes (Table S1) were excluded by targeted analysis of WES data, as described previously.[6] Subjects were not preselected based on theirHI phenotype.

4.1

Homozygosity mapping
Genomic DNA was isolated from peripheral blood lymphocytes by standard procedures. The samples of subjects II:1 and II:3 of family W05-682 (Figure 1) were genotyped using the Affymetrix mapping 250K SNP array, according to the manufacturer's protocol (Santa Clara, CA, USA). Genotype calling was performed with the Genotyping Console software (Affymetrix) with default settings. Homozygosity mapping was performed with the online tool HomozygosityMapper[13] to identify significant shared homozygous regions. Other shared homozygous regions larger than 1 Mb and regions of shared heterozygous genotypes were identified manually.

VNTR marker analysis
Genotyping of variable number of tandem repeats (VNTR) markers was performed by DNA amplification with touchdown PCR and analysis on an ABI Prism 3730 Genetic Analyzer (Applied Biosystems). Primers for amplification of VNTR loci were designed with Primer3Plus. Genetic location of the markers was derived online from the Marshfield genetic map and marker order was confirmed in the human genome assembly GRCh37/hg19. Alleles were assigned with GeneMapper v.4.0 software, according to the manufacturer's protocol (Applied Biosystems, Foster City, CA, USA).

Whole Exome Sequencing
Exome DNA was enriched using the Agilent SureSelect version 4 or version 5 kits. WES was performed on an Illumina HiSeq system by BGI-Europe (Denmark). Variants in genes associated with hearing impairment (HI) were selected and analyzed.[14] A list of the analyzed HI-related genes and their coverage is provided in Table S1. Mean ≥20x coverage per sample was 95.9% to 96.5% of the enriched regions. The effect of identified variants on the protein and on splicing was predicted with Alamut (Interactive Biosoftware, Rouen, France). To predict the pathogenicity of variants, they were classified according to the guidelines from the Association for Clinical Genetic Science and the Dutch Society of Clinical Genetic Laboratory Specialists.[15]

Sanger sequencing

Primers for amplification of exons and exon-intron boundaries of *MPZL2* (NM_005797.3) and *TECTA* (ENST00000392793), and for mRNA analysis of *TECTA* were designed with Primer3Plus and Oligo Primer Analysis Software. Amplification by PCR was performed under standard conditions. For *TECTA* mRNA analysis, total RNA was isolated from Epstein–Barr virus-transformed lymphoblastoid cells of affected subjects II:1 and II:3 of family W05-682, using the NucleoSpin RNA II kit (Machery Nagel,) according to the manufacturer's protocol. Poly A$^+$ RNA was isolated from total RNA using the OligoTEX mRNA Spin Column kit (Qiagen), according to the manufacturer's protocol. Subsequently, cDNA synthesis was performed with 0.5 µg poly A$^+$ RNA as starting material by using the iScript cDNA Synthesis Kit (Bio-Rad Laboratories), according to the manufacturer's protocol. PCRs were performed on 2 µl cDNA with Taq DNA polymerase (Roche). PCR fragments were purified with ExoI/FastAP or ExoSAP-IT (Thermo Fisher Scientific), in accordance with manufacturers' protocols. Sequence analysis was performed with the ABI PRISM BigDye Terminator Cycle Sequencing v.2.0 Ready Reaction kit and analyzed with the ABI PRISM 3730 DNA analyzer or the 3130 Genetic Analyzer (Applied Biosystems). Possibly deleterious effects of the identified variants on the MPZL2 and TECTA proteins and on splicing was predicted with Alamut (Interactive Biosoftware). Primer sequences and PCR conditions are provided in Table S2.

Quantitative PCR (qPCR) analysis for identification of intragenic deletions

We quantified copy numbers of *MPZL2* exons 2, 3 and 5 by using genomic qPCR. Specific primers (Table S2) were designed with Primer3Plus and reference sequence NM_005797.3. qPCRs were performed with 5 µg genomic DNA and reaction mixtures were prepared with the GoTaq qPCR Master Mix (Promega) in accordance with the manufacturer's protocol. qPCRs were performed with the Applied Biosystem Fast 7900 System in accordance with the manufacturer's protocol (Applied Biosystems). *SLC16A2* (MIM: 300095) was employed as a reference gene. All reactions were performed in duplicate.

MPZL2 expression in human tissues

Total RNA derived from fetal heart, skeletal muscle, lung, brain, colon, kidney, stomach, spleen and thymus, and from adult skeletal muscle, liver, duodenum, stomach, spleen, thymus and testis, was purchased from Stratagene (La Jolla, CA, USA). Adult heart, lung, brain, kidney, bone marrow and placenta total RNA was purchased from Bio-chain (Newark, CA, USA). In addition, total RNA was isolated from fetal cochlea (8 weeks of gestation) as described previously.[16] Subsequently, cDNA synthesis was performed with 2 µg total RNA as starting material by using the SuperScript cDNA Synthesis Kit (Thermo Fisher Scientific, Waltham, MA, USA), according to the manufacturer's protocol. Specification on primer

design, qPCR system and reaction mixtures are mentioned above. Primer sequences and conditions are provided in Table S2. The human beta glucuronidase gene (*GUSB,* MIM 611499) was employed as a reference gene. All reactions were performed in duplicate. Relative gene expression levels were determined with the delta-delta Ct method[17].

Audiometric characterization of Mpzl2[ko/ko] mice

Hearing was evaluated in C57BL6J wild-type (WT) and *Mpzl2[ko/ko]* mice.[9] In the *Mpzl2[ko/ko]* mice, exons 2 and 3 were deleted by standard gene targeting methods.[9] This is predicted to result in an in-frame deletion of the coding sequences for amino acid residues 20-145, encompassing part of the signal sequence and the majority of the extracellular region of the 215-residue MPZL2 protein (cf. Figure S1). Auditory brainstem responses (ABR) were registered in 4, 8 and 12 week-old mice (n=5 per genotype and age group), essentially as reported by Cediel et al. (2006)[18] with the modifications reported by Murillo-Cuesta et al. (2015).[19] Briefly, ABR recordings were obtained under anesthesia with ketamine (75 mg/kg, Imalgene, Merial) and xylacine (5 mg/kg, Rompun, Bayer). Click (0.1 ms, 30 pps rate) and tone burst stimuli (8, 16, 20, 28 and 40 kHz, 5 ms, 50 pps rate) were generated with SigGenRP™ software (Tucker-Davis Technologies, Alachua, FL, USA). Stimuli were presented from 90 to 10 decibels, relative to sound pressure level (dB SPL) in 5–10 dB SPL steps with a MF1 speaker (TDT). The electrical responses were amplified, recorded and averaged, and hearing thresholds were determined in the ABR recordings. Amplitudes of ABR waves I, II, and IV and interpeak latencies of peaks I-II, II-IV, and I-IV were analyzed for 70 dB SPL click stimuli.

Statistical analysis was performed with IBM SPSS 23.0 software. Nonparametric Mann-Whitney U-tests were used to compare ABR parameters between genotypes because of the small sample sizes. Differences were considered significant if $p<0.05$.

Animal experiments were conducted in accordance with Spanish and European legislation, and approved by the local bioethics committees.

Histology and immunohistochemistry of wild-type and Mpzl2[ko/ko] cochleae

Cochleae from 12 weeks old mice (n=3 per genotype) were dissected, decalcified and embedded in paraffin or Tissue-Tek OCT (Sakura Finetek). Deparaffinized cochlear sections (5 mm) were stained with hematoxylin and eosin, and images for general cytoarchitecture evaluation were taken with 10x, 20x and 40x magnification objectives with an Olympus DP70 digital camera as described previously.[20] For immunofluorescence assays of 12-week cochleae, cryosections (10 mm) were treated overnight at 4ºC with the following primary antibodies: rabbit anti-Kir4.1 (1:200 AB5818 Chemicon), rat anti-ZO-1 (1:200 sc-33725 Santa Cruz); rabbit anti-KCNQ1 (1:200 sc-20816 Santa Cruz), rabbit anti-Myosin VIIa (1:250

25-6790 Proteus), or goat anti-SOX2 (1:100 sc-17320 SantaCruz). After washing, sections were incubated with the corresponding secondary Alexa conjugated antibodies for 2 hrs at room temperature (RT), essentially as reported in Sanchez-Calderon *et al.* (2010).[21]

Images were taken with epifluorescence (Nikon 90i, Tokyo, Japan) and/or confocal (Leica TCS SP2; Leica, Wetzlar, Germany) microscopes. SOX2 and Myosin VIIa positive cells were counted from base to apex in five serial cryosections (10 μm) per animal separated by 50 μm, prepared from 3 mice of each genotype. The intensities of KCNQ1, ZO-1, and Kir4.1 immunostainings were determined in areas of the stria vascularis, delimited by thresholding the marker's fluorescent signal using Fiji software v1.51n (National Institutes of Health, Bethesda, MD, USA). The fluorescence optical density was thus determined from base to apex in 3-5 serial cryosections (10 μm) per animal separated by 50 μm, prepared from 3 mice of each genotype. Statistical significance was determined by Student's t test for unpaired samples.

For evaluation of early postnatal cytoarchitecture of the cochlea and for localization of MPZL2, inner ears of postnatal day four (P4) C57BL6J wild-type and *Mpzl2^{ko/ko}* mice (n=3) were dissected, cryoprotected with 10% sucrose in PBS before embedding in Tissue-Tek OCT. For analysis of the cytoarchitecture, cryosections (7 μm) were fixed with paraformaldehyde (PFA) 4% (10 min), stained with hematoxylin and eosin, and analyzed on a Zeiss Axioskop light microscope. For immunofluorescence, cryosections were permeabilised with 0.01% Tween20 in PBS (20 min) and after rinsing with PBS and blocking with blocking buffer (ovalbumin 0.1% and fish gelatin 0.5% in PBS; 1 hr) incubated overnight at 4 °C with primary antibodies diluted in blocking buffer. After rinsing with PBS, cryosections were incubated (1 hr) with secondary antibodies diluted in blocking buffer with DAPI (1:8000; D1306; Molecular Probes). After rinsing in PBS, sections were fixed in PFA 4% in PBS (10 min), rinsed and mounted in anti-fade Prolong Gold (P36930; Molecular Probes). Analyses were performed on a Zeiss Axio Imager fluorescence microscope and for higher resolution on a Zeiss LSM880 confocal microscope. As primary antibodies were used: Rabbit anti-MPZL2 (1:200 11787-1-AP Proteintech), rabbit anti-Myosin VIIa (1:200 25-6790 Proteus), goat anti-Collagen IV (1:200 1340-01 SouthernBiotech), and mouse anti-Na$^+$-K$^+$ATPase α1 (1:5 α6F Developmental Studies Hybridoma Bank). As secondary antibodies were utilized: Alexa Fluor (AF) conjugated immunoglobulins (Molecular Probes): AF 568-goat anti-rabbit (A11011), AF 488-donkey anti-goat (A11055), AF 488-goat anti-mouse (A11029) and AF 488-goat anti-rat (A11006), at a 1:800 dilution.

Results

Homozygosity mapping and WES revealed loss-of-function variants of MPZL2

Homozygosity mapping in a Dutch consanguineous family with HI (W05-682; Figure1, Figure S2) revealed a single significant homozygous region of 23.8 Mb on chromosome 11q23.1-q25, flanked by single nucleotide polymorphisms (SNPs) rs4936310 and rs10458997 (Figure S3). VNTR marker analysis confirmed homozygosity of the region and segregation of marker alleles in the family was compatible with linkage of the HI with a region flanked by D11S1893 at the centromeric side and including D11S2359 at the telomeric side (Figure 1a). D11S2359 is the most telomeric VNTR marker of chromosome 11q (UCSC Genome Browser, GRCh37/hg19). By combining VNTR marker and SNP data, the critical region is delimited to Chr11:110,803,280-134,746,130. Two hundred and nine RefSeq genes have been annotated in this region (UCSC Genome Browser, GRCh37/hg19), including *TECTA,* a known deafness gene. However, pathogenic variants in *TECTA* were excluded by Sanger sequencing of all exons and exon-intron boundaries and by mRNA analysis. The homozygous region did not contain or overlap with any other known deafness gene or locus. Fifteen additional homozygous regions larger than 1 Mb and shared by individuals II:1 and II:3 were identified (Table S3). There were no regions with shared heterozygous genotypes larger than 1 Mb.

As a next step, WES was performed in the index case (II:1) of family W05-682. The mean ≥20x coverage of genes in the homozygous region of chromosome 11q23.1-q25 was 98.1%. Variants within this region were filtered and classified as depicted in Figure S4. This revealed four rare homozygous variants in coding sequences and splice sites. Based on variant classification guidelines[15], one of these variants was predicted to be likely benign (*OR8G2* c.537C>G (p.Leu179Leu)). Two variants were predicted to be of uncertain significance (*BSX* c.263-5T>C (p.?) and *GRAMD1B* c.1111G>A (p.Val371Ile). The fourth variant was a homozygous one-base-pair deletion of *MPZL2,* c.72del (Figure S4) that is predicted to result in premature termination of protein synthesis (p.Ile24Metfs*22). As *MPZL2* was known to be transcribed in the cochlea, it seemed the most promising candidate gene.[22,23] The *MPZL2* variant c.72del has only been reported heterozygously in gnomAD, with a global minor allele frequency (MAF) of 0.00077, and is most common in the non-Finnish European population with a MAF of 0.00127. Segregation analysis by Sanger sequencing demonstrated co-segregation of the variant and HI in the family (Figure 1a). Targeted analysis of WES data for a panel of 120 HI-associated genes (Table S1) revealed no other (likely) pathogenic variants.

4.1
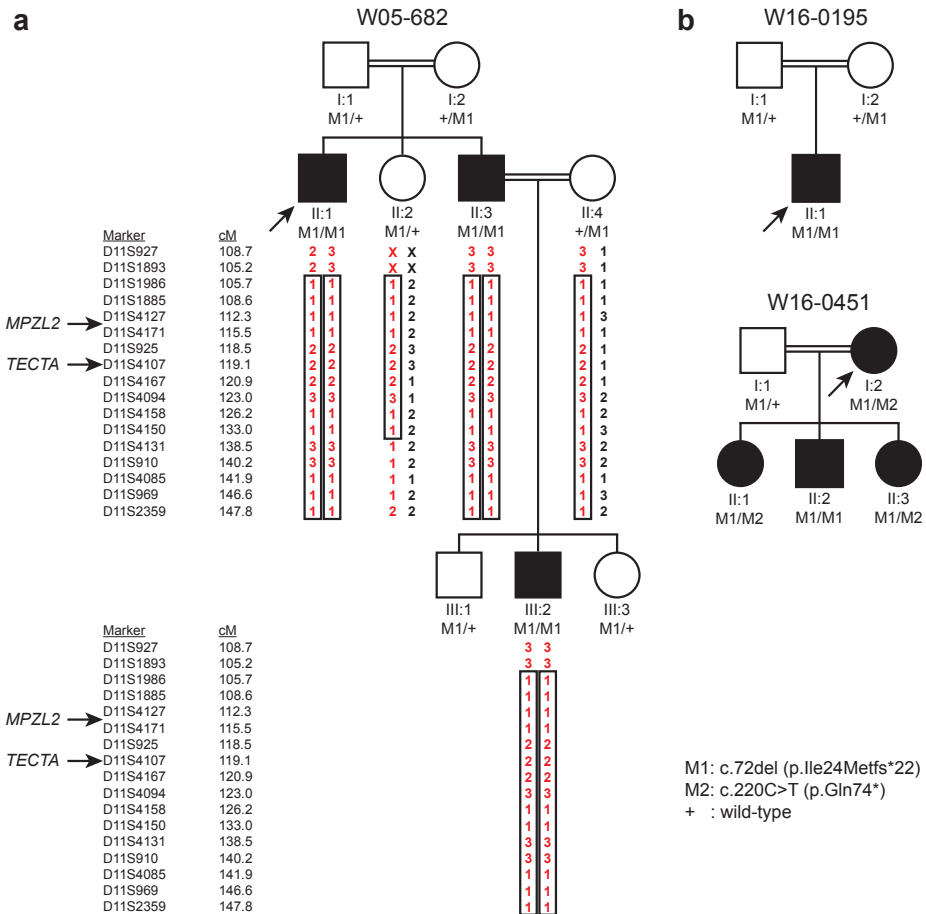
Figure 1 Pedigrees, VNTR genotypes and segregation of variants of *MPZL2*.
(**a**) Genotypes of VNTR markers and segregation of identified truncating variants of *MPZL2* in family W05-682. Besides *MPZL2*, *TECTA* (DFNB21) is also located within the homozygous region shared by the affected individuals. Pathogenic variants in the coding and intronic regions of *TECTA* were excluded. (**b**) Pedigrees and segregation analyses of two additional families with deleterious variants in *MPZL2*. Index cases are indicated by arrows. Double lines indicate consanguinity (for extended pedigrees, see Figure S1).

Identification of additional families with deleterious MPZL2 variants

We addressed further involvement of *MPZL2* variants in recessive NSHI. A phenotype-based cohort of 138 unrelated probands with a phenotype similar to that of affected individuals in family W05-682, was screened for variants of *MPZL2*. This revealed the variant c.72del (p.Ile24Metfs*22) in homozygous state in a family of Turkish origin, W16-0195. The variant was present heterozygously in the unaffected consanguineous parents (Figure 1b, Figure S5).

In two other individuals of the phenotype-based cohort, rare heterozygous variants of *MPZL2* were identified, namely c.268C>T (p.Arg90Trp) and c.544C>T (p.Arg182*). To identify possible intragenic deletions of the second allele, genomic qPCR was performed for exons in which no heterozygous SNPs were detected (Table S4). No deletions could be identified. Therefore, defects of *MPZL2* are unlikely to be causative of HI in these subjects. However, a deleterious variant in non-coding regions of the gene cannot be excluded.

Subsequently, data of a WES cohort of 270 genetically undiagnosed NSHI subjects was analyzed for rare *MPZL2* variants. This unveiled a third family, W16-0451, of Turkish origin with truncating variants in *MPZL2*. Segregation analysis demonstrated that the c.72del and c.220C>T (p.Gln74*) variants were present in compound heterozygous state in the index case and that her affected offspring also carried biallelic truncating *MPZL2* variants (Figure 1b, Figure S5). The c.220C>T variant has been reported only heterozygously in gnomAD, with a global MAF of 0.00038 and 0.00003 in the non-Finnish population, which represents a significant part of the Turkish ancestry.[24] The MAF of c.220C>T is 0.00515 in the East Asian population and 0.00016 in the South Asia as indicated in gnomAD. There is admixture of the Turkish population from Asia, mainly from West and Central Asia.[24] The c.220C>T variant has not been observed in other populations represented in gnomAD.

4.1

The c.72del MPZL2 variant is derived from a common founder
VNTR marker analysis was performed in families W05-682, W16-0195 and W16-0451 to determine the haplotypes in the *MPZL2* region (Figure S6). All c.72del *MPZL2* alleles shared a haplotype of at least 0.5 Mb, delimited by markers D11S1341 and D11S4104, suggesting that it is a founder variant rather than a recurrent variant due to a mutational hotspot. Since the families have a different ethnic background, the c.72del variant is likely to be of ancient origin.

MPZL2 is expressed in human fetal cochlea
The relative expression of *MPZL2* was determined in human fetal cochlea and various other fetal and adult human tissues (Figure 2). As the fetal tissues were not derived from embryos of the same gestational age, mRNA transcript levels are not directly comparable. Among the tested fetal tissues, *MPZL2* expression was highest in inner ear, with 70-fold higher transcript levels compared to skeletal muscle, which displayed the lowest detectable expression. Also in all other fetal tissues, *MPZL2* transcript levels were significantly lower as compared to that in the inner ear. In the analysis of *MPZL2* expression in adult tissues, mRNA levels of *MPZL2* in fetal inner ear were included for comparison. *MPZL2* mRNA was detected in all analyzed adult tissues, with highest levels in thymus and lung, which were in the range of those in fetal inner ear.
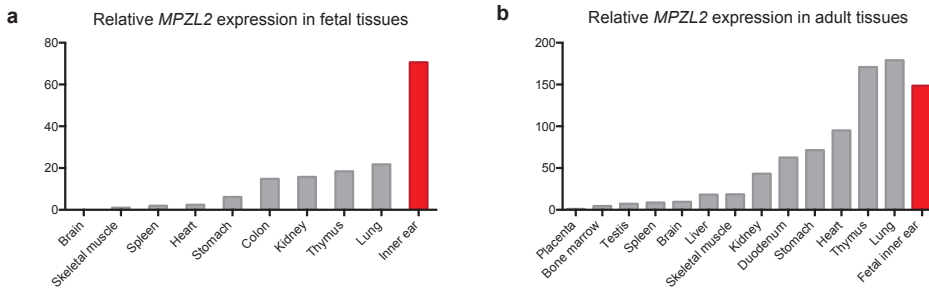
Figure 2 *MPZL2* expression profile in human tissues.
Relative *MPZL2* mRNA levels as determined by RT-qPCR in human fetal (**a**) and adult (**b**) tissues. The relative expression values were determined by the delta-delta Ct method with *GUSB* as a reference gene.[17] Expression levels are relative to those in skeletal muscle (**a**) and placenta (**b**), which displayed the lowest detectable *MPZL2* expression of tested fetal and adult tissues, respectively. In fetal brain, no expression of *MPZL2* could be detected.

Mpzl2^{ko/ko} mice are hearing impaired

Mpzl2^{ko/ko} mice showed early-onset progressive HI, with significantly increased ABR thresholds in response to click and tone burst stimuli along the ages studied, when compared to age-matched C57BL6J normal hearing wild-type mice. Four-week-old *Mpzl2^{ko/ko}* mice showed a mild HI, that affected the detection of click stimuli and pure tone frequencies above 16 kHz (Figures 3a and 3b) with statistically significant higher thresholds (P<0.05) as compared to wild-type mice. HI in *Mpzl2^{ko/ko}* mice rapidly progressed to moderate and severe at the ages of 8 and 12 weeks, respectively, with statistically significant elevated thresholds for all tested stimuli as compared to wild-type mice. At 12 weeks of age, ABR thresholds in response to 16-40 kHz are above 70 dB SPL in the *Mpzl2^{ko/ko}*, while wild-type mice maintained normal hearing with thresholds below 30 dB SPL. Accordingly, significant alterations in ABR peak amplitudes, latencies and interpeak latencies were observed in *Mpzl2^{ko/ko}* mice. The maximum amplitudes of wave I, which represents cochlear activity, were approximately 30% lower in the knock-out animals than in the wild-type mice at all ages studied (Figure 3c), and differences reached significance in 4 week-old mice (Figure 3d). In addition, wave I peaks showed increased latencies in the *Mpzl2^{ko/ko}* as compared to wild-type mice which progressed over time. Peaks were increased in young animals (4 weeks-old) at the level of intensity near the threshold, whereas in 12 weeks-old mice they were increased for all intensities tested (Figure 3e). Also, *Mpzl2^{ko/ko}* showed significantly shorter interpeak latencies (IPL) I-II, II-IV and I-IV compared to wild-type mice (Figure 3f). These data suggest a compensatory central response to the delayed peripheral transmission, as already shown in the *Igf1* knock-out.[25]

4.1
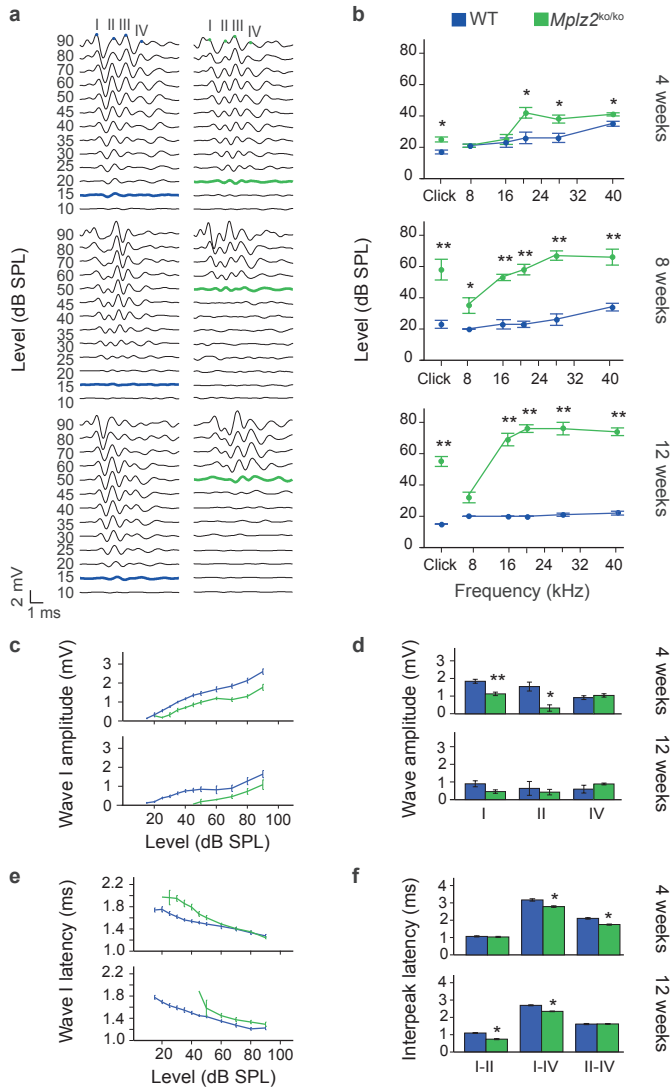
Figure 3 Hearing phenotype of *Mpzl2ko/ko* mice.
(**a**) Representative click-evoked ABR recordings at decreasing intensities (dB SPL) in 4, 8 and 12 week-old wild-type and *Mpzl2ko/ko* mice. Waves are labeled I to IV and reflect the evoked activity of the auditory nerve (I) and ascending points of the auditory pathway in the midbrain (II-IV). As the stimulus level is reduced, amplitudes of ABR waves decrease and latencies of waves increase. The lowest intensity at which the ABR wave profile is higher than the background noise signal is the threshold (bold line; WT, blue; *Mpzl2ko/ko* mice, green). (**b**) ABR thresholds in response to click and 8-40 kHz tone bursts, of the different genotypes and age groups. (**c,e**) ABR wave I amplitude/intensity (**c**) and latency/intensity (**e**) curves in response to click stimuli of increasing intensities were determined in 4- and 12-week-old wild-type and *Mpzl2ko/ko* mice. (**d, f**) Peak amplitude of ABR waves I, II and IV (**d**), and interpeak latencies I-II, II-IV and I-IV (**f**), in response to a 70 dB SPL click stimulus in 4- and 12-week-old wild-type and *Mpzl2ko/ko* mice. Data are shown as mean±SEM. Statistical significance, *p<0.05; **p<0.01.

Mpzl2^{ko/ko} mice display alterations in cell organization and cell loss in the organ of Corti.
Evaluation of the general cochlear cytoarchitecture was performed in the basal, medial and apical turns of the cochlea of 12 week-old mice (Figure S7) to assess the integrity of the principal structures. Namely, the organ of Corti with inner and outer hair cells (IHCs and OHCs, respectively) responsible, respectively, for the mechanotransduction and amplification and tuning of the sound, and different types of supporting cells. Furthermore, the spiral ganglion neurons that connect the hair cells with the central auditory pathway; the stria vascularis in the lateral wall, involved in the formation of the high potassium containing endolymph, and the spiral ligament. Loss of hair and supporting cells of the organ of Corti (asterisk in Figure S7d) and of neurons in the spiral ganglion (asterisks in Figure S7d-1) were observed in the basal cochlear turn of *Mpzl2^{ko/ko}*, but not in wild-type mice. No evident structural abnormalities were seen in the stria vascularis and spiral ligament. Expression of markers of the stria vascularis was not altered in *Mpzl2^{ko/ko}* mice, as compared to age-matched wild-type animals (Figure S8).

A closer evaluation of the organ of Corti (Figure 4) showed clear differences between wild-type and *Mpzl2^{ko/ko}* mice at 12 weeks of age. At the basal turn of the cochlea, two *Mpzl2^{ko/ko}* mice showed a flat epithelium at the basilar membrane with complete loss of hair and supporting cells (asterisks in Figure 4n and Figure 4o). At the medial and apical turns of the cochlea, hair and supporting cells were present in both genotypes, as were tunnel forming inner (IP) and outer pillar cells (OP) (Figure 4e). However, *Mpzl2^{ko/ko}* mice showed an aberrant mosaic pattern of OHCs and supporting Deiters cells (DCs), with collapse of the spaces between OHCs and displacement of DC nuclei with respect to OHC nuclei (asterisks in Figure 4g, h, j-l, n-p).

Specific immunolabeling for Myosin VIIa and SOX2 evidenced that IHCs, OHCs and supporting cells were present (Figure 5). Also, this analysis confirmed *Mpzl2^{ko/ko}* mice to display a disorganized arrangement of OHCs and DCs in the apical (asterisks in Figures 5b and 5c) and middle turns (asterisk in Figure 5h), and absence or decreased numbers of all cell types in the basal turn of the cochlea (asterisks in Figure 5j-l), when compared to wild-type mice. Statistically significant differences were found in the number of OHCs in the basal turn only due to the differences in severity of the phenotype in *Mpzl2^{ko/ko}* mice (Figure S9). At P4, no indications were obtained for an abnormal cellular organization in the developing organ of Corti (Figure S10).

Mouse MPZL2 is expressed in the organ of Corti and the stria vascularis
Cochlear expression and localization of MPZL2 was assessed in wild-type mice at P4 by immunofluorescence, which revealed a signal in DCs and most intensely in the basal region of DCs in all three cochlear turns (Figure 6a and Figure S11). Staining of serial sections with
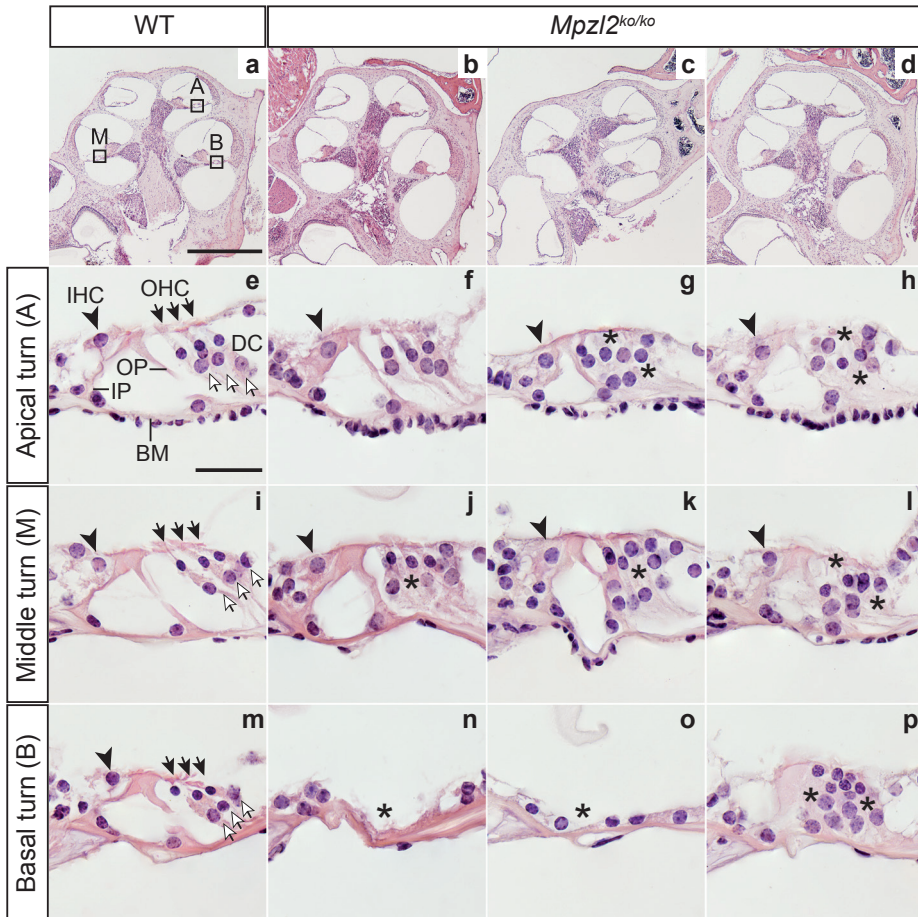
Figure 4 Cochlear morphology of 12-week-old wild-type and *Mpzl2ko/ko* mice.
Microphotographs show representative midmodiolar cross sections of the cochlea from one representative wild-type mouse (**a**) and three *Mpzl2ko/ko* mice (**b-d**). The apical (A), middle (M) and basal (B) organs of Corti are boxed in image a. Close-ups of the organ of Corti from one wild-type mouse (**e, i, m**) and three *Mpzl2ko/ko* mice (**f-h, j-l, n-p**). Arrowheads point to inner hair cells (IHC), blackhead arrows to outer hair cells (OHC) and arrows to Deiters cells (DC). BM; basilar membrane, IP; inner pillar cell, OP; outer pillar cell. Asterisks mark abnormalities. Scale bar a-d: 500 mm, e-p: 25 mm.

anti-collagen IV suggests that MPZL2 is present at the contact sites of DCs with the basilar membrane (Figures 6a and 6b). A weaker MPZL2 immunostaining is observed in both IHCs and OHCs (Figure 6a and Figure S11). In the stria vascularis, MPZL2 was detected in the basal cell layer as confirmed by co-staining with anti-Na$^+$K$^+$ATPase that demarcates the intermediate cell layer (Figures 6c and 6d). Specificity of the anti-MPZL2 antibody was confirmed by analyzing cochleae of *Mpzl2ko/ko* mice in the same experiments (Figure S11).
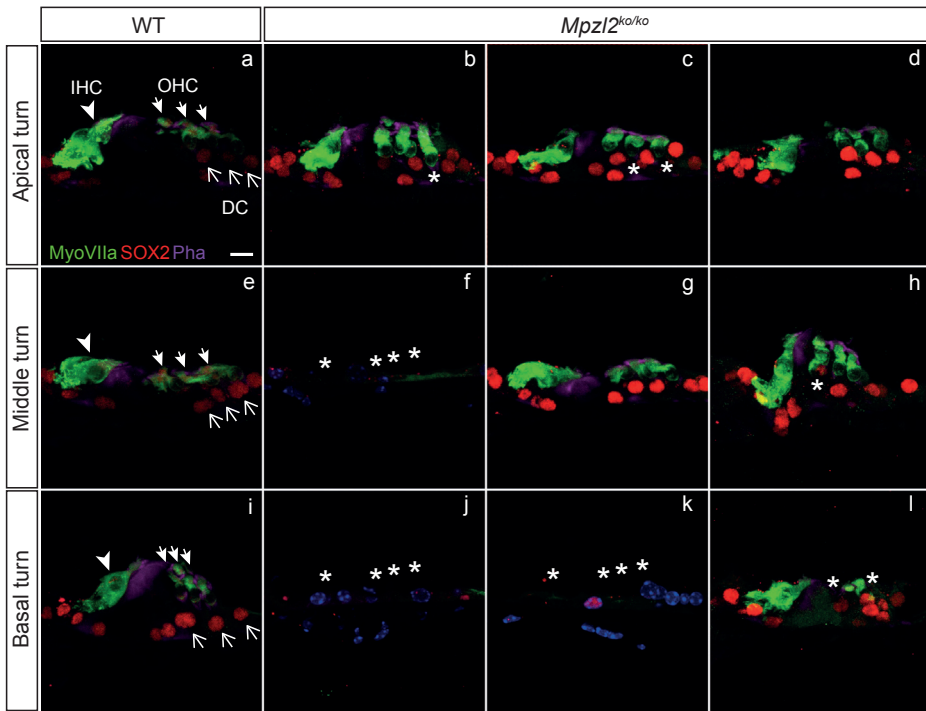
Figure 5 Organ of Corti cytoarchitecture of wild-type and *Mpzl2*^{ko/ko} mice.
Close-ups of the organ of Corti from representative frozen sections (10 µm) prepared from one representative wild-type mouse (**a, e, i**) and three *Mpzl2*^{ko/ko} mice (**b-d, f-h, j-l**). Hair cells and supporting cells were immunolabeled for Myosin VIIa (green) and SOX2 (red), respectively, in the apical, middle and basal turns of the cochlea. Actin in the organ of Corti was stained with phalloidin (purple). Arrowheads point to inner hair cells (IHC), whitehead arrows to outer hair cells (OHC) and arrows to Deiters cells (DC). Asterisks mark abnormalities. Scale bar: 10 mm.

Clinical characterization of individuals with pathogenic variants of MPZL2

All affected and unaffected subjects of families W05-682, W16-0195 and W16-0451 underwent clinical examinations. One of the siblings (II:1) of family W16-0451 was not able to participate in the current clinical evaluation; only retrospective data of this subject were used for analysis. History revealed that this individual previously underwent surgery for cholesteatoma of the left ear. Therefore, audiometric data of the right ear only were used for this study, which showed pure sensorineural HI. However, she also had osteogenesis imperfecta, which might contribute to her sensorineural HI. Nevertheless, her hearing thresholds were very similar to age-matched hearing thresholds of other affected family members and therefore we decided to include her in the audiometric evaluations.

None of the affected subjects (family W05-682, II:1, II:3, III:2; family W16-0195, II:1; family W16-0451, I:2, II:1, II:2, II:3) demonstrated abnormalities on otoscopy and tympanometry
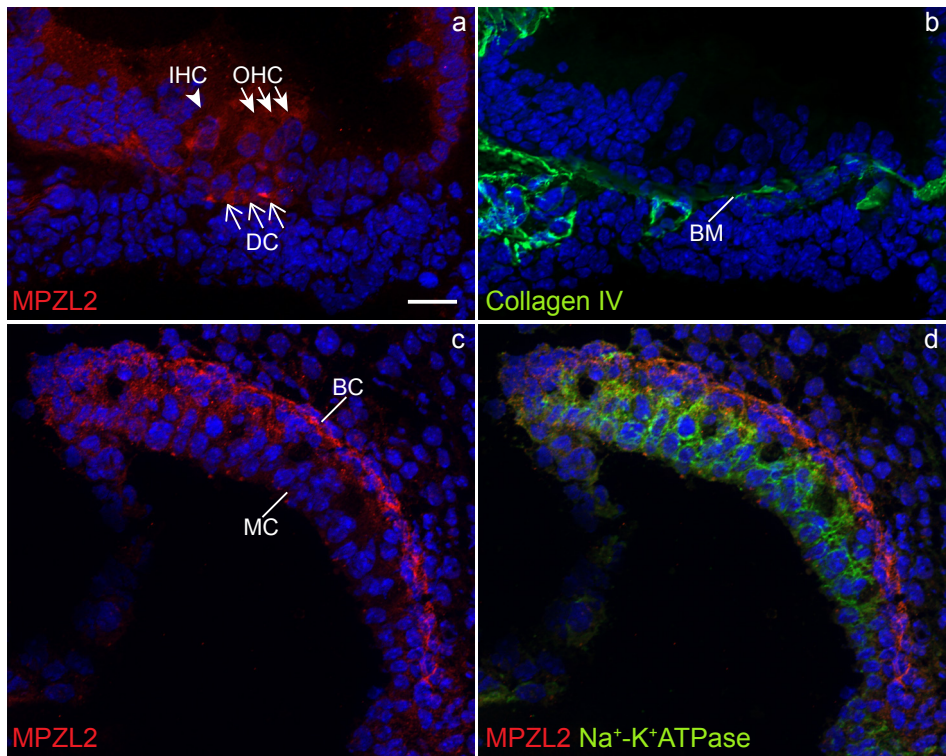
Figure 6 Localization of MPZL2 in the organ of Corti and stria vascularis.
MPZL2 displayed a distinct localization in the cochlear organ of Corti and stria vascularis at P4 in wild-type mice. (**a**) MPZL2 (red) localizes in the organ of Corti in the basal region of Deiters cells (DC) present below the three rows of outer hair cells (OHC) and diffusely in inner hair cells (IHC), OHCs and DCs. (**b**) In a serial section, collagen IV (green) immunostaining marked basement membranes including the basilar membrane (BM) thereby indicating the localization of MPZL2 at the DC-BM contact region. (**c**) In the stria vascularis, MPZL2 (red) immunostaining was observed predominantly in the basal cell (BC) region. (**d**) Co-immunostaining of MPZL2 and Na$^+$-K$^+$ATPase (green), a marker for marginal cells (MC), confirms immunostaining of MPZL2 (red) in the basal cells. Cell nuclei were stained with DAPI (blue). Arrowheads point to IHC, whitehead arrows to OHCs and arrows to DCs. Scale bar a-d, 20 μm.

(Table S5a). Pure tone audiometry of these individuals revealed no signs of conductive HI but did demonstrate a symmetric mild to moderate HI with a gently downsloping audiogram configuration for all of them (Figure 7a). The mean reported onset age of HI was 4 years (min-max: 3-9 years) (Table S5a). Four affected individuals had a disturbed speech-language development, whereas this was normal in three cases and unknown in one case. Speech perception thresholds were lower than the pure tone average thresholds at 0.5, 1 and 2 kHz, and maximum speech recognition scores were 90-100% for the better hearing ear, both suggesting absence of retrocochlear pathology. Acoustic reflexes were present (both ipsi- and contralateral) without decay, which also suggested absence of

retrocochlear pathology. OAEs could only be detected in individuals II:2 and II:3 of family W16-0451, for frequencies with hearing thresholds lower than 30 dB HL. This is indicative of residual function of cochlear OHCs in these subjects.[26] OAEs were absent in all other affected subjects. The index cases of families W05-682 and W16-0195 displayed normal ABR wave latencies, which indicated normal auditory neural processing. Additional information on otologic and audiometric evaluation of individual cases is provided in Table S5a.

Individual longitudinal regression analyses of hearing thresholds revealed that HI was progressive in all affected adults. No progression could be demonstrated in the affected children, for whom follow-up time was probably too short (1-11 years) to establish significant progression. Cross-sectional linear regression analysis revealed progression of HI for all frequencies. The increase of hearing thresholds was significant at 1 kHz (0.8 dB/year), 2 kHz (0.5 dB/year) and 4 kHz (0.6 dB/year). In Figure 7b, the ARTA is depicted, which demonstrates gradual progression of HI.
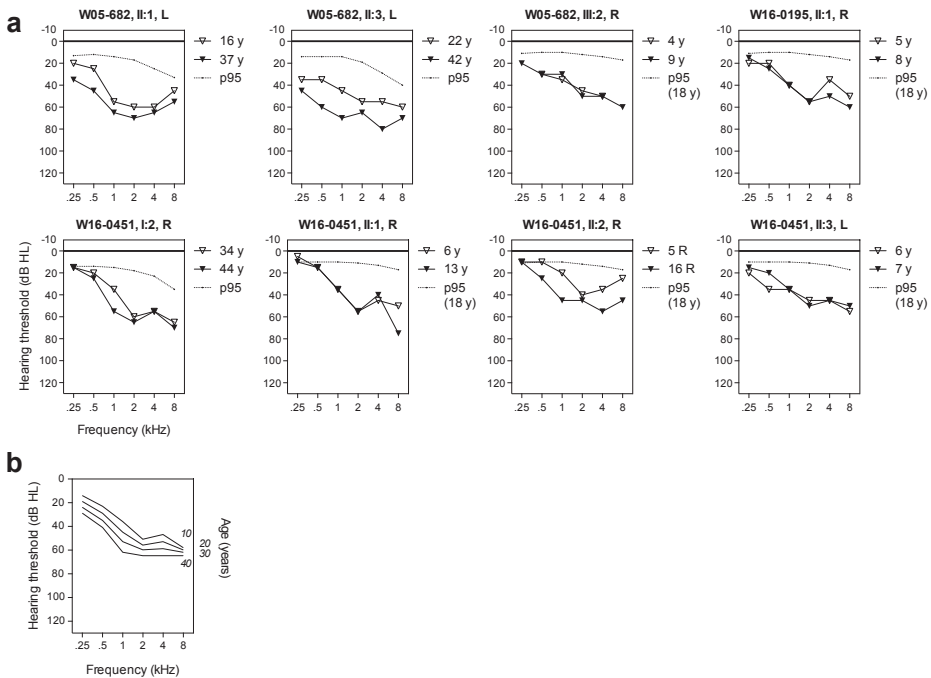
Figure 7 Audiometric characterization of families affected by pathogenic *MPZL2* variants.
(**a**) Air conduction thresholds of the better hearing ear of all affected individuals. The better hearing ear was determined by calculating the mean of the pure-tone thresholds for 0.5, 1, 2 and 4 kHz of the last audiogram. First-visit and last-visit audiograms are depicted. Subject II:1 of family W16-0451 was not able to participate in the clinical evaluation; only retrospective data of this subject were used for analysis. R, right ear; L, left ear. (**b**) ARTA (Age Related Typical Audiogram) constructed by cross-sectional linear regression analysis of last-visit audiograms of all affected individuals (n=8).

None of the affected subjects or their parents reported vestibular symptoms, such as vertigo, dizziness, instability or delayed motor development, except for the index case of family W16-0451 (I:2) who reported two periods of vertigo in the past without persisting complaints. Vestibular function was assessed in three of the hearing impaired individuals (family W05-682, II:1; family W16-0451, I:2 and II:2) and normal to slight hyperreactive vestibular responses were measured (Table S5b).

Because *MPZL2* is highly homologous to *MPZ* (MIM: 159440), which is associated with distinct types of hereditary motor and sensory neuropathy[27-33], we performed neurological screening of the affected individuals (family W05-682, II:1, II:3, III:2; family W16-0195, II:1; family W16-0451, I:2, II:2, II:3). No symptoms or signs of neuropathy were present.

Hearing-impaired subjects were also screened for immunological abnormalities, because *MPZL2* is involved in early thymocyte development.[34-36] None of them had symptoms of immunodeficiency, allergies or autoimmune disease. CD4 and CD8 T cell counts, including double positive (CD4+CD8+) cell counts, double negative (CD4-CD8-) cell counts, as well as the CD4/CD8 ratios, were normal (Figure S11), indicating normal CD4 and CD8 expression on T cells.

As gene expression studies have shown that *MPZL2* transcript levels are relatively high in the cornea of the eye (Ocular Tissue Database)[37], affected individuals were screened for corneal abnormalities. There were no eye problems, slit lamp biomicroscopy did not show abnormalities and visual acuity was normal.

4.1

Discussion

This study provides evidence for the association of biallelic defects of *MPZL2* with recessively inherited sensorineural NSHI in man and mouse. Affected human subjects displayed moderate to severe, slowly progressive HI from the first decade onwards, and intra- and interfamilial phenotypic similarity was high. The causal relationship between *MPZL2* defects and HI in the families was confirmed by functional and morphological inner ear defects in *Mpzl2*$^{ko/ko}$ mice. HI of these mice and affected family members was similar with regard to the early onset, the progressive nature and high-frequency hearing being most severely affected. The latter is reflected by the decreasing severity of disorganization and loss of OHCs and DCs from cochlear base to apex.[38]

OHCs function as cochlear amplifiers that enhance hearing thresholds by more than 40 dB, and loss of the amplifying function leads to 40-60 dB HI.[39,40] As subjects with deleterious *MPZL2* variants displayed a 35 to 65 dB increase of hearing thresholds, the HI phenotype is compatible with predominant loss of OHCs. In addition, the remarkably good

speech discrimination compared to the hearing thresholds and absence of OAEs in the affected individuals indicate abnormal OHC function.[41,42] Given the only moderate HI of the affected adult subjects of family W05-682 and subject I:2 of family W16-0451 at the age of about 40 years, we hypothesize that IHCs do not, or very slowly degenerate over time.

MPZL2 (Myelin Protein Zero-like 2), alternatively called EVA1 (Epithelial V-like Antigen 1), is a low-affinity adhesion molecule and a member of the immunoglobulin superfamily, more specifically of the family of immunoglobulin-like cell adhesion molecules (Ig-CAMs).[34] Ig-CAMs form a large family of cell surface molecules broadly expressed in for example epithelial and endothelial cells and in the nervous system. Ig-CAMs are known to interact directly with other classes of cell surface molecules such as cadherins, integrins, tyrosine kinase receptors and intracellularly also with proteins of the cytoskeleton such as actin and ankyrin. (for review see [43,44])

The biological function of MPZL2 is likely to be related to its ability to mediate both homophilic and heterophilic cell-cell adhesions. In mouse, *Mpzl2* is already expressed early in embryogenesis in various epithelial tissues as well as in adult tissues.[34,45] An adhesive function of *MPZL2* has been indicated in thymus histogenesis and T-cell development[34,35], placental morphogenesis[46], blood-cerebrospinal barrier[47], lymphocyte adhesion to choroid plexus epithelial cells[48], and in mammary epithelial cell differentiation.[45] Upregulation of *Mpzl2* in spermatogenic cells of cell adhesion molecule 1-deficient mice further supports the cell adhesive function.[49] Also, MPZL2 was demonstrated to function in proliferation and tumorigenesis of glioblastoma-initiating cells.[50] Despite these manifold indications of functional significance of MPZL2, HI is to our knowledge the first phenotype found to be associated with MPZL2 deficiency.[50,51] However, more phenotypic effects might emerge under stress conditions, as is suggested by increased severity of experimentally induced autoimmune encephalomyelitis and white matter tissue injury in MPZL2-deficient mice.[51]

In the developing and adult inner ear, several CAMs, belonging to different protein families including the Ig-CAM superfamily, display a specific spatiotemporal pattern of expression and several of these Ig-CAMs are critical for hearing and/or balance in both mice and humans.[52-59] The Ig-CAMs nectin-1 and -3, for example, are critical for establishing the checkerboard-like organization of hair cells and supporting cells in the cochlea.[60] The abnormal organization of DCs and OHCs, and their loss in *Mpzl2ko/ko* mice at 12 weeks of age indicate that MPZL2 is essential for maintenance of the DC-OHC organization and integrity. A role in maintenance is supported by the moderate transcript levels of MPZL2 in adult human cochleae.[23] Although no structural abnormalities were detected in cochleae of *Mpzl2ko/ko* mice at P4, MPZL2 is likely to function in prenatal cochlear development as well, in both man and mouse, as transcription of the gene was demonstrated in human embryos at 8 weeks of gestation and in mouse developing hair cells and their surrounding cells from

embryonic day 16 (E16) to P16.[61](See also the SHIELD database). From the present study it is unclear whether *MPZL2*-associated HI is congenital or has an early childhood onset. As speech-language development was disturbed in a number of cases, onset of HI was prelingual these individuals. If HI was congenital in the cases with prelingual HI, thresholds were below 35 dB HL as two of three individuals with prelingual HI had a neonatal hearing screening, which they passed. These tests are calibrated to pick up HI of more than 35 dB HL.[62]

To our knowledge, MPZL2 is the first CAM that is specifically expressed at the base of DCs where they contact the basilar membrane. DCs develop a narrow infranuclear region that ends in feet-like junctions with the basal membrane.[63] The stripe-shaped signal in DCs in MPZL2-immunohistochemistry might represent the developing feet-like structures. It is tempting to speculate that MPZL2 is involved in the morphogenesis and/or maintenance of the characteristic structure of DCs by anchoring the actin-rich cytoskeletal core of the feet-like structures or the surrounding microtubules to the basilar membrane.[63] The relatively weak MPZL2 signal in immunohistochemistry at P4 in OHCs, IHCs and the cytoplasm of DCs, suggest that MPLZ2 (transiently) functions in homophilic or heterophilic cellular junctions of these cells and that absence of these junctions in *Mpzl2^{ko/ko}* mice might contribute to the disorganization and degeneration of the organ of Corti.

Although not much is known about the adhesive function of MPZL2 at the molecular level, some hints towards molecular interactions have been obtained. A co-association of MPZL2 and CLCA2 with ZO-1 has been described.[45] ZO-1 is an adapter protein that functions in the coupling of TJs and adherens junctions (AJs) to the cytoskeleton.[64] Also, ZO-1 binds directly to occludin *in vitro*.[58] Interestingly, an association of MPZL2 and occludin has been observed in a high-throughput human protein interaction study.[65] Occludin is a tight junction (TJ) protein and essential for functional integrity of the reticular lamina of the organ of Corti.[56] The organ of Corti of *Occ^{-/-}* mice degenerates, starting in the OHC region. Because of these associations and the organ of Corti defects of *Mpzl2^{ko/ko}* mice, it is tempting to speculate that MPZL2 is essential for (functional) integrity of cell junctions in the reticular lamina, especially in the OHC region, and thereby for ion homeostasis in the cochlea. The associations of MPZL2 with TJ and AJ proteins and their co-function in the cochlea have to be validated with other protein interaction assays, and co-localization assays in the inner ear. The latter assays were impaired by failure of antibodies to detect MPZL2 in the experimental conditions to be used in immunofluorescence of adult cochleae.

Recently, it was demonstrated that MPZL2 can activate the NF-κB signaling pathway, likely by binding TRAF2, for which a consensus binding site is present in the cytoplasmic domain of MPLZ2.[50] This pathway was indicated to be protective for hair cell loss by environmental factors such as noise and aminoglycosides.[66,67] Therefore, defects of MPZL2

4.1

might lead to an increased sensitivity to noise and other environmental cues.

Although MPZL2 was detected in the basal cell layer of the developing stria vascularis, no gross histological abnormalities were observed in this region of the cochlea in *Mpzl2*[ko/ko] mice neither at the age of four days nor at 12 weeks of age. However, this does not fully exclude functional defects. A mild loss of spiral ganglion neurons was observed in the basal turn of the cochlea of *Mpzl2*[ko/ko] mice, which might be secondary to hair cell loss.

In conclusion, we demonstrated that MPZL2 is essential for normal cochlear function in man and mouse. In the latter species, defects of MPZL2 resulted in disorganization of the OHCs and DCs that is likely to interfere with mechanical and other functional properties of that region of the cochlea and ultimately in loss of organ of Corti integrity. Humans affected by biallelic truncating *MPZL2* variants displayed slowly progressive NSHI, which is important in (genetic) counseling of subjects and their families.

Acknowledgements

Web Resources

The URLs for data presented herein are as follows:

Alamut Visual, http://www.interactive-biosoftware.com/alamut- visual/

ExAC Browser, http://exac.broadinstitute.org/

GnomAD Browser, http://gnomad.broadinstitute.org/

Hereditary Hearing loss Homepage, http://hereditaryhearingloss.org/

HomozygosityMapper, http://www.homozygositymapper.org/

Marshfield Genetic Maps, http://research.marshfieldclinic.org/genetics/GeneticResearch/compMaps.asp

Ocular Tissue Database, https://genome.uiowa.edu/otdb/

Oligo Primer Analysis Software, http://www.oligo.net/

OMIM, http://www.omim.org/

OMIM Phenotypic Series, http://www.omim.org/phenotypicSeriesTitle/all

Primer3Plus, http://www.bioinformatics.nl/cgi-bin/primer3plus/primer3plus.cgi

SMART, http://smart.embl-heidelberg.de/

UCSC Genome Browser, https://genome.ucsc.edu

4.1

References

1. Sommen M, Schrauwen I, Vandeweyer G, et al. DNA Diagnostics of Hereditary Hearing Loss: A Targeted Resequencing Approach Combined with a Mutation Classification System. *Human mutation.* Aug 2016;37(8):812-819.

2. Yan D, Tekin D, Bademci G, et al. Spectrum of DNA variants for non-syndromic deafness in a large cohort from multiple continents. *Human genetics.* Aug 2016;135(8):953-961.

3. Sloan-Heggen CM, Bierer AO, Shearer AE, et al. Comprehensive genetic testing in the clinical evaluation of 1119 patients with hearing loss. *Human genetics.* Apr 2016;135(4):441-450.

4. Shearer AE, Black-Ziegelbein EA, Hildebrand MS, et al. Advancing genetic testing for deafness with genomic technology. *Journal of medical genetics.* Sep 2013;50(9):627-634.

5. Atik T, Onay H, Aykut A, et al. Comprehensive Analysis of Deafness Genes in Families with Autosomal Recessive Nonsyndromic Hearing Loss. *PloS one.* 2015;10(11):e0142154.

6. Zazo Seco C, Wesdorp M, Feenstra I, et al. The diagnostic yield of whole-exome sequencing targeting a gene panel for hearing impairment in The Netherlands. *European journal of human genetics : EJHG.* Feb 2017;25(3):308-314.

7. Zazo Seco C, Serrao de Castro L, van Nierop JW, et al. Allelic Mutations of KITLG, Encoding KIT Ligand, Cause Asymmetric and Unilateral Hearing Loss and Waardenburg Syndrome Type 2. *American journal of human genetics.* Nov 05 2015;97(5):647-660.

8. Zazo Seco C, Castells-Nobau A, Joo SH, et al. A homozygous FITM2 mutation causes a deafness-dystonia syndrome with motor regression and signs of ichthyosis and sensory neuropathy. *Disease models & mechanisms.* Feb 01 2017;10(2):105-118.

9. Garabatos N, Blanco J, Fandos C, et al. A monoclonal antibody against the extracellular domain of mouse and human epithelial V-like antigen 1 reveals a restricted expression pattern among CD4- CD8- thymocytes. *Monoclonal antibodies in immunodiagnosis and immunotherapy.* Oct 2014;33(5):305-311.

10. Mazzoli M, Van Camp G, Newton V, Giarbini N, Declau F, Parving A. Recommendations for the description of genetic and audiological data for families with nonsyndromic hereditary hearing impairment. *Audiological Medicine.* 2003;1:148-150.

11. Huygen PLM, Pennings RJE, Cremers CWRJ. Characterizing and distinguishing progressive phenotypes in nonsyndromic autosomal dominant hearing impairment. . *Audiol. Med.* . 2003;1:37-46.

12. Bosman AJ, Smoorenburg GF. Intelligibility of Dutch CVC syllables and sentences for listeners with normal hearing and with three types of hearing impairment. *Audiology : official organ of the International Society of Audiology.* Sep-Oct 1995;34(5):260-284.

13. Seelow D, Schuelke M, Hildebrandt F, Nurnberg P. HomozygosityMapper--an interactive approach to homozygosity mapping. *Nucleic acids research.* Jul 2009;37(Web Server issue):W593-599.

14. Neveling K, Feenstra I, Gilissen C, et al. A post-hoc comparison of the utility of sanger sequencing and exome sequencing for the diagnosis of heterogeneous diseases. *Human mutation.* Dec 2013;34(12):1721-1726.

15. Wallis Y, Payne S, McAnulty C, et al. Practice Guidelines for the Evaluation of Pathogenicity and the Reporting of Sequence Variants in Clinical Molecular Genetics. *ACGS /VGKL.* 2013.

16. Luijendijk MW, van de Pol TJ, van Duijnhoven G, et al. Cloning, characterization, and mRNA expression analysis of novel human fetal cochlear cDNAs. *Genomics.* Oct 2003;82(4):480-490.

17. Pfaffl MW. A new mathematical model for relative quantification in real-time RT-PCR. *Nucleic acids research.* May 1 2001;29(9):e45.

18. Cediel R, Riquelme R, Contreras J, Diaz A, Varela-Nieto I. Sensorineural hearing loss in insulin-like growth factor I-null mice: a new model of human deafness. *Eur J Neurosci.* Jan 2006;23(2):587-590.

19. Murillo-Cuesta S, Rodriguez-de la Rosa L, Contreras J, et al. Transforming growth factor beta1

inhibition protects from noise-induced hearing loss. *Frontiers in aging neuroscience.* 2015;7:32.

20. Martinez-Vega R, Garrido F, Partearroyo T, et al. Folic acid deficiency induces premature hearing loss through mechanisms involving cochlear oxidative stress and impairment of homocysteine metabolism. *FASEB J.* Feb 2015;29(2):418-432.

21. Sanchez-Calderon H, Rodriguez-de la Rosa L, Milo M, Pichel JG, Holley M, Varela-Nieto I. RNA microarray analysis in prenatal mouse cochlea reveals novel IGF-I target genes: implication of MEF2 and FOXM1 transcription factors. *PloS one.* Jan 25 2010;5(1):e8699.

22. Skvorak AB, Weng Z, Yee AJ, Robertson NG, Morton CC. Human cochlear expressed sequence tags provide insight into cochlear gene expression and identify candidate genes for deafness. *Human molecular genetics.* Mar 1999;8(3):439-452.

23. Schrauwen I, Hasin-Brumshtein Y, Corneveaux JJ, et al. A comprehensive catalogue of the coding and non-coding transcripts of the human inner ear. *Hearing research.* Mar 2016;333:266-274.

24. Hodoglugil U, Mahley RW. Turkish population structure and genetic ancestry reveal relatedness among Eurasian populations. *Ann Hum Genet.* Mar 2012;76(2):128-141.

25. Fuentes-Santamaria V, Alvarado JC, Rodriguez-de la Rosa L, et al. IGF-1 deficiency causes atrophic changes associated with upregulation of VGluT1 and downregulation of MEF2 transcription factors in the mouse cochlear nuclei. *Brain structure & function.* Mar 2016;221(2):709-734.

26. Brownell WE. Outer hair cell electromotility and otoacoustic emissions. *Ear and hearing.* Apr 1990;11(2):82-92.

27. Su Y, Brooks DG, Li L, et al. Myelin protein zero gene mutated in Charcot-Marie-tooth type 1B patients. *Proceedings of the National Academy of Sciences of the United States of America.* Nov 15 1993;90(22):10856-10860.

28. Mastaglia FL, Nowak KJ, Stell R, et al. Novel mutation in the myelin protein zero gene in a family with intermediate hereditary motor and sensory neuropathy. *Journal of neurology, neurosurgery, and psychiatry.* Aug 1999;67(2):174-179.

29. Marrosu MG, Vaccargiu S, Marrosu G, Vannelli A, Cianchetti C, Muntoni F. Charcot-Marie-Tooth disease type 2 associated with mutation of the myelin protein zero gene. *Neurology.* May 1998;50(5):1397-1401.

30. Chapon F, Latour P, Diraison P, Schaeffer S, Vandenberghe A. Axonal phenotype of Charcot-Marie-Tooth disease associated with a mutation in the myelin protein zero gene. *Journal of neurology, neurosurgery, and psychiatry.* Jun 1999;66(6):779-782.

31. Hayasaka K, Himoro M, Sawaishi Y, et al. De novo mutation of the myelin P0 gene in Dejerine-Sottas disease (hereditary motor and sensory neuropathy type III). *Nature genetics.* Nov 1993;5(3):266-268.

32. Warner LE, Hilz MJ, Appel SH, et al. Clinical phenotypes of different MPZ (P0) mutations may include Charcot-Marie-Tooth type 1B, Dejerine-Sottas, and congenital hypomyelination. *Neuron.* Sep 1996;17(3):451-460.

33. Plante-Bordeneuve V, Guiochon-Mantel A, Lacroix C, Lapresle J, Said G. The Roussy-Levy family: from the original description to the gene. *Annals of neurology.* Nov 1999;46(5):770-773.

34. Guttinger M, Sutti F, Panigada M, et al. Epithelial V-like antigen (EVA), a novel member of the immunoglobulin superfamily, expressed in embryonic epithelia with a potential role as homotypic adhesion molecule in thymus histogenesis. *The Journal of cell biology.* May 18 1998;141(4):1061-1071.

35. DeMonte L, Porcellini S, Tafi E, et al. EVA regulates thymic stromal organisation and early thymocyte development. *Biochemical and biophysical research communications.* May 04 2007;356(2):334-340.

36. Iacovelli S, Iosue I, Di Cesare S, Guttinger M. Lymphoid EVA1 expression is required for DN1-DN3 thymocytes transition. *PloS one.* Oct 23 2009;4(10):e7586.

37. Wagner AH, Anand VN, Wang WH, et al. Exon-level expression profiling of ocular tissues.

4.1

Experimental eye research. Jun 2013;111:105-111.

38. Mann ZF, Kelley MW. Development of tonotopy in the auditory periphery. *Hearing research.* Jun 2011;276(1-2):2-15.

39. Ryan A, Dallos P. Effect of absence of cochlear outer hair cells on behavioural auditory threshold. *Nature.* Jan 03 1975;253(5486):44-46.

40. Liberman MC, Gao J, He DZ, Wu X, Jia S, Zuo J. Prestin is required for electromotility of the outer hair cell and for the cochlear amplifier. *Nature.* Sep 19 2002;419(6904):300-304.

41. Dorn PA, Piskorski P, Gorga MP, Neely ST, Keefe DH. Predicting audiometric status from distortion product otoacoustic emissions using multivariate analyses. *Ear and hearing.* Apr 1999;20(2):149-163.

42. Hoben R, Easow G, Pevzner S, Parker MA. Outer Hair Cell and Auditory Nerve Function in Speech Recognition in Quiet and in Background Noise. *Frontiers in neuroscience.* 2017;11:157.

43. Bombardelli L, Cavallaro U. Immunoglobulin-like cell adhesion molecules: novel signaling players in epithelial ovarian cancer. *Int J Biochem Cell Biol.* May 2010;42(5):590-594.

44. Rougon G, Hobert O. New insights into the diversity and function of neuronal immunoglobulin superfamily molecules. *Annu Rev Neurosci.* 2003;26:207-238.

45. Ramena G, Yin Y, Yu Y, Walia V, Elble RC. CLCA2 Interactor EVA1 Is Required for Mammary Epithelial Cell Differentiation. *PloS one.* 2016;11(3):e0147489.

46. Teesalu T, Grassi F, Guttinger M. Expression pattern of the epithelial v-like antigen (Eva) transcript suggests a possible role in placental morphogenesis. *Developmental genetics.* 1998;23(4):317-323.

47. Chatterjee G, Carrithers LM, Carrithers MD. Epithelial V-like antigen regulates permeability of the blood-CSF barrier. *Biochemical and biophysical research communications.* Aug 01 2008;372(3):412-417.

48. Wojcik E, Carrithers LM, Carrithers MD. Characterization of epithelial V-like antigen in human choroid plexus epithelial cells: potential role in CNS immune surveillance. *Neuroscience letters.* May 16 2011;495(2):115-120.

49. Nakata H, Wakayama T, Adthapanyawanich K, et al. Compensatory upregulation of myelin protein zero-like 2 expression in spermatogenic cells in cell adhesion molecule-1-deficient mice. *Acta histochemica et cytochemica.* Feb 29 2012;45(1):47-56.

50. Ohtsu N, Nakatani Y, Yamashita D, Ohue S, Ohnishi T, Kondo T. Eva1 Maintains the Stem-like Character of Glioblastoma-Initiating Cells by Activating the Noncanonical NF-kappaB Signaling Pathway. *Cancer research.* Jan 01 2016;76(1):171-181.

51. Wright E, Rahgozar K, Hallworth N, Lanker S, Carrithers MD. Epithelial V-like antigen mediates efficacy of anti-alpha(4) integrin treatment in a mouse model of multiple sclerosis. *PloS one.* 2013;8(8):e70954.

52. Whitlon DS. E-cadherin in the mature and developing organ of Corti of the mouse. *Journal of neurocytology.* Dec 1993;22(12):1030-1038.

53. Simonneau L, Gallego M, Pujol R. Comparative expression patterns of T-, N-, E-cadherins, beta-catenin, and polysialic acid neural cell adhesion molecule in rat cochlea during development: implications for the nature of Kolliker's organ. *J Comp Neurol.* Apr 28 2003;459(2):113-126.

54. Nakano Y, Kim SH, Kim HM, et al. A claudin-9-based ion permeability barrier is essential for hearing. *PLoS genetics.* Aug 2009;5(8):e1000610.

55. Ben-Yosef T, Belyantseva IA, Saunders TL, et al. Claudin 14 knockout mice, a model for autosomal recessive deafness DFNB29, are deaf due to cochlear hair cell degeneration. *Human molecular genetics.* Aug 15 2003;12(16):2049-2061.

56. Kitajiri S, Katsuno T, Sasaki H, Ito J, Furuse M, Tsukita S. Deafness in occludin-deficient mice with dislocation of tricellulin and progressive apoptosis of the hair cells. *Biology open.* Jul 25 2014;3(8):759-766.

57.	Kamitani T, Sakaguchi H, Tamura A, et al. Deletion of Tricellulin Causes Progressive Hearing Loss Associated with Degeneration of Cochlear Hair Cells. *Scientific reports.* Dec 18 2015;5:18402.

58.	Riazuddin S, Ahmed ZM, Fanning AS, et al. Tricellulin is a tight-junction protein necessary for hearing. *American journal of human genetics.* Dec 2006;79(6):1040-1051.

59.	Wilcox ER, Burton QL, Naz S, et al. Mutations in the gene encoding tight junction claudin-14 cause autosomal recessive deafness DFNB29. *Cell.* Jan 12 2001;104(1):165-172.

60.	Togashi H, Kominami K, Waseda M, et al. Nectins establish a checkerboard-like cellular pattern in the auditory epithelium. *Science.* Aug 26 2011;333(6046):1144-1147.

61.	Scheffer DI, Shen J, Corey DP, Chen ZY. Gene Expression by Mouse Inner Ear Hair Cells during Development. *The Journal of neuroscience : the official journal of the Society for Neuroscience.* Apr 22 2015;35(16):6366-6380.

62.	van der Ploeg CP, Uilenburg NN, Kauffman-de Boer MA, Oudesluys-Murphy AM, Verkerk PH. Newborn hearing screening in youth health care in the Netherlands: National results of implementation and follow-up. *International journal of audiology.* Aug 2012;51(8):584-590.

63.	Parsa A, Webster P, Kalinec F. Deiters cells tread a narrow path--the Deiters cells-basilar membrane junction. *Hearing research.* Aug 2012;290(1-2):13-20.

64.	Gonzalez-Mariscal L, Betanzos A, Avila-Flores A. MAGUK proteins: structure and role in the tight junction. *Semin Cell Dev Biol.* Aug 2000;11(4):315-324.

65.	Huttlin EL, Ting L, Bruckner RJ, et al. The BioPlex Network: A Systematic Exploration of the Human Interactome. *Cell.* Jul 16 2015;162(2):425-440.

66.	Tamura A, Matsunobu T, Tamura R, Kawauchi S, Sato S, Shiotani A. Photobiomodulation rescues the cochlea from noise-induced hearing loss via upregulating nuclear factor kappaB expression in rats. *Brain Res.* Sep 01 2016;1646:467-474.

67.	Dinh CT, Bas E, Chan SS, Dinh JN, Vu L, Van De Water TR. Dexamethasone treatment of tumor necrosis factor-alpha challenged organ of Corti explants activates nuclear factor kappa B signaling that induces changes in gene expression that favor hair cell survival. *Neuroscience.* Aug 11 2011;188:157-167.

4.1

Supplemental Data

Supplemental methods
Screening protocol for polyneuropathy in subjects with *MPZL2* variants.

Medical history was obtained regarding sensory disturbances, muscle weakness, functional impairment (walking, walking stairs, cycling), and use of medication. Participants also underwent physical neurological examination.

Neurological examination included testing of:
- Cranial nerves, according to current standards
- Muscle strength using the Medical Research Council (MRC) scores (0-5) of 18 predefined muscle groups, including shoulder abduction, elbow flexion, wrist extension, hip flexion, knee extension, foot dorsiflexion (extension) and plantar flexion, and toe dorsiflexon (extension); muscle tone and bulk
- Muscle mass of the extensor digitorum brevis muscle (normal / atrophic)
- Vigorimeter grip strength, as described previously[1]
- Coordination with use of nose-finger test and tandem gait (normal / abnormal).
- Sensation, using the Modified INCAT Sensory Sum Score (mISSReflexes) and the Romberg test (1= abnormal; 0 = normal), according to the European Federation of Neurological Societies/Peripheral Nerve Society guideline on management of chronic inflammatory demyelinating polyradiculoneuropathy[2]
- Deep tendon reflexes (biceps, triceps, patellar and ankle jerks) bilaterally (absent / reduced / normal)

Supplemental figures and tables
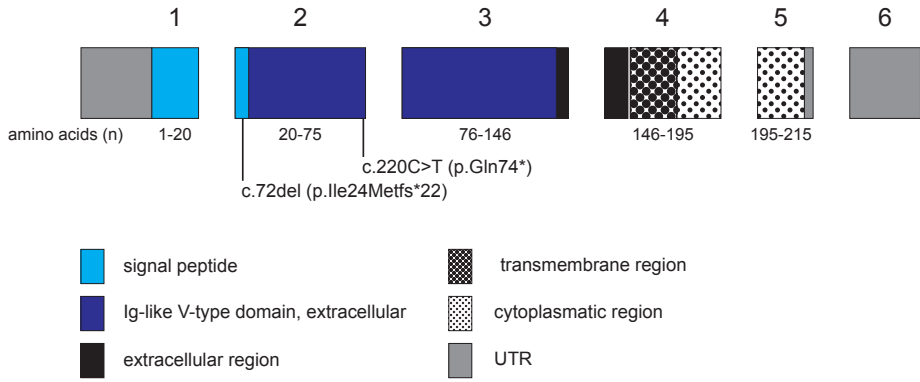
Figure S1 Exonic and protein structure of *MPZL2*/MPZL2 and pathogenic variants.
Schematic representation of the genomic structure and the encoded protein domains of *MPZL2* (NM_005797.3). Identified pathogenic variants are indicated. Protein domain predictions were extracted from the SMART domain database (http://smart.embl-heidelberg.de/), using the *PFAM domains* setting.
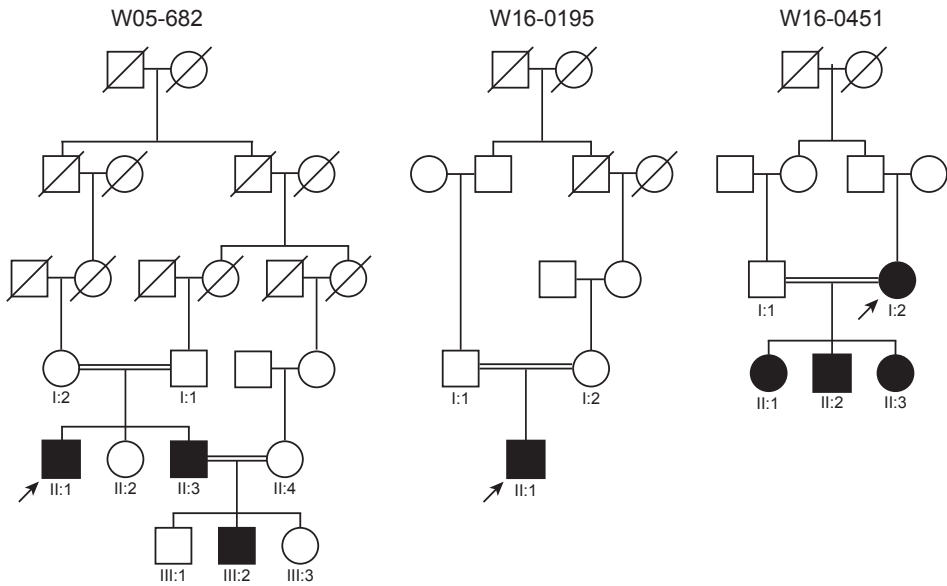
Figure S2 Extended pedigrees of families affected by *MPZL2* variants.
Index cases are marked by arrows. Double lines indicate consanguinity.
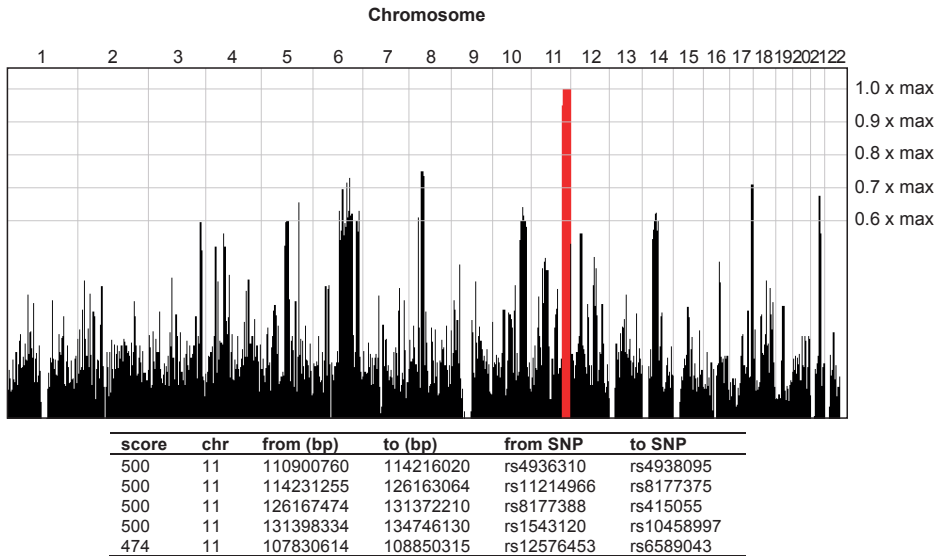
Figure S3 Homozygosity mapping in family W05-682.

Graphical representation of the genome-wide homozygosity scores in family W05-682, produced by HomozygosityMapper.[3] Homozygosity mapping was performed by genotyping of subjects II:1 and II:3 of family W05-682 with the Affymetrix mapping 250K SNP array, and subsequent genotype calling with Genotype Console software (Santa Clara, CA, USA) and homozygosity mapping with the online tool HomozygosityMapper (http://www.homozygositymapper.org/). This revealed a single homozygous region of 23.8 Mb on chromosome 11q23.1-q25, flanked by rs4936310 and rs10458997. There were no other significant regions of homozygosity.
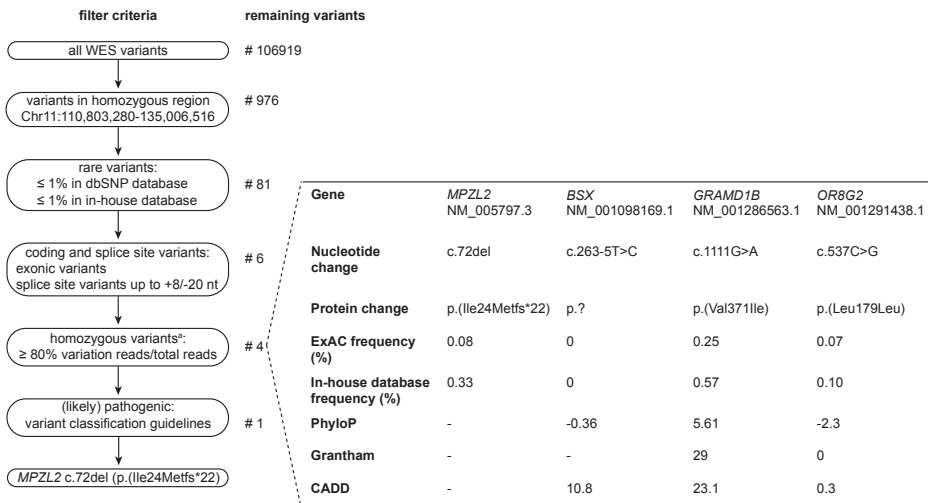
Figure S4 Filtering of WES variants in the largest homozygous region on chromosome 11q23.1-q25 of family W05-682.

Criteria of variant filtering and resulting number of variants of WES data for the index case (II:1) of family W05-682. The in-house database contains WES data of 13314 individuals, the vast majority of Dutch origin, affected by a large number of different diseases (including 810 subjects with HI) and also non-affected individuals. The variants in *BSX, GRAMD1B* and *OR8G2* were considered not to be (likely) pathogenic, based on variant classification guidelines.[4] [a]No compound heterozygous variants were resulting from the first three filtering steps.

4.1
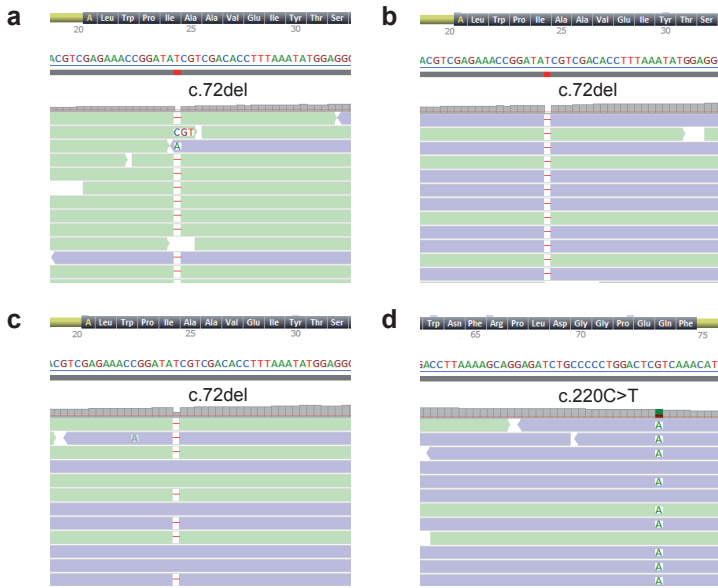
Figure S5 Sequences of *MPZL2* c.72del and c.220C>T.
Analysis of the WES paired-reads demonstrated a homozygous point deletion, *MPZL2* c.72del, in the index cases of families W05-682 (**a**) and W16-0195 (**b**). In the index case of family W16-0451, WES revealed the c.72del variant heterozygously (**c**) and the heterozygous missense variant *MPZL2* c.220C>T (**d**). NM_005797.3 was used as reference sequence. Figures were obtained using Alamut Visual (Interactive Biosoftware, Rouen, France).
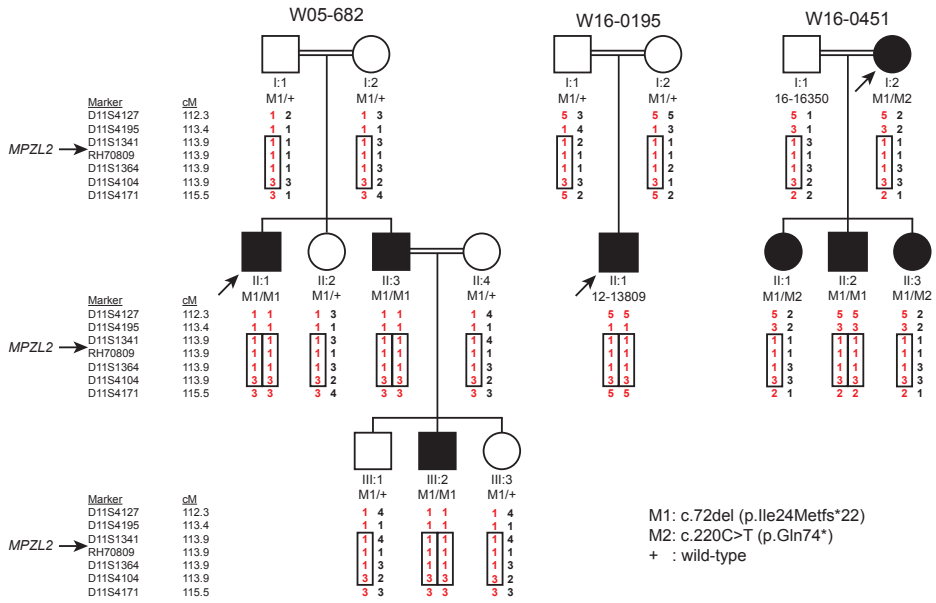
Figure S6 Haplotype analysis of the genomic region harboring *MPZL2*.

MPZL2 haplotypes were determined by genotyping VNTR-markers in families W05-682, W16-0195 and W16-0451. All c.72del *MPZL2* alleles (depicted in red) shared a haplotype of at least 0.5 Mb, delimited by markers D11S1341 and D11S4104 (boxed), suggesting that it is derived from a common ancestor. Index cases are marked by arrows.
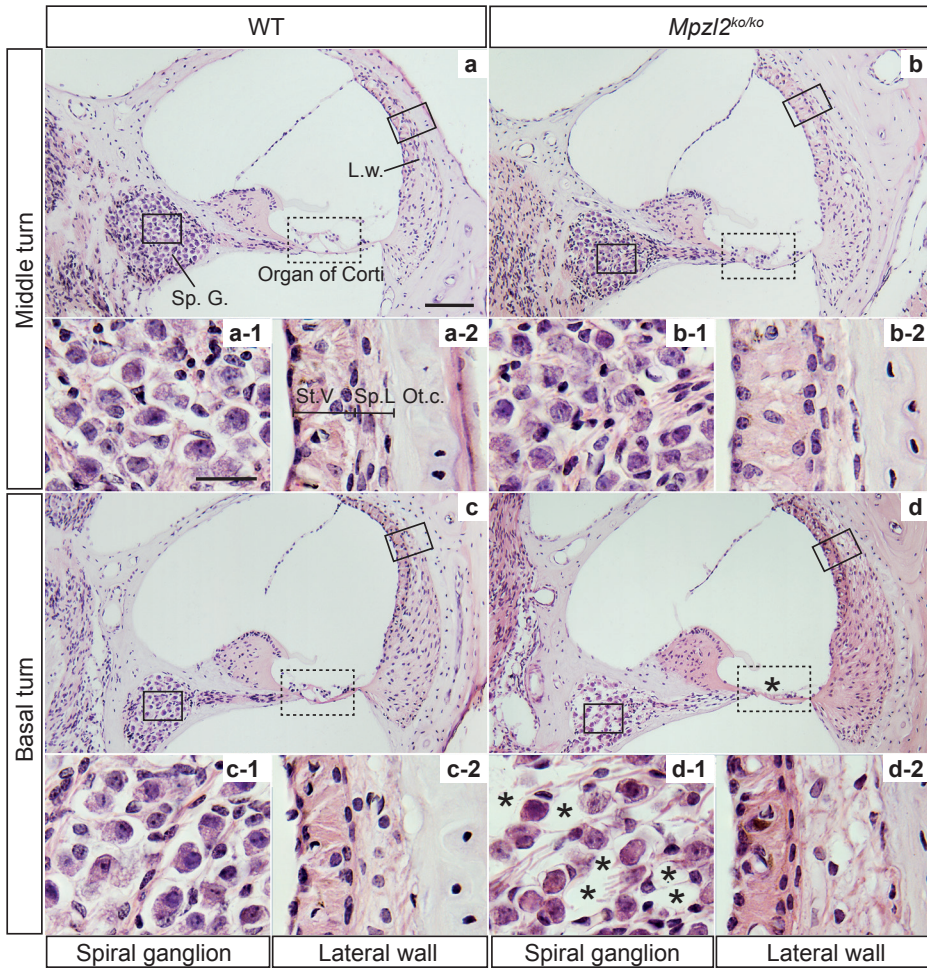
Figure S7 Cochlear morphology of 12-week-old wild-type mice and *Mpzl2^{ko/ko}* mice.
Representative microphotographs from the middle (**a** and **b**) and basal (**c** and **d**) cochlear turns from midmodiolar cross sections. The second and fourth rows include close-ups of the boxed areas, from left to right: spiral ganglion (1), and stria vascularis (2). Asterisks mark abnormalities. L.w., lateral wall; Ot.c., otic capsule; Sp.G., spiral ganglion; Sp.L., spiral ligament; St.V., stria vascularis. Scale bar a-d, 100 μm, close-ups 25 μm.
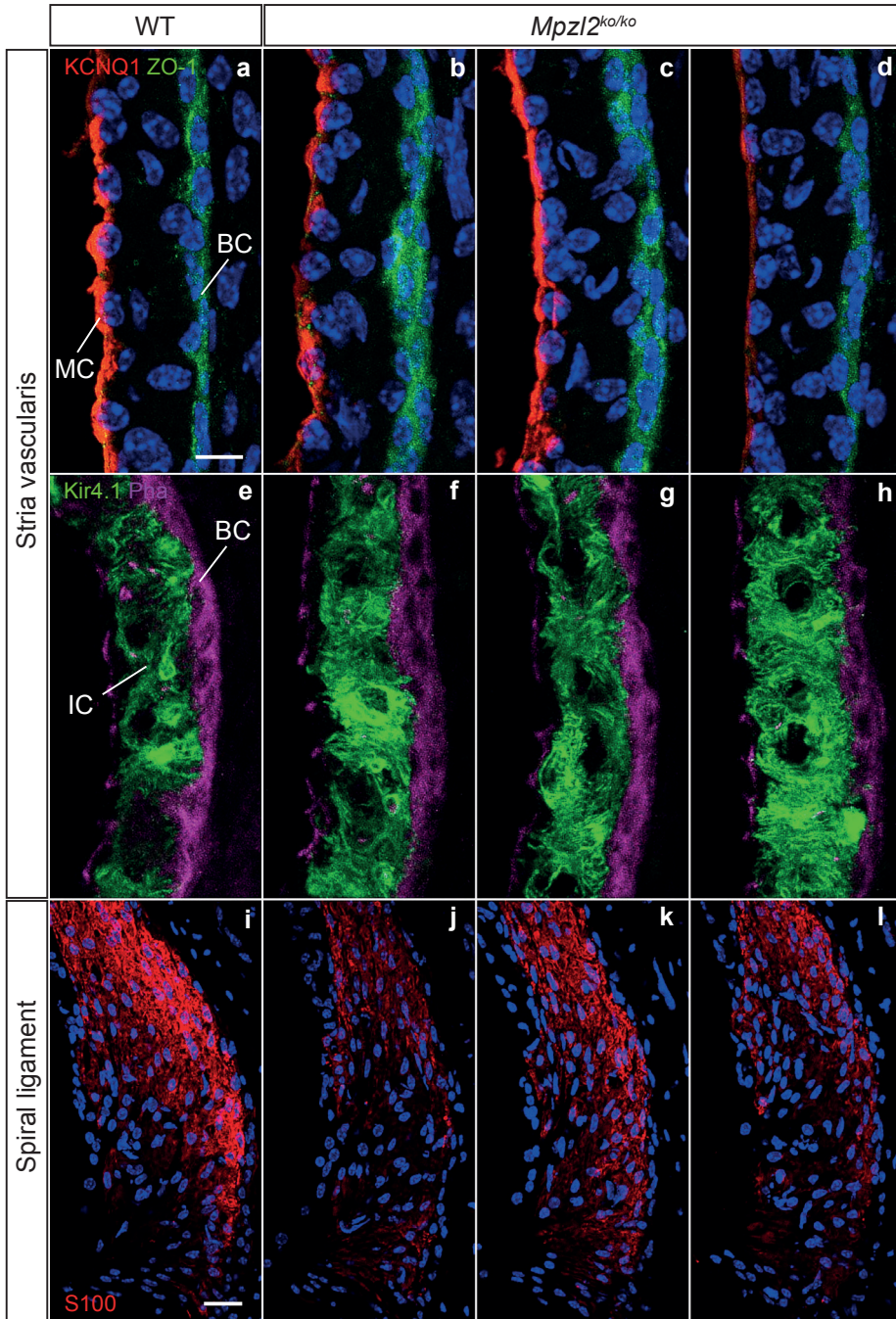
Figure S8 Normal cellular organization of the stria vascularis in wild-type mice and *Mpzl2*^ko/ko^ mice.
Close-ups of the stria vascularis (**a-h**) of the basal turn of the cochlea from representative cryosections (10

μm) prepared from a wild-type mouse (**a,e**) and three *Mpzl2^(ko/ko)^* mice (**b-d, f-h**). Strial marginal (MC), basal (BC) and intermediate cells (IC) were immunostained for KCNQ1 (red), ZO-1 (green) (**a-d**) and Kir4.1 (green) (**e-h**) respectively. Actin in the stria vascularis was stained with phalloidin (purple). Scale bar a-h: 10 μm.
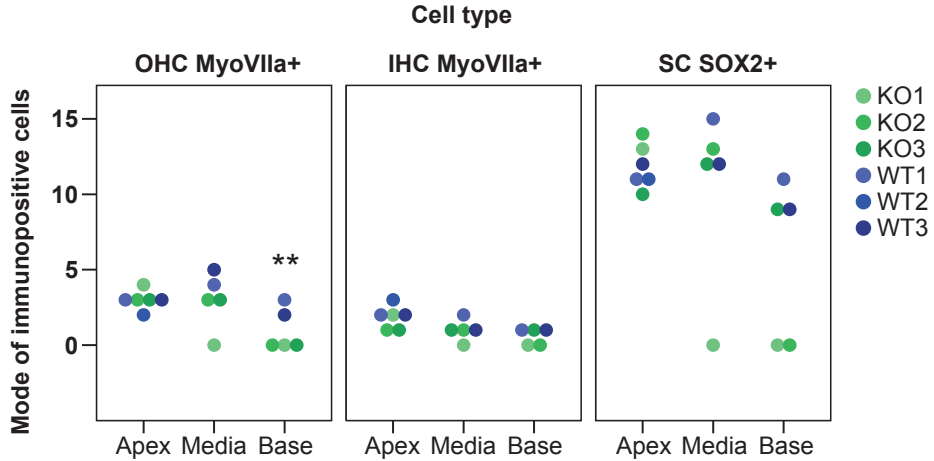
Figure S9 Quantification of MyoVIIa and SOX2 positive cells.

Cell numbers were evaluated for wild-type (blue) and *Mpzl2^(ko/ko)^* mice (green) for each turn of the cochlea. Data were obtained counting MyoVIIa and SOX2 positive cells in each cochlear region from 5 serial cryosections (10 μm) per animal (apex, n=3 mice per genotype in IHC and SC, n=2 wild-type, n= 3 KO in OHC; middle region, n= 2 wild-type, n=3 KO for each cell type; base, n=3 mice per genotype for each cell type). Data are expressed as the sum of each cell type per animal. Statistical analysis was performed by Student t-test between groups for each marker and level of the cochlea. **p<0.01 (KO *versus* WT). IHC, inner hair cells; KO, *Mpzl2^(ko/ko)^*; OHC, outer hair cells; SC, supporting cells.
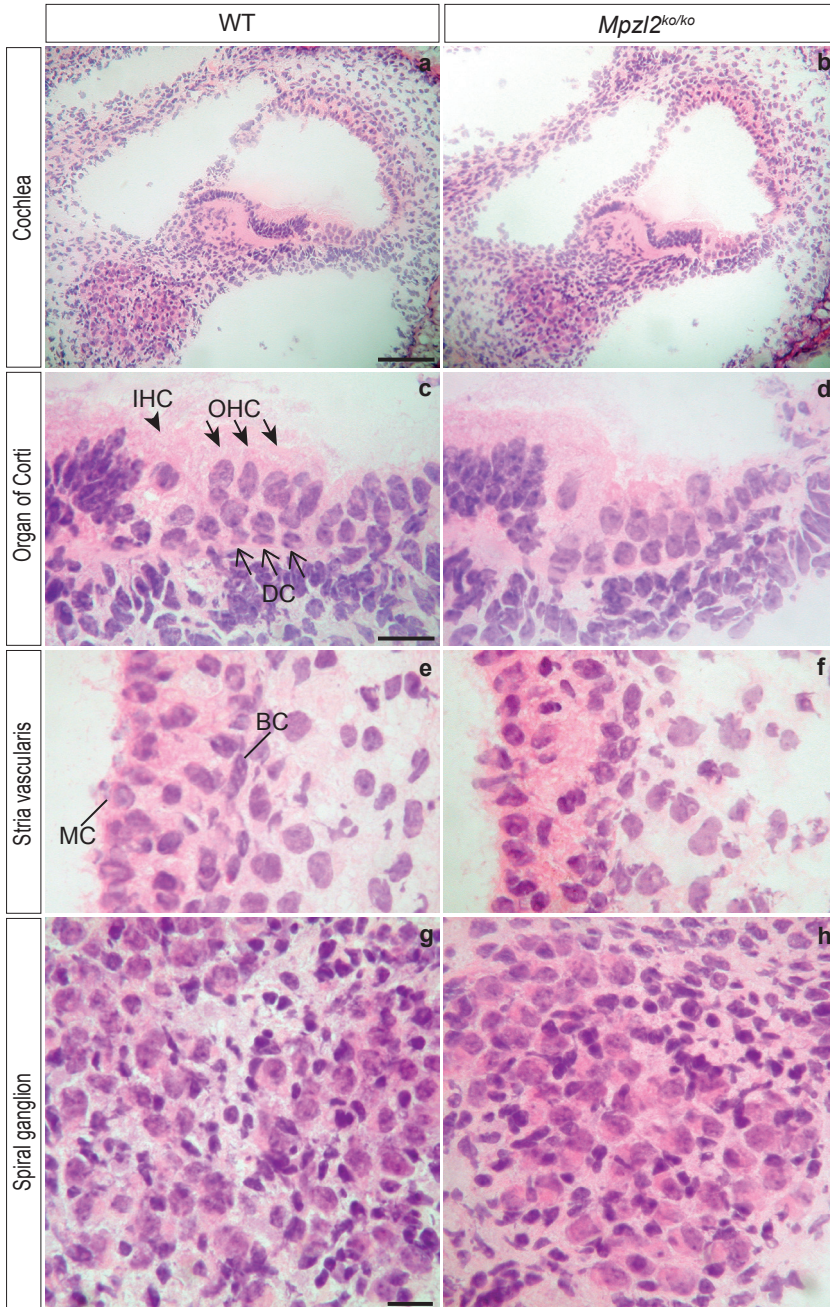
Figure S10 Normal histology of the cochlear basal turn at P4 in wild-type and *Mpzl2ko/ko* mice.
Overview of the basal turn of cochleae (**a, b**) and higher magnifications of organs of Corti (**c, d**), striae vascularis (**e, f**) and spiral ganglions (**g, h**). Arrowheads point to inner hair cells (IHC), blackhead arrows to outer hair cells (OHC) and arrows to Deiters cells (DC). BC, basal cells; MC, marginal cells; WT, wild-type. Scale bars a, b: 100 μm, c-f: 20 μm and g, h: 20 μm.
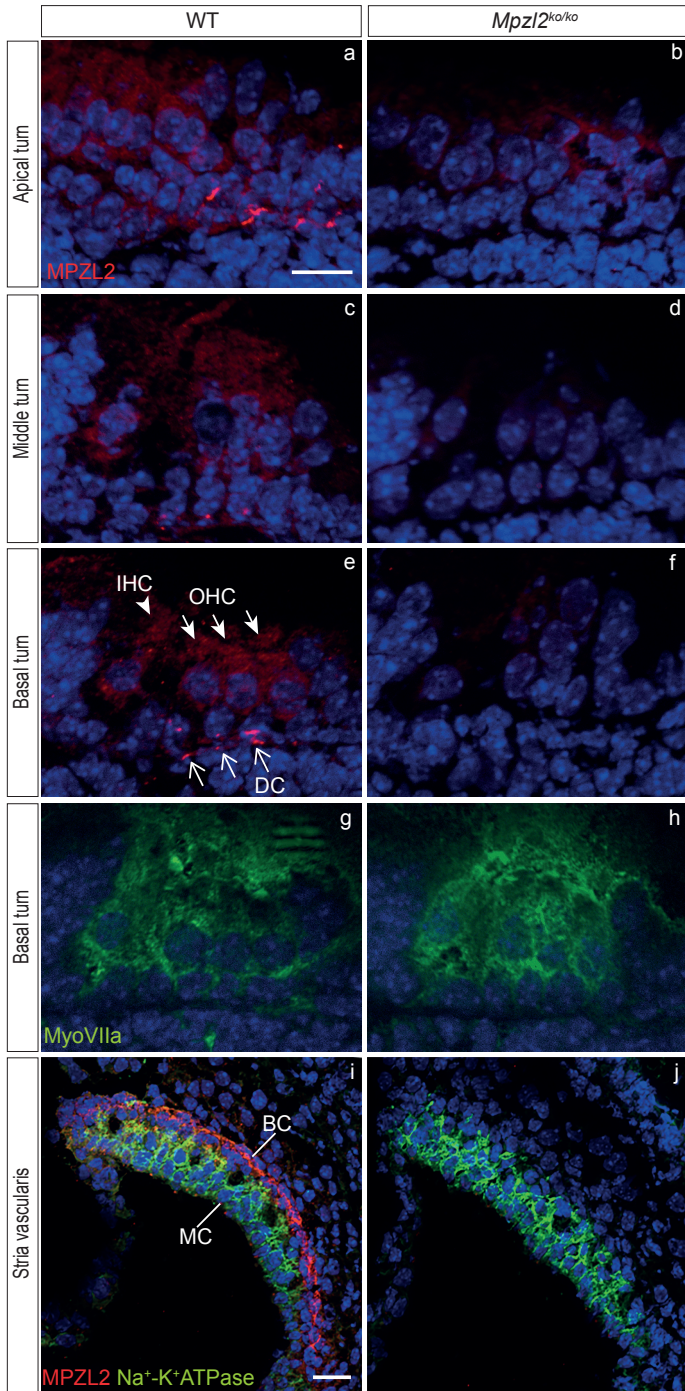
Figure S11 Specificity of immunostaining of MPZL2 in hair cells and Deiters cells of the organ of Corti and basal cells of the stria vascularis in P4 wild-type and *Mpzl2ko/ko* mice.

Immunostaining of MPZL2 (red) is observed diffusely in the hair cells and Deiters cells and with higher intensity at the basal part of the Deiters cells in the apical (**a**), middle (**c**) and basal (**e**) turns of the cochlea in wild-type mice. Antibody-specificity is confirmed by absence of immunostaining in these cells in the apical (**b**), middle (**d**) and basal (**f**) turns in *Mpzl2*[ko/ko] mice. Myosin VIIa (green) immunostaining shows the inner and outer hair cells of the organ of Corti in wild-type (**g**) and *Mpzl2*[ko/ko] (**h**) mice. In the basal cells of the stria vascularis immunostaining of MPZL2 (red) was observed in the wild-type (**i**) mice and not in *Mpzl2*[ko/ko] (**j**) mice. Na^{+}/K^{+}-ATPase (green) immunostaining was employed for marking marginal cells (**i, j**). Cell nuclei were stained with DAPI (blue). IHC: inner hair cell, OHC: outer hair cell, DC: Deiters cell, MC: marginal cells, BC: basal cells. Scale bars a-h: 20 µm and i, j: 20 µm.
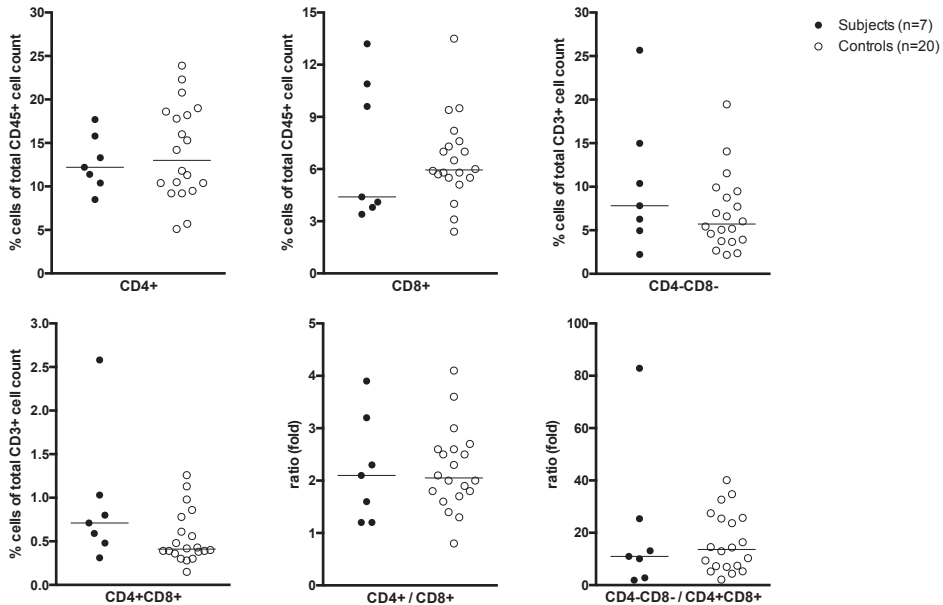
Figure S12 CD4 and CD8 expression on human T cells.
The number of CD4 and CD8 expressing human T cells was analyzed in affected individuals (family W05-682, II:1, II:3, III:2; family W16-0195, II:1; family W16-0451, I:2, II:2, II:3), as described in detail before.[5] In brief, peripheral blood was collected in EDTA-tubes, and after red cell lysis, leucocytes were stained with fluorochrome labelled antibodies against CD3 (UCHT-1 pe), CD4 (13B8.2 pacific blue), CD8 (B9.11 APC-AF750) and CD45 (J33 Krome Orange) (all from Beckman Coulter, Brea, USA). Data was acquired on a Navios flow cytometer (Beckman Coulter) and analyzed using Kaluza® software version 1.3 (Beckman Coulter). Presented cell counts are a percentage of total CD45+ cells (CD4+ and CD8+), a percentage of total CD3+ cells (CD4-CD8- and CD4+CD8+) or a fold ratio. Data of 20 healthy individuals was used as control. Individual and median cell counts and ratios are shown. Numbers of cells and ratios are comparable between subjects and controls, indicating normal CD4 and CD8 T cell counts. Mann-Whitney U tests did not demonstrate significant differences.

Table S1 Details on analyzed panels of HI-related genes, and coverage

Gene name	RefSeq transcript ID	Mean % covered ≥ 20x		
		HI panel DGD 20062014 family W05-682, II:1	HI panel DG 2.4 family W16-0195, II:1	HI panel DG 2.5 family W16-0451, I:2
Total		120 genes coverage 95.9%	132 genes coverage 96.5%	138 genes coverage, 95.8%
ACTB	NM_001101.3	x	x	x
ACTG1	NM_001199954.1	x	x	x
ADCY1	NM_021116.2	x	x	x
ADGRV1	NM_032119.3	x	x	x
AIFM1	NM_004208.3	not included	not included	x
APOPT1	NM_032374.4	not included	x	x
ATP1A2	NM_000702.3	not included	x	x
ATP6V1B1	NM_001692.3	x	x	x
BDP1	NM_018429.2	x	x	x
BSND	NM_057176.2	x	x	x
CABP2	NM_016366.2	x	x	x
CACNA1D	NM_000720.3	x	x	x
CCDC50	NM_178335.2	x	x	x
CD164	NM_006016.5	not included	not included	x
CDH23	NM_022124.5	x	x	x
CEACAM16	NM_001039213.3	x	x	x
CIB2	NM_006383.3	x	x	x
CLDN14	NM_144492.2	x	x	x
CLIC5	NM_001114086.1	x	x	x
CLPP	NM_006012 .2	x	x	x
CLRN1	NM_001195794.1	x	x	x
COCH	NM_001135058.1	x	x	x
COL11A1	NM_001854.3	x	x	x
COL11A2	NM_080680.2	x	x	x
COL2A1	NM_001844.4	x	x	x
COL4A3	NM_000091.4	x	x	x
COL4A4	NM_000092.4	x	x	x
COL4A5	NM_033380.2	x	x	x
COL4A6	NM_001287758.1	x	x	x
COL9A1	NM_001851.4	x	x	x
COL9A2	NM_001852.3	x	x	x
CRYM	NM_001888.4	x	x	x
DCDC2	NM_016356.4	not included	x	x
DFNA5	NM_004403.2	x	x	x
DFNB59	NM_001042702.3	x	x	x
DIABLO	NM_019887.5	x	x	x
DIAPH1	NM_005219.4	x	x	x

4.1

Table S1 (continued)

Gene name	RefSeq transcript ID	Mean % covered ≥ 20x		
		HI panel DGD 20062014 family W05-682, II:1	HI panel DG 2.4 family W16-0195, II:1	HI panel DG 2.5 family W16-0451, I:2
DIAPH3	NM_001042517.1	x	x	x
DSPP	NM_014208.3	x	x	x
EDN3	NM_207034.2	x	x	x
EDNRB	NM_001201397.1	x	x	x
ELMOD3	NM_032213.4	x	x	x
EPS8	NM_004447.5	x	x	x
ESPN	NM_031475.2	x	x	x
ESRRB	NM_004452.3	x	x	x
EYA1	NM_000503.5	x	x	x
EYA4	NM_001301013.1	x	x	x
FAM65B	NM_014722.3	not included	x	x
FGF3	NM_005247.2	x	x	x
FOXI1	NM_012188.4	x	x	x
GIPC3	NM_133261.2	x	x	x
GJB2	NM_004004.5	x	x	x
GJB3	NM_024009.2	x	x	x
GJB6	NM_001110219.2	x	x	x
GPSM2	NM_013296.4	x	x	x
GRHL2	NM_024915.3	x	x	x
GRXCR1	NM_001080476.2	x	x	x
GRXCR2	NM_001080516.1	x	x	x
HARS	NM_002109.5	x	x	x
HARS2	NM_012208.2	x	x	x
HGF	NM_000601.4	x	x	x
HOMER2	NM_004839.3	not included	not included	x
HSD17B4	NM_001199291.1	x	x	x
ILDR1	NM_001199799.1	x	x	x
KARS	NM_001130089.1	x	x	x
KCNE1	NM_000219.4	x	x	x
KCNJ10	NM_002241.4	x	x	x
KCNQ1	NM_000218.2	x	x	x
KCNQ4	NM_004700.3	x	x	x
KITLG	NM_000899.4	not included	x	x
LARS2	NM_015340.3	x	x	x
LHFPL5	NM_182548.3	x	x	x
LOXHD1	NM_144612.6	x	x	x
LRTOMT	NM_001145309.3	x	x	x
MARVELD2	NM_001038603.2	x	x	x
MCM2	NM_004526.3	not included	not included	x

Table S1 (continued)

Gene name	RefSeq transcript ID	Mean % covered ≥ 20x		
		HI panel DGD 20062014 family W05-682, II:1	HI panel DG 2.4 family W16-0195, II:1	HI panel DG 2.5 family W16-0451, I:2
MIR96	NR_029512.1	x	x	x
MITF	NM_198159.2	x	x	x
MSRB3	NM_198080.3	x	x	x
MYH14	NM_001145809.1	x	x	x
MYH9	NM_002473.5	x	x	x
MYO15A	NM_016239.3	x	x	x
MYO3A	NM_017433.4	x	x	x
MYO6	NM_004999.3	x	x	x
MYO7A	NM_000260.3	x	x	x
NARS2	NM_024678.5	not included	x	x
NLRP3	NM_001079821.2	x	x	x
OPA1	NM_130837.2	x	x	x
OSBPL2	NM_144498.2	not included	x	x
OTOA	NM_144672.3	x	x	x
OTOF	NM_194248.2	x	x	x
OTOG	NM_001277269.1	x	x	x
OTOGL	NM_173591.3	x	x	x
P2RX2	NM_170683.3	x	x	x
PAX3	NM_181459.3	x	x	x
PCDH15	NM_033056.3	x	x	x
PDZD7	NM_001195263.1	x	x	x
PET100	NM_001171155.1	not included	x	x
PNPT1	NM_033109.4	x	x	x
POU3F4	NM_000307.4	x	x	x
POU4F3	NM_002700.2	x	x	x
PRPS1	NM_002764.3	x	x	x
PTPRQ	NM_001145026.1	x	x	x
RDX	NM_002906.3	x	x	x
S1PR2	NM_004230.3	not included	not included	x
SERPINB6	NM_001271823.1	x	x	x
SIX1	NM_005982.3	x	x	x
SIX5	NM_175875.4	x	x	x
SLC17A8	NM_139319.2	x	x	x
SLC26A4	NM_000441.1	x	x	x
SLC26A5	NM_198999.2	x	x	x
SLC33A1	NM_004733.	x	x	x
SLITRK6	NM_032229.2	x	x	x
SMPX	NM_014332.2	x	x	x
SNAI2	NM_003068.4	x	x	x

4.1

Table S1 (continued)

Gene name	RefSeq transcript ID	Mean % covered ≥ 20x		
		HI panel DGD 20062014 family W05-682, II:1	HI panel DG 2.4 family W16-0195, II:1	HI panel DG 2.5 family W16-0451, I:2
SOX10	NM_006941.3	x	x	x
STRC	NM_153700.2	x	x	x
SYNE4	NM_001039876.2	x	x	x
TBC1D24	NM_001199107.1	x	x	x
TECTA	NM_005422.2	x	x	x
TIMM8A	NM_004085.3	x	x	x
TJP2	NM_004817.3	not included	x	x
TMC1	NM_138691.2	x	x	x
TMEM132E	NM_001304438.1	not included	x	x
TMIE	NM_147196.2	x	x	x
TMPRSS3	NM_024022.2	x	x	x
TNC	NM_002160.3	x	x	x
TPRN	NM_001128228.2	x	x	x
TRIOBP	NM_001039141.2	x	x	x
TSPEAR	NM_144991.2	x	x	x
TYR	NM_000372.4	not included	x	x
USH1C	NM_153676.3	x	x	x
USH1G	NM_173477.4	x	x	x
USH2A	NM_206933.2	x	x	x
WBP2	NM_012478.3	not included	not included	x
WFS1	NM_006005.3	x	x	x
WHRN	NM_015404.3	x	x	x
YAP1	NM_001130145.2	not included	x	x

Coverage was calculated per sample on a base pair resolution, using the *coverage* function of BEDtools (v2.19.1; PMID 20110278). Subsequently, the mean percentage of base pairs with at least 20 reads (≥20x coverage) was determined per sample, for the enriched regions of each gene.

Table S2 Primer sequences and PCR conditions

Target	Primer	Oligonucleotides	Amplicon size (bp)	Annealing temperature (°C)
MPZL2 exon 1	Forward	cattcacttcccaggcaagc	552	58
	Reverse	agagtgagcagtgaaggagg		
MPZL2 exon 1	Forward	tggggtggtgctttgagaagtg	652	60
	Reverse	gctcaggctcccaaacaaaagtc		
MPZL2 exon 2	Forward	gtaagtttgggagatggggc	422	58
	Reverse	ttccgagcttaaccttgtgc		
MPZL2 exon 2	Forward	gatggggcatctcagtttcactttac	365	60
	Reverse	ggaaaggagaaatggactggcttatt		
MPZL2 exon 3	Forward	tttcacttccgctcccac	381	58
	Reverse	tgtccctctctctcagcc		
MPZL2 exon 3	Forward	ctgggtgctgagtaagaagacctttt	316	60
	Reverse	gcccctttcttttctacaagctctc		
MPZL2 exon 4	Forward	tggggcctaagatttccatg	542	58
	Reverse	tctgtcctgcaaatgtgaattc		
MPZL2 exon 4	Forward	cctattgctagtaggattcacaaggtaat	369	60
	Reverse	caaaataccaagagtcgccataaga		
MPZL2 exon 5	Forward	ggcaccagtttagctctgtg	366	58
	Reverse	ctgacccagctcctctaatttc		
MPZL2 exon 5	Forward	acccacttgcttcttgtcttgttca	555	60
	Reverse	aagctctcctgtaaaaactgccagata		
MPZL2 exon 6	Forward	ggtcatccaagtgtccatgc	694	58
	Reverse	cgaggaggcttagctcacc		
MPZL2 exon 2 (genomic qPCR)	Forward	ctgtggaaatttatacctcccgg	84	60
	Reverse	gggcaaagctggagaaagtg		
MPZL2 exon 3 (genomic qPCR)	Forward	atgggaatcctgagcggtac	110	60
	Reverse	caccccatcaacatcaggtg		
MPZL2 exon 5 (genomic qPCR)	Forward	tcccaagtgcatgtaattcttcc	99	60
	Reverse	tcaggtgaacaagacaagaagc		
MPZL2 mRNA exons 2-3	Forward	gtgggtgatgctctaacagtg	115	60
	Reverse	ccttaaaccgcccactcatg		
MPZL2 mRNA exons 3-4	Forward	cagttcgacgacaatgggac	109	60
	Reverse	cagagaagcgtacagtgtgc		
TECTA exon 2	Forward	gttgaacttcggaggacctg	489	58
	Reverse	ggcaagctggtacatacaaatag		

4.1

Table S2 (continued)

Target	Primer	Oligonucleotides	Amplicon size (bp)	Annealing temperature (°C)
TECTA exon 3	Forward	accaagatgcatgaaagtgc	509	58
	Reverse	gccaataaatcctcccttcc		
TECTA exon 4	Forward	ggtgtttgggggttctaattc	576	58
	Reverse	tttcctgcaaagtgggtagc		
TECTA exon 5	Forward	aggagtcagagctggaggg	423	60
	Reverse	tagcctcgtagtccacctgc		
TECTA exon 6	Forward	acctagaatgctggcccc	455	58
	Reverse	aaaattaccttgatctccattaccc		
TECTA exon 7	Forward	gggtgaccatacctccctaac	645	58
	Reverse	cagagacaaacagcagaaccag		
TECTA exon 8	Forward	ttcctgatctctgctggaac	833	56
	Reverse	tggttgtggtattaggtggg		
TECTA exon 9_1	Forward	cctcaattctgtcttccccg	485	58
	Reverse	gaagcagccctggtagcc		
TECTA exon 9_2	Forward	caatgcctgtgcgaggag	499	58
	Reverse	cagatcattagaaaacgctccc		
TECTA exon 10	Forward	ggcagaccgtgtctttatcc	746	58
	Reverse	cctggaagggaagtcctgag		
TECTA exon 11_1	Forward	gcacgcacacttctgtctc	490	56
	Reverse	agctggtctggaagtcaaag		
TECTA exon 11_2	Forward	agtggcacagacaacaggg	495	58
	Reverse	tctctagggcctctctctgc		
TECTA exon 12	Forward	ctgctcaaacttccctctgg	754	58
	Reverse	tctagggagttggaagactgg		
TECTA exon 13	Forward	agacccaggctttctgtgag	565	58
	Reverse	tgacactcagtgcccaagag		
TECTA exon 14	Forward	gtttccccactgctgcc	679	58
	Reverse	tttgattctttaaaacctggtcac		
TECTA exon 15	Forward	gggacagaatggagtcgttg	623	58
	Reverse	ttactggggtctctgatgtgc		
TECTA exon 16	Forward	tggcacaatgcactagcttc	552	58
	Reverse	ctgcagctcacagctctctac		

Table S2 (continued)

Target	Primer	Oligonucleotides	Amplicon size (bp)	Annealing temperature (°C)
TECTA exon 17	Forward	agctaatccaggcccacag	555	58
	Reverse	aatgtggcctcagatggaac		
TECTA exon 18	Forward	tggaggtcatttgcctcttc	551	58
	Reverse	ccacagtaggcatcccaaac		
TECTA exon 19	Forward	cccaagtaaatgctaagg	456	56
	Reverse	tggttgaaagcatttaggctc		
TECTA exon 20	Forward	cccatgtggctagcagg	600	58
	Reverse	cttgattgtctgtaaaatgaggc		
TECTA exon 21	Forward	atgcagtccaggggtcac	456	58
	Reverse	tcactgtcccatcaaagatgac		
TECTA exon 22	Forward	ccagtggattcaatgatcaag	391	56
	Reverse	ctttaaggaagcaggtgatg		
TECTA exon 23	Forward	gatctcctgaccgcgtg	443	58
	Reverse	aattccttgggcatgttcc		
TECTA exon 24	Forward	gctgccttagggccatttag	398	58
	Reverse	ctggtttctggaccttggac		
TECTA mRNA exons 1-4	Forward	ttattggcaacaagttgaggag	572	57
	Reverse	cttcctcccatgtcacaatg		
TECTA mRNA exons 1-4 nested	Forward	actcagttcctccagcctctac	447	57
	Reverse	gaaggttgccatgtctttgaag		
TECTA mRNA exons 4-7	Forward	cttcaaagacatggcaaccttc	477	57
	Reverse	tcattgttgaaatccagacagc		
TECTA mRNA exons 6-8	Forward	gaccacaaacgtcaatgttcc	589	57
	Reverse	tgtttccacggcagtagatatg		
TECTA mRNA exons 7-9	Forward	agtggaggtgaatggctacaag	672	57
	Reverse	cacacggagtagtggctgaag		
TECTA mRNA exons 9-10	Forward	caggcctatgctcttgtgtg	747	57
	Reverse	ccactgtcgtactgtttttgtttc		
TECTA mRNA exons 9-11	Forward	aggtcaagataggaggcatcg	723	57
	Reverse	gacatccctcagagcagctatc		
TECTA mRNA exons 10-12	Forward	aacagctccttcctggagtg	896	57
	Reverse	acaaccttcaggccaaaatc		
TECTA mRNA exons 10-12 nested	Forward	gagtgggggcaatgagtcag	786	57
	Reverse	acgtggaagccaaaggaaaag		

4.1

Table S2 (continued)

Target	Primer	Oligonucleotides	Amplicon size (bp)	Annealing temperature (°C)
TECTA mRNA exons 11-13	Forward	ctctttccccaagtttgttgtc	785	57
	Reverse	agtcactcttcaggcggatg		
TECTA mRNA exons 12-15	Forward	aagaactgcctgtttgactcttgc	781	57
	Reverse	tgctgtagattttggttgccaaac		
TECTA mRNA exons 14-16	Forward	gcttatcatcaacttcgacaagtg	494	57
	Reverse	agtagccatcaccctgcatc		
TECTA mRNA exons 15-18	Forward	ttaaaatcagcatcagcgagag	597	57
	Reverse	tcacctctgcatcgataatgtc		
TECTA mRNA exons 17-20	Forward	agtggttgaagatccctgtgtg	556	57
	Reverse	atgtttgtaggaggcgtttttg		
TECTA mRNA exons 19-22	Forward	caacactggcaacatcatcac	599	57
	Reverse	taggtcccactgaaatgatctg		
TECTA mRNA exons 21-24	Forward	tcaccgtctttaaattcataggg	476	57
	Reverse	ttaagggcacacactttttatcc		

For primer design to amplify *MPZL2*, reference sequence NM_005797.3 was used, and for *TECTA*, ENST00000392793.

Table S3 Homozygous regions larger than 1 Mb and WES variants in family W05-682

Start SNP	End SNP	Chr	Start position	End position	Size (Mb)	Known deafness gene(s)	Total WES variants	Rare variants (≤1%)	Coding & splice site variants	Homozygous variants	(likely) pathogenic variants[a]
rs4936310	rs10458997	11	110,803,280	134,746,130	23,94	*TECTA*	976	81	6	*MPZL2* c.72del *BSX* c.263-5T>C *GRAMD1B* c.1111G>A *OR8G2* c.537C>G	*MPZL2* c.72del
rs9910295	rs7406119	17	74,124,040	78,599,918	4,48	*ACTG1*[b]	397	32	1	0	-
rs2353200	rs7835152	8	47,043,376	49,785,649	2,74	-	20	2	1	0	-
rs28870	rs803137	5	129,555,034	132,160,546	2,61	-	80	7	1	0	-
rs7125329	rs1648142	11	107,401,046	109,376,162	1,98	-	67	5	0	-	-
rs10520657	rs12443195	15	85,915,598	87,872,738	1,96	-	77	4	0	-	-
rs9992997	rs17027362	4	133,177,516	134,863,883	1,69	-	7	0	-	-	-
rs2236047	rs9472138	6	42,234,377	43,919,740	1,69	-	86	9	1	0	-
rs4766455	rs12308836	12	108,125,961	109,772,342	1,65	-	114	11	0	-	-
rs7688203	rs17088085	4	66,251,451	67,739,917	1,49	-	8	0	-	-	-
rs2451256	rs10755578	6	159,427,326	160,889,728	1,46	-	147	7	0	-	-
rs1533075	rs9900927	17	60,469,835	61,853,472	1,38	-	80	5	2	0	-
rs8135828	rs5753355	22	28,259,239	29,589,658	1,33	-	52	3	1	0	-
rs7152200	rs8022938	14	65,905,908	66,925,080	1,02	-	10	0	-	-	-
rs7574269	rs6735340	2	14,617,908	15,623,366	1,01	-	46	3	0	-	-

Homozygous regions of shared genotypes. Genomic positions were determined using the UCSC Genome Browser, GRCh37/hg19 (https://genome.uccsc.edu/). [a]Based on variant classification guidelines by the American College of Medical Genetics and Genomics and the Association for Molecular Pathology.[4] [b]All coding and splice site pairs of *ACTG1* were covered by at least 15 reads.

4.1

Table S4 Analysis of intragenic deletions in subjects with a heterozygous variant in *MPZL2*

Sample	Identified heterozygous variant	Gender	Mean Ct value *MPZL2* exon 2	Mean Ct value *MPZL2* exon 3	Mean Ct value *MPZL2* exon 5	Mean Ct value *SLC16A2* exon 6
DNA11-22171	c.544C>T (p.(Arg182*)), exon 4	female	25	24	25	24
DNA11-23140	c.268C>T (p.(Arg90Trp)), exon 3	male	25	24	25	25
Control		female	25	24	25	24

In two individuals of the phenotype-based cohort, rare mono-allelic variants of *MPZL2* were identified. As no variants could be detected of the second allele by Sanger sequencing, genomic qPCR was performed to identify possible intragenic deletions. qPCR was performed for exons without a heterozygous SNP (*MPZL2* exons 2, 3 and 5). Temperatures and reaction times for qPCR were as follows: 10 min at 95 °C, followed by 40 cycles of 15 sec at 95 °C and 30 sec at 60 °C. qPCRs were performed with the Applied Biosystem Fast 7900 System in accordance with the manufacturer's protocol (Applied Biosystems, Foster City, CA, USA). *SLC16A2* (MIM: 300095) was employed as a reference gene. All reactions were performed in duplicate, mean Ct values are indicated. These Ct values do not provide any indication for the presence of intragenic deletions encompassing exons 2, 3, or 5 of *MPZL2*.

4.1

Table S5a Individual results of otoscopy, tympanometry, pure-tone audiometry, OAEs, acoustic reflexes, HI progression and speech discrimination

Family	Subject	Age at evaluation (years)	Reported onset age of HI (years)	Otoscopic examination	Tympano-metry	PTA (dB HL)	OAEs	Mean ART (dB HL)	Significant HI progression (follow-up)	SRT (dB)	Max SRS (%)
W05-682	II:1	37	4	normal	R+L type A	60	R+L ND	100	yes (21 years)	50	100
	II:3	42	9	R+L myringo-sclerosis	R+L type A	65	R+L ND	100	yes (20 years)	53	100
	III:2	9	4	normal	R+L type A	37	R+L ND	90	no (4 years)	32	90
W16-0195	II:1	8	3	normal	R type A L type Ad	40	R+L ND	90	no (3 years)	30	100
W16-0451	I:2	44	childhood	normal	R+L type A	48	R+L ND	90	yes (10 years)	31	92
	II:1	13	3	NT	NT	35	NT	NT	no (7 years)	NT	NT
	II:2	16	5	normal	R+L type A	38	R ND L detected at 1 kHz	90	no (5 years)	27	95
	II:3	7	6	normal	R+L type A	35	R+L detected at 1.4kHz	90	no (1 year)	28	95

PTA, pure tone average, mean thresholds of 0.5, 1 and 2 kHz in dB HL; OAEs, otoacoustic emissions; ART, acoustic reflex threshold; SRT, speech reception threshold; Max, maximum; SRS, speech recognition score; R, right; L, left; ND, not detected; NT, not tested. Tympanometry type A means a normal curve, indicating normal pressure in the middle ear with normal mobility of the eardrum and ossicles; type Ad means a higher curve, indicating increased mobility of the eardrum and/or ossicles. Progression of HI was considered significant if at least 2 frequencies showed significant progression (p≤0.05). Results of audiometry, acoustic reflexes and speech discrimination from the better hearing ear are presented. One of the siblings (II:1) of family W16-0451 was not able to participate in the clinical evaluation; only retrospective data of this subject were used for analysis.

Table S5b Individual results of ABR and vestibular tests

Family	Subject	Click-evoked ABR	History of vestibular symptoms	Rotary chair test	Caloric irrigation test	vHIT	cVEMP
W05-682	II:1	symmetric, normal wave latencies	no	normal	normal	normal	normal (slightly lower)
	II:3	NT	no	NT	NT	NT	NT
	III:2	NT	no	NT	NT	NT	NT
W16-0195	II:1	symmetric, normal wave latencies	no	NT	NT	NT	NT
W16-0451	I:2	NT	two periods of vertigo in the past, without persisting complaints	normal	normal	normal	normal (slightly lower)
	II:1	NT	unknown	NT	NT	NT	NT
	II:2	NT	no	normal	slight asymmetry to the detriment of the left vestibulum	normal	normal (slightly lower)
	II:3	NT	no	NT	NT	NT	NT

ABR, auditory brainstem response; vHIT, video head impulse test; cVEMP, cervical vestibular evoked myogenic potentials; NT, not tested.

References

1. Vanhoutte EK, Latov N, Deng C, et al. Vigorimeter grip strength in CIDP: a responsive tool that rapidly measures the effect of IVIG--the ICE study. *European journal of neurology* 2013;20:748-755.
2. Van den Bergh PY, Hadden RD, Bouche P, et al. European Federation of Neurological Societies/ Peripheral Nerve Society guideline on management of chronic inflammatory demyelinating polyradiculoneuropathy: report of a joint task force of the European Federation of Neurological Societies and the Peripheral Nerve Society - first revision. *European journal of neurology* 2010;17:356-363.
3. Seelow D, Schuelke M, Hildebrandt F, Nurnberg P. HomozygosityMapper--an interactive approach to homozygosity mapping. *Nucleic acids research* 2009;37:W593-599.
4. Wallis Y, Payne S, McAnulty C, et al. Practice Guidelines for the Evaluation of Pathogenicity and the Reporting of Sequence Variants in Clinical Molecular Genetics. *ACGS /VGKL.* 2013.
5. Aguirre-Gamboa R, Joosten I, Urbano PC, et al. Differential Effects of Environmental and Genetic Factors on T and B Cell Immune Traits. *Cell reports.* 2016;17:2474-2487.

4.1

4.2

Heterozygous missense variants of *LMX1A* lead to nonsyndromic hearing impairment and vestibular dysfunction

Mieke Wesdorp, Pia A.M. de Koning Gans, Margit Schraders, Jaap Oostrik, Martijn A. Huynen, Hanka Venselaar, Andy J. Beynon, Judith van Gaalen, Vitória Piai, Nicol Voermans, Michelle M. van Rossum, Bas P. Hartel, Stefan H. Lelieveld, Laurens Wiel, Berit Verbist, Liselotte J. Rotteveel, Marieke F. van Dooren, Peter Lichtner, Henricus P.M. Kunst, Ilse Feenstra, Ronald J.C. Admiraal, DOOFNL Consortium, Helger G. Yntema, Lies H. Hoefsloot, Ronald J.E. Pennings* and Hannie Kremer*

*These authors contributed equally to this work

Submitted for publication

Abstract

We identified heterozygous pathogenic missense variants of *LMX1A* in two families of Dutch origin with nonsyndromic hearing impairment (HI), using whole exome sequencing. One variant, c.721G>C (p.Val241Leu), occurred *de novo* and affected an amino acid of LMX1A's homeodomain, which is essential for DNA binding. The second variant, c.290G>C (p.Cys97Ser), affected a zinc binding residue of the second LIM domain that is involved in protein-protein interactions. Bi-allelic deleterious variants of *Lmx1a* are associated with a complex phenotype in mice, including deafness and vestibular defects, due to early-stage arrest of inner ear development. Although *Lmx1a* mouse mutants demonstrate neurological, skeletal, pigmentation and reproductive system abnormalities, no syndromic features were present in the participating subjects of either family. *LMX1A* has previously been suggested as a candidate gene for intellectual disability, but our data do not support this, as affected subjects displayed normal cognition. Phenotype characterization of the affected individuals revealed large phenotypic variability in the age of onset (congenital to 35 years), (a)symmetry, severity (mild to profound) and progression rate of HI. About half of the affected individuals displayed vestibular dysfunction and experienced symptoms thereof. The late-onset progressive phenotype, and absence of cochleovestibular malformations on computed tomography scans indicate that heterozygous defects of *LMX1A* do not result in severe developmental abnormalities in humans. We hypothesize that a single *LMX1A* copy encoding wild-type protein causes minor cochleovestibular developmental abnormalities that eventually lead to a progressive phenotype, or that it is sufficient for normal development but insufficient for maintenance of cochleovestibular function.

Report

Hereditary nonsyndromic hearing impairment (NSHI, MIM: 500008) is genetically very heterogeneous. Currently, more than 100 deafness genes have been identified, and still every year novel ones are discovered (Hereditary Hearing Loss Homepage). Since 2010, whole exome sequencing (WES) and targeted next generation sequencing have enabled the rapid and cost-efficient identification of deafness genes.[1] However, we need to beware of seemingly causative variants that segregate in small families or occur in several unique individuals with HI by coincidence, especially in dominant NSHI. This is illustrated by the recent disqualification of *MYO1A* (MIM: 601478) as a deafness gene.[2,3] Ideally, unique pathogenic variants are identified in several families with a similar phenotype and not in a significant number of controls. Genetic studies are preferably supported by functional and animal studies that prove the deleterious effect of a variant and demonstrate the function of a gene in hearing. As this is often very time- and money-consuming, (homology) protein modeling or existing data on studies in mice can be supportive in the discovery of novel deafness genes, as has recently been the case for *KITLG* (MIM: 184745)[4] and *S1PR2* (MIM: 605111).[5]

In the present study, we identified pathogenic missense variants of *LMX1A* (MIM: 600298), a gene associated with a complex phenotype in mice, including recessive deafness and vestibular defects[6-8], as a cause of dominant NSHI and vestibular dysfunction in human. This study was approved by the medical ethics committee of the Radboud university medical center and is in accordance with the principles of the World Medical Association Declaration of Helsinki. Written informed consent was obtained from all participants or their legal representatives.

   A family of Dutch origin (W15-0551, Figure 1a), was investigated to identify the underlying genetic defect of the dominant NSHI segregating in the family. We performed WES in the index case (III:8). The exome was enriched with the Agilent SureSelect version 4 kit (Santa Clara, CA, USA), and WES was performed on an Illumina HiSeq system by BGI Europe (Denmark)[9]. As a first step, variants in genes associated with hearing impairment (HI) were selected (gene list DGD20062014) and classified according to the existing guidelines from the American College of Medical Genetics and Genomics[10], as described previously.[9] Mean ≥20x coverage was obtained for 96% for the enriched regions. No (likely) pathogenic variants were identified. As a next step, all WES variants were analyzed. To reduce the number of candidate variants, WES was performed in subject II:7 as well, under the same conditions and using the Agilent SureSelect version 5 kit. After filtering for shared, rare (≤0.5%), and missense, nonsense, indels, and splice site variants, 186 variants remained

(Table 1). One of these variants was a heterozygous missense variant of *LMX1A*, c.721G>C (p.Val241Leu) (Figure S1). This variant has not been reported in ExAC and segregated with the HI in the family (Figure 1a). As it was unknown whether the grandmother (subject I:2) was hearing impaired, based on conflicting subjective information provided by family members, we investigated whether the variant of *LMX1A* was inherited or occurred *de novo* in subject II:7. Haplotypes in the *LMX1A* region were determined by genotyping variable number of tandem repeats (VNTR) markers, as described previously[4]. This revealed that the c.721G>C containing haplotype was also present in individuals in the second generation, who did not carry this variant (Figure 1a). This indicates that the variant occurred *de novo* in subject II:7. *LMX1A* c.721G is highly conserved (PhyloP 5.53) and p.Val241 is fully conserved in the LIM-homeodomain protein family (Figure 2). Defects of *Lmx1a* have been associated with HI and vestibular defects in mouse.[6-8] All together, we considered the identified *LMX1A* variant a promising candidate to underlie the HI in family W15-0551.
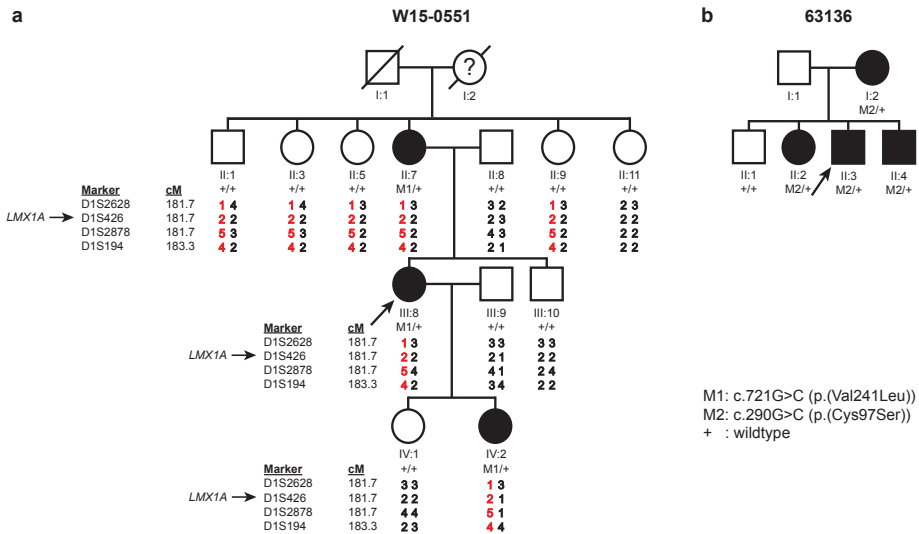
Figure 1 Pedigrees, VNTR genotypes and segregation of *LMX1A* variants.
(**a**) Genotypes of VNTR markers and segregation of the identified missense variant of *LMX1A* in family W15-0551. Genetic locations of the markers were derived online from the Marshfield genetic map and maker order was confirmed in the human genome assembly GRCh37/hg19. As the variant resides on an allele (depicted in red) that is shared by non-affected siblings of subject II:7, the variant was concluded to be *de novo* in subject II:7. It remained unclear whether subject I:2 was affected only at high age or earlier, based on conflicting subjective information provided by her family members. (**b**) Pedigree and segregation analyses of a missense variant in *LMX1A* in family 63136. Index cases are indicated by arrows. +, wild-type.

Table 1 Filter steps applied on variants identified in WES for family W15-0551

Filter steps	No. of variants
Shared by subjects II:7 and III:8	85798
≤0.5% in ExAC, dbSNP database and in-house database[a]	1039
Exonic missense, nonsense, indels, and splice site variants[b]	186

[a]In-house database contains WES data of 13314 individuals, the vast majority of Dutch origin, affected by a large number of different diseases (including 810 subjects with HI) and also non-affected individuals. [b]Splice site variants up to +8/-20 nucleotides were selected

To exclude other candidate DNA variants (n=185) shared by individuals II:7 and III:8, linkage analysis was performed by genotyping of all subjects of family W15-0551, using the 700K SNP Global Screening Array (Illumina, San Diego, CA, USA). Superlink online SNP 1.1 software was employed for approximate multipoint LOD score calculations, and a window size of 20 SNPs was used.[11] The inheritance pattern was assumed to be autosomal dominant with a disease allele frequency of 0.001. The penetrance of the disease allele was set at 99%. There were 54 regions in which linkage could not be excluded by a LOD score ≥ -2. (Figure S2, Table S1). DNA variants in these regions were filtered and classified as described above, which resulted in seven candidate variants (Table S1). None of them segregated with the HI in the family, as determined by Sanger sequencing. As ten of the 54 regions not excluded by linkage analysis harbored known deafness genes (Table S1), coverage of all exons and exon-intron boundaries of these genes, including *MYO6* (MIM: 600970), was manually checked to be at least 10x. Subsequently, Sanger sequencing was performed for regions with a lower coverage, which did not reveal any rare variants (allele frequency ≤ 0.5%). Since the HI associated with dominant defects of *MYO6* is similar to that in the affected subjects of family W15-0551[12,13], this gene was also excluded by segregation analysis of SNPs located in and flanking *MYO6* (Figure S3).

We addressed further involvement of deleterious *LMX1A* variants in dominant NSHI. WES data of genetically undiagnosed individuals with NSHI were evaluated for rare variants of *LMX1A*. Only subjects with suspected dominant inheritance or without family history of HI were included (n=405) This revealed a heterozygous variant c.290G>C (p.Cys97Ser) in the index case of family 63136 (Figure S1), which segregated with the dominantly inherited HI in the family (Figure 1b). *LMX1A* c.290G>C is highly conserved (PhyloP 5.45) and has not been reported in the ExAC database. Residue Cys97 is located within the second LIM domain, and is fully conserved in the LIM-homeodomain protein family (Figure 2). Screening of WES data also revealed a heterozygous variant c.376G>A (p.Gly126Lys) in the index case of family W05-233, but this variant was inherited from the normal hearing mother. As can be seen in Figure 2, p.Gly126 is not conserved in the LIM-homeodomain protein family.
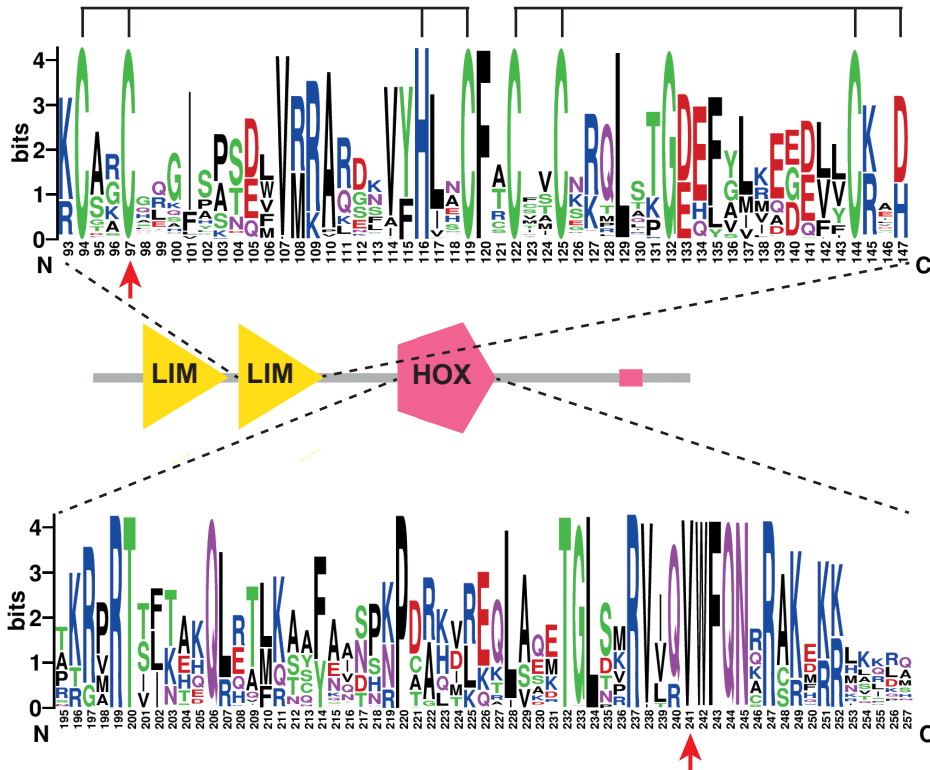
Figure 2 Domains and conservation of (mutated) residues in the LIM-homeodomain protein family. Domain architecture of the LIM-homeodomain protein family. All ~600 members of the family were extracted from the SMART domain database and aligned. Sequence logos for the second LIM domain and the homeodomain within this family were created with WebLogo[14], which shows the perfect conservation of the mutated residues Cys97 and Val241 (indicated by arrows). Within the second LIM domain, the residues that together bind two zinc atoms are indicated with black lines above the amino acid sequence.

The affected subjects of family W15-0551 (II:7, III:8 and IV:2) were clinically examined to characterize their audiovestibular phenotype. Medical history was obtained; otoscopy, tympanometry and pure-tone audiometry were performed, and otoacoustic emissions and acoustic reflexes were assessed, according to current standards. Family 63136 did not participate in our clinical evaluation; only retrospective data from the affected subjects (I:2, II:2, II:3 and II:4) were analyzed. There was no evidence of acquired causes of HI. All affected subjects had sensorineural HI except for individual II:7 of family W15-0551, who had bilateral fenestral otosclerosis and mixed HI of the left ear. We assume that the sensorineural HI was unlikely to be caused by otosclerosis, because there were no radiological signs of cochlear otosclerosis and her vestibular test results fit with the defect in *LMX1A*. There were no preoperative audiograms available before stapedectomy of the right ear in 1973 for comparison of the pre- and postoperative bone conduction thresholds of the right ear.

The reported age of onset varied from congenital to 35 years (Table S3). Affected subjects had mild to profound HI, with overall a downsloping audiogram configuration (Figure 3). Subject IV:2 of family W15-0551 and subject II:2 of family 63136 displayed asymmetric HI, whereas the other affected individuals demonstrated symmetric HI. Longitudinal linear regression analysis of hearing thresholds revealed significant progression in all affected subjects of both families, except for subject IV:2 of family W15-0551, probably because follow-up time was too short (3 years) to measure significant deterioration of hearing in this individual. Progression of HI was not analyzed in subject II:7 of family W15-0551, as we cannot exclude deterioration of hearing due to her otosclerosis. The progression rate and severity of HI varied widely among the affected subjects (Table S3). Speech reception thresholds were lower than or comparable to pure tone average thresholds at 0.5, 1 and 2 kHz for the better hearing ear, indicating absence of retrocochlear pathology (Table S3). This is confirmed by results from acoustic reflex measurements in all affected subjects and brainstem evoked response audiometry in subject II:2 of family 63136, which showed no indications of retrocochlear pathology (data not shown). CT scans in subject II:7 of family W15-0551 and the index case (II:3) of family 63136 did not show cochleovestibular malformations, except for known fenestral otosclerosis in the former individual.

4.2
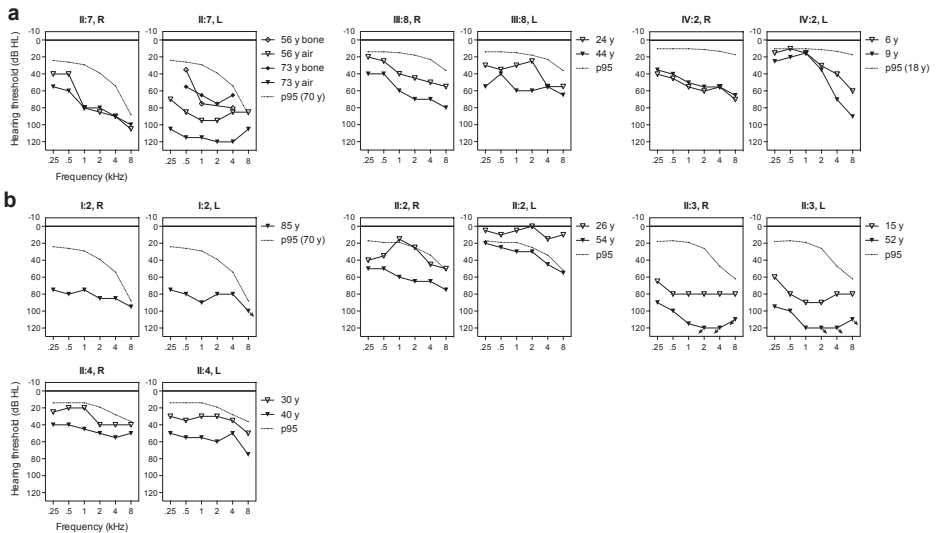
Figure 3 Audiometric characterization of families affected by deleterious *LMX1A* variants.
Air conduction thresholds of both ears of the affected individuals are shown of first-visit and last-visit audiometry. The 95th percentile threshold values of presbyacusis (p95) were calculated for the last-visit audiogram, and matched to the individual's sex and age, according to the ISO 7029 standard. (**a**) Family W15-0551. For subject II:7, also bone conduction thresholds of the left ear are depicted, because of mixed HI due to fenestral otosclerosis (conductive HI) and the *LMX1A* variant (sensorineural HI). (**b**) Family 63136. Subjects did not participate in our clinical evaluation; only retrospective data were used for analysis. R, right ear; L, left ear.

Four of the affected individuals reported sudden episodes of vertigo in the past that lasted minutes to days, with or without tinnitus, but without simultaneous deterioration of hearing (Table S3). Individuals could not identify triggers for the vertigo episodes. Vestibular function was assessed in subjects II:7 and III:8 (family W15-0551) and the index case of family 63136, using electronystagmography rotary chair stimulation and caloric irrigation testing, according to current standards. The vestibular tests revealed bilateral symmetric hyporeflexia in subject III:8 of family W15-0551 (42 years old), asymmetric severe hyporeflexia to areflexia to the detriment of the left vestibulum in subject II:3 of family 63136 (52 years old), and bilateral areflexia in subject II:7 of family W15-0551 (73 years old). Subjects II:7 and III:8 of family W15-0551 also underwent a video head impulse test (vHIT) and cervical vestibular evoked myogenic potential (cVEMP) recordings. The vHIT displayed bilateral weakness of the posterior semicircular canals in individual II:7 and normal function in individual III:8. cVEMPs showed no responses up to 100 dBnHL in both subjects, indicating dysfunction of the saccule. Since vestibular abnormalities are more severe in the older individuals, we hypothesize that there is progressive deterioration of vestibular function. There were, however, no longitudinal data available to confirm this. Apart from the vestibular abnormalities, the observed HI phenotype fits with DFNA7, for which the underlying defect has been localized to chromosome 1q21-q23 encompassing *LMX1A*.[15] Therefore, *LMX1A* is a candidate gene for DFNA7.

LMX1A is a transcription factor that belongs to the highly conserved LIM-homeodomain protein family. LIM-homeodomein proteins are characterized by two cysteine-rich zinc-binding LIM motifs that are known to be involved in protein-protein interactions[16], and a homeodomain that is known to bind DNA.[17] The mutated *LMX1A* residues identified in this study are located within the second LIM domain and the homeodomain. The p.Cys97Ser affects one of the two zinc binding residues, which is highly likely to be deleterious for protein folding and function. LIM-homeodomain transcription factors play a pivotal role in various developmental processes, and can be divided into subgroups based on sequence similarities. The vertebrate Lmx subgroup consists of paralogs *LMX1A* and *LMX1B* that have identical homeodomain sequences (Figure S4).[17]

Bi-allelic loss-of-function variants of the murine *Lmx1a* gene cause congenital deafness, vestibular defects, and neurological, skeletal, pigmentation, and reproductive system abnormalities.[6-8] However, upon screening (Supplemental Methods), none of the affected individuals of families W15-0551 and 63136 displayed any cutaneous abnormalities, signs of cognitive dysfunction, or peripheral or central nervous system involvement. History taking did not indicate fertility problems. In contrast to humans, there is no auditory phenotype in heterozygous *Lmx1a* mouse mutants, but occasionally mild pigmentation

abnormalities are seen.[8,18] Normal hearing thresholds have been measured up to 16 weeks[8] and 3 months (unpublished data, kindly provided by Dr. Johnson, Jackson Laboratory, Bar Harbor, Maine, concerning heterozygous *Lmx1a^dr-J* mice). Interestingly, the genetic defect in the well-studied mouse model *Lmx1a^dr-J* is p.Cys82Tyr and affects one of the zinc-binding cysteine residues of the LIM1 domain[19], which supports the pathogenicity of the identified p.Cys97Ser variant.

Heterozygous loss-of-function variants in *LMX1B* (MIM: 602575), a paralog of *LMX1A,* have been associated with nail-patella syndrome in human (NPS, MIM: 161200).[20-22] NPS is characterized by dysplastic nails, absent or hypoplastic patellae, elbow dysplasia, and iliac horns, and may be accompanied with nephropathy and/ or glaucoma.[23,24] There are important similarities between genetic defects in *LMX1A* and *LMX1B*. The mutated residues Cys97 and Val241 identified in LMX1A, are in the sequence alignments at the same positions as the amino acids Cys118 and Val265 in LMX1B (Figure S4). Amino acid variant p.Val265Leu of LMX1B is known to be disease-causing and aligns with p.Val241Leu of *LMX1A* in the present study.[25] The equivalent of *LMX1A* variant p.Cys97Ser has not been identified in *LMX1B*, but other substitutions at this position that would also impair the binding of a zinc atom, p.Cys118Phe[22] and p.Cys118Tyr[26], and the equivalent Cysteine to Serine substitution in LIM domain 1 (p.Cys59Ser), have been associated with NPS. Resemblance of the identified *LMX1A* variants with disease-causing variants in *LMX1B* supports the former's pathogenicity.

4.2

We hypothesize that the identified deleterious *LMX1A* variants lead to haploinsufficiency, which is also the proposed pathogenic mechanism of NPS, caused by variants of *LMX1B*.[27-29] A number of LMX1B variants have been tested for a dominant-negative effect, including p.Val265Leu, the equivalent of LMX1A p.Val241Leu, but no inhibitory effect on wild-type protein function was found.[28,29] Mono-allelic *Lmx1b* loss-of-function mice do not have a phenotype, except mice with the heterozygous *Lmx1b* variant p.Val265Asp, for which a dominant-negative effect has been suggested.[30] Our hypothesis that heterozygous *LMX1A* variants result in haploinsufficiency is strengthened by the fact that sensorineural HI and impaired speech development were diagnosed in a subject with a heterozygous interstitial 1q23.3q24.1deletion encompassing *LMX1A*.[31] Additional cases with heterozygous deletions of this region are reported to have impaired speech development.[31,32] However, it remains unclear whether impaired speech development in these cases was associated with HI or with the determined intellectual disability (ID). Our data do not support the suggested involvement of *LMX1A* in ID[31,32], as affected subjects of families W15-0551 and 63136 displayed normal cognition. Based on our findings and those of Chatron *et al.* (2015) and Mackenroth *et al.* (2016), we recommend screening for HI in subjects with mono-allelic loss

of *LMX1A*. The fact that a single copy of *LMX1A* encoding wild-type protein does not lead to a phenotype in mouse, whereas it does in man, suggests a difference in dosage sensitivity for this gene.[27] However, it cannot be excluded that heterozygous *Lmx1a* mouse mutants develop HI later in adulthood, as mice have only been measured up to 3 months, whereas some subjects developed HI in the third decade of life.

In mouse, Lmx1a expression in the inner ear starts at the otocyst stage (from E10.5 onwards) and is later restricted to non-sensory epithelia of the developing cochlea and vestibular system.[8,33-35] Bi-allelic *Lmx1a* defects lead to disorganization of the inner ear and lack of differentiation and separation of sensory, non-sensory and neurogenic domains of the vestibulocochlear system. As a result, *Lmx1a* mouse mutants have a short and malformed cochlear duct, no endolymphatic duct and sac, no semicircular canals, and the sacculus and utriculus remain rudimentary.[8,34,35] Hair cells in the basal part of the cochlea display severe disorganization, whereas hair cells in the apical turn are only mildly disorganized.[35] Although expression of *Lmx1a* in the inner ear is reduced from E16.5 onwards[33], Lmx1a has been suggested to function in the maintenance of hair cells, as there is progressive hair cell loss in adult mutant mice.[35]

There is large phenotypic variability within families W15-0551 and 63136, regarding age of onset, (a)symmetry, severity and progression rate of HI. Large intrafamilial phenotypic variation has also been reported for NPS.[36] The variable HI phenotype suggests involvement of environmental and/or genetic factors in the expression of the phenotype. The expression level of the wild-type *LMX1A* allele might well be one of the genetic factors. The overall downsloping audiogram configuration observed in the affected subjects corresponds to the abnormal development of the sensory epithelium in the organ of Corti in homozygous *Lmx1a* mouse mutants, displaying severe abnormalities of this epithelium in the basal part of the cochlea compared to mild defects in the apical regions.[34]

The onset of HI caused by *LMX1A* defects was in the 2nd or 3rd decade in most of the cases, which suggests that one *LMX1A* copy is sufficient for normal cochlear development. As homozygous *Lmx1a* mutant mice displayed loss of cochlear hair cells in the adult stage, the gene has been suggested to be essential for long-term maintenance of hair cells.[35] It is therefore tempting to speculate that the deterioration of HI over time is due to progressive loss of hair cells. Since vestibular complaints occurred during adulthood and vestibular dysfunction seemed progressive, we speculate that LMX1A is also critical for maintenance of the adult vestibular organs. Interestingly, it has been demonstrated that both *Lmx1a* and *Lmx1b* not only function in the developing mouse brain, as expression of both genes was found to be sustained in the adult midbrain and to be essential for survival of adult dopaminergic neurons in the midbrain.[37] A function in the regulation of genes with a

mitochondrial function was indicated. It remains to be determined whether LMX1A has a similar function in the adult inner ear. So far, there are no indications for *LMX1A*/*Lmx1a* expression in the adult inner ear.[33,38] An explanation for the HI in the presented families is that a single copy of *LMX1A* causes minor cochleovestibular developmental abnormalities that eventually lead to a progressive disease-phenotype. Currently, the recessive phenotype of deleterious *LMX1A* variants in humans remains unclear. As suggested by Steffes *et al.* (2012), bi-allelic loss-of-function variants of *LMX1A* might well be lethal in human.[8]

In conclusion, mono-allelic missense variants of *LMX1A* were found to underlie nonsyndromic HI and vestibular defects. The HI phenotype has a variable age of onset, severity and progression rate. Haploinsufficiency is the most likely pathogenic mechanism. Like in *LMX1B,* we expect that both truncating and missense variants can lead to the identified phenotype, with a preferential presence of missense variants in the conserved residues of the LIM domains and homeodomain of *LMX1A.*

4.2

Acknowledgements

Web resources

The URLs for data presented herein are as follows:
Alamut Visual, http://www.interactive-biosoftware.com/alamut- visual/
ExAC Browser, http://exac.broadinstitute.org/
Hereditary Hearing loss Homepage, http://hereditaryhearingloss.org/
Marshfield Genetic Maps, http://research.marshfieldclinic.org/genetics/GeneticResearch/compMaps.asp
OMIM, http://www.omim.org/
OMIM Phenotypic Series, http://www.omim.org/phenotypicSeriesTitle/all
SMART, http://smart.embl-heidelberg.de/
UCSC Genome Browser, https://genome.ucsc.edu
WebLogo, http://weblogo.berkeley.edu/

References

1. Vona B, Nanda I, Hofrichter MA, Shehata-Dieler W, Haaf T. Non-syndromic hearing loss gene identification: A brief history and glimpse into the future. *Molecular and cellular probes.* Oct 2015;29(5):260-270.

2. Eisenberger T, Di Donato N, Baig SM, et al. Targeted and genomewide NGS data disqualify mutations in MYO1A, the "DFNA48 gene", as a cause of deafness. *Human mutation.* May 2014;35(5):565-570.

3. Patton J, Brewer C, Chien W, Johnston JJ, Griffith AJ, Biesecker LG. A genotypic ascertainment approach to refute the association of MYO1A variants with non-syndromic deafness. *European journal of human genetics : EJHG.* Jan 2016;25(1):147-149.

4. Zazo Seco C, Serrao de Castro L, van Nierop JW, et al. Allelic Mutations of KITLG, Encoding KIT Ligand, Cause Asymmetric and Unilateral Hearing Loss and Waardenburg Syndrome Type 2. *American journal of human genetics.* Nov 05 2015;97(5):647-660.

5. Santos-Cortez RL, Faridi R, Rehman AU, et al. Autosomal-Recessive Hearing Impairment Due to Rare Missense Variants within S1PR2. *American journal of human genetics.* Feb 04 2016;98(2):331-338.

6. Bergstrom DE, Gagnon LH, Eicher EM. Genetic and physical mapping of the dreher locus on mouse chromosome 1. *Genomics.* Aug 01 1999;59(3):291-299.

7. Chizhikov V, Steshina E, Roberts R, Ilkin Y, Washburn L, Millen KJ. Molecular definition of an allelic series of mutations disrupting the mouse Lmx1a (dreher) gene. *Mammalian genome : official journal of the International Mammalian Genome Society.* Oct 2006;17(10):1025-1032.

8. Steffes G, Lorente-Canovas B, Pearson S, et al. Mutanlallemand (mtl) and Belly Spot and Deafness (bsd) are two new mutations of Lmx1a causing severe cochlear and vestibular defects. *PloS one.* 2012;7(11):e51065.

9. Zazo Seco C, Wesdorp M, Feenstra I, et al. The diagnostic yield of whole-exome sequencing targeting a gene panel for hearing impairment in The Netherlands. *European journal of human genetics : EJHG.* Feb 2017;25(3):308-314.

10. Wallis Y, Payne S, McAnulty C, et al. Practice Guidelines for the Evaluation of Pathogenicity and the Reporting of Sequence Variants in Clinical Molecular Genetics. *ACGS /VGKL.* 2013.

11. Silberstein M, Weissbrod O, Otten L, et al. A system for exact and approximate genetic linkage analysis of SNP data in large pedigrees. *Bioinformatics.* Jan 15 2013;29(2):197-205.

12. Miyagawa M, Nishio SY, Kumakawa K, Usami S. Massively parallel DNA sequencing successfully identified seven families with deafness-associated MYO6 mutations: the mutational spectrum and clinical characteristics. *The Annals of otology, rhinology, and laryngology.* May 2015;124 Suppl 1:148S-157S.

13. Hilgert N, Topsakal V, van Dinther J, Offeciers E, Van de Heyning P, Van Camp G. A splice-site mutation and overexpression of MYO6 cause a similar phenotype in two families with autosomal dominant hearing loss. *European journal of human genetics : EJHG.* May 2008;16(5):593-602.

14. Crooks GE, Hon G, Chandonia JM, Brenner SE. WebLogo: a sequence logo generator. *Genome research.* Jun 2004;14(6):1188-1190.

15. Fagerheim T, Nilssen O, Raeymaekers P, et al. Identification of a new locus for autosomal dominant non-syndromic hearing impairment (DFNA7) in a large Norwegian family. *Human molecular genetics.* Aug 1996;5(8):1187-1191.

16. Kadrmas JL, Beckerle MC. The LIM domain: from the cytoskeleton to the nucleus. *Nature reviews. Molecular cell biology.* Nov 2004;5(11):920-931.

17. Hobert O, Westphal H. Functions of LIM-homeobox genes. *Trends in genetics : TIG.* Feb 2000;16(2):75-83.

18. Patrylo PR, Sekiguchi M, Nowakowski RS. Heterozygote effects in dreher mice. *Journal of neurogenetics.* Apr 1990;6(3):173-181.

19. Millonig JH, Millen KJ, Hatten ME. The mouse Dreher gene Lmx1a controls formation of the roof plate in the vertebrate CNS. *Nature.* Feb 17 2000;403(6771):764-769.

20. Dreyer SD, Zhou G, Baldini A, et al. Mutations in LMX1B cause abnormal skeletal patterning and renal dysplasia in nail patella syndrome. *Nature genetics.* May 1998;19(1):47-50.

21. McIntosh I, Dreyer SD, Clough MV, et al. Mutation analysis of LMX1B gene in nail-patella syndrome patients. *American journal of human genetics.* Dec 1998;63(6):1651-1658.

22. Vollrath D, Jaramillo-Babb VL, Clough MV, et al. Loss-of-function mutations in the LIM-homeodomain gene, LMX1B, in nail-patella syndrome. *Human molecular genetics.* Jul 1998;7(7):1091-1098.

23. Sweeney E, Fryer A, Mountford R, Green A, McIntosh I. Nail patella syndrome: a review of the phenotype aided by developmental biology. *Journal of medical genetics.* Mar 2003;40(3):153-162.

24. Mimiwati Z, Mackey DA, Craig JE, et al. Nail-patella syndrome and its association with glaucoma: a review of eight families. *The British journal of ophthalmology.* Dec 2006;90(12):1505-1509.

25. Dunston JA, Hamlington JD, Zaveri J, et al. The human LMX1B gene: transcription unit, promoter, and pathogenic mutations. *Genomics.* Sep 2004;84(3):565-576.

26. Clough MV, Hamlington JD, McIntosh I. Restricted distribution of loss-of-function mutations within the LMX1B genes of nail-patella syndrome patients. *Human mutation.* 1999;14(6):459-465.

27. Bongers EM, de Wijs IJ, Marcelis C, Hoefsloot LH, Knoers NV. Identification of entire LMX1B gene deletions in nail patella syndrome: evidence for haploinsufficiency as the main pathogenic mechanism underlying dominant inheritance in man. *European journal of human genetics : EJHG.* Oct 2008;16(10):1240-1244.

28. Dreyer SD, Morello R, German MS, et al. LMX1B transactivation and expression in nail-patella syndrome. *Human molecular genetics.* Apr 12 2000;9(7):1067-1074.

29. Sato U, Kitanaka S, Sekine T, Takahashi S, Ashida A, Igarashi T. Functional characterization of LMX1B mutations associated with nail-patella syndrome. *Pediatric research.* Jun 2005;57(6):783-788.

30. Cross SH, Macalinao DG, McKie L, et al. A dominant-negative mutation of mouse Lmx1b causes glaucoma and is semi-lethal via LDB1-mediated dimerization [corrected]. *PLoS genetics.* May 2014;10(5):e1004359.

31. Chatron N, Haddad V, Andrieux J, et al. Refinement of genotype-phenotype correlation in 18 patients carrying a 1q24q25 deletion. *American journal of medical genetics. Part A.* May 2015;167A(5):1008-1017.

32. Mackenroth L, Hackmann K, Klink B, et al. Interstitial 1q23.3q24.1 deletion in a patient with renal malformation, congenital heart disease, and mild intellectual disability. *American journal of medical genetics. Part A.* Sep 2016;170(9):2394-2399.

33. Huang M, Sage C, Li H, Xiang M, Heller S, Chen ZY. Diverse expression patterns of LIM-homeodomain transcription factors (LIM-HDs) in mammalian inner ear development. *Developmental dynamics : an official publication of the American Association of Anatomists.* Nov 2008;237(11):3305-3312.

34. Koo SK, Hill JK, Hwang CH, Lin ZS, Millen KJ, Wu DK. Lmx1a maintains proper neurogenic, sensory, and non-sensory domains in the mammalian inner ear. *Developmental biology.* Sep 01 2009;333(1):14-25.

35. Nichols DH, Pauley S, Jahan I, Beisel KW, Millen KJ, Fritzsch B. Lmx1a is required for segregation of sensory epithelia and normal ear histogenesis and morphogenesis. *Cell and tissue research.* Dec 2008;334(3):339-358.

36. Ghoumid J, Petit F, Holder-Espinasse M, et al. Nail-Patella Syndrome: clinical and molecular data in 55 families raising the hypothesis of a genetic heterogeneity. *European journal of human genetics : EJHG.* Jan 2016;24(1):44-50.

4.2

37.   Doucet-Beaupre H, Gilbert C, Profes MS, et al. Lmx1a and Lmx1b regulate mitochondrial functions and survival of adult midbrain dopaminergic neurons. *Proceedings of the National Academy of Sciences of the United States of America.* Jul 26 2016;113(30):E4387-4396.

38.   Schrauwen I, Hasin-Brumshtein Y, Corneveaux JJ, et al. A comprehensive catalogue of the coding and non-coding transcripts of the human inner ear. *Hearing research.* Mar 2016;333:266-274.

Supplemental data

Supplemental methods
Screening protocol for syndromic abnormalities in subjects with *LMX1A* variants.

Medical history was obtained from all affected subjects of families W15-0551 and 63136, regarding neurological, cognitive and dermatological abnormalities, and sub/infertility. Special attention was paid to symptoms related to ataxia. Participants of family W15-0551 also underwent physical neurological and dermatological examination.

Neurological examination included testing of:
- Mental status, language and articulation
- Cranial nerves
- Muscle strength using the Medical Research Council (MRC) scores (0-5) of 18 predefined muscle groups, including shoulder abduction, elbow flexion, wrist extension, hip flexion, knee extension, foot dorsiflexion (extension) and plantar flexion, and toe dorsiflexon (extension); muscle tone and bulk
- Sensory function including pain and light touch sensation, vibration sense and position sense (absent; reduced; normal)
- Coordination with use of nose-finger test, diadochokinesis, heel-shin slide, and tandem gait (normal / abnormal)
- Deep tendon reflexes (biceps, brachioradialis, triceps, patellar, ankle jerks and plantar reflex) bilaterally (absent / reduced / normal)
- Posture and gait, including heel and toe walking (normal / abnormal)
- SARA Score (Scale for the Assessment and Rating of Ataxia)[1]

Cognitive screening of II:7 and III:8 included:
- Montreal cognitive assessment[2]
- National adult reading test[3]
- Rey auditory verbal learning test[4]

Cognitive screening of IV:2 included:
- Wechsler Intelligence scale for children, similarities subset[5]
- Wechsler Intelligence scale for children, coding subtest[5]
- Beery-Buktenice developmental test of visual motor integration, visual motor integration subset[6]
- Rey auditory verbal learning test

4.2

Dermatological screening included evaluation of skin type (I–VI), skin depigmentation, hypopigmentation, and hyperpigmentation, number of naevi, allergic reactions, other observed skin abnormalities, and treatment of skin abnormalities in the past. The whole body was examined and a Wood's lamp was used to analyze hypo-, hyper-, and depigmentations. If necessary, skin abnormalities were reviewed with a dermatoscope.

Supplemental figures and tables
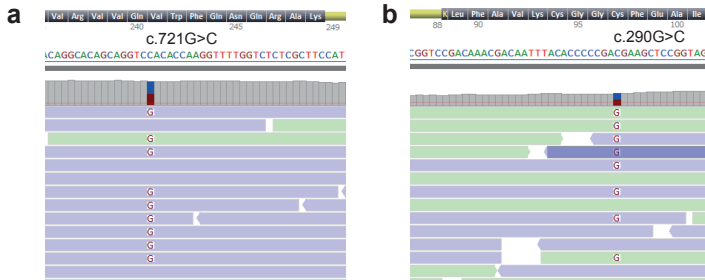
Figure S1 Sequences of *LMX1A* c.721G>C and c.290G>C.
Analysis of the WES paired-reads demonstrated a heterozygous missense variant in the index cases of family W15-0551, c.721G>C (p.Val241Leu) (**a**) and of family 63136, c.290G>C (p.Cys97Ser) (**b**). NM_177398.3 was employed as reference sequence. Figures show reverse sequences and were obtained using Alamut Visual version 2.7.1 (Interactive Biosoftware, Rouen, France).
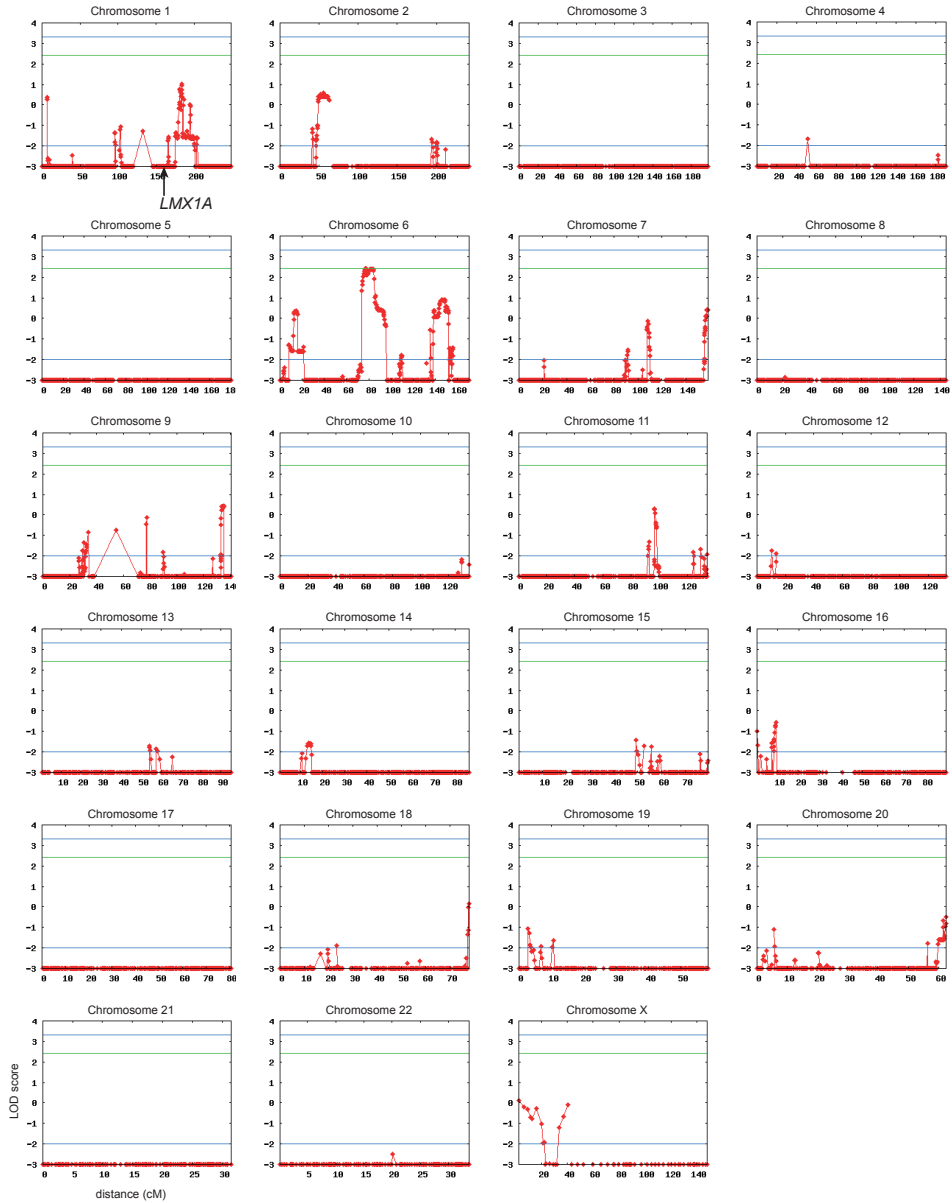
Figure S2 Genome wide LOD scores per chromosome of family W15-0551.

Linkage analysis was performed in family W15-0551 and LOD scores were calculated using SuperLink online SNP 1.1 software. The blue lines define the customary LOD score range, with a LOD score of ≥3.3 indicating significant linkage and a LOD score <-2 indicating exclusion of linkage. The green line indicates the maximum LOD score (2.4) measured in family W15-0551. In the calculations, window size was set at 20 SNPs, disease allele frequency at 0.001 and penetrance at 99%. There were 54 regions in which linkage could not be excluded (LOD score ≥ -2), but none of them had a significant maximum LOD score. The region with the highest LOD score of 2.4 was located on chromosome 6 and delimited by rs16883199 and rs2143437 (chr6:73,739,831-96,400,830; GRCh37, hg19).
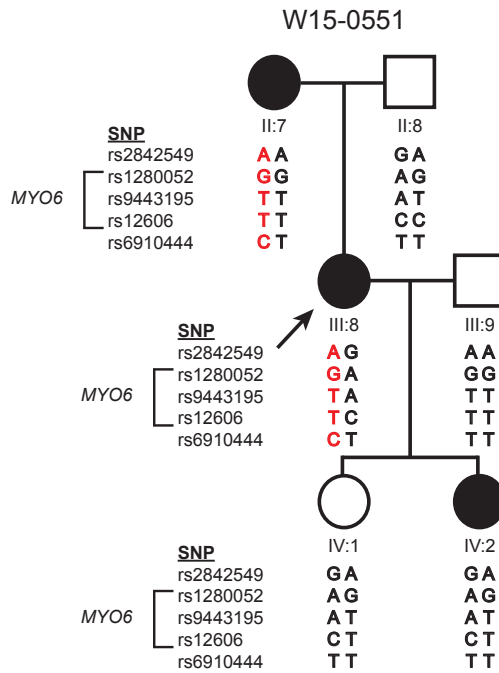
Figure S3 Haplotype analysis of the genomic region harboring *MYO6*.

MYO6 haplotypes were determined by genotyping SNPs in and flanking *MYO6* using Sanger sequencing and WES data of family W15-0551. As subject IV:2 does not inherit the grandmaternal haplotype, the causative variant does not reside in the coding or regulatory regions of *MYO6*. Black arrow indicates the index case.

```
             1
LMX1A  ----------------------MLDGLKMEENFQSAIDTSASFSSLLGRAVSPKSVCEG
LMX1B  MDIATGPESLERCFPRGQTDCAKMLDGIKMEEHALR--PGPATLGVLLGSDCPHPAVCEG
       1                      ****:****:       *::. ***      :****
             LIM 1                                              97
LMX1A  CQRVILDRFLLRLNDSFWHEQCVQCASCKEPLETTCFYRDKKLYCKYDYEKLFAVKCGGC
LMX1B  CQRPISDRFLMRVNESSWHEECLQCAACQQALTTSCYFRDRKLYCKQDYQQLFAAKCSGC
       *** * ****:*:*:* ***:*:***:*:: * *:*:::**:***** **::***.**.*
                                                                118
             LIM 2
LMX1A  FEAIAPNEFVMRAQKSVYHLSCFCCCVCERQLQKGDEFVLKEGQLLCKGDYEKERELLSL
LMX1B  MEKIAPTEFVMRALECVYHLGCFCCCVCERQLRKGDEFVLKEGQLLCKGDYEKEKDLLSS
       :* ***.****** :.****.***********:*****************::***
LMX1A  VSPAASDSGKSDDEESLCKSAHGAG---KGTAEEGKDHKRPKRPRTILTTQQRRAFKASF
LMX1B  VSPDESDSVKSEDEDGDMKPAKGQGSQSKGSGDDGKDPRRPKRPRTILTTQQRRAFKASF
       ***   *** **:**.   * *:* *   **:.::*** :******************
             HOX              241
LMX1A  EVSSKPCRKVRETLAAETGLSVRVVQVWFQNQRAKMKKLARRQQQQQQDQQNTQRLSSAQ
LMX1B  EVSSKPCRKVRETLAAETGLSVRVVQVWFQNQRAKMKKLARRHQQQQE-QQNSQRLGQE-
       *******************************************:****: ***:***..
                              265
LMX1A  TNGGGSAGMEGIMNPYTALPTPQQ-LLAIEQSVY-SSDPFRQGLTPPQMPGDHMHPYGAE
LMX1B  ---VLSSRMEGMMASYTPLAPPQQQIVAMEQSPYGSSDPFQQGLTPPQMPGN-------D
          *: ***:*  ** *  *** ::*:*** * *****:***********:       :
LMX1A  PLFHDLDSDDTSLSNLGDCFLATSEAGPLQSRVGNPIDHLYSMQNSYFTS
LMX1B  SIFHDIDSD-TSLTSLSDCFLGSSDVGSLQARVGNPIDRLYSMQSSYFAS
        :***:*** ***:*.****.:*:.* **:*******:*****.***:*
```

Figure S4 Alignment of LMX1A and LMX1B.
Protein alignment of LMX1A (NP_796372.1) and LMX1B (NP_002307.1) performed with Clustal Omega version 1.2.4 (EMBL-EBI, http://www.ebi.ac.uk/Tools/msa/clustalo/). An asterisk (*) indicates positions which have a single, fully conserved residue; a colon (:) indicates conservation between groups of strongly similar properties, a period (.) indicates conservation between groups of weakly similar properties. There is a high percentage of similarity between the two proteins and the homeodomain of the two proteins is identical. The mutated residues identified in LMX1A (Cys97 and Val241) are boxed and indicated by a red arrow head, and demonstrate that the amino acids at these positions are identical in LMX1B (Cys118 and Val265, respectively). LIM, LIM domain; HOX, homeodomain.

Table S1 Overview of chromosomal regions, and WES variants in these regions, with a LOD score ≥ -2 in family W15-0551

Start SNP	End SNP	Chr	Start position	End position	Size (Mb)	Max LOD score	Known deafness genes	Shared exome variants[a]	Rare variants[b] (≤ 0.5%)	Coding & splice site variants	VUS & (likely) pathogenic variants[c]	Candidate variants
rs4908619	rs2797685	1	7,369,931	7,879,063	0,51	0.3683	-	26	1	0	-	-
rs12402233	rs10875048	1	96,144,365	97,595,033	1,45	-1.3532	-	2	0	-	-	-
rs1470436	rs4434842	1	102,253,545	104,492,118	2,24	-1.0535	COL11A1	49	1	0	-	-
rs478093	rs12129861	1	120,255,126	145,725,689	25,47	-1.2788	-	195	0	-	-	-
rs10918345	rs12041287	1	166,065,145	167,052,988	0,99	-1.5703	-	8	0	-	-	-
rs4233164	rs10800771	1	175,651,786	201,240,182	25,59	1.0027	-	607	3	1	1	NR5A2 c.1570G>A
rs10920621	rs10751435	1	203,335,113	205,318,321	1,98	-1.6129	-	152	0	-	-	-
rs1372165	rs10153860	2	41,420,957	42,722,516	1,31	-1.1611	-	13	0	-	-	-
rs34136947	rs115417046	2	46,584,059	68,108,933	21,52	0.5203	PNPT1	397	8	2	2	NRXN1 c.342G>C PEX13 c.89T>C
rs17697617	rs16838302	2	193,564,025	196,067,526	2,50	-1.6675	-	0	-	-	-	-
rs1374360	rs2348129	2	200,125,150	201,644,232	1,52	-1.7975	-	31	1	0	-	-
rs17609761	rs458514	4	48,496,804	54,074,642	5,58	-1.6693	-	40	0	-	-	-
rs621896	rs5011719	6	8,269,415	22,138,150	13,87	0.3627	-	226	2	0	-	-
rs16883199	rs2143437	6	73,739,831	96,400,830	22,66	2.3974	MYO6	388	5	0	-	-
rs76359180	rs4947084	6	108,810,769	110,947,440	2,14	-1.7656	CD164	121	5	2	1	CD164 c.106-6dup
rs6912287	rs72977538	6	135,597,263	136,736,714	1,14	-0.5684	-	21	0	-	-	-
rs34261503	rs2813487	6	138,240,225	152,466,582	14,23	0.8980	-	290	2	2	0	-
rs2296254	rs1902064	6	152,555,112	156,722,390	4,17	-1.4288	-	107	1	0	-	-
rs17863123	rs112640327	7	90,111,371	91,863,363	1,75	-1.5439	-	16	1	1	1	FZD1 c.1571G>C
rs2108225	rs17157870	7	107,453,103	110,287,125	2,83	-0.1203	-	58	0	-	-	-
rs10949787	rs16868174	7	155,720,971	159,138,663	3,42	0.4142	-	146	2	0	-	-
rs7040084	rs13290342	9	29,483,651	30,175,188	0,69	-1.7456	-	0	-	-	-	-
rs117403619	rs10511880	9	30,652,864	31,540,903	0,89	-1.3325	-	0	-	-	-	-
rs10970585	rs13301121	9	31,895,373	34,701,352	2,81	-0.8431	-	134	1	0	-	-
rs10119417	rs6560420	9	38,686,734	71,512,668	32,83	-0.7518	-	4	0	-	-	-
rs77600772	rs12340637	9	77,299,919	78,185,039	0,89	-0.1230	-	34	2	0	-	-
rs12551266	rs12551927	9	89,986,101	90,772,863	0,79	-1.8168	-	38	0	-	-	-
rs602924	rs11243915	9	133,371,501	135,675,305	2,30	0.4537	-	196	0	-	-	-
rs117496585	rs2511376	11	91,771,186	93,670,388	1,90	-1.3298	-	70	3	1	0	-
rs74896377	rs74536307	11	96,771,009	98,955,361	2,18	0.3051	-	0	-	-	-	-

Table S1 (continued)

Start SNP	End SNP	Chr	Start position	End position	Size (Mb)	Max LOD score	Known deafness genes	Shared exome variants[a]	Rare variants[b] (≤ 0.5%)	Coding & splice site variants	VUS & (likely) pathogenic variants[c]	Candidate variants
rs4282990	rs2014365	11	124,386,011	125,049,965	0,66	-1.8146	-	41	0	-	-	-
rs3734078	rs58045934	11	129,772,013	130,644,486	0,87	-1.6628	-	41	0	-	-	-
rs61908863	rs34226067	11	134,416,490	134,616,366	0,20	-1.9277	-	0	-	-	-	-
rs521040	rs6488433	12	10,147,850	11,768,462	1,62	-1.7581	-	186	0	-	-	-
rs1806201	rs79974352	12	13,717,508	14,930,869	1,21	-1.9018	-	40	0	-	-	-
rs1886449	rs76588355	13	73,932,114	74,797,460	0,87	-1.7232	-	3	0	-	-	-
rs283956	rs76661894	13	77,117,984	79,330,073	2,21	-1.8628	-	27	0	-	-	-
rs10144623	rs10137285	14	31,242,086	34,049,850	2,81	-1.5711	COCH	64	1	0	-	-
rs1837763	rs77968073	15	71,707,375	73,236,886	1,53	-1.4074	-	50	0	-	-	-
rs351175	rs75192007	15	74,528,985	77,518,629	2,99	-1.7094	-	128	6	2	0	-
rs117104971	rs117140491	15	78,018,233	78,524,231	0,51	-1.7302	CIB2	19	0	0	-	-
rs78641696	rs448653	16	1	1,081,348	1,08	-1.0024	-	82	3	0	-	-
rs17562963	rs8044409	16	7,452,583	7,715,577	0,26	-1.5463	-	5	1	0	-	-
rs11077287	rs74569016	16	8,337,001	9,781,606	1,44	0.5677	-	85	1	0	-	-
rs138769038	rs16942334	18	23,381,462	24,026,191	0,64	-1.8843	-	5	1	0	-	-
rs117246954	rs117483780	18	77,241,715	78,077,248	0,84	0.1636	-	40	0	-	-	-
rs4807391	rs10415208	19	3,054,567	4,496,046	1,44	-1.0559	GIPC3	230	1	1	-	-
rs2250656	rs1423096	19	6,718,534	7,739,177	1,02	-1.9221	-	191	1	0	0	-
rs1644731	rs116049570	19	10,131,999	11,574,443	1,44	-1.6460	S1PR2	196	2	2	1	RAVER1 c.2002G>A
rs1401828	rs2144936	20	4,977,788	6,118,980	1,14	-1.0977	-	51	1	0	-	-
rs56055585	rs4811952	20	56,296,576	56,583,939	0,29	-1.7923	-	0	-	-	-	-
rs2093140	rs55872076	20	59,692,266	63,025,520	3,33	-0.4991	OSBPL2	415	7	1	0	-
rs1726175	rs4141087	X	1	26,252,686	26,25	0.1244	SMPX	240	0	-	-	-
rs4271113	rs4239965	X	34,892,503	47,244,180	12,35	-0.0783	-	82	2	1	1	BCOR c.3407G>A

Genomic positions are according to the UCSC Genome Browser, GRCh37/hg19 (https://genome.ucsc.edu/). Coverage of all exons and exon-intron boundaries of the ten known deafness genes located in one of the regions not excluded by linkage analysis, was manually checked to be at least 10x. Sanger sequencing was performed for regions with a lower coverage, which did not reveal any rare variants (allele frequency ≤ 0.005). VUS, variant of uncertain significance. [a]Total number of WES variants shared by subject II:7 and III:8 of family W15-0551. [b]Based on population frequency data of the dbSNP database and our in-house database. The latter contains WES data of 13314 individual, the vast majority of Dutch origin, affected by a large number of different diseases (including 810 subjects with HI). [c]Based on variant classification guidelines by the American College of Medical Genetics and Genomics and the Association for Molecular Pathology.[7]

4.2

185

Table S2 Primer sequences and PCR conditions

Target	Primer	Oligonucleotides	Size (bp)	Annealing Temperature (°C)
LMX1A exon 3	Forward	gttctttcccaggagtgcg	299	58
	Reverse	tgtatgaagaggggcgctag		
LMX1A exon 4	Forward	tggttgattagcaggagttcc	461	58
	Reverse	ctgaagggaagttctgctcg		
LMX1A exon 5	Forward	tgaatgactcaactgaatgcttc	500	58
	Reverse	agggaagaaacaatgcagacag		
LMX1A exon 6	Forward	tgctctcatacataaagccatcc	376	58
	Reverse	caatgcccactgagatccca		
LMX1A exon 7	Forward	aggcaagagaggagaccaag	576	58
	Reverse	acctggcagcaagtacaatg		
LMX1A exon 8	Forward	tggccactgttgctccttta	395	58
	Reverse	ccctctcacaagttcctcgt		
LMX1A exon 9	Forward	ggaatcaggacccagggaaa	347	58
	Reverse	tggaacttcggtgagcatct		
LMX1A exon 10	Forward	cagctgaatatcctagcactga	395	58
	Reverse	GGAAATGCTGAGCTACACCA		
LMX1A mRNA exons 3-4	Forward	AGAACTTCCAAAGCGCGATC	105	60
	Reverse	TCCAAGATGACCCGCTGAC		
LMX1A mRNA exons 4-5	Forward	TCTACCGGGACAAGAAGCTG	111	60
	Reverse	GGGCCCGCATAACAAACTC		
LMX1A mRNA exons 6-7	Forward	CTCAACAGAGGCGAGCATTC	97	60
	Reverse	ACACTCAGCCCTGTCTCTG		
MYO6 c.2417-1758T>G	Forward	ccattcatttgtggactgtg	283	58
	Reverse	tgaaatgtgaataggtatgtcctg		
NR5A2 exon 8	Forward	AATGTGTAACTACCCGCAGC	396	58
	Reverse	AGCCTTTGATTCACAGTTTGC		
NRXN1 exon 2	Forward	CCAGCTCAAGACTCGCAGC	300	58
	Reverse	CCGACGAAAAGGCCGCTG		
PEX13 exon 1	Forward	GTTGTGTCTTACGCTCCAGG	294	58
	Reverse	ggttgggtattggttaaagggg		
CD164 exon 3	Forward	tttgggtttgatttcatagagc	264	58
	Reverse	ctgaaacaaggctttctgagg		
FZD1 exon 1	Forward	CTTCGTGGGGCTTAACAACG	273	58
	Reverse	CTGCGTTCCCACTGGTCC		

Table S2 (continued)

Target	Primer	Oligonucleotides	Size (bp)	Annealing Temperature (°C)
RAVER1 exon 11	Forward	acaaagggctgggtactaca	280	58
	Reverse	ggttacagagccccggtg		
BCOR exon 8	Forward	CACCGTGATCCCTTTGAAGC	248	58
	Reverse	ggctcacCTTTAGAGACTCGT		
COL11A1 exon 26	Forward	tgaattgaagccagtgactcag	370	58
	Reverse	agtttccacaaaagccaccg		
COL11A1 exon 56	Forward	tgctgtttttcagtattctaagagg	657	58
	Reverse	gaaagtaaaatatgggagcacattag		
PNPT1 exon 7	Forward	tacaaagcccctgcttttagc	397	58
	Reverse	gccatatgccattgctgtaac		
PNPT1 exon 9	Forward	gaaatcaaggtggatctatcactaag	398	58
	Reverse	tccatgggaagtttctctcc		
COCH exon 2	Forward	ATCAGTCACCATGTCCGCAG	497	58
	Reverse	cttcctcgacctcctgctg		
GIPC3 exon 1	Forward	cctgtccctgtccttatttg	746	58
	Reverse	gctagtcctaagacctgccc		

Primers for amplification of exons and exon-intron boundaries were designed with Primer3Plus (http://www.bioinformatics.nl/cgi-bin/primer3plus/primer3plus.cgi). The following reference sequences were used: *LMX1A*, NM_177398.3; *MYO6*, NM_004999.3; *NR5A2*, NM_205860.2; *NRXN1*, NM_004801.5; *PEX13*, NM_002618.3; *CD164*, NM_006016.5; *FZD1*, NM_003505.1; *RAVER1*, NM_133452.2; *BCOR*, NM_001123385.1; *COL11A1*, NM_001854.3; *PNPT1*, NM_033109.4; *COCH*, NM_001135058.1; *GIPC3*, NM_133261.2. Amplification by PCR was performed under standard conditions. PCR fragments were purified with ExoI/FastAP (Thermo Fisher Scientific, Waltham, MA, USA), in accordance with manufacturers' protocols. Sequence analysis was performed with the ABI PRISM BigDye Terminator Cycle Sequencing v.2.0 Ready Reaction kit and analyzed with the ABI PRISM 3730 DNA analyzer or the 3130 Genetic Analyzer (Applied Biosystems, Foster City, CA, USA). A possibly deleterious effect of the identified variants on the proteins and splicing was predicted with Alamut Visual version 2.7.1 (Interactive Biosoftware, Rouen, France).

4.2

Table S3 Individual results of otoscopy, pure-tone audiometry, HI progression analysis, speech discrimination and vestibular complaints

Family	Subject	Age at evaluation (yrs)	Reported age of HI onset (yrs)	Otoscopic examination	PTA (dB HL)		Significant progression of HI				SRT (dB)[c]	Max. SRS (%)[c]	Vestibular complaints
					R	L	R	L	rate[b]	YOF			
W15-0551	II:7	73	27	R+L myringo-sclerosis	73	65[d]	no	no	-	17	67	58	no
	III:8	44	puberty	R+L hypermobile eardrum	57	53	yes	yes	1.2	20	51	92	vertigo episodes at age of 32 and 40 years lasting for days
	IV:2	9	congenital	normal	48	23	no	no	-	3	22	100	no
63136[e]	I:2	85	childhood	NT	80	83	-	-	-	0	82	90	no
	II:2	54	26	normal	58	28	yes	yes	1.0	28	28	100	vertigo episodes with tinnitus during puberty and at age of 40 years lasting for days
	II:3	52	congenital	normal	112	113	yes	yes	1.1	37	ND	10	vertigo episodes with tinnitus in the past lasting for hours
	II:4	40	35	normal	45	57	yes	yes	1.6	10	36	92	vertigo episodes with tinnitus around the age of 40 years lasting minutes to hours, and BPPV

yrs, years; PTA, pure tone average, mean of 0.5, 1 and 2 kHz air conduction thresholds; R, right; L, left; HI, hearing impairment; YOF, years of follow-up; SRT, speech reception threshold; Max, maximum; SRS, speech recognition score; NT, not tested. [a]Individual progression of HI was calculated with longitudinal linear regression analyses, using all available audiograms for the better hearing ear. Audiograms were used only if they were obtained after the age of 5 years. The onset level of HI (threshold intercept, in dB HL at age 0 years) and progression of HI (slope in dB/year), were determined for each frequency (0.25, 0.5, 1, 2, 4 and 8 kHz). Progression of HI was considered to be significant, if the regression coefficient differed significantly (p ≤ 0.05) from 0 for at least two of the six evaluated frequencies, and if the slopes were positive. Progression of HI could not be calculated in subject I:2 of family 63136, because only one audiogram was available. [b]Progression rate is the mean (PTA$_{0.5-4 kHz}$) increase in dB per year for the better hearing ear. [c]Results of speech discrimination for the better hearing ear are presented. [d]PTA of bone conduction thresholds is displayed, because of mixed HI due to fenestral otosclerosis conductive HI) and the *LMX1A* variant (sensorineural HI). [e]Family 63136 did not participate in our clinical evaluation; only retrospective data were analyzed.
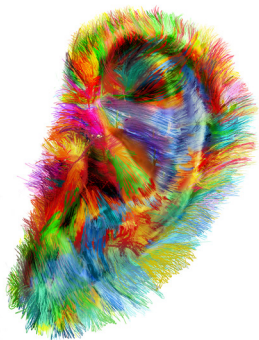
References

1.   Schmitz-Hubsch T, du Montcel ST, Baliko L, et al. Scale for the assessment and rating of ataxia: development of a new clinical scale. *Neurology.* Jun 13 2006;66(11):1717-1720.

2.   Nasreddine ZS, Phillips NA, Bedirian V, et al. The Montreal Cognitive Assessment, MoCA: a brief screening tool for mild cognitive impairment. *Journal of the American Geriatrics Society.* Apr 2005;53(4):695-699.

3.   Schmand B, Lindeboom J, van Harskamp F. Nederlandse leestest voor volwassenen. . Lisse: Swets en Zeitlinger; 1992.

4.   Schmidt M. *Rey auditory verbal learning test: A handbook.* Los Angeles, CA: Western Psychological Services; 1996.

5.   Wechsler D. The Wechsler intelligence scale for children. San Antonio: TX: The Psychological Corporation; 1991.

6.   Beery KE, Buktenica NA, N.A. B. The Beery-Buktenica developmental test of visual-motor integration: Administration, scoring, and teaching manual Minneapolis: MN: NSC Pearson; 2010.

7.   Wallis Y, Payne S, McAnulty C, et al. Practice Guidelines for the Evaluation of Pathogenicity and the Reporting of Sequence Variants in Clinical Molecular Genetics. *ACGS /VGKL.* 2013.

4.2

5

General discussion

This thesis had the aim to contribute to optimal diagnostics and counseling for patients with hereditary HI in the Netherlands and beyond, by identification of novel deafness genes and (further) characterization of correlations between types of HI and underlying genetic causes. Chapter 2 evaluated the yield and outcomes of the most commonly used diagnostic test for hereditary HI in the Netherlands: whole exome sequencing (WES) with targeted analysis of a deafness gene panel. Here, the (dis)advantages and ethical issues of this technique are discussed, as well as developments in molecular diagnostics. In chapter 3, we have described phenotype characterizations and genotype-phenotype correlations of two recessive types of HI. The importance of these types of studies will be commented, and we shall discuss phenotype characteristics that should be described when publishing a (novel) genotype-phenotype correlation. Chapter 4 described two novel deafness genes and the associated phenotype. Here, we will discuss strategies for identification of novel deafness genes.

5

Diagnostic yield, (dis)advantages, and ethical issues of WES with targeted analysis of a deafness gene panel

Retrospective research into test outcomes of 200 Dutch patients with HI, described in chapter 2 of this thesis, revealed that in only 33.5% of cases a genetic diagnosis could be established. This diagnostic yield is comparable to other studies[1-7], which means that worldwide in circa 65% of HI patients no genetic diagnosis can be provided. There are several reasons why the diagnostic yield for hereditary HI is low. First of all, at least tens of deafness genes are to be identified, illustrated by the number of deafness loci for which the causative gene is currently unknown (Hereditary Hearing Loss Homepage, http://hereditaryhearingloss.org/). The number of monogenic forms of nonsyndromic HI (NSHI) that await identification is probably even higher, as there are many genes known to be expressed in the cochlea or involved in hearing in animals, that are possibly also involved in HI in human. An example of this *LMX1A*. This gene was found to be associated with dominant NSHI in humans (described in chapter 4.2), but was already associated with deafness in mice since 1999.[8] Each unidentified gene is most likely involved in less than 1% of the cases, or even in only one or a few families with NSHI, as most frequently involved genes are already known. This is illustrated by recently identified deafness genes, such as *KITLG*[9] and *CLIC5*[10], that have so far been associated with HI in three families and one family, respectively. The prevalence of the identified founder variant in *MPZL2* (c.72del, chapter 4.1) in the Dutch population is 0.33%, based on population-frequency data of the Radboud university medical center in-house exome database. This reveals that the prevalence of

homozygotes is 1 in 100.000 individuals, demonstrating that mutations in *MPZL2* are rare, but occur in a significant number of Dutch HI patients.

The second reason for the low diagnostic yield might be the suboptimal technological WES conditions. Part of causal variants in known deafness genes probably remained unidentified due to insufficient enrichment or coverage. In our study, two enrichment kits (Agilent version 50 Mb and version 4) were used, both not targeting 121 of the 2347 exons of the analyzed deafness genes, of which 51 exons (50 Mb kit) and 56 exons (version 4 kit) were coding. We have not investigated whether poor enrichment has a significant impact on the diagnostic yield. We expect that the number of causative variants might slightly increase with improved enrichment, as more than half of coding exons was not targeted for a few genes (*PTPRQ* in the 50 Mb kit, and *OTOA* and *STRC* in the version 4 kit). However, poor enrichment of *OTOA* and *STRC* does not affect the identification of large copy number variations (CNVs) in these genes, although small CNVs can be missed. Indeed, large deletions could be identified in the investigated cohort despite bad enrichment. In addition, the coverage was suboptimal, as the median coverage of at least 20x was reached for 72.0% to 97.8% of the targeted genes. Coverage, however, seemed not to be the major cause of the high percentage of unidentified variants, as the identification rate of causative variants remained stable with improvement of coverage over time. Diagnostic yield was not influenced by improvement of sequence quality and read length by using a better sequencing system (switch from the 5500xl SOLiD system to the Illumina HiSeq2000TM machine).

Third, in 5% of cases, variants of uncertain significance were identified. Further research into these variants and subsequent classification as pathogenic or (likely) benign will probably increase the diagnostic yield. Functional validation is the gold standard to prove pathogenicity of a variant, but this is usually not feasible in diagnostic settings. Although population based frequency data, such as the Exome Aggregation Consortium browser[11], and computational tools for variant prioritization, such as CADD[12], are increasingly available, interpretation of variants is still a challenge. This is especially true for interpretation of missense and splice site variants. In addition, these tools have important drawbacks, as variant frequency data are often not population-specific, and pathogenic founder variants can be misinterpreted because of high prevalence. Validation of computational tools has shown that the predictive value is limited, as variants that are predicted to be pathogenic are often benign and vice versa.[13] Scores for intolerance to genetic variation are not applicable for HI, as many deafness genes have a high tolerance to variation, because HI does not (significantly) reduce fitness. This is illustrated by the relatively high residual variation intolerance score of *USH2A* (4.2, overall range -8.3 to 29.8), as calculated by Petrovski *et al.* (2013).[14] In our study, variants of uncertain significance were

mainly reported in patients for whom no DNA of family members was available, which hampered segregation analysis. This highlights the importance of taking an accurate family history and collecting clinical data and DNA samples of as many as possible family members.

Fourth, deep intronic variants affecting splicing, complex chromosomal rearrangements, and variants in non-coding exons, repeat regions and regulatory regions are missed in WES, which probably explains the largest part of unidentified variants. Several pathogenic intronic variants in frequently involved HI genes have been described, for example in *MYO6*[15], *SLC26A4*[16], and *USH2A*[17,18]. These variants can only be found using other techniques, such as whole genome sequencing (WGS) or targeted genome sequencing.

Finally, involvement of non-genetic causes or a combination of (multiple) genetic and non-genetic factors cannot be excluded for cases in which no causative variants could be identified. We expect that the number of patients with non-genetic and multifactorial HI is significant. This is strengthened by the fact that the diagnostic yield declined significantly with increased age of HI onset. Whereas the percentage of identified causal variants was 37-49% in individuals with congenital or 1st decade HI onset, this declined radically to 8-18% in individuals with 2nd to 4th decade HI onset. No causal variants were identified in the subjects with an age of HI onset in the fifth or sixth decade.

Besides WES, targeted next-generation sequencing (NGS) of a deafness gene panel is commonly used as a diagnostic test for HI (*e.g.* OtoSCOPE[19]). The advantage of WES targeting a gene panel compared to targeted NGS, is that the gene panel can be constantly updated according to newest insights on genes involved in HI, and reanalysis of previously tested cases on novel deafness genes is possible. Besides, if gene panel analysis is negative, analysis of all WES data (open exome analysis) can be performed.[20] Since WGS can identify variants in non-coding regions, it could be questioned whether this has a better diagnostic applicability and yield for HI, compared to WES. WGS has the mentioned advantages of WES and outperforms WES regarding coverage and sequencing biases (*e.g.* problems with mapping, strand coverage, or allele distribution)[21], partly because the enrichment step is entirely omitted in WGS. In addition, complex rearrangements, such as inversions and translocations, can be identified in WGS.[22] Despite the superiority of WGS, only one case of diagnostic use of WGS for syndromic HI has been described.[23] This is due to the high costs of WGS, making WES currently more cost-effective.[20] But in the nearby future, lower costs of WGS will enable the application of WGS as a diagnostic test, and will eventually replace WES. There are, however, also other hurdles to take, such as storage of the enormous amount of data that is generated by WGS, and strategies for analysis and interpretation of the large number of sequencing variants.

The rapid progress in unraveling exomes, and soon genomes, obliges us to be guided by ethical principles. As described in chapter 2 of this thesis, we identified variants of uncertain significance in *USH2A*, which is associated with Usher syndrome type 2, in children without symptoms of retinitis pigmentosa. This is difficult for genetic counseling, as parents have to be informed about the *possible* development of Usher syndrome later in life. Therefore, development of better computational tools for prediction of variant pathogenicity and/or novel techniques for cost-effective functional validation is urgent. Although presymptomatic testing enables effective management and rehabilitation, parents should be counseled on the risk of diagnosing a syndrome, to make an informed decision on whether or not to perform genetic testing.[24] A presymptomatic diagnosis can have a huge psychosocial impact, although this has not been studied for HI. Therefore, if presymptomatic diagnostics is applied, one should be able to provide aftercare for patients and their relatives if needed.

Another ethical issue is the risk of incidental findings, which only occurs when performing open exome (or genome) sequencing. Whereas some argue that incidental findings should be reported and actively searched for, others are of the opinion that they should be avoided if possible.[25] In the Radboud university medical center, the risk of incidental findings with WES is 0.7% (unpublished data). If an incidental finding occurs, the results are discussed in a panel of independent experts who decide whether the incidental finding is important for the patient to know, in accordance with the recommendations of the European Society of Human Genetics[26], and the guidelines for diagnostic NGS, as published by Eurogentest (http://www.eurogentest.org/). In the scientific research team of the Radboud university medical expertise center Hearing & Genes, 59 genes associated with severe disease are excluded from analysis, to exclude incidental findings. For this purpose, the list of genes compiled and updated by the American College of Medical Genetics and Genomics, for reporting of secondary findings in clinical exome and genome sequencing, is used.[27] Since the diagnostic yield of open exome analysis for HI is extremely low, even lower than the chance of incidental findings, it could be questioned whether open exome analysis should be performed in a diagnostic setting. When a *de novo* approach is applied, *i.e.* analyzing exome or genome sequencing data in parent-child trios, the probability of an incidental finding is low (no numbers available). The risk of incidental findings can also be lowered by analysis of shared exomic or genomic variants of several affected family members, although the risk will remain significantly higher compared to a *de novo* approach.

Finally, we demonstrated in chapter 2 that we could not find any pathogenic variants in patients with an HI onset in the 5th or 6th decade. These results demonstrate that – at

least in the Dutch population – WES should probably not be performed in patients with an age of onset after the 4th decade of life, as the costs of the test do certainly not outweigh the chance of finding the genetic defect. In these individuals, *COCH* (DFNA9) should be tested when clinically suspected, and special attention should be paid to non-genetic causes. Probably, combinations of multiple genetic factors are involved, as in age-related multifactorial HI.[28]

The importance of thorough characterization of the phenotype and establishment of genotype-phenotype correlations

The reported phenotype of several cases described in chapter 2, was different from the type of HI known to be associated with mutations in the gene. An example of this is the identification of pathogenic variants in *TRIOBP*, a gene known for severe to profound HI, in two patients with mild and moderate HI (further described in chapter 3.1). This illustrates that novel genotype-phenotype correlations can be identified by targeted analysis of a deafness gene panel, provided that one does not discard these variants because the phenotype does not match with the reported type of HI. In addition, it underlines the enormous phenotypic heterogeneity that can result from pathogenic variants in an HI-related gene. Many deafness genes are associated with a highly variable phenotype, such as *TRIOBP* (chapter 3.1 of this thesis), *LOXHD1* (chapter 3.2), *LMX1A* (chapter 4.2), *CDH23*[29,30], *TECTA*[31,32], and *DFNA9*[33,34].

Establishment of well characterized phenotypes and genotype-phenotype correlations is essential for adequate counseling, to prevent further diagnostic testing, and to identify possible medical comorbidities.[35,36] In addition, knowledge on the phenotype and genotype-phenotype correlations can help to understand the function of the gene in humans. Patients with HI pursue a genetic diagnosis to obtain information on treatment options, prognosis and risk of inheritance.[37] However, phenotype information is scarce for many types of HI, due to the limited number of patients diagnosed with a specific type of HI and due to insufficient description of the phenotype. Evaluation of a phenotype of a small kindred is considered less reliable and precise than characterization of a large number of patients with a genetic defect in the same gene, preferably from several families and origin. Examples of insufficient phenotype descriptions are described in chapter 3, as a number of publications on DFNB28 (chapter 3.1) and DFNB77 (chapter 3.2) do not provide a phenotype description at all. We endorse the recommendations of the GENDEAF study group for description of the HI phenotype, who propose that all published HI phenotypes at least describe type and severity of HI, audiometric configuration, (a)symmetry of HI, estimated

age of onset, HI progression, tinnitus, vestibular symptoms and function, and intrafamilial/interfamilial variability.[38] It is obvious that the description of sequence variants should be in accordance with the HGVS recommendations[39], and that classification of the identified DNA variant should meet the globally accepted recommendations of the American College of Medical Genetics and Genomics.[40] The ClinGen Hearing Loss Working Group is currently working on a variant assessment framework for HI-related genes, which will describe, amongst others, a cut-off point of the minor allele frequency for specific genes.

Strategies for identification of novel genes for nonsyndromic deafness

As described at the start of this chapter, it is very likely that HI in part of genetically undiagnosed patients is caused by pathogenic variant(s) in yet undiscovered deafness genes. Identification of these genes increases the efficacy of genetic testing and enables adequate genetic counseling on prognosis, recurrence risk, rehabilitation options and, if applicable, diagnosing of additional symptoms. In addition, identification of underlying genetic defects opens the doors for development of genetic therapies for HI. Unraveling the pathophysiological mechanisms that result from a specific genetic defect, or identification of specific types of causative variants, enable future development of targeted therapy. There are a number of strategies that can be used for therapy, depending on the type of causal variant and the effect of the genetic defect on protein function. For example, dominant-negative effects can be addressed with an allele silencing approach[41], whereas compounds that enhance read-through can abolish effects of a nonsense mutation[42]. Mis-splicing of pseudo-exons that are inserted due to intronic variants can be prevented using antisense oligonucleotide-mediated exon skipping[43].

Before the introduction of NGS, identification of NSHI-related genes relied on Sanger sequencing of candidate deafness genes and/or positional cloning, usually after identification of a shared genotype region by homozygosity mapping or linkage analysis. Since 2010, targeted NGS and WES have enabled the rapid and more cost-efficient identification of genes involved in NSHI (Figure 1).[44] Up to now, genes involved in NSHI have not been identified with WGS, although recently three syndromic HI-related genes have been discovered by WGS.[45-47] The identification rate of deafness genes has not increased as fast as expected, as can be seen in Figure 1, mainly due to difficulties in variant interpretation.

DNA variant interpretation is all about reducing the number of sequence variants, typically tens of thousands when using WES, to a manageable number of candidate variants, which are to be further investigated. This eventually leads to identification of

one or two (likely) causative variants.[48] The first step in reducing the number of candidate variants is based on variant quality, population frequency of the variant, the type of variant, and the predicted effect of the variant on protein level using computational tools. The remaining candidate variants are further analyzed using (homology) protein modeling, segregation analysis, available information on function and expression of the candidate gene, interactions of the candidate gene/protein with genes/proteins involved in hearing, and existing phenotype data of animal models. If indicated, functional or animal studies can be performed to prove the deleterious effect of the variant(s) and the function of the gene in hearing.
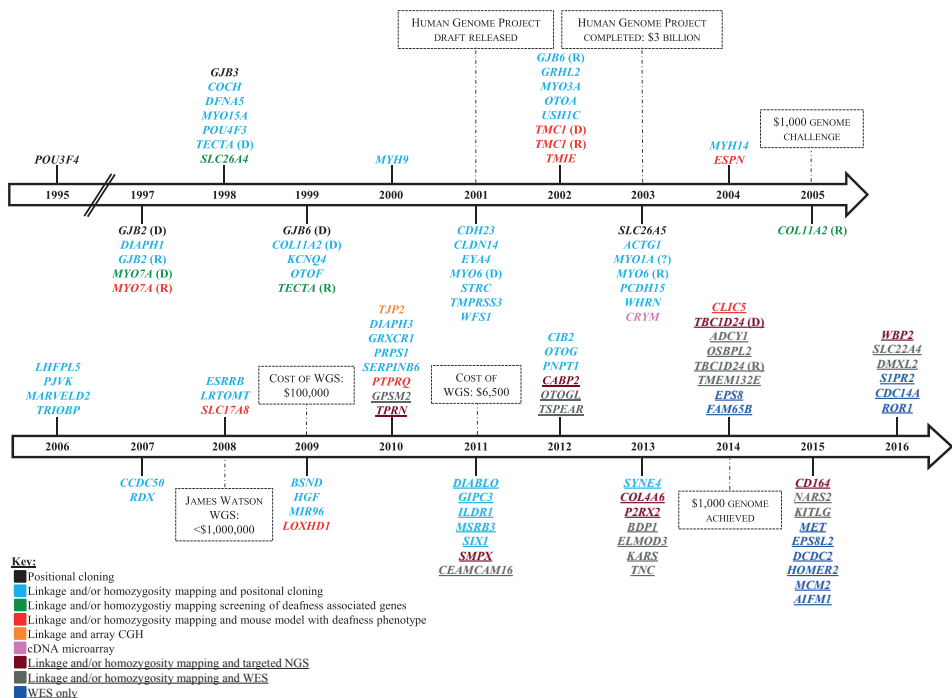
Figure 1 Identification of NSHI-related genes and method of discovery, from 1995 to 2016. The figure was adapted from Vona *et al.* (2015).[44] CGH, comparative genomic hybridization.

Elucidating pathogenic variant(s) by analyzing WES or WGS data of one affected individual is often not successful, because too many candidate variants remain. If the (likely) causative variant can be identified, we need to beware of seemingly causative variants that segregate by chance, especially in dominant NSHI. This is illustrated by the recent disqualification of *MYO1A* as a deafness gene.[49,50] Both the remaining of too many variants and the risk of classifying a benign variant as causative, are reasons to combine WES or WGS with other molecular techniques, or to perform WES or WGS in several patients from one or

a number of families. These strategies have been described by Gilissen *et al.* (2012), and are depicted in Figure 2.[48] The linkage based (Figure 2a) and homozygosity based (Figure 2b) strategies are often used for identification of novel deafness genes, as can be seen in Figure 1, and we have applied them for discovery of several deafness genes (*e.g. MPZL2,* described in chapter 4.1). These strategies have the advantage of statistical support for the variant's causality.[51] However, for linkage analysis and homozygosity mapping a significant number of (affected) family members is needed, whereas in many cases there is no family history of HI, the number of affected family members is small, or DNA and clinical information of family members is not available. In addition, these strategies always lead to identification of only one novel deafness gene at a time.
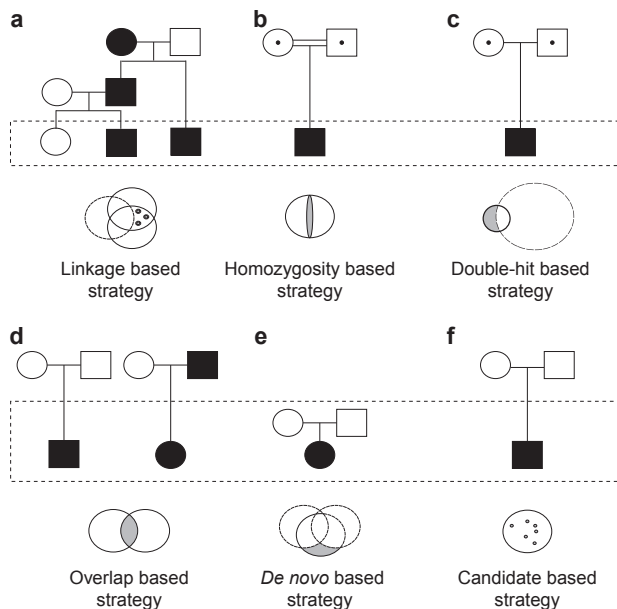
Figure 2 Strategies for identification of disease-causing variant(s) using WES or WGS. The figure was obtained from Gilissen *et al.* (2012)[48], with approval from the Nature Publishing Group. Dashed rectangles indicate subjects in which WES is performed. Circles below the pedigrees represent WES variants of the different subjects and grey dots (**a** en **f**) and grey filled spaces (**b-e**) symbolize candidate variants that remain after application of the strategy. Details on the strategies are described in the main text.

If only WES or WGS data is available, one of the alternative strategies for identification of causative variant(s) can be used. Whichever of these strategies is used, one should search for a number of families segregating unique pathogenic variant(s) in the same gene, and prove that these variants do not occur in a significant number of normal hearing controls. Although rareness of the involvement of a deafness gene can impede the identification of additional families, (inter)national collaborations and databases may offer a solution

(*e.g.* the online database GeneMatcher).[52] In chapter 2, we demonstrate that 2% of the investigated cases harbors a *de novo* variant, which shows that a *de novo* based strategy (Figure 2e) can be effective. However, the relative number of causative *de novo* variants in HI is expected to be low, as HI does not (significantly) reduce fitness and consequently most variants are inherited. In chapter 4.2, we describe the discovery of *LMX1A* as a novel deafness gene, identified by a candidate based strategy (Figure 2f). This strategy, and the double-hit based strategy (Figure 2c) are only successful if a clear candidate variant is present based on current (biological) knowledge, for example because defects in a candidate gene are associated with HI in mice.[48] The a priori chance of identifying disease-causing variant(s) using the candidate based or double-hit based strategy is low.

The overlap based strategy (Figure 2d) has, as far as we know, never been used extensively for NSHI. This strategy requires accurate and systematic phenotyping and genotyping, and can only be applied if the disease is a monogenic disorder.[48] Although di-, oligo-, or polygenic inherited forms of HI probably exist[53,54], we assume that the majority of early-onset NSHI causes is monogenic. The genetic and phenotypic heterogeneity of NSHI complicates the use of the overlap based strategy. Genetic heterogeneity and rareness of involvement of a specific disease-causing gene can be circumvented by analyzing a large cohort of NSHI patients in a meta-analysis. This strategy has been used for other disorders, and could effectively identify a number of disease-related genes at once.[55,56] One could analyze WES data of uncategorized patients, or a subset with a specific mode of inheritance or a distinct phenotype. However, it could be questioned whether the phenotype of the latter subset can be characterized well enough for proper categorization, as we lack tools for deep phenotyping of HI. Although audiometric and vestibular examination give objective phenotype information, there are no tests available that can determine which part of the inner ear is affected (*e.g.* outer or inner hair cells, tectorial membrane, stria vascularis, or the cochlear nerve). Additional techniques, such as determination of the auditory profile through psychophysical measurements[57], sophisticated imaging techniques, or even the use of organoids[58,59], could enable deep phenotyping. As described in the first paragraph of this chapter, environmental factors can often not be excluded, especially in cases without a family history of HI and in patients with late-onset HI, in particular patients with an age of onset after the 4th decade of life. These cases could be excluded from analysis.

A preliminary meta-analysis of 117 exomes revealed that the number of candidate variants that remain after a first selection – based on variant quality, population frequency, type of variant, and predicted pathogenicity based on computational tools – is excessive (M. Wesdorp and S. Lelieveld, Radboud university medical center, unpublished data). To reduce this number, only families could be included of which exomic or genomic data of at least two affected or affected and unaffected family members is available, and only

shared variants could be used for analysis. Statistical calculations on genetic variation rates in functional domains could be used to significantly reduce the number of variants and to unveil novel candidate deafness genes.

Conclusions and implications of this thesis

In conclusion, the studies described in this thesis contribute to identification of all genes involved in hearing and their associated phenotype. Enhanced knowledge on genes and proteins essential for hearing in humans enables further elucidation of the physiology of hearing and provides clues for genetic therapies. We should seek for sophisticated ways to unveil the disease-causing variants in yet undiagnosed patients, such as a meta-analysis of WES or WGS data. In addition, we should thoroughly characterize the associated phenotypes, ideally using strategies for deep phenotyping, such as psychophysical measurements. Rarity of specific genetic types of HI and difficulties encountered during sequence analysis could be tackled if we collaborate (inter)nationally with bio-informaticians, biologists, physicians, and molecular geneticists. Finally, we should not only focus on coding variants and monogenic causes, as has been done in the last decades. We now have the tools to address intronic splice variants, regulatory variants, and multifactorial causes, which might well explain a significant part of HI cases.

References

1.   Sommen M, Schrauwen I, Vandeweyer G, et al. DNA Diagnostics of Hereditary Hearing Loss: A Targeted Resequencing Approach Combined with a Mutation Classification System. *Human mutation.* Aug 2016;37(8):812-819.

2.   Yan D, Tekin D, Bademci G, et al. Spectrum of DNA variants for non-syndromic deafness in a large cohort from multiple continents. *Human genetics.* Aug 2016;135(8):953-961.

3.   Shearer AE, Black-Ziegelbein EA, Hildebrand MS, et al. Advancing genetic testing for deafness with genomic technology. *J Med Genet.* Sep 2013;50(9):627-634.

4.   Sloan-Heggen CM, Babanejad M, Beheshtian M, et al. Characterising the spectrum of autosomal recessive hereditary hearing loss in Iran. *J Med Genet.* 2015;52:823-829.

5.   Sloan-Heggen CM, Bierer AO, Shearer AE, et al. Comprehensive genetic testing in the clinical evaluation of 1119 patients with hearing loss. *Human genetics.* Apr 2016;135(4):441-450.

6.   Atik T, Onay H, Aykut A, et al. Comprehensive Analysis of Deafness Genes in Families with Autosomal Recessive Nonsyndromic Hearing Loss. *PLoS One.* 2015;10(11):e0142154.

7.   Bademci G, Diaz-Horta O, Guo S, et al. Identification of copy number variants through whole-exome sequencing in autosomal recessive nonsyndromic hearing loss. *Genetic testing and molecular biomarkers.* Sep 2014;18(9):658-661.

8.   Bergstrom DE, Gagnon LH, Eicher EM. Genetic and physical mapping of the dreher locus on mouse chromosome 1. *Genomics.* Aug 01 1999;59(3):291-299.

9.   Zazo Seco C, Serrao de Castro L, van Nierop JW, et al. Allelic Mutations of KITLG, Encoding KIT Ligand, Cause Asymmetric and Unilateral Hearing Loss and Waardenburg Syndrome Type 2. *American journal of human genetics.* Nov 05 2015;97(5):647-660.

10.   Seco CZ, Oonk AM, Dominguez-Ruiz M, et al. Progressive hearing loss and vestibular dysfunction caused by a homozygous nonsense mutation in CLIC5. *European journal of human genetics : EJHG.* Feb 2015;23(2):189-194.

11.   Lek M, Karczewski KJ, Minikel EV, et al. Analysis of protein-coding genetic variation in 60,706 humans. *Nature.* Aug 18 2016;536(7616):285-291.

12.   Kircher M, Witten DM, Jain P, O'Roak BJ, Cooper GM, Shendure J. A general framework for estimating the relative pathogenicity of human genetic variants. *Nature genetics.* Mar 2014;46(3):310-315.

13.   Lelieveld SH, Veltman JA, Gilissen C. Novel bioinformatic developments for exome sequencing. *Human genetics.* Jun 2016;135(6):603-614.

14.   Petrovski S, Wang Q, Heinzen EL, Allen AS, Goldstein DB. Genic intolerance to functional variation and the interpretation of personal genomes. *PLoS genetics.* 2013;9(8):e1003709.

15.   Hilgert N, Topsakal V, van Dinther J, Offeciers E, Van de Heyning P, Van Camp G. A splice-site mutation and overexpression of MYO6 cause a similar phenotype in two families with autosomal dominant hearing loss. *European journal of human genetics : EJHG.* May 2008;16(5):593-602.

16.   Yang T, Vidarsson H, Rodrigo-Blomqvist S, Rosengren SS, Enerback S, Smith RJ. Transcriptional control of SLC26A4 is involved in Pendred syndrome and nonsyndromic enlargement of vestibular aqueduct (DFNB4). *American journal of human genetics.* Jun 2007;80(6):1055-1063.

17.   Liquori A, Vache C, Baux D, et al. Whole USH2A Gene Sequencing Identifies Several New Deep Intronic Mutations. *Human mutation.* Feb 2016;37(2):184-193.

18.   Vache C, Besnard T, le Berre P, et al. Usher syndrome type 2 caused by activation of an USH2A pseudoexon: implications for diagnosis and therapy. *Human mutation.* Jan 2012;33(1):104-108.

19.   Shearer AE, DeLuca AP, Hildebrand MS, et al. Comprehensive genetic testing for hereditary hearing loss using massively parallel sequencing. *Proceedings of the National Academy of Sciences of the United States of America.* Dec 07 2010;107(49):21104-21109.

20.   Sun Y, Ruivenkamp CA, Hoffer MJ, et al. Next-generation diagnostics: gene panel, exome, or

5

whole genome? *Human mutation*. Jun 2015;36(6):648-655.

21. Lelieveld SH, Spielmann M, Mundlos S, Veltman JA, Gilissen C. Comparison of Exome and Genome Sequencing Technologies for the Complete Capture of Protein-Coding Regions. *Human mutation*. Aug 2015;36(8):815-822.

22. Gilissen C, Hehir-Kwa JY, Thung DT, et al. Genome sequencing identifies major causes of severe intellectual disability. *Nature*. Jul 17 2014;511(7509):344-347.

23. Goodwin G, Hawley PP, Miller DT. A Case of HDR Syndrome and Ichthyosis: Dual Diagnosis by Whole-Genome Sequencing of Novel Mutations in GATA3 and STS Genes. *The Journal of clinical endocrinology and metabolism*. Mar 2016;101(3):837-840.

24. Hartnett ME. *Pediatric Retina*. Philadelphia, USA: Lippincott Williams & Wilkins; 2005.

25. Yu JH, Harrell TM, Jamal SM, Tabor HK, Bamshad MJ. Attitudes of genetics professionals toward the return of incidental results from exome and whole-genome sequencing. *American journal of human genetics*. Jul 03 2014;95(1):77-84.

26. van El CG, Cornel MC, Borry P, et al. Whole-genome sequencing in health care: recommendations of the European Society of Human Genetics. *European journal of human genetics : EJHG*. Jun 2013;21(6):580-584.

27. Kalia SS, Adelman K, Bale SJ, et al. Recommendations for reporting of secondary findings in clinical exome and genome sequencing, 2016 update (ACMG SF v2.0): a policy statement of the American College of Medical Genetics and Genomics. *Genetics in medicine : official journal of the American College of Medical Genetics*. Feb 2017;19(2):249-255.

28. Uchida Y, Sugiura S, Sone M, Ueda H, Nakashima T. Progress and prospects in human genetic research into age-related hearing impairment. *BioMed research international*. 2014;2014:390601.

29. Bork JM, Peters LM, Riazuddin S, et al. Usher syndrome 1D and nonsyndromic autosomal recessive deafness DFNB12 are caused by allelic mutations of the novel cadherin-like gene CDH23. *American journal of human genetics*. Jan 2001;68(1):26-37.

30. Miyagawa M, Nishio SY, Usami S. Prevalence and clinical features of hearing loss patients with CDH23 mutations: a large cohort study. *PLoS One*. 2012;7(8):e40366.

31. Balciuniene J, Dahl N, Jalonen P, et al. Alpha-tectorin involvement in hearing disabilities: one gene--two phenotypes. *Human genetics*. Sep 1999;105(3):211-216.

32. Plantinga RF, de Brouwer AP, Huygen PL, Kunst HP, Kremer H, Cremers CW. A novel TECTA mutation in a Dutch DFNA8/12 family confirms genotype-phenotype correlation. *Journal of the Association for Research in Otolaryngology : JARO*. Jun 2006;7(2):173-181.

33. Bae SH, Robertson NG, Cho HJ, et al. Identification of pathogenic mechanisms of COCH mutations, abolished cochlin secretion, and intracellular aggregate formation: genotype-phenotype correlations in DFNA9 deafness and vestibular disorder. *Human mutation*. Dec 2014;35(12):1506-1513.

34. Kim BJ, Kim AR, Han KH, et al. Distinct vestibular phenotypes in DFNA9 families with COCH variants. *European archives of oto-rhino-laryngology : official journal of the European Federation of Oto-Rhino-Laryngological Societies*. Oct 2016;273(10):2993-3002.

35. Shearer AE, Smith RJ. Genetics: advances in genetic testing for deafness. *Current opinion in pediatrics*. Dec 2012;24(6):679-686.

36. Korver AM, Smith RJ, Van Camp G, et al. Congenital hearing loss. *Nature reviews. Disease primers*. Jan 12 2017;3:16094.

37. Oonk AMM, Ariens S, Kunst HPM, Admiraal RJC, Kremer H, Pennings RJE. Psychological impact of a genetic diagnosis on hearing impairment - an exploratory study. *Clinical otolaryngology : official journal of ENT-UK ; official journal of Netherlands Society for Oto-Rhino-Laryngology & Cervico-Facial Surgery*. May 29 2017.

38. Mazzoli M, Van Camp G, Newton V, Giarbini N, Declau F, Parving A. Recommendations for the description of genetic and audiological data for families with nonsyndromic hereditary hearing impairment. *Audiological Medicine*. 2003;1:148-150.

39. den Dunnen JT, Dalgleish R, Maglott DR, et al. HGVS Recommendations for the Description of Sequence Variants: 2016 Update. *Human mutation.* Jun 2016;37(6):564-569.

40. Wallis Y, Payne S, McAnulty C, et al. Practice Guidelines for the Evaluation of Pathogenicity and the Reporting of Sequence Variants in Clinical Molecular Genetics. *ACGS /VGKL.* 2013.

41. Maeda Y, Sheffield AM, Smith RJ. Therapeutic regulation of gene expression in the inner ear using RNA interference. *Advances in oto-rhino-laryngology.* 2009;66:13-36.

42. Goldmann T, Rebibo-Sabbah A, Overlack N, et al. Beneficial read-through of a USH1C nonsense mutation by designed aminoglycoside NB30 in the retina. *Investigative ophthalmology & visual science.* Dec 2010;51(12):6671-6680.

43. Slijkerman RW, Vache C, Dona M, et al. Antisense Oligonucleotide-based Splice Correction for USH2A-associated Retinal Degeneration Caused by a Frequent Deep-intronic Mutation. *Molecular therapy. Nucleic acids.* Nov 01 2016;5(10):e381.

44. Vona B, Nanda I, Hofrichter MA, Shehata-Dieler W, Haaf T. Non-syndromic hearing loss gene identification: A brief history and glimpse into the future. *Molecular and cellular probes.* Oct 2015;29(5):260-270.

45. White J, Beck CR, Harel T, et al. POGZ truncating alleles cause syndromic intellectual disability. *Genome medicine.* Jan 06 2016;8(1):3.

46. Guan J, Wang D, Cao W, et al. SIX2 haploinsufficiency causes conductive hearing loss with ptosis in humans. *Journal of human genetics.* Nov 2016;61(11):917-922.

47. Fu Q, Xu M, Chen X, et al. CEP78 is mutated in a distinct type of Usher syndrome. *J Med Genet.* Mar 2017;54(3):190-195.

48. Gilissen C, Hoischen A, Brunner HG, Veltman JA. Disease gene identification strategies for exome sequencing. *European journal of human genetics : EJHG.* May 2012;20(5):490-497.

49. Eisenberger T, Di Donato N, Baig SM, et al. Targeted and genomewide NGS data disqualify mutations in MYO1A, the "DFNA48 gene", as a cause of deafness. *Human mutation.* May 2014;35(5):565-570.

50. Patton J, Brewer C, Chien W, Johnston JJ, Griffith AJ, Biesecker LG. A genotypic ascertainment approach to refute the association of MYO1A variants with non-syndromic deafness. *European journal of human genetics : EJHG.* Jan 2016;25(1):147-149.

51. Ott J, Wang J, Leal SM. Genetic linkage analysis in the age of whole-genome sequencing. *Nature reviews. Genetics.* May 2015;16(5):275-284.

52. Sobreira N, Schiettecatte F, Valle D, Hamosh A. GeneMatcher: a matching tool for connecting investigators with an interest in the same gene. *Human mutation.* Oct 2015;36(10):928-930.

53. Yang T, Gurrola JG, 2nd, Wu H, et al. Mutations of KCNJ10 together with mutations of SLC26A4 cause digenic nonsyndromic hearing loss associated with enlarged vestibular aqueduct syndrome. *American journal of human genetics.* May 2009;84(5):651-657.

54. Ebermann I, Phillips JB, Liebau MC, et al. PDZD7 is a modifier of retinal disease and a contributor to digenic Usher syndrome. *The Journal of clinical investigation.* Jun 2010;120(6):1812-1823.

55. Akawi N, McRae J, Ansari M, et al. Discovery of four recessive developmental disorders using probabilistic genotype and phenotype matching among 4,125 families. *Nature genetics.* Nov 2015;47(11):1363-1369.

56. Lelieveld SH, Reijnders MR, Pfundt R, et al. Meta-analysis of 2,104 trios provides support for 10 new genes for intellectual disability. *Nature neuroscience.* Sep 2016;19(9):1194-1196.

57. van Esch TE, Kollmeier B, Vormann M, et al. Evaluation of the preliminary auditory profile test battery in an international multi-centre study. *International journal of audiology.* May 2013;52(5):305-321.

58. Koehler KR, Nie J, Longworth-Mills E, et al. Generation of inner ear organoids containing functional hair cells from human pluripotent stem cells. *Nature biotechnology.* May 01 2017.

59. Hartley BJ, Brennand KJ. Neural organoids for disease phenotyping, drug screening and developmental biology studies. *Neurochemistry international.* Jun 2017;106:85-93.
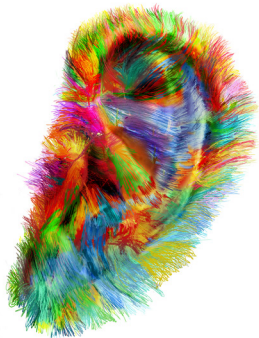
5

6

Addendum

English summary

Hearing impairment (HI) is the most common sensorineural disorder, and can have a significant impact on life. To cope with HI, it is essential that patients and their relatives are well informed about their diagnosis. In case of presumed hereditary HI, it starts with establishing a (genetic) diagnosis, after which counseling on prognosis, recurrence risk, rehabilitation options, and, if applicable, additional symptoms can take place. This thesis has the aim to contribute to optimal diagnostics and counseling for patients with hereditary HI in the Netherlands and beyond, by identification of novel deafness genes and (further) characterization of phenotypes and correlations between types of HI and underlying genetic causes.

Chapter 1 provides a general introduction on hearing and hereditary hearing impairment, and describes the scope of this thesis.

Chapter 2 serves as the starting point of this thesis. We evaluated the yield and outcomes of the most commonly used diagnostic test for hereditary HI in the Netherlands: whole exome sequencing (WES) with targeted analysis of a deafness gene panel. Retrospective analysis of test outcomes of 200 Dutch patients with presumed hereditary, mainly nonsyndromic, HI revealed that in 33.5% of cases a genetic diagnosis could be established, which is comparable to other studies. Variants in *GJB2*, *USH2A, MYO15A* and *STRC*, and in *MYO6* were the leading causes for autosomal recessive and dominant HI, respectively. Evaluation of the utility of prescreening single genes prior to gene panel analysis led to the conclusion that prescreening should be reduced to a minimum. Our recommendations, which particularly apply for the Dutch population, are to prescreen *GJB2* in case of congenital or 1st decade onset nonsyndromic HI, and specific genes associated with recognizable phenotypes such as DFNA9, DFNB4/Pendred syndrome and Usher syndrome. In all other cases, we recommend to perform WES targeting a panel of deafness genes as a first diagnostic test.

In **chapter 3**, the phenotypes of two recessive types of HI are further characterized and genotype-phenotype correlations are extended, which enables better counseling. **Chapter 3.1** describes the identification of pathogenic variants of *TRIOBP* in two isolated cases of Dutch origin. Disease-causing variants in *TRIOBP* have previously been associated with prelingual, severe to profound HI, known as DFNB28. Audiovestibular characterization of the two individuals in this study, however, displayed moderate HI, demonstrating that DFNB28 can be milder than reported so far. Vestibular function was normal. The relatively mild phenotype cannot be explained by predicted effects of the causative variants on

protein function. In the second presented subject, location of one of the underlying variants might well contribute to the milder HI, as it only affects isoform class TRIOBP-5, whereas all previously reported variants affect both TRIOBP-4 and TRIOBP-5. The identification of a pathogenic variant that only affects TRIOBP-5, suggests that a single *TRIOBP* copy encoding wild-type TRIOBP-4 is insufficient for normal hearing, and that at least one *TRIOBP* copy encoding TRIOBP-5 is indispensable for normal inner ear function.

In **chapter 3.2**, we report on nine families with DFNB77, caused by deleterious variants of *LOXHD1*. Twelve of fifteen identified variants were novel. There was high inter- and intrafamilial variation of the audiovestibular phenotype with regard to both severity and progression of HI. This is in line with previous studies. The phenotypic differences could not be related to type or location of the variants. Since objective evaluation of the vestibular function has not been reported before for DFNB77, we extensively assessed the vestibular system, which revealed normal function. Rare heterozygous missense variants of *LOXHD1* have been associated with Fuchs corneal dystrophy (FCD), a dominantly inherited disorder of the corneal endothelium. To assess whether family members who carry a heterozygous pathogenic *LOXHD1* variant are at risk for FCD, we screened them for corneal abnormalities. None of the carriers showed (preclinical) symptoms of FCD. We argue that rare *LOXHD1* alleles are a risk factor for FCD, rather than a monogenic cause. In addition, there are indications for *LOXHD1* variants associated with HI to induce a loss-of-function effect and for gain-of function variants to be related to FCD.

Chapter 4 describes the identification of two novel deafness genes, the associated phenotypes. In addition, we investigated and/or discussed the function of these genes in the inner ear. In **chapter 4.1**, we describe the discovery of *MPZL2* as a novel gene for recessive deafness. Phenotype characterization of three families with truncating variants of *MPZL2* showed early-onset, moderate, slowly progressive HI, without vestibular involvement or syndromic features. One of the identified variants is a founder mutation, which occurs homozygously in 0.001% of the Dutch population. We demonstrate that *MPZL2* is relatively highly expressed in the human fetal cochlea. Audiometric evaluation of mutant mice confirmed that *MPZL2* is essential for normal hearing, as these mice displayed progressive moderate to severe HI, similar to the human phenotype. Histological studies in three-month-old *Mpzl2* mouse mutants revealed loss of cochlear hair cells and supporting cells, which was most severe in the basal cochlear turn, corresponding to the downsloping audiogram configuration in the investigated individuals. We hypothesize that *MPZL2* mediates epithelial adhesions in the inner ear and that defects of *MPZL2* therefore lead to loss of structural integrity of the organ of Corti and progressive degeneration of hair cells and supporting cells.

Chapter 4.2 describes the identification of mono-allelic variants in *LMX1A* as a cause of HI and vestibular dysfunction in two families of Dutch origin. There was large phenotypic variability in the age of onset (congenital to 35 years), (a)symmetry, severity (mild to profound) and progression rate of HI. About half of the affected individuals displayed vestibular dysfunction and experienced symptoms thereof. Bi-allelic variants of *Lmx1a* have previously been associated with a complex phenotype in mice, including deafness and vestibular defects, caused by early-stage arrest of inner ear development. In humans, however, *LMX1A* seems to be (also) involved in maintenance of the inner ear, as most investigated subjects displayed a late-onset progressive phenotype, and absence of cochleovestibular malformations on computed tomography scans. Although *Lmx1a* mouse mutants demonstrate neurological, skeletal, pigmentation and reproductive system abnormalities, no syndromic features were seen in the participating subjects of either family. *LMX1A* has previously been suggested to be a candidate gene for intellectual disability, but our data do not support this, as affected subjects displayed normal cognition. We argue that haploinsufficiency is probably the main pathogenic mechanism of HI and vestibular dysfunction caused by mono-allelic *LMX1A* variants.

6

Lastly, **chapter 5** provides an overview of our main findings and implications of our results. In addition, we discuss strategies for future research into hereditary HI. The studies described in this thesis contribute to optimal diagnostics and counseling for patients with hereditary HI in the Netherlands and beyond. They expand knowledge on the epidemiology of hereditary HI in the Netherlands, (dis)advantages of our currently used diagnostic test, characteristics of phenotypes and genotype-phenotype correlations, and genes involved in hearing.

Nederlandse samenvatting

Slechthorendheid is de meest voorkomende zintuigstoornis en kan een aanzienlijke impact hebben op de kwaliteit van leven. Het is essentieel dat patiënten en hun familieleden goed worden geïnformeerd over hun aandoening, omdat dit hen kan helpen bij het omgaan met hun slechthorendheid. Bij verdenking op erfelijke slechthorendheid wordt geprobeerd eerst een (genetische) diagnose gesteld, waarna counseling plaatsvindt ten aanzien van prognose, herhalingsrisico, mogelijke revalidatie-opties en, indien van toepassing, bijkomende symptomen. Dit proefschrift heeft als doel om bij te dragen aan optimale diagnostiek en counseling van patiënten met erfelijke slechthorendheid in Nederland en ook daarbuiten, door nieuwe genen voor erfelijke slechthorendheid te ontdekken, en door fenotypen en correlaties tussen type slechthorendheid en genetische oorzaak (verder) in kaart te brengen.

Hoofstuk 1 geeft een algemene introductie over het gehoor en erfelijke slechthorendheid, en beschrijft de kaders van dit proefschrift.

6

Hoofdstuk 2 dient als het startpunt van dit proefschrift. Hierin hebben we de opbrengst en resultaten geëvalueerd van de meest gebruikte diagnostische test voor erfelijke slechthorendheid in Nederland: *whole exome sequencing* (WES) met gerichte analyse van een panel van doofheidsgenen. Uit een retrospectieve analyse van de testuitslagen van 200 Nederlandse patiënten met, voornamelijk niet-syndromale, erfelijke slechthorendheid bleek dat in 33.5% van de gevallen een genetische diagnose kon worden vastgesteld. Dit is vergelijkbaar met andere studies. Varianten in *GJB2, USH2A, MYO15A* en *STRC,* en in *MYO6*, waren de belangrijkste oorzaken van respectievelijk autosomaal recessieve en dominante slechthorendheid. Onderzoek naar het nut van het testen van een specifiek gen voorafgaand aan genpanel analyse leidde tot de conclusie dat deze testen tot een minimum moeten worden beperkt. Onze aanbevelingen, die specifiek gelden voor de Nederlandse populatie, luiden dat een *GJB2* voortest dient te worden gedaan in het geval van niet-syndromale slechthorendheid die congenitaal of in het eerste levensjaar is ontstaan. Daarnaast dienen voortesten te worden gedaan voor specifieke genen die geassocieerd zijn met herkenbare fenotypen zoals DFNA9, DFNB4/Pendred syndroom of Usher syndroom. In alle andere gevallen adviseren we om WES gericht op het doofheidspanel als eerste diagnostische test uit te voeren.

In **hoofdstuk 3** worden de fenotypen van twee recessieve vormen van slechthorendheid verder gekarakteriseerd en worden genotype-fenotype correlaties beschreven. Deze

studies hebben als doel om meer kennis te vergaren ten behoeve van verbeterde counseling. **Hoofdstuk 3.1** beschrijft de identificatie van pathogene varianten in *TRIOBP* in twee patiënten van Nederlandse afkomst. Mutaties in *TRIOBP* zijn in eerdere studies geassocieerd met prelinguale, ernstige tot zeer ernstige slechthorendheid, bekend als DFNB28. Echter, audiovestibulair onderzoek bij de twee aangedane personen in deze studie liet zien dat er sprake is van matige slechthorendheid. Dit toont aan dat DFNB28 kan leiden tot een milder gehoorverlies dan tot nu toe gerapporteerd. De evenwichtsfunctie was normaal. Het relatief milde fenotype kan niet worden verklaard door het voorspelde effect van de varianten op de functie van het eiwit. De locatie van één van de gevonden varianten draagt bij één van de patiënten mogelijk wel bij aan het milde gehoorverlies. Deze variant heeft namelijk alleen invloed op isovormklasse TRIOBP-5, terwijl alle eerder gerapporteerde varianten invloed hebben op zowel TRIOBP-4 als TRIOBP-5. De identificatie van deze variant suggereert dat één enkele kopie van *TRIOBP* coderend voor wildtype TRIOBP-4 onvoldoende is voor normaal gehoor, en dat tenminste één *TRIOBP* kopie coderend voor TRIOBP-5 nodig is voor een normale functie van het binnenoor.

In **hoofdstuk 3.2** rapporteren we over negen families met DFNB77, veroorzaakt door pathogene varianten in *LOXHD1*. Twaalf van de vijftien geïdentificeerde varianten waren nog niet eerder beschreven. Het audiovestibulaire fenotype laat een hoge inter- en intrafamiliaire variatie zien ten aanzien van ernst en progressie van de slechthorendheid. Dit komt overeen met resultaten van eerdere studies. De verschillen in fenotype kunnen niet worden toegeschreven aan het type of de locatie van de variant. Aangezien objectieve evaluatie van de vestibulaire functie tot op heden niet was beschreven, werden uitgebreide vestibulaire metingen uitgevoerd, welke een normale vestibulaire functie lieten zien. Heterozygote pathogene missense varianten in *LOXHD1* zijn in een eerdere studie geassocieerd met Fuchse corneale dystrofie (FCD), een dominant overervend ziektebeeld van het endotheel van de cornea. Om te beoordelen of familielieden met een heterozygote *LOXHD1* variant een verhoogd risico hebben op FCD, werden zij gescreend op corneale afwijkingen. Bij geen van hen werden (pre)klinische symptomen van FCD gevonden. We beargumenteren dat pathogene varianten in *LOXHD1* een risicofactor zijn voor FCD in plaats van een monogene oorzaak. Daarnaast zijn er aanwijzingen dat *LOXHD1*-varianten geassocieerd met slechthorendheid leiden tot een *loss-of-function* effect, terwijl varianten met een *gain-of-function* effect gerelateerd zijn aan FCD.

Hoofdstuk 4 beschrijft de identificatie van twee nieuwe doofheidsgenen en de bijbehorende fenotypen. Daarnaast onderzoeken en/of bediscussiëren we de functie van deze genen in het binnenoor. In **hoofdstuk 4.1** beschrijven we de identificatie van

MPZL2, een nieuw doofheidsgen voor recessieve slechthorendheid. Onderzoek naar het fenotype in drie families met defecten in *MPZL2* laat zien dat er sprake is van een matige, langzaam progressieve slechthorendheid, die ontstaat in de eerste levensdecade. Er was geen sprake van vestibulaire of syndromale afwijkingen. Eén van de geïdentificeerde varianten is zeer waarschijnlijk afkomstig van een gemeenschappelijk voorouder van de patiënten en komt in 0.001% van de Nederlandse bevolking homozygoot voorkomt. We laten zien dat *MPZL2* relatief hoog tot expressie komt in de humane foetale cochlea. Dat *MPZL2* een rol speelt bij het gehoor werd bevestigd middels audiometrie bij mutante muizen. Hierbij werd een progressieve milde tot ernstige slechthorendheid vastgesteld, vergelijkbaar met het humane fenotype. Histologische studies bij 3 maanden oude *Mpzl2* mutante muizen toonde een verlies van cochleaire haarcellen en ondersteunende cellen. Dit verlies was het meest ernstig in de basale winding van de cochlea, wat overeenkomt met de aflopende audiogramconfiguratie bij de onderzochte individuen. We suggereren dat MPZL2 bijdraagt aan celadhesie in het binnenoor en dat *MPZL2*-defecten leiden tot verlies van structurele integriteit van het orgaan van Corti, en een progressief verlies van haarcellen en ondersteunende cellen.

6

Hoofdstuk 4.2 beschrijft de identificatie van mono-allelische varianten in *LMX1A* als oorzaak van slechthorendheid en vestibulaire dysfunctie in twee families van Nederlandse afkomst. Er is sprake van een zeer variabel fenotype ten aanzien van ontstaansleeftijd (congenitaal tot 35 jaar), (a)symmetrie, ernst (mild tot zeer ernstig) en snelheid van progressie van de slechthorendheid. Bij ongeveer de helft van de aangedane personen was er sprake van vestibulaire dysfunctie, waar zij ook klachten van ondervinden. Bi-allelische *Lmx1a* varianten zijn in eerdere studies geassocieerd met een complex fenotype in de muis, waaronder doofheid en vestibulaire defecten. Dit wordt veroorzaakt door vroegtijdige beëindiging van de ontwikkeling van het binnenoor. Aangezien de meesten van de onderzochte patiënten pas op latere leeftijd een progressief fenotype ontwikkelden en de CT-scans geen cochleovestibulaire malformaties lieten zien, lijkt *LMX1A* in de mens (ook) betrokken te zijn bij het behouden van de binnenoorfunctie. Hoewel muizen met een defect in het *Lmx1a*-gen afwijkingen hebben van het centrale zenuwstelsel, het skelet, huidpigmentatie en het voortplantingssysteem, werden er geen syndromale afwijkingen waargenomen bij de patiënten van beide families. In de literatuur is gesuggereerd dat *LMX1A* een kandidaatgen is voor mentale retardatie. De resultaten van onze studie ondersteunen dit niet, aangezien de aangedane personen een normale cognitie hadden. We beargumenteren dat de geïdentificeerde mono-allelische *LMX1A*-defecten slechthorendheid en vestibulaire dysfunctie veroorzaken, doordat één kopie van het gen onvoldoende is voor het behoud van volledige cochleovestibulaire functie.

Tot slot geeft **hoofdstuk 5** een overzicht van de belangrijkste bevindingen en de implicaties van onze resultaten. Daarnaast bediscussiëren we strategieën voor verder onderzoek naar erfelijke slechthorendheid. De studies beschreven in dit proefschrift zijn een stap in de richting van optimale diagnostiek en counseling van patiënten met erfelijke slechthorendheid in Nederland en daarbuiten. Ze dragen bij aan kennis over de epidemiologie van slechthorendheid in Nederland, voor- en nadelen van de huidige diagnostiek, fenotypen en genotype-fenotype correlaties, en genen betrokken bij het gehoor.

List of abbreviations

ABR	auditory brainstem response
adHI	autosomal dominant hearing impairment
adNSHI	autosomal dominant nonsyndromic hearing impairment
AJ	adherens junction
arHI	autosomal recessive hearing impairment
arNSHI	autosomal recessive nonsyndromic hearing impairment
ART	acoustic reflex threshold
ARTA	age-related typical audiogram
BERA	brainstem evoked response audiometry
bp	base pair
cDNA	complementary deoxyribonucleic acid
cM	centiMorgan
CMV	cytomegalovirus
CNV	copy number variation
CT	computed tomography
cVEMP	cervical vestibular evoked myogenic potentials
dB	decibel
dBnHL	decibel normal hearing level
dbSNP	database of single nucleotide polymorphism
DNA	deoxyribonucleic acid
DFN	deafness
DFNA	autosomal dominantly inherited hearing impairment
DFNB	autosomal recessively inherited hearing impairment
DFNX	X-linked inherited hearing impairment
DFNY	Y-linked inherited hearing impairment
DFNM	modifier of hereditary hearing impairment
ENG	electronystagmography
ENT	ear-nose-throat
ExAC	exome aggregation consortium database
FCD	fuchs corneal dystrophy
HI	hearing impairment
HI	hearing level
Hz	hertz
IHC	inner hair cell
ISO	international organization for standardisation

6

ISO	isolated
Kb	kilobase
kHz	kilo hertz
LOVD	leiden open variation database
MAF	minor allele frequency
Mb	megabase
MIPS	molecular inversion probes
MLPA	multiplex ligation-dependent probe amplification
MRI	magnetic resonance imaging
mRNA	messenger ribonucleic acid
NGS	next generation sequencing
NSHI	nonsyndromic hearing impairment
nt	nucleotide
OAE	otoacoustic emission
OHC	outer hair cell
OMIM	Online Mendelian Inheritance in Man
PCR	polymerase chain reaction
PTA	pure tone acerage
qPCR	quantative polymerase chain reaction
RNA	ribonucleic acid
SNP	single-nucleotide polymorphism
SPL	sound pressure level
SRS	speech recognition score
SRT	speech reception threshold
TJ	tight junction
vHIT	video head impulse test
VNTR	variable number tandem repeat
VRA	visual reinforcement audiometry
VOR	vestibulo-ocular reflex
WES	whole exome sequencing
WGS	whole genome sequencing

List of publications

Wesdorp M, van de Kamp JM, Hensen EF, Schraders M, Oostrik J, Yntema HG, Feenstra I, Admiraal RJ, Kunst HP, Tekin M, Kanaan M, Kremer H[#], Pennings RJ[#]. Broadening the Phenotype of DFNB28: Mutations in TRIOBP are associated with Moderate, Stable Hereditary Hearing Impairment. *Hearing Research* 2017 Apr;347:56-62.

Zazo Seco C*, Wesdorp M*, Feenstra I*, Pfundt R, Hehir-Kwa JY, Lelieveld SH3, Castelein S, Gilissen C, de Wijs IJ, Admiraal RJ, Pennings RJ, Kunst HP, van de Kamp JM, Tamminga S, Houweling AC, Plomp AS, Maas SM, de Koning Gans PA, Kant SG, de Geus CM, Frints SG, Vanhoutte EK, van Dooren MF, van den Boogaard MH, Scheffer H, Nelen M, Kremer H, Hoefsloot L, Schraders M[#], Yntema HG[#]. The diagnostic yield of whole-exome sequencing targeting a gene panel for hearing impairment in The Netherlands. *European Journal of Human Genetics* 2017 Feb;25(3):308-314.

Zazo Seco C*, Serrão de Castro L*, van Nierop JW*, Morín M*, Jhangiani S, Verver EJ, Schraders M, Maiwald N, Wesdorp M, Venselaar H, Spruijt L, Oostrik J, Schoots J; Baylor-Hopkins Center for Mendelian Genomics, van Reeuwijk J, Lelieveld SH, Huygen PL, Insenser M, Admiraal RJ, Pennings RJ, Hoefsloot LH, Arias-Vásquez A, de Ligt J, Yntema HG, Jansen JH, Muzny DM, Huls G, van Rossum MM, Lupski JR, Moreno-Pelayo MA[#], Kunst HP[#], Kremer H[#]. Allelic mutations of KITLG, encoding KIT ligand, cause asymmetric and unilateral hearing loss and Waardenburg syndrome type II. *American Journal of Human Genetics* 2015 Nov 5;97(5):647-60.

Hoekstra CE, Wesdorp FM, van Zanten GA. Socio-demographic, health, and tinnitus related variables affecting tinnitus severity. *Ear and Hearing* 2014 Sep-Oct;35(5):544-54.

*,[#] These authors contributed equally to this work

6

Dankwoord

Niet voor niets is het dankwoord het meest gelezen deel van een proefschrift, en wel om drie redenen. Dit is het enige hoofdstuk dat makkelijk te lezen en te begrijpen is, wat ervoor zorgt dat de lezer niet na drie zinnen de weg kwijt is. Ten tweede is dit hoofdstuk in beperkte oplage verkrijgbaar, want je kunt 'm niet vinden op pubmed – dat maakt een mens nieuwsgierig. Maar de belangrijkste reden is dat de mensen die op deze pagina's worden genoemd een (groot) aandeel hebben gehad aan dit proefschrift, of mij na aan het hart liggen.

In de allereerste plaats wil ik alle patiënten die hebben deelgenomen aan het onderzoek bedanken voor hun inzet, tijd, geduld en doorzettingsvermogen. De onderzoeksdagen waren soms lang en vermoeiend, maar jullie enthousiasme en bereidwilligheid leken oneindig. Bij velen ben ik thuis langs geweest, bedankt voor de gastvrijheid!

Beste Hannie, je hebt je rol als promotor met verve vervuld. Dankzij jou is elk woord in dit proefschrift en elke assay of hypothese goed doordacht. Waar ik in het begin vaak moest slikken als ik een manuscript rood van de revisies van je terug kreeg, zijn we in de loop der jaren steeds dichter naar elkaar toe gegroeid. Vooral in het laatste jaar hebben we veel leuke en leerzame discussies gehad over de inhoud, maar ook over allerlei dingen die ons bezig houden in het leven. Ik waardeer je enorm om je kennis, eerlijkheid en oprechte interesse. Je hebt me oneindig veel geleerd!

Beste Ronald, ik had me geen betere copromotor kunnen wensen. Vanaf dag één heb je me bij de hand genomen en wegwijs gemaakt in de (politieke) wereld van de wetenschap. Maar je had vooral ook oog voor mijn persoonlijke ontwikkeling en ambities, en dat is absoluut jouw kracht. Het is jammer dat ik je teleur heb moeten stellen, omdat ik geen KNO-arts wil worden, maar zoals je weet heeft jouw enthousiasme voor het vak en de fantastische sfeer op de afdeling me erg doen twijfelen. Ik heb ontzettend genoten van de promovendi-etentjes bij jou thuis. Bedankt voor de fantastische tijd!

Dit proefschrift is mede tot stand gekomen in samenwerking met onze nationale werkgroep DOOFNL (Diagnostiek & Onderzoek Oto-genotype-Fenotype Nederland), waarbij het ErasmusMC, LUMC, MUMC+ en UMCG betrokken zijn. Hierbij wil ik Jet de Gier, Lies Hoefsloot, Marc van der Schroeff, Marieke van Dooren, Liselotte Rotteveel, Pia de Konings Gans, Sarina Kant, Els Vanhoutte, Janny Hof, Robert Stokroos, Suzanne Frints, Jolien Klein Wassink, Rolien Free en Ton van Essen bedanken voor de goede samenwerking en het

6

warme onthaal tijdens mijn bezoekjes aan jullie afdelingen. Ik hoop dat dit proefschrift het begin zal zijn van een vruchtbare samenwerking!

Leden van de otogenetica werkgroep, de leerzame woensdagmiddagen hebben mij niet alleen meer inzicht gegeven in de otogenetica, maar ook in het beleid en management van ziekenhuisdiagnostiek en poliklinische zorg. Fijn dat jullie me deze kans hebben geboden. Helger, we hebben vaak samengewerkt, vooral aan hoofdstuk 2: de opbrengst van het WES genpanel. Ik heb veel van je geleerd, met name door de tijd die je hebt genomen om samen de revisies te schrijven. Bedankt! Ronald Admiraal, jouw kennis over erfelijke slechthorendheid is van onschatbare waarde. Dat, in combinatie met je onuitputtelijke enthousiasme voor je vak, maakten dat ik graag bij je langskwam om te discussiëren over patiënten en de klinische implicaties van ons onderzoek. Ilse, je hebt me op een hele leuke en persoonlijke manier wegwijs gemaakt in de klinische genetica en het counselen van patiënten. Dank daarvoor!

Margit, jouw kennis en ervaring op het gebied van de otogenetica waren voor mij onmisbaar. Fijn dat we zoveel uur samen hebben kunnen werken! Jaap, jouw engelengeduld gecombineerd met goede humor zorgde ervoor dat ik uit keek naar de dagen op het lab. Erwin, ik bewonder je enthousiasme en liefde voor je vak, het werkt aanstekelijk! Alle mensen uit de 'Usher-groep': het was fantastisch om jullie te kennen. Ik heb goede herinneringen aan de etentjes en vooral de escape room!

Stefan, ondanks mijn eindeloze vraag om bio-informatische analyses was je altijd bereid om ze uit te voeren. Ik ben je daar heel erg dankbaar voor. Het heeft je, naast co-auteurschappen, in ieder geval een chocoladetaart opgeleverd!

Andy, bedankt voor alle leerzame momenten waarin je me telkens geduldig hebt uitgelegd hoe ons ingewikkelde evenwichtssysteem in elkaar zit. Je bent een fantastische leermeester!

Lieve Loes, ik bewonder je nuchtere, maar ó zo betrokken houding. Het was heerlijk om met je te praten over werk en privé, en om samen voorbereidingen te treffen voor symposia en vergaderingen. Dank voor alle gezelligheid en administratieve ondersteuning!

Beste medewerkers en staf van de afdeling KNO, de fantastische sfeer en de leuke samenwerkingen hebben ervoor gezorgd dat ik elke dag met veel plezier naar mijn werk ging. Dank voor alle mogelijkheden die jullie mij hebben geboden.

Lieve (oud)-assistenten, het was heerlijk om deel uit te maken van jullie gezellige, uitbundige groep! Ik ben blij dat jullie mij als vreemde-huisarts-in-de-bijt hebben opgenomen in de groep. Ik heb genoten van elk moment! Ik verlaat jullie met pijn in mijn hart, maar met fantastische herinneringen aan de assistentenweekenden, skivakanties, véle borrels, research-uitjes en KNO-dagen.

Lieve Ivo, wat heb jij een heerlijke kritische blik op de wetenschap en alles wat los en vast zit. Ik bewonder je nuchterheid en tegelijkertijd betrokkenheid in je werk en daarbuiten. We hebben aardig wat gezellige feestjes en borrels gehad; sorry voor de vechtpartijtjes, je bent een goede tegenpartij. Maar er zal toch altijd één ding op mijn netvlies blijven staan: assistentenweekend, een Duits accent en een megafoon. Je bent echt te gek!

Lieve Bas, tweeënhalf jaar lang hebben wij bijna elke dag onze onderzoekskamer gedeeld, dat is zeker 4000 uur! We hebben lief en leed gedeeld: van een artikel dat binnen 5 minuten na submissie werd afgewezen, tot eindeloze discussies over ons onderzoek en het leven, vele biertjes in Anneke, logeerpartijtjes van jou en Eva bij ons thuis, en niet te vergeten: onze trip naar Hinxton! Ik mis je gezelligheid, je goede smaak voor muziek, eten en wijn, maar vooral je goede smaak voor het leven. Mochten we elkaar ooit uit het oog verliezen (ik ga er alles aan doen om dat te voorkomen), weet dan dat je nooit uit mijn hart bent.

Lieve Anne-Marie, jouw nuchtere kijk op ons beroep en onze gezamenlijke interesse in de niet-klinische geneeskunde maken dat ik het heerlijk vind om met je te sparren over het dokter-zijn. Maar los van dat, ben je vooral een hele leuke, vrolijke en attente vriendin!

Lieve Marjolein en Frank, vanwege mijn promotieonderzoek zijn we tijdelijk verhuisd naar Nijmegen en woonden jullie ineens heel dicht bij ons. Het was fantastisch om elkaar zo vaak te kunnen zien! Onze tijd in Nijmegen is mede dankzij jullie een prachtige tijd geweest. Ik hoop dat onze vriendschap altijd zo mag blijven. Marjolein, onze hechte band kan na al die jaren niet meer stuk, ik vind je geweldig!

Lieve Leontien, je bent er altijd voor me, je begrijpt me en voelt me feilloos aan. Ik ben zo blij dat ik je ken! Hoewel het jou verschrikkelijk lijkt om te promoveren wilde je toch altijd weten waar ik mee bezig was en kreeg ik telkens weer lofbetuigingen van je. Ik waardeer je enorm om wie je bent. Je bent me ontzettend dierbaar! Pat, fijn dat jij, inmiddels als man van, achter Leontien staat, met je nuchtere en vrolijke kijk op het leven.

Marlies en Emmy, wat ben ik blij dat ik zulke lieve, attente, zorgzame zussen heb! Ondanks

6

dat we allemaal ambitieus zijn en drukke agenda's hebben is er gelukkig altijd tijd om even bij te kletsen en te horen hoe het met de ander gaat. Fijn dat we nu weer dichter bij elkaar wonen en zo vaker bij elkaar kunnen binnenlopen.

Lieve mam, bij jou ligt de oorsprong van het doorzetten en dicht bij jezelf blijven. Dank voor je nuchtere opvoeding en je onvoorwaardelijke, liefdevolle steun. Het maakt niet uit of je dichtbij of ver weg woont, want onze band overstijgt tijd en afstand. Waar je me vroeger hielp om mijn eerste kleine stapjes te zetten, helpen we elkaar nu om grote, nieuwe stappen te zetten. Op naar de toekomst!

Lieve, lieve Steev, onze liefde en geluk kan ik niet in woorden uitdrukken. Je bent er altijd voor me met je eindeloze optimisme en (dezelfde) grapjes, je geloof en vertrouwen in mij, en je geduld en luisterend oor als ik weer eens ongeduldig ben. Je bent een levensgenieter, en als ik het nodig heb herinner je me er aan dat genieten van het leven altijd boven werk gaat. Je hebt me geholpen en gesteund om keuzes te maken voor een toekomst die bij mij en bij ons past. Ik ben verschrikkelijk gek op je en gelukkig met je, en ik wil niks liever dan een leven samen met jou!

Mieke

Curriculum Vitae

Mieke Wesdorp werd op 29 april 1989 geboren in Goes. Ze groeide op met haar moeder en twee zussen in de prachtige provincie Zeeland. In 2007 haalde ze haar eindexamen Gymnasium aan het Buys Ballot College in Goes, waarna ze verhuisde naar Utrecht. Hier volgde ze haar opleiding geneeskunde aan de Universiteit van Utrecht. Vanwege haar brede interesse in de mensheid en organisatie & management volgde ze twee minors, een in Culturele Antropologie en een in Bestuurs- en Organisatiewetenschappen in 2009-2010. Ze vervolgde de geneeskundeopleiding in 2010 en volbracht haar coschappen in Nederland en aan de University of Malaya, Maleisië. In 2013 liep zij stage bij de beleidsstaf van de Raad van Bestuur van het UMC Utrecht, waar zij een intern rapport schreef over het meten van kwaliteit in de gezondheidszorg. Tijdens haar studie deed zij bestuurswerk binnen diverse verenigingen. Gedurende het coschap huisartsgeneeskunde werd duidelijk dat de diversiteit van het huisartsen vak, de persoonlijke relatie met de patiënt en de holistische werkwijze past bij haar interesses en persoonlijkheid. Maar haar interesses en ambities liggen ook binnen het wetenschappelijk onderzoek en beleid & management. Om die reden startte zij in september 2014 met haar promotieonderzoek naar de genetische oorzaken van slechthorendheid en correlaties tussen oorzaken en fenotypen aan de afdeling KNO van het Radboudumc, waarvoor ze naar Nijmegen verhuisde. Tevens heeft zij bijgedragen aan de oprichting van werkgroep DOOFNL, een landelijke samenwerking van vijf academische centra gericht op diagnostiek en onderzoek naar erfelijke slechthorendheid. De liefde voor de stad Utrecht deed haar terug verhuizen naar het midden van het land. In augustus 2017 startte zij als ANIOS beschouwende specialismen in het St. Antonius Ziekenhuis in Utrecht. In de toekomst ambieert zij een carrière als huisarts, waarbij zij daarnaast een rol hoopt te vervullen op het gebied van verbeteringen in de zorg.

6

Hearing impairment is the most common sensorineural disorder, and can have a significant impact on life. To cope with HI, it is essential that patients and their relatives are well informed about their diagnosis. In case of hereditary hearing impairment, it starts with establishing a (genetic) diagnosis, after which counseling on prognosis, recurrence risk, rehabilitation options, and, if applicable, additional symptoms can take place.

This thesis aims to contribute to optimal diagnostics and counseling for patients with hereditary hearing impairment in the Netherlands and beyond, by identification of novel deafness genes and (further) characterization of correlations between types of hearing impairment and underlying genetic causes.